

TILLAGE EROSION -  
AN IMPORTANT DRIVER OF YIELD VARIABILITY AND CARBON DYNAMICS  
IN A HUMMOCKY ARABLE LANDSCAPE IN NORTHEAST GERMANY

Kumulative Dissertation  
zur Erlangung des akademischen Grades  
"doctor rerum naturalium"  
(Dr. rer. nat.)

in der Wissenschaftsdisziplin  
KLIMA- & UMWELTWISSENSCHAFTEN

eingereicht an der  
Fakultät für Angewandte Informatik  
der Universität Augsburg



vorgelegt von  
LENA KATHARINA ÖTTL

2023

Ort und Tag der Disputation:  
Augsburg, 4. Dezember 2023



## GUTACHTER

PROF. DR. PETER FIENER  
Boden- & Wasserressourcenforschung  
Institut für Geographie  
Universität Augsburg

PROF. DR. KARL-FRIEDRICH WETZEL  
Hydrogeographie & Angewandte Physische Geographie  
Institut für Geographie  
Universität Augsburg

PROF. JOHN QUINTON  
Lancaster Environment Centre  
Lancaster University  
Lancaster, UK

Lena Katharina Öttl

*Tillage erosion - An important driver of yield variability and carbon dynamics  
in a hummocky arable landscape in Northeast Germany, 2023*

Picture Titlepage © Lena Katharina Öttl 2020.

Paper Chapter 3 © Authors 2022, CC BY 4.0.

Paper Chapter 4 © Authors 2021, CC BY-NC-ND 4.0.

Paper Chapter 5 © Authors 2022, under exclusive licence to Springer  
Nature Limited.

Paper Chapter 6 © Authors 2023, CC BY 4.0.

Paper Chapter A © Authors 2023.

Document typeset using the L<sup>A</sup>T<sub>E</sub>X template classicthesis developed  
by André Miede with style inspired by Robert Bringhurst: “The Ele-  
ments of Typographic Style”. classicthesis is available at <https://bitbucket.org/amiede/classicthesis/>.

“What we do to the land, we do to ourselves.”

– *Wendell Berry*



## PREFACE - VORWORT

---

“Alle guten Handlungen haben ihren Anfang in guten Gedanken.”  
“All good actions begin with good thoughts.”

— Swami Shivananda

My passion for science developed from the will to take action to combat climate change already at a time when I was still in school. At university, I learned the necessary tools for doing research in several positions as a student assistant. After conducting my bachelor thesis in the field of climate research I realised that it is difficult to directly influence the climate (except for fundamentally reducing one’s carbon footprint with a sustainable lifestyle). However, maintaining soil fertility and protecting soils from being polluted or degraded has a direct impact on the well-being of all life on earth. Only very few people are concerned about the “*dirt*” below our feet, although nearly all of the world’s food comes from the land. For those reasons my heart (and mind) opened up for soil science. To this day, I see an urgent need for protecting our soils as an active measure to ensure food security and to mitigate climate change. I tried my best to contribute to this research need with the work I conducted during my PhD.

The present thesis was prepared within the framework of the German Research Foundation (DFG) project “*Tillage erosion affects crop yields and carbon balance in hummocky landscapes (TilEro)*”. I am grateful for the financial support of the DFG and that Peter Fiener and Michael Sommer made this project possible. More importantly, I would not have been able to produce this thesis without the personal support of many people to whom I would like to express my special thanks.

I am deeply grateful to my doctoral advisor Peter Fiener. Peter, thank you for the more than self-evident support and motivation, for the trust in me and my scientific skills when I have already given up, and the freedom you gave me, e. g. regarding time management and the field campaigns. Thank you for the encouraging and inspiring discussions throughout the last five years that always improved the study results. I also highly appreciate the support I received regarding several trainings to improve my teaching, writing, and presentation skills.

My journey to the Uckermark and the topic of tillage erosion began in the *Landscape Pedology* working group led by Michael Sommer at ZALF e.V. in Müncheberg. Thank you Michael, for hosting me during my four-months internship in 2018, for introducing me to the wonderful and interesting soil landscape of the Northwestern Uckermark, for your support during the preparation of the field campaigns, and for connecting me to important people, especially the

staff from ZALF's research station and the *Landscape Pedology* working group.

Special thanks go to my colleague Florian Wilken. Thank you Florian, for your support in so many ways, e. g. modelling, preparing and conducting the field campaigns, (spatial) data analysis, reviews of figures and manuscripts as well as proof-reading parts of this thesis. I would not have been able to do my PhD without your (technical) advice and your continuous good mood. I especially enjoyed the time we spent together during field campaigns and student courses.

Additionally, I am deeply grateful for my colleague and dear friend Anna Juřicová. What started as a scientific exchange turned into a real friendship, where we supported each other in many ways. I especially thank you for your help during the field campaign and for your feedback to this thesis.

Particular thanks also go to my colleague Pedro Batista for sharing the office with me, for the fruitful discussions, for helping me to improve my programming skills and figures for publications, and to become more critical regarding publications of other researchers.

My thanks also go to all colleagues that were part of the *Soil & Water Resource Research* working group during the last five years. Thank you Alessandro Fabrizi, Ana Carolina Cugler, Anna Stegmann, Annette Dietmaier, Benjamin Bukombe, Joseph Tamale, Mario Reichenbach, Raphael Rehm, Silvia Schrötter, and Tabea Zeyer. I will keep all events and shared memories in mind, e. g. after-work beer evenings, birthdays, summer and christmas parties, weddings, and births. I would also like to thank my student assistants Rosi Degg and Patricia Borel for the support regarding the field campaigns and data processing.

I am grateful for the so-called "*Erfolgsteam*" (i. e. "*success team*") – Annette Straub, Maximilian Graf, and Sebastian Purwins – for the support during very difficult times. Thank you for the endless motivation and faith in me.

Last but not least, I thank my family and friends who supported me equally in good and hard times. Special thanks go to Alex, who was always one step ahead in her studies and had an answer to (nearly) all PhD-related questions (e. g. organisational issues or regarding L<sup>A</sup>T<sub>E</sub>X and R). Thanks go to all friends that listened to me when my motivation and the faith in myself was low but also celebrated successful moments with me.

Danke Papa & Linda dafür, dass ihr immer an mich geglaubt habt, jede meiner Entscheidungen hinsichtlich meines Lebensweges akzeptiert habt und mich darin unterstützt, ab jetzt einen anderen Weg zu gehen. Danke Ami, dass du immer für mich da warst und bist. Es hat mich motiviert, dass du nie damit aufgehört hast zu fragen, wann ich denn endlich mit der "Arbeit" fertig bin. ***Jetzt ist es soweit!***

## ABSTRACT

---

Soils are a non-renewable, precious resource providing numerous ecosystem services that enable life on land. However, they are threatened by various human-induced land degradation processes since the onset of settled agriculture a few thousand years ago. One of the most severe threats is soil erosion that not only jeopardises soil health and fertility but also redistributes large amounts of soil organic carbon (SOC). These lateral SOC fluxes modify the biogeochemical cycling and vertical fluxes of carbon (C). The latter have the potential to influence the atmospheric concentration of carbon dioxide (CO<sub>2</sub>) and as a consequence, received increasing political and scientific attention in the last decades.

There is political interest in enhancing C sequestration and storing large amounts of atmospheric CO<sub>2</sub> in soils. Thereby, soils can potentially act as a tool to mitigate climate change. However, research has demonstrated that different methods lead to contrasting results on whether soil redistribution contributes to increased C mineralisation or sequestration (loss of CO<sub>2</sub> to the atmosphere) or storage of atmospheric CO<sub>2</sub> in the SOC compartment of the soil, respectively. The magnitude of the C sink or source term depends on the temporal and spatial scales that are considered as well as on the types of erosion that are included in the analysis. Most studies focus on water erosion, while tillage erosion has only been regarded on small temporal (decades to a century) and spatial scales (plot to field scale).

This thesis aims to assess the impact of long-term (1000 years) soil redistribution by tillage and water on crop yields and the C balance at landscape scale (ca. 200 km<sup>2</sup>). Therefore, the spatially explicit soil redistribution and C turnover model SPEROS-C was used for simulating soil redistribution by tillage and water as well as SOC dynamics. The model simulations are performed for the catchment of the River Quillow in the Uckermark region, Northeast Germany. To analyse the impact of soil redistribution on landscape-scale crop yields, the model simulations were compared to the Enhanced Vegetation Index (EVI) of different crops and coupled with the crop biomass model AQUACROP. The study region is characterised by large-field farming with heavy machinery and a rolling landscape, which favour tillage-induced soil redistribution. Field experiments were carried out to compare a conventional inversion and a conservative non-inversion plough regarding their soil redistribution rates. The development of agricultural management in the study area over the past millennium was included in a modelling approach to determine the historical and recent role of tillage erosion on current SOC patterns.

Soil redistribution by tillage was found to be the dominant erosion process in the study region, leading to soil thinning at erosional areas and soil accumulation at depositional areas. Overall, this results in a reduction in mean crop yields at the landscape scale. The crop yield reduction is amplified in dry years, while in normal-to-wet years, the reduction in crop yields at erosional sites can be compensated by the increases in yields in depositional zones.

Field experiments demonstrated that non-inversion conservative chisel tillage resulted in larger soil redistribution compared to conventional mouldboard ploughing at the same tillage depth and speed.

The historical reconstruction of the land use history in the study region shows that tillage is a non-negligible soil redistribution agent throughout the past millennium. The combined effect of soil redistribution by tillage and water can more than compensate for C losses due to land conversion from forest to agricultural land. This effect can turn the study region into a slight C sink when the time since the onset of widespread agricultural management in the study region and C turnover processes in erosional and depositional soils are considered at the landscape scale.

The results of this thesis suggest that soil redistribution by tillage has an underestimated effect on crop yields and SOC turnover. The topic will gain importance in the future due to increasing tillage intensity and changes in crop growth conditions facing climate change effects. This highlights the potential of land management adaptations to control C dynamics and mitigate atmospheric CO<sub>2</sub> concentrations.

## ZUSAMMENFASSUNG

---

Böden sind nicht erneuerbare, wertvolle Ressourcen von unschätzbarem Wert, die zahlreiche Ökosystemleistungen erbringen und Leben auf der Erde ermöglichen. Sie sind jedoch durch verschiedene vom Menschen verursachte Prozesse der Bodendegradation bereits seit Anbeginn der Landwirtschaft vor einigen Jahrtausenden bedroht. Eine der schwerwiegendsten Bedrohungen ist die Bodenerosion, die nicht nur die Bodengesundheit und -fruchtbarkeit gefährdet, sondern auch große Mengen an organischem Bodenkohlenstoff verlagert. Diese lateralen Kohlenstoffflüsse verändern den biogeochemischen Kohlenstoffkreislauf und damit vertikale Kohlenstoffflüsse. Letztere sind aufgrund ihres Potentials, die Kohlendioxid-Konzentration in der Atmosphäre beeinflussen zu können, in den letzten Jahrzehnten zunehmend in den Fokus von Politik und Wissenschaft gelangt.

Das politische Interesse liegt dabei auf den Prozessen der verstärkten Kohlenstoff-Sequestrierung und damit auf der Speicherung großer Mengen an atmosphärischem Kohlendioxid in Böden, wodurch sie potentiell als Klimaschutzinstrument dienen könnten. Unterschiedliche Forschungsmethoden resultieren jedoch in gegensätzlichen Ergebnissen hinsichtlich der Frage, ob Bodenverlagerung zu einer verstärkten Mineralisierung oder Sequestrierung von Kohlenstoff (Verlust von Kohlendioxid an die Atmosphäre) bzw. zu einer Speicherung von atmosphärischem Kohlendioxid im Boden beiträgt. Die Größe der Kohlenstoffsенke oder -quelle hängt von der Analyse der zeitlichen und räumlichen Skala sowie von den betrachteten Erosionsarten ab. Die meisten Studien befassen sich mit Wassererosion, während die vom Menschen verursachte Bodenverlagerung (d.h. Erosion durch Bodenbearbeitung) bisher meist nur auf kleinen zeitlichen (Jahrzehnte bis zu einem Jahrhundert) und räumlichen Skalen (Parzelle bis Feld/Schlag) betrachtet wurde.

Vor diesem Hintergrund untersucht diese Arbeit die Auswirkungen der langfristigen (1000 Jahre) Bodenverlagerung durch Bodenbearbeitung und Wasser auf die Ernteerträge sowie die Kohlenstoffbilanz auf Landschaftsebene (ca. 200 km<sup>2</sup>). Mithilfe des räumlich expliziten Bodenverlagerungs- und Kohlenstoffumsatzmodells SPEROS-C wurde die Bodenverlagerung durch Bodenbearbeitung und Wasser sowie die Dynamik von organischem Bodenkohlenstoff simuliert. Die Modellsimulationen wurden für das Einzugsgebiet des Flusses Quillow in der Uckermark im Nordosten Deutschlands durchgeführt. Um die Auswirkungen der Bodenverlagerung auf die mittleren Ernteerträge auf Landschaftsskala zu analysieren, wurden die Modellsimulationen mit einem aus Satellitenbildern abgeleiteten Vegetationsindex verschiedener Nutzpflanzen verglichen und mit dem Biomassemodell

AQUACROP gekoppelt. Die Untersuchungsregion ist durch intensive Landwirtschaft mit schweren Maschinen auf großen Schlägen und eine hügelige Landschaft gekennzeichnet, die eine durch die Bodenbearbeitung verursachte Bodenverlagerung begünstigen. In Feldexperimenten wurden ein konventioneller, wendender Pflug und ein konservativer, nicht-wendender Pflug hinsichtlich ihrer Bodenverlagerungsraten verglichen. Um die historische und aktuelle Rolle der Bearbeitungserosion zu ermitteln, wurde in einer Modellstudie die Entwicklung der Landwirtschaft im Untersuchungsgebiet im letzten Jahrtausend berücksichtigt.

Die Bodenverlagerung durch Bearbeitung ist die vorherrschende Erosionsart in der Untersuchungsregion. Sie führt zu einer Abnahme der Bodentiefe auf Erosionsflächen und zu Bodenauftrag auf Depositionsflächen. Als Resultat nehmen die durchschnittlichen Ernteerträge auf Landschaftsebene ab. Dieser Effekt ist in trockenen Jahren verstärkt, während in normalen bis feuchten Jahren die reduzierten Erträge auf Erosionsstandorten durch höhere Erträge in Depositionsgebieten ausgeglichen werden. Die Feldversuche resultieren in einer größeren Bodenverlagerung durch den konservativen, nicht wendenden Grubber im Vergleich zum konventionellen, wendenden Pflug, wenn beide Geräte mit der gleichen Bearbeitungstiefe und -geschwindigkeit eingesetzt werden. Die historische Rekonstruktion der Landnutzungsgeschichte in der Untersuchungsregion zeigt, dass die Bodenbearbeitung während des vergangenen Jahrtausends einen nicht zu vernachlässigenden Faktor der Bodenverlagerung darstellt. Der kombinierte Effekt der Bodenverlagerung durch Bodenbearbeitung und Wasser kann die Kohlenstoffverluste aufgrund der Landnutzungsänderung von Wald in Ackerland mehr als kompensieren und in einer geringen Kohlenstoffsenke resultieren, wenn die Zeit seit Beginn der landwirtschaftlichen Nutzung in der Region sowie die Kohlenstoff-Umsatzprozesse in erodierten und akkumulierten Böden auf Landschaftsebene berücksichtigt werden.

Die Ergebnisse dieser Arbeit zeigen, dass die Bodenverlagerung durch Bodenbearbeitung einen bisher unterschätzten Einfluss auf die Ernteerträge und den Kohlenstoffumsatz im Boden hat. Das Thema wird in Zukunft aufgrund der zunehmenden Intensität der Bodenbearbeitung und der veränderten Wachstumsbedingungen der Pflanzen angesichts der Wirkungen des Klimawandels zunehmend an Bedeutung gewinnen. Dies unterstreicht das Potenzial von Anpassungen in der Landwirtschaft zur Kontrolle der Kohlenstoffdynamik und zur Minderung der atmosphärischen Kohlendioxid-Konzentrationen.

## CONTENTS

---

1	GENERAL INTRODUCTION	1
1.1	Thesis overview . . . . .	4
1.2	Author contributions . . . . .	6
2	THEORETICAL BACKGROUND	9
2.1	Soil redistribution . . . . .	10
2.2	SOC redistribution and dynamics . . . . .	16
2.3	Impact of soil redistribution on crop yields . . . . .	20
3	NON-INVERSION CONSERVATION TILLAGE AS AN UNDER-ESTIMATED DRIVER OF TILLAGE EROSION	23
3.1	Introduction . . . . .	24
3.2	Materials & Methods . . . . .	25
3.3	Results . . . . .	30
3.4	Discussion . . . . .	34
3.5	Conclusions . . . . .	38
4	TILLAGE EROSION AS AN IMPORTANT DRIVER OF IN-FIELD BIOMASS PATTERNS IN AN INTENSIVELY USED HUMMOCKY LANDSCAPE	41
4.1	Introduction . . . . .	42
4.2	Materials & Methods . . . . .	45
4.3	Results . . . . .	51
4.4	Discussion . . . . .	56
4.5	Conclusions . . . . .	60
5	TILLAGE EXACERBATES THE VULNERABILITY OF CROPS TO DROUGHT	61
5.1	Introduction . . . . .	61
5.2	Methods . . . . .	63
5.3	Results . . . . .	71
5.4	Discussion . . . . .	76
5.5	Supplementary information . . . . .	80
6	A MILLENNIUM OF ARABLE LAND USE – THE LONG-TERM IMPACT OF WATER AND TILLAGE EROSION ON LANDSCAPE-SCALE CARBON DYNAMICS	87
6.1	Introduction . . . . .	88
6.2	Materials and methods . . . . .	90
6.3	Results . . . . .	102
6.4	Discussion . . . . .	107
6.5	Conclusion . . . . .	112
6.6	Supplementary material . . . . .	112
7	GENERAL DISCUSSION AND CONCLUSION	119
7.1	Summary and general discussion . . . . .	119
7.2	Concluding remarks and outlook . . . . .	128

BIBLIOGRAPHY	129
A TILLAGE EROSION AS AN UNDERESTIMATED DRIVER OF CARBON DYNAMICS	161
A.1 Introduction . . . . .	162
A.2 Materials and methods . . . . .	163
A.3 Results . . . . .	172
A.4 Discussion . . . . .	177
A.5 Conclusions . . . . .	179
A.6 Supplementary material . . . . .	180
List of Figures	181
List of Tables	182
List of Abbreviations	183

## GENERAL INTRODUCTION

---

Soils are invaluable and non-renewable resources providing numerous ecosystem services that are essential for life on land (Lal, 1998). Most importantly, soils support plant growth, thereby providing food and raw materials. Moreover, soils regulate water availability and purification, are habitat for soil organisms, provide the foundation for human infrastructure, and maintain cultural heritage (Adhikari and Hartemink, 2016; Buckwell et al., 2022; Weil and Brady, 2017). The interplay of soil functions operating at the nexus of lithos-, hydros- and atmosphere, influences land-atmosphere interactions and thus, the composition and physical condition of the atmosphere (Blum, 2005; Weil and Brady, 2017).

Soils play a major role in the global carbon (C) cycle, as they represent the largest terrestrial organic C pool, store thrice the amount of C held in the atmosphere, and more than four times the amount stored in terrestrial vegetation (IPCC, 2019; Lal, 2018; Stockmann et al., 2013). C in soils can be either inorganic or organic, whereby inorganic C derives from the parent material or from biogeochemical reactions in the soils (Buckwell et al., 2022). Soil organic carbon (SOC) is the C contained in the organic component of soil (i. e. soil organic matter (SOM)), consisting of plant and animal residue as well as soil organisms and is essential for soil health (Buckwell et al., 2022; IPCC, 2019).

A large proportion of global surface soils has been degraded and depleted in SOC stocks due to unsustainable management (Bellamy et al., 2005; IPCC, 2019). Soils are imperiled by humans since the onset of agricultural land use (Lang and Bork, 2006; Montgomery, 2007a). One of the most widespread land degradation processes threatening soil fertility and crop production is soil erosion (Amundson et al., 2015; Lal, 2003; Pimentel and Burgess, 2013). For European soils it is estimated that 71 % of soil degradation are caused by water and wind erosion, while globally this number reaches 84 %. Human-induced soil compaction, sealing, and crusting causes 17 % of soil degradation in Europe, whereby the main causative factor is the use of heavy machinery (Oldeman, 1992). The soil erosion rates on arable land caused by these factors often exceed soil formation rates (Evans et al., 2019; Montgomery, 2007b).

Soil erosion and deposition (i. e. soil redistribution) lead to a lateral redistribution of C resulting in reduced SOC stocks at eroded sites and enhanced SOC stocks in depositional zones (e. g. depressions or alluvial sites Blanco-Canqui and Lal, 2010). These lateral fluxes further modify the biogeochemical cycling and vertical C fluxes leading to soil

C mineralisation (i. e. release as carbon dioxide (CO<sub>2</sub>)) on one side and C sequestration (i. e. transferring CO<sub>2</sub> from the atmosphere into the soil system) on the other side. These vertical fluxes have the potential to directly influence the atmospheric concentration of CO<sub>2</sub> (Doetterl et al., 2016; IPCC, 2019). Soil management strongly determines whether soils act as a C sink or source as well as the strength of that term (Smith et al., 2009). The SOC sequestration potential is highest in soils that have been depleted in C, e. g. agricultural and degraded soils (Lal, 2018; Paustian et al., 1997; Smith et al., 2009). This can be achieved by increasing C input by adding manure or cereal straw, by slowing decomposition, and by storing a larger proportion of C in the longer term C pools of the soil (Lal, 2018; Smith et al., 2009).

Due to their sequestration potential, soils and SOC have received increasing political attention. A set of global conventions to protect and conserve the Earth's resources was created starting with the Kyoto Protocol to the United Nations Framework Convention on Climate Change (UNFCCC) (Blum and Eswaran, 2004; UNFCCC, 1998). Although soils and agricultural management were not included in the Paris Agreement (21<sup>st</sup> Conference of the Parties to the UNFCCC (COP<sub>21</sub>) in 2015), a soil-related initiative was launched at COP<sub>21</sub> by the French Minister of Agriculture (Minasny et al., 2017; UNFCCC, 2015). The so-called *4 %-initiative* aims at increasing SOC stocks globally by 4 % per year by environmentally sound agronomic practices to compensate for anthropogenic greenhouse gas emissions (Chabbi et al., 2017; Minasny et al., 2017). Furthermore, the Intergovernmental Panel on Climate Change (IPCC) Special Report on Climate Change and Land (IPCC, 2019) names SOC management and reduced soil erosion as a land-related action that contributes to climate change adaptation, mitigation and sustainable development.

However, the implementation of the agreements signed in the mentioned global conventions is hampered by environmental and social circumstances. The potential of increasing SOC content is threatened by a declining capacity of soils to act as C sinks at higher temperatures that are expected from an ongoing climate change. A further threat is the expansion of land use that leads to increasing soil degradation and decreasing SOC stocks (IPCC, 2019). National political frameworks and legislations have to be adapted in order to achieve the quantified emission limitation and reduction commitments (Paustian et al., 2016). Moreover, existing social barriers to the adoption of sustainable soil management have to be removed (e. g. economic, technical, and knowledge barriers; Buckwell et al., 2022) and scientific knowledge gaps in assessing SOC dynamics have to be closed.

Scientific attention on SOC and erosion started in the 1990s and increased nearly exponentially since the 2000s (Clarivate *Web of Science* search result, 07/02/2023). A systematic scientometric analysis with the software *VOSviewer* (version 1.6.18; Eck and Waltman, 2010) re-

vealed three main research clusters regarding SOC and erosion: (i) field studies assessing soil properties, (ii) modelling soil redistribution and sediment export at sloping land and at different spatial scales, and (iii) improvements of management practices. The latter is the most prominent cluster including topics such as soil management, soil fertility, conservation tillage, crop yields, SOC depletion and sequestration, sustainability, and climate change mitigation. The latest publications deal with climate change, ecosystem services, and the Chinese loess plateau, while research about management practices, soil fertility, and crop production is already of concern for at least one decade (Clarivate *Web of Science* search result, 07/02/2023). Refining the search result regarding erosion types showed nearly 5 times the amount of studies dealing with the relation of water erosion and SOC compared to that with tillage erosion (Clarivate *Web of Science* search result, 07/02/2023). The long-term, historical impact of tillage on soil and SOC redistribution has not received attention until now, although soil redistribution rates since the 1950s are not sufficient to explain current soil truncation and accumulation rates (Pimentel, 2000; Wilken et al., 2020). Studies assessing long-term soil erosion rates or the impact of historical land use changes only considered water erosion (e. g. Bouchoms et al., 2017; Lang and Bork, 2006).

Large scale (e. g. national, continental or global) estimates of soil redistribution and related SOC dynamics are mostly based on average values derived from plot or field experiments (Boardman, 1998). This is problematic because these experiments are mostly conducted at steep, eroding landscape positions thereby overemphasizing the erosion effect and omitting depositional positions (Auerswald et al., 2009). A holistic landscape scale approach including the historical evolution of tillage-induced soil redistribution is needed to assess the fate of eroded, redistributed, and deposited SOC and to determine whether soil redistribution is a source or sink of atmospheric CO<sub>2</sub> (Lal, 2005).

Especially in areas with large-field farming and hilly, undulating topography, soil degradation and enhanced C fluxes play a major role in the context of food security and climate change as they constitute important crop production areas globally, such as parts of Canada (e. g. Manitoba, Ontario, and Saskatchewan), Northeast Europe (e. g. Czech Republic, Denmark, and Northeast Germany), Russia, and the USA (e. g. Indiana, Michigan, and Ohio). The study area of this thesis is located in the young morainic area of Northeast Germany and is characterised by a gently rolling (so-called *hummocky*) terrain, highly mechanised large-field farming, and a long history of agricultural land use (several millennia). These characteristics favour the occurrence of tillage-induced soil redistribution. As the area is located in one of the driest regions in Germany (mean annual precipitation of 466 mm compared to 781 mm in Germany, 20-year average 2001 - 2020; DWD, 2021; UBA, 2022), soil redistribution by water is restricted to single

erosive rain events and bare soil conditions (7-11 events per year; Deumlich, 1999; Vahrson and Frielinghaus, 1998).

Another peculiarity of the study area regarding soil redistribution by water is the low connectivity to the river network. Due to the rare occurrence of streams or rivers, eroded sediment is mostly exported to and deposited in drainless kettle holes that are only connected to the groundwater (Lischeid et al., 2017; OpenStreetMap contributors, 2017). When soil redistribution due to water occurs, it mainly leads to offsite damages such as sedimentation and water pollution in kettle holes (Frielinghaus and Schmidt, 1993). Soil redistribution by tillage was until now only assessed at single fields (Kietzer, 2007; Wilken et al., 2020; Winnige et al., 2003).

A better understanding of the impact of soil redistribution on C dynamics is crucial to protect and maintain affected soils. Hence, the overarching aim of this thesis is to improve the understanding of the impact of agricultural management on soil redistribution since the onset of widespread land use and related soil-atmosphere C exchange on a regional scale.

### 1.1 THESIS OVERVIEW: AIMS AND STRUCTURE

The specific goal of this dissertation is to quantify the impact of management-specific, tillage-induced soil redistribution on crop yields and resulting feedbacks on the C cycle on a regional scale (200 km<sup>2</sup>) and historical timespan (1000 years). Based on the motivation presented in the previous section the following questions have evolved and are addressed regarding the study area of this thesis:

- 1) To which extent does soil redistribution by tillage and water affect crop yields?
- 2) What is the dominant driver of soil redistribution – tillage or water?
- 3) What role did tillage-induced soil redistribution play since the onset of agricultural management and what is its role today?
- 4) What implications arise from long-term soil redistribution by tillage and water on the C balance after forest has been converted to crop land?

The hypotheses that are tested on a regional scale are as follows:

- 1) Soil redistribution by tillage and water leads to a mean landscape-scale decrease in crop yields.
- 2) Tillage erosion is the dominant driver of soil redistribution because of specific characteristics of the study region.

- 3) Tillage played a minor role in soil redistribution at the onset of agricultural management but its impact increased with mechanisation of agriculture.
- 4) The lateral redistribution of SOC by tillage and water leads to increased vertical C fluxes, whereby the processes of dynamic replacement and deep burial generate a sink of atmospheric CO<sub>2</sub>.

This dissertation is organised as a cumulative thesis that consists of individual and independent research articles for international ISI-listed and peer-reviewed scientific journals. These articles are presented in the four main chapters. Chapters 3-5 are published, while Chapter 6 is a submitted manuscript. The framework is given by a theoretical background introducing the main topic of the research articles and an overall discussion of their results. All articles deal with the same study area, namely the ca. 200 km<sup>2</sup>-sized catchment of the River Quillow in the Uckermark region, Northeast Germany.

Chapter 2 provides the scientific background for the thesis and the individual articles. It provides the necessary knowledge for a self-contained understanding of the thesis chapters and highlights the challenges common to all of the presented research articles.

Chapter 3 assesses differences in soil redistribution between a conventional, inversion mouldboard plough and a conservative, non-inversion chisel plough. Tracer experiments were performed at three sites mainly differing in slope (steep, moderate, and gentle slope). The results reveal that non-inversion tillage produces significantly more lateral soil movement compared to inversion tillage. The largest difference in soil translocation distance between the tillage implements was found on the gentle slope that exhibited lowest soil cohesion.

Chapter 4 analyses the interrelation between the Enhanced Vegetation Index (EVI) as proxy for crop biomass and modelled soil redistribution by tillage and water on a regional scale. The findings indicate that eroded areas have the lowest values of the EVI, while the highest values were found at depositional areas. The differences in the EVI between the contrasting areas affected by soil loss or accumulation are more pronounced in the analysed normal-to-dry year than in the wet year. Although the increase in crop biomass at depositional sites can partly outweigh losses at erosional sites, soil redistribution leads to an overall decline in mean crop yields at the landscape scale.

Chapter 5 determines how the changes in soil depth and soil properties due to tillage affect crop yields. The impact of tillage-induced soil redistribution on winter wheat and maize yields was assessed by modelling the past millennial and future 50 - 100 years of agricultural

management. A combination of literature review, coupled soil redistribution and crop growth modelling as well as remote sensing data reveals that soil loss negatively impacts crop yields. Deeper soils in depositional areas can partly compensate for yield losses in erosional areas leading to continuing agricultural production. For consistency of the structure of this thesis the order of the original publication was changed by inserting the methods section between the introduction and results instead of having it after the discussion.

Chapter 6 estimates the impact of 1000 years of tillage and water erosion on C dynamics and the C balance of the study region. The model approach incorporates different realisations of historical land management and rain erosivity. Tillage-induced soil redistribution was found to be the dominant erosion process in this area. The soil redistribution-induced C fluxes can compensate for C losses due to land conversion from forest to crop land and turn the study region into a slight C sink.

In the overall discussion and conclusion (Chapter 7), the main findings of the individual publications are discussed and put into context with respect to the general aims of this thesis.

Finally, Appendix A presents another submitted manuscript. This modelling study assesses the impact of soil redistribution by tillage and water on the C balance for a modelling period of 58 years (1961 - 2018) using the same spatially explicit soil redistribution model as in Chapter 6. Since the study is performed at a smaller temporal and spatial scale (ca. 200 ha) in the Czech Republic and is therefore not directly linked to the study area of this thesis it is only included in the Appendix. Nevertheless, the work gives additional insights into the region-specific importance of soil redistribution by tillage and water on C dynamics.

## 1.2 AUTHOR CONTRIBUTIONS TO PUBLISHED MANUSCRIPTS

This section lists the detailed author contributions to the individual research articles included in this thesis and in the Appendix.

Chapter 3 – *Non-inversion conservation tillage as an underestimated driver of tillage erosion (Öttl et al., 2022)*: P. Fiener, M. Sommer, L. K. Öttl, and F. Wilken conceived and planned the study design. A. Hupfer set up the RFID detection system. L. K. Öttl and F. Wilken carried out the field work. Data processing and illustration were done by L. K. Öttl, while data analysis and interpretation were carried out by L. K. Öttl, F. Wilken, and P. Fiener. The manuscript was drafted by L. K. Öttl, F. Wilken, and P. Fiener, while all authors reviewed and approved the

final version of the manuscript.

Chapter 4 – *Tillage erosion as an important driver of in-field biomass patterns in an intensively used hummocky landscape (Öttl et al., 2021)*: The study design was conceived and planned by M. Sommer, P. Fiener, L. K. Öttl and F. Wilken. L. K. Öttl and M. Wehrhan evaluated the remote sensing data. L. K. Öttl conducted the modelling with support of F. Wilken. The statistical analysis of the data was done by L. K. Öttl and K. Auerswald. L. K. Öttl, F. Wilken, and P. Fiener drafted the manuscript, while all authors reviewed and approved the final version of the manuscript. K. Auerswald supported the review process.

Chapter 5 – *Tillage exacerbates the vulnerability of cereal crops to drought (Quinton et al., 2022)*: J. N. Quinton and P. Fiener contributed equally to the design, literature review, modelling and manuscript preparation. L. K. Öttl supported the modelling and evaluated the remote sensing data for the test site.

Chapter 6 – *A millennium of arable land use – the long-term impact of water and tillage erosion on landscape-scale carbon dynamics (Öttl et al., submitted to Soil)*: The modelling approach was designed by L. K. Öttl, P. Fiener, and F. Wilken. L. K. Öttl reviewed relevant literature, developed the model, conducted the modelling, processed the data, and designed the figures and tables. Model development was supported by F. Wilken and A. Juřicová. Data analysis and interpretation were carried out by all authors. The manuscript was drafted by L. K. Öttl, F. Wilken, and P. Fiener, while all authors contributed to the discussion and reviewed the final version of the manuscript.

Appendix A – *Tillage erosion as an underestimated driver of carbon dynamics (Juřicová et al., submitted to Soil & Tillage Research)*: A. Juřicová and P. Fiener designed the study. A. Juřicová conducted the field work and processed the samples with the contribution of T. Chuman. L. K. Öttl modified the model code. A. Juřicová prepared the input data, performed the model simulations, and created the figures for the paper. A. Juřicová and L. K. Öttl processed the data and interpreted the model output with the support of P. Fiener and F. Wilken. The manuscript was drafted by A. Juřicová with a substantial contribution of L. K. Öttl and F. Wilken. D. Žížala provided the validation dataset, R. Minařík helped with statistics and all authors reviewed the manuscript.

In the manuscript chapters, obvious typing errors in the original publications have been corrected. Larger changes are marked by the symbol \* and explained in footnotes at the respective page.



## THEORETICAL BACKGROUND

---

This chapter describes the relationship between lateral soil and soil organic carbon (SOC) redistribution as well as vertical SOC turnover in agricultural landscapes and thus, is essential to understand the background of this thesis and the following chapters. Moreover, the requirements and methods for answering the research questions are presented.

Figure 2.1 illustrates the main topic of this thesis, namely the impact of soil redistribution by tillage and water on SOC dynamics. Soil redistribution is the detachment, transport, and deposition of soil particles caused by one or more natural or anthropogenic erosive forces (e. g. rain, surface runoff, tillage, wind, gravity, land levelling, and crop harvesting; Boardman and Poesen, 2006). Globally, water erosion is the major agent of soil redistribution, followed by tillage and wind erosion (Quinton et al., 2010).

Soil redistribution leads to lateral removal and application of soil material, or in other words, soil profile truncation and accumulation. This is accompanied with a reduction in SOC stocks and other nutrients (e. g. nitrogen (N) and phosphorous (P)), rooting depth, and available plant water at erosional and an increase of those favourable soil conditions at depositional areas (Gerke and Hierold, 2012; Herbrich et al., 2018). The change in soil properties due to erosion and deposition also modifies crop biomass production and the in-field yield pattern (Stadler et al., 2015; Taylor et al., 2003). The soil redistribution induced lateral removal of SOC does not only change SOC stocks but also the vertical biogeochemical cycling (Berhe et al., 2014; Doetterl et al., 2016; Quinton et al., 2010). Carbon (C) cycling is altered due to the modified sequestration and mineralisation of SOC in eroded and deposited soils (Doetterl et al., 2016). The processes of *dynamic replacement* and *deep burial* mentioned in Figure 2.1 are described in more detail in the following sections.

In the study area of this thesis, today's soils are not only a result of soil development since the retreat of the Weichselian glaciation (ca. 15 ky ago; Lüthgens et al., 2011). They are also highly influenced by human land management that already started a few thousand years ago (Behre, 2008; Kappler et al., 2019). For this thesis the last millennium is considered as agricultural practices clearly intensified since that time (Kappler et al., 2019; Van der Meij et al., 2019).

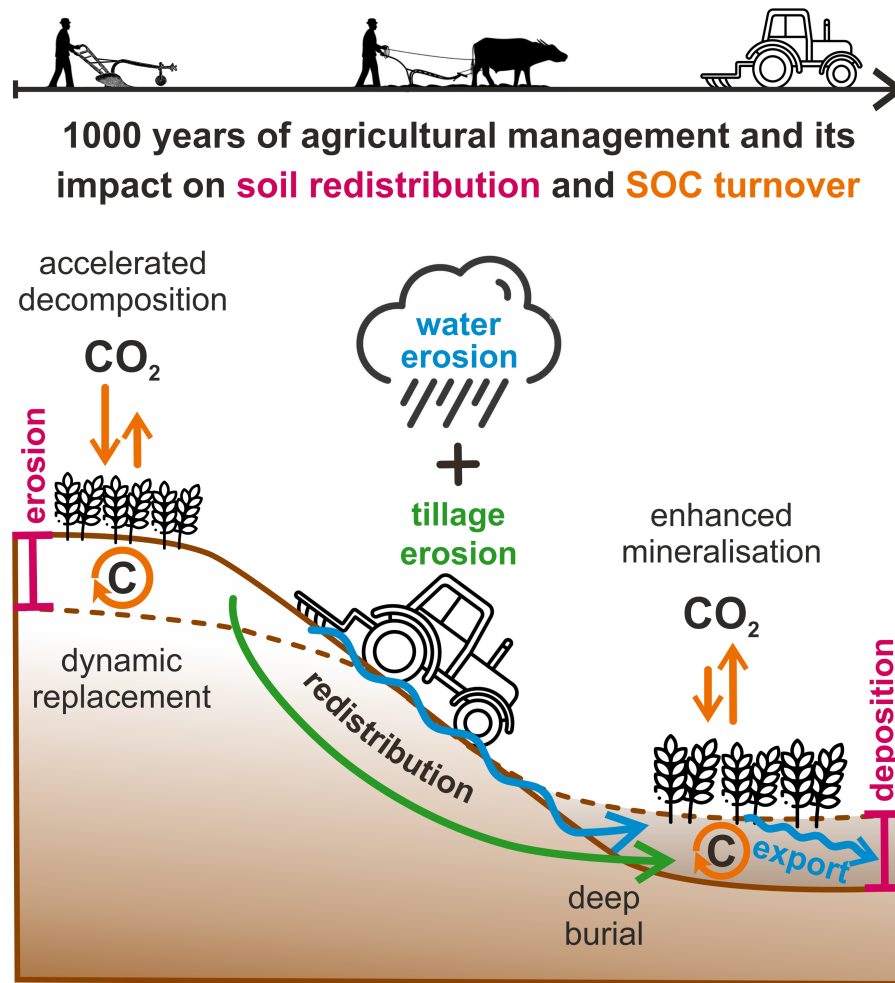


Figure 2.1: Summary of the thesis. Impact of soil redistribution by tillage and water on soil organic carbon (SOC) turnover and resulting carbon (C) fluxes into the soil or the atmosphere. Detailed explanation can be found in the text.

## 2.1 SOIL REDISTRIBUTION

The focus of this thesis lies on tillage- and water-induced soil redistribution, i. e. erosion and deposition. However, there are several other erosion processes which are not included in this thesis for individual reasons, e. g. land levelling, soil loss due to crop harvesting (SLCH), and wind erosion. Little is known about land levelling in our study area, which generally results in significant soil profile truncation and often induces other soil erosion processes such as sheet, rill, gully, and pipe erosion (Boardman and Poesen, 2006). SLCH, also called *harvest erosion*, occurs during the harvest of crops when the harvested crop is in direct contact with the soil. The export of loose soil, soil adhering to the crop, and rock fragments from the field occurs with root and tuber crops, e. g. sugar beet (*Beta vulgaris* L.), potato (*Solanum tuberosum* L.), chicory (*Cichorium intybus* L.), and carrot (*Daucus carota* L.; Kuhwald et al., 2022; Ruysschaert et al., 2004). This erosion process was not

considered as root and tuber crops together only account for ca. 2 % of the crops grown in the study area (Destatis, 2015-2019). Wind erosion was not considered as it is of minor importance in the study area due to the typical soil texture ranging from loamy sand to sandy clay loam soils (Deumlich et al., 2006, 2017).

### 2.1.1 *Soil redistribution processes and patterns*

Tillage is the mechanical manipulation of the soil profile for modifying soil conditions and managing crop residues, weeds or incorporating chemicals for crop production (Soil Science Society of America, 2008). Whenever soil is tilled up- and downslope on sloping land, tillage erosion (or rather *tillage translocation*) takes place. This term comprises the displacement of the cultivation layer (i. e. erosion) at slope shoulders, transport of the detached soil material and deposition at places with lower slope (i. e. foot slopes and depressions; Van Oost and Govers, 2006; Van Oost et al., 2006a). Hence, tillage-induced soil redistribution smoothens the landscape by degrading convex hilltops and aggrading concave areas (Figure 2.1; Van Oost et al., 2006a; Weil and Brady, 2017). The amount of soil moved and the translocation distance mainly depend on slope gradient, whereby greater movement occurs on steeper slopes and positions of changing slope gradient (Van Oost et al., 2006a). Other important influencing factors are the design of the tillage implement, depth of tillage, tillage speed, and soil properties at time of tillage such as soil moisture and bulk density (Montgomery et al., 1999; Van Oost et al., 2006a; Weil and Brady, 2017). Net soil movement occurs in the direction of tillage, whereby translocation distance is higher when the tillage implement is traveling downslope than upslope due to gravity. For the same reason, soil is also slightly moved downslope when tillage is on the contour (Govers et al., 1999; Van Oost et al., 2000).

Soil erosion by water is also a three-step process, including detachment of soil particles by rain drops or floating water, transportation of the detached soil particles downhill (by floating, rolling, dragging, and splashing), deposition of the transported soil particles at a lower elevated position or export to the river network (Figure 2.1; Weil and Brady, 2017). Water erosion comprises sheet, rill, gully, and pipe erosion. Severe water erosion typically occurs on bare, temporarily unprotected arable land, overgrazed rangelands and on badlands (Boardman and Poesen, 2006).

Spatial patterns of tillage- and water-induced soil redistribution differ markedly because of the different principal driving forces. Soil loss by tillage can be greatest from landscape positions where water erosion is minimal, i. e. on slope convexities and near upslope field borders, while soil deposition by tillage typically occurs in areas where water erosion is often maximal, i. e. in concavities (Van Oost

et al., 2006a). However, both erosion types lead to soil deposition at footslopes (Wilken et al., 2020). Mean soil erosion rates induced by present-day soil tillage techniques on sloping land reported for Europe range from 3 to 93 t ha<sup>-1</sup> yr<sup>-1</sup> (Boardman and Poesen, 2006). They are of the same order of magnitude as rates of water-induced soil erosion (Van Oost et al., 2000) or can even exceed them (Gerontidis et al., 2001; Lobb et al., 1995; Van Oost et al., 2003). Generally, tillage erosion rates in Europe have increased over the last decades because of an increase in tillage depth and speed (Boardman and Poesen, 2006).

In some areas of the world, tillage is known to be the dominant erosion process (e. g. in parts of Europe and Canada; Govers et al., 1996a, 1994; Lobb and Kachanoski, 1999; Lobb et al., 1995; Schimmack et al., 2002; Wilken et al., 2020). For the study region of this thesis it was also shown that recent soil degradation is dominated by tillage translocation (small catchment of ca. 4.2 ha in the center of the study area; Wilken et al., 2020). Water-induced soil redistribution in this area is determined by the specific, limited hydrological and sedimentological connectivity to the river system. Water-induced erosion has a minor contribution because it is distributed over a greater spatial extent, but the eroded material concentrates in significant deposition around and in kettle holes (i. e. typical landscape features; agriculturally not used depressions often filled with water or peat; Anderson, 1998; Frielinghaus and Vahrson, 1998; Wilken et al., 2020). Although single heavy rain events can contribute to relatively high soil loss and especially to soil accumulation in depressions (Frielinghaus and Vahrson, 1998), they are of minor importance when longer timescales are taken into account.

Both, tillage- and water-induced soil redistribution lead to severe on-site damage. At eroding sites, soil depth is reduced resulting in modified physical, chemical, and biological properties described in more detail in Section 2.3. Tillage is a non-selective process removing the plough layer and redistributing relatively fertile, loose soil material within an agricultural field (Blanco-Canqui and Lal, 2010). In contrast, water erodes valuable organic matter and fine mineral particles leaving behind less fertile coarser fractions (Batista et al., 2023; Weil and Brady, 2017). The selective sedimentation of water-erosion induced deposition can lead to unfavourable deposition of coarse material and soil crusting due to fine material. Moreover, the sediment may bury seeds and small plants, while dense crusts reduce water infiltration and increase water runoff (Weil and Brady, 2017).

As eroded and transported soil material does not leave the agricultural field in case of tillage erosion, only water erosion leads to off-site damages. Thereby, exported sediment and water masses lead to several, partly severe damages that depend on the characteristics of the catchment's surrounding and its connectivity to the stream network (Boardman et al., 2019). When the sediment reaches rivers

or water bodies it can modify ecosystem properties by changing the water quality (e. g. increasing turbidity and concentration of N and P), covering pebbles and rocks that act as habitat for several organisms, and can even raise the river level leading to a higher probability of flooding (Frielinghaus and Schmidt, 1993; Weil and Brady, 2017). Infrastructure such as roads, basins and dams can be damaged by the exported sediment and muddy floods leading to high costs (Boardman et al., 2019; Graves et al., 2015; Weil and Brady, 2017).

### 2.1.2 *Effect of tillage implements on soil redistribution*

“The age-old practice of turning the soil before planting a new crop is a leading cause of farmland degradation. Many farmers are thus looking to make ploughing a thing of the past.”

— *Huggins and Reganold (2008)*

For a better understanding of the use of different tillage implements nowadays, the development of tillage practices in North Germany is elaborated in the following. The onset of agricultural land use in this region can be dated back to at least 5500 years BCE based on archeological findings of the linear pottery culture (Behre, 2008; Herrmann, 1985). These farmers used hand-held wooden hooks, hoes or digging sticks to produce ridges and furrows with an estimated plough depth of 2 - 3 cm (Behre, 2008; Ehlers and Claupein, 2017; Herrmann, 1985). The first simple wooden plough, the so-called *ard*, which was drawn by oxen at relatively small fields of approximately 1000 - 2000 m<sup>2</sup>, was introduced in this area in the bronze and iron age (1800 - 750 BCE; Figure 2.2 a; Behre, 2008; Herrmann, 1985; Lüning, 1997). It further evolved into the *Roman plough* with an iron plough share (Figure 2.2 b; Lal et al., 2007). This symmetric plough did not invert the soil but already reached a plough depth of up to 0.18 m (Behre, 2008; Herrmann, 1985; Lüning, 1997). A few hundred years later, the first soil-inverting mouldboard plough was invented and horses were preferred over oxen (Behre, 2008; Herrmann, 1985). However, the widespread replacement of the hook by the mouldboard plough on a large scale lasted until the beginning of the 11<sup>th</sup> century (Ehlers and Claupein, 2017). In the middle ages, average tillage depths were around 0.15 m (Bork et al., 1998). At the beginning of the 19<sup>th</sup> century, the so-called *Ruchadlo* revolutionised agricultural management as it not only turned the soil but also crumbled soil clods (Herrmann, 1985; Leser, 1931). In the 20<sup>th</sup> century, average tillage depths increased to 0.2 m. Further mechanisation and the introduction of modern, turning mouldboard ploughs with several plough shares enabled deeper ploughing (average tillage depths of up to 0.4 m in the 1970s; Bork et al., 1998). Until today, the mouldboard plough is the most widespread and important implement of primary tillage in Germany (Ehlers and Claupein, 2017; Zikeli and Gruber, 2017).

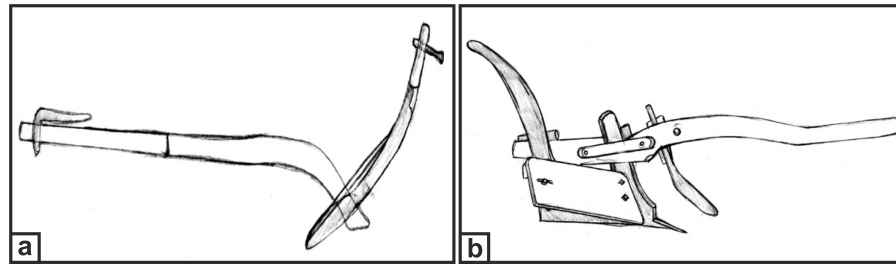


Figure 2.2: Drawing of historical ploughs taken from Lal et al. (2007). (a) Wooden ard plough and (b) Roman plough with an iron share.

In agricultural systems, tillage has multiple functions that influence crop production such as modifying soil structure, weed control, incorporating fertilisers and soil amendments as well as alleviating edaphic and climatic constraints (Carter, 2004). Inversion tillage by mouldboard ploughing enables burying and thereby deactivating annual and perennial weeds as well as volunteer crops. Moreover, it loosens the topsoil, cleans the soil surface, which enables precision seeding, and prevents the leaching of nutrients such as base-forming cations. On light, sandy soils the ability to integrate organic residues, manure or semiliquid manure mixed with straw is important for improving the water holding capacity and fertility of these soils (Ehlers and Claupein, 2017). However, present-day modern mouldboard ploughing with heavy machinery promotes excessive pan formation as well as subsoil compaction and the bare soil surface increases the susceptibility to soil erosion by water and wind (Ehlers and Claupein, 2017; Lal et al., 2007).

In contrast to that long history of intensive soil cultivation, conservation tillage is only taken into account since a few decades (Ehlers and Claupein, 2017; Lal et al., 2007). Conservation tillage is a general term including all tillage methods that omit mouldboard ploughing and have the potential to conserve soil and water by reducing their loss relative to conventional tillage (Carter, 2004; Ehlers and Claupein, 2017; Lal et al., 2007). Precise definitions of conservation tillage can only be made in a specific context taking into account the crop types grown, the local soil types and conditions as well as the respective climate. However, a well-accepted operational definition of conservation tillage is a tillage (or tillage and planting combination) that retains a 30% or greater crop residue cover on the soil surface after seeding or planting (Carter, 2004; CTIC, 2017; Zikeli and Gruber, 2017). There are several variants of conservation tillage that do not meet the operational definition of 30% crop residue cover but lead to soil and water conservation, such as mulch, reduced, minimum, shallow, non-inversion or zero tillage (also called *no tillage* or *direct drilling/seeding*). Some of these variants are restricted to a shallower tillage depth (e. g.  $< 0.15$  m) and no soil inversion (Carter, 2004).

Inversion tillage was necessary as long as N fertilisation was limited and herbicides for deactivating weeds and volunteer crops were lacking (Carter, 2004; Lal et al., 2007). Although the scientific community proved that soil inversion was not a prerequisite of crop production anymore, the acceptance of conservation tillage remained generally low, at least for German farmers (Ehlers and Claupein, 2017). Constraints to the adoption of conservation tillage practices can mostly be traced back to economic and sociocultural factors such as the need for purchasing specialised planting equipment, applying additional herbicides, and acquiring new management skills (Carter, 2004; FAO, 2001; Huggins and Reganold, 2008). In Germany, conservation tillage was applied on ca. 40 % of the arable land in the year 2010, while 53 % of the arable land was tilled conventionally (year 2016; Destatis, 2017). At global or European scale conservation agriculture is less common, with 12.5 % and 5.0 % of the cropland area, respectively (year 2015/16; Kassam et al., 2019).

There are various benefits of conservation tillage that go beyond soil conservation, e. g. saving time due to reduced work steps of seedbed preparation and seeding accompanied by reduced costs for labour and fuel. Ecologic benefits for implementing conservation agriculture are a reduction in wind and water erosion as well as resulting nonpoint pollution. It also comes along with enhanced soil fertility and health due to sequestration of SOC in the topsoil as well as increased microbial activity (Franzluebbers, 2010; Helsel, 2007; Madarász et al., 2021).

Tillage erosion rates also vary between inversion and non-inversion implements because of the different soil movement. Examples of a conventional and a conservative tillage implement can be seen in Figure 3.2 in Chapter 3. A conventionally used mouldboard plough picks up and inverts large quantities of soil. Thereby, the turning direction (to the left or right) is determined by the implement shape and can be static or changing per pass (Figure 2.3 a). Conservative non-inversion implements, e. g. a chisel plough or disk harrow, stir up the soil and spread it over distances of several meters (Figure 2.3 b). Conventional inversion tillage is accompanied with soil erosion rates mostly exceeding those of other tillage implements such as chisel ploughs or field cultivators (e. g. Govers et al., 1994; Lobb et al., 1999; Marques da Silva et al., 2004).



Figure 2.3: Comparison of soil movement by exemplary, contrasting tillage implements. (a) Conventional mouldboard plough (Albatros, Raabe, Germany) turning the soil. (b) Conservative non-turning chisel plough (Smaragd, Lemken, Germany) stirring up the soil. Screenshots from videos taken with a remotely piloted aircraft system (RPAS) by F. Wilken.

## 2.2 SOIL ORGANIC CARBON (SOC) REDISTRIBUTION AND DYNAMICS

As soil redistribution highly depends on terrain attributes such as hillslope inclination, length, and curvature, those are important factors controlling the movement, stock, sequestration, and decomposition of SOC in the landscape (Berhe and Kleber, 2013). During the three phases of soil redistribution - detachment, transport, and deposition - complex, competing processes such as mineralisation, sequestration, and biomass production affect the C budget of the landscape prone to soil redistribution (Doetterl et al., 2016; Kirkels et al., 2014).

### 2.2.1 *The fate of soil organic carbon (SOC) upon soil redistribution*

At eroded landscape positions SOC stocks are generally reduced by soil removal (Kirkels et al., 2014). However, in eroded soils there are two contrary processes taking place simultaneously: First, former stable subsoil SOC is exposed due to erosion of surface soil and mixed with fresh labile topsoil SOC. This readily available energy source for decomposers accelerates SOC decomposition (so-called *priming effect*) and the release of carbon dioxide ( $\text{CO}_2$ ) to the atmosphere (Figure 2.1; Doetterl et al., 2016; Fontaine et al., 2007; Van Oost and Six, 2023). Second, if at least some of the eroded C is replaced by fresh biomass-C, then the so-called *dynamic replacement* takes place (Berhe et al., 2008; Harden et al., 1999). Due to this process, erosion enhances terrestrial sequestration of  $\text{CO}_2$  from the atmosphere and increases SOC storage (Berhe et al., 2014; IPCC, 2019; Paustian et al., 2000). This process leads to the counterintuitive situation where soils represent a net atmospheric C sink although SOC was lost laterally due to erosion (Figure 2.1; Van Oost and Six, 2023). The soil's C sink strength depends

on soil depth, landscape position, clay content, mineralogy, and the antecedent SOC stock (Lal, 2018).

Soil detachment leads to a disruption of soil aggregates, thereby exposing SOC to loss by decomposition or transport in soluble or particulate form (Berhe et al., 2014). Soil aggregates get further disrupted leading to increased C mineralisation during transport, whereby this source term is only short-lived (seconds to days; Berhe et al., 2014; Doetterl et al., 2016; Van Oost and Six, 2023). Mixing of mineral and organic matter as well as subsequent formation of new soil aggregates can counteract the mineralisation and reduce C loss (Berhe et al., 2014). The extent to which C (and other nutrients) is lost from eroded hillslopes through decomposition or dissolved loss depends on the physico-chemical characteristics of the soil (e. g. soil texture and water content), the nature of C in the transported material, the type and intensity of the erosion process, the duration of transport, and the characteristics of the depositional area in which the eroded material accumulates (Berhe et al., 2014; Doetterl et al., 2016).

In deposited soils the delivery of freshly eroded topsoil material stimulates mineralisation of soil surface SOC by soil organisms leading to enhanced C loss to the atmosphere (Lal, 2003). There is again a counterintuitive situation: although laterally delivered SOC is accumulated, it represents a source for atmospheric C (Figure 2.1; Van Oost and Six, 2023). However, C mineralisation after deposition is also a short-lived process due to the rapid mineralisation and of minor importance on landscape scale (Quinton et al., 2010; Van Hemelryck et al., 2010, 2011). A competing process that leads to an increase in SOC stocks and a net removal of CO<sub>2</sub> from the atmosphere is the preservation of SOC from decomposition in depositional soils, the so-called *deep burial* (Berhe et al., 2008; Stallard, 1998; VandenBygaart et al., 2015). This process leads to a transfer from an active SOC pool that interacts with the biosphere to a passive pool of storage (McCarty and Ritchie, 2002).

### 2.2.2 Soil redistribution - carbon (C) sink or source? A matter of perspective

“Sedimentologists argue that soil erosion is a C sink [...] –  
Soil scientists and agronomists argue that soil erosion is a net C source [...].”

— Lal (2005)

There is an ongoing controversy between researchers since approximately two decades whether soil-redistribution enhanced SOC mineralisation or sequestration prevails or in other words, whether soil redistribution leads to a C source or sink (see e. g. comments on *Managing soil carbon*; Lal et al., 2004; Renwick et al., 2004; Van Oost et al., 2004b). The criterion for soil redistribution acting as C sink is that dynamic replacement of eroded C and reduced decomposition of deeply buried, depositional C together more than compensate for erosional C losses from the studied catchment (Berhe et al., 2007).

The review of Kirkels et al. (2014) systematically describes the C source or sink controversy. The research of Lal R. and other authors results in soil redistribution constituting a source of atmospheric CO<sub>2</sub> due to (i) reduced net primary production on eroded soils that are not able to sufficiently replace removed SOC, (ii) enhanced SOC mineralisation due to breakdown of soil aggregates during detachment and transport, and (iii) increased SOC decomposition in buried sediments (Jacinthe and Lal, 2001; Lal, 2019; Lal et al., 2004).

Van Oost K. and co-workers describe soil redistribution as a sink of atmospheric CO<sub>2</sub> due to (i) new C fixation at eroded sites (*dynamic replacement*), (ii) reduced turnover rates and thus, reduced mineralisation in C depleted subsoils that are exposed at erosional sites, and (iii) reduced SOC mineralisation in deeply buried, deposited soil material (Liu et al., 2003; Van Oost et al., 2005a, 2007).

Tillage erosion plays a special role in this debate as soil eroded by tillage is deposited within the same field and no transport-related mineralisation of SOC occurs as it would be the case for water-induced soil redistribution (Van Oost et al., 2004b). Tillage-induced soil redistribution thus leads to relatively high C inventories at depositional sites by moving SOC enriched topsoil from relatively reactive to rather unreactive sites (Blanco-Canqui and Lal, 2010; Renwick et al., 2004; Van Oost et al., 2004b).

A consensus on the direction and magnitude of the soil-redistribution induced land-atmosphere C exchange is still lacking although methodological advances, especially regarding modelling, nowadays enable an improved representation of the relation between soil redistribution processes and C cycling (Doetterl et al., 2016; Van Oost and Six, 2023). The contradiction regarding soil redistribution and SOC can be reconciled by considering the range of temporal and spatial scales at which soil redistribution impacts SOC dynamics (Van Oost and Six, 2023). In their review, Van Oost and Six (2023) conclude that water erosion is a source for atmospheric CO<sub>2</sub> when only small temporal and spatial scales are considered. When multi-scaled approaches are used, both C sinks and sources appear (Van Oost and Six, 2023).

### 2.2.3 Modelling soil redistribution and soil organic carbon (SOC) dynamics

The latter paragraph leads to the question of which computer models can be used to assess the effect of soil redistribution processes on SOC dynamics. Spatially integrated approaches that link soil redistribution and C dynamics across the landscape are needed to deal with the intrinsic complexity of the key mechanisms (Van Oost et al., 2009b). However, there are only few models that are able to simulate the combination of both mechanisms in a spatially distributed way (e. g. Harden et al., 1999; Liu et al., 2003; Rosenbloom et al., 2001; Van Oost et al., 2005b; Yadav and Malanson, 2009). A detailed overview of all

coupled soil erosion and SOC turnover models is given in Doetterl et al. (2016).

Modelling spatially explicit water-induced soil redistribution can be performed either event based or at greater time steps ( $\geq 1$  year; Doetterl et al., 2016). The former are well suited to model event-based SOC redistribution including C depletion and enrichment processes during detachment, transport, and deposition (e. g. De Roo et al., 1996; Nearing, 1989; Schmidt et al., 1999; Van Oost et al., 2004a). Coupling soil redistribution to SOC turnover models at a larger temporal and spatial scale is in most cases based on Universal Soil Loss Equation (USLE) type models for quantifying water erosion (Wischmeier and Smith, 1978). They only require a relatively small amount of input data that is in most countries available through environmental agencies (Doetterl et al., 2016).

Tillage-induced soil redistribution is simulated as a diffusion-type geomorphological process (Govers et al., 1993, 1994; Quine et al., 1994). The rate of tillage erosion is determined by (i) slope curvature, i. e. the rate of change in slope in the direction of tillage, and (ii), the tillage transport coefficient ( $k_{til}$ ), a constant expressing the erosivity of tillage defined by tillage speed and depth, bulk density, texture, and soil moisture at time of tillage (Van Oost et al., 2006a).

The spatial distribution of SOC due to soil redistribution is then updated with yearly time steps and fed into coupled SOC turnover models (Doetterl et al., 2016). Thereby, the most commonly used SOC turnover models are the Introductory Carbon Balance Model (ICBM) (Andr n and K tterer, 1997), Century (Parton et al., 1987), and RothC (Coleman and Jenkinson, 2014). The main differences of these models lie in the number of C pools defined by different turnover times (two pools in ICBM and multiple pools in Century and RothC) and the use of annual (ICBM) versus monthly input data (Century and RothC; Bolinder et al., 2006; Chappell et al., 2016; Smith et al., 1997). There is one modification of the SOC turnover model RothC that includes a simple (not spatially distributed) soil redistribution parameter and runs at an annual time step (RothCE; Chappell et al., 2016). In general, these models were designed for stable landscapes and changes in soil characteristics due to lateral fluxes were not included (Doetterl et al., 2016). SPEROS-C (Fiener et al., 2015; Van Oost et al., 2005a) is a model that is used to combine soil redistribution and SOC dynamics on arable land (based on ICBM) in a spatially explicit way, with an annual time step, over decadal to centennial time-scales including tillage- and water-induced soil redistribution (Doetterl et al., 2016).

### 2.3 IMPACT OF SOIL REDISTRIBUTION ON CROP YIELDS

The changes in the physical, chemical, and biological properties of soils due to soil redistribution do not only affect SOC turnover and vertical C fluxes but also modify aboveground biomass (AGBM) production of crops (Bakker et al., 2004; Den Biggelaar et al., 2001).

Soil erosion affects the phenological development of crops, and consequently crop yields, via several mechanisms. In general, soil redistribution processes increase the in-field variability of soil properties due to the non-uniform removal and deposition of topsoil. The removal of the fertile topsoil due to erosion leads to a reduction in soil depth when the distance to an impenetrable layer and accompanied rooting depth is reduced. This affects nutrient and water availability as these plant growth limiting factors depend on soil depth. The exposure of subsoil material or the mixing of subsoil into topsoil (by tillage or biological activity) leads to a reduction in soil quality because the subsoil is often poorer in main nutrients (e. g. N and P) and SOC. This also induces changes in soil physical properties such as bulk density, texture, water infiltration and water holding capacity in a way that is unfavourable for crop growth (Den Biggelaar et al., 2001; Van Oost and Bakker, 2012).

Globally, the impact of erosion has been estimated at a 0.4 % reduction in global crop yields per year (FAO, 2019). In contrast, at depositional sites, enhanced crop growth conditions due to the delivery of nutrient-rich eroded topsoil, deeper rooting space, and improved hydrological properties were recorded to result in an increase in crop yields (Heckrath et al., 2005; Kosmas et al., 2001; Papiernik et al., 2005). Therefore, a landscape scale approach is required for capturing the combined effect of erosion and deposition on agronomic productivity (Lal, 2001).

However, the yield-reducing effect of soil erosion varies with climatic conditions and soil properties (Bakker et al., 2004; Den Biggelaar et al., 2001). It is more pronounced in dry years resulting in a more distinct in-field pattern of crop growth and overall lower crop yields compared to years with normal or above-average rainfall (Den Biggelaar et al., 2001; Stadler et al., 2015; Taylor et al., 2003). Relatively shallow soils where root growth is restricted by a compact layer or the parent material (e. g. the soils of the young moraine landscape in Northeast Germany) are more vulnerable to soil erosion effects compared to soils with a relatively deep and uniform topsoil depth (e. g. soils developed on loess or alluvial parent material; Lal, 1998).

There are several concerns arising from the impact of soil redistribution on agronomic productivity. First, the loss of crop yields due to severe water erosion leads to annual costs that are estimated at around € 1 billion for Europe (Panagos et al., 2018). For Germany, 1.7 % of the total agricultural area are estimated to be affected by severe

water erosion leading to an annual productivity loss of 0.14 % (equal to approximately € 50 million; Panagos et al., 2018). As this assessment is only based on water erosion, thereby neglecting tillage erosion, the values can be seen as conservative. Second, the in-field variability and reduction of crop AGBM production due to soil redistribution has a profound impact on SOC sequestration and mineralisation, thereby modifying soil-atmosphere C exchange (Doetterl et al., 2016; Gregorich et al., 1998; Kirkels et al., 2014).

To conclude, the nexus of soil redistribution, net primary production, and SOC dynamics in the context of climate change is a complex feedback system that has to be regarded at broader scales – both temporally and spatially.



## NON-INVERSION CONSERVATION TILLAGE AS AN UNDERESTIMATED DRIVER OF TILLAGE EROSION

---

LENA K. ÖTTL<sup>1</sup>, FLORIAN WILKEN<sup>1</sup>, ALEXANDER HUPFER<sup>1</sup>, MICHAEL SOMMER<sup>2,3</sup>, AND PETER FIENER<sup>1</sup>

<sup>1</sup> *Water and Soil Resource Research, Institute of Geography, University of Augsburg, Augsburg, Germany*

<sup>2</sup> *Landscape Pedology Working Group, Leibniz Centre for Agricultural Landscape Research ZALF e. V., Müncheberg, Germany*

<sup>3</sup> *Institute of Environmental Science and Geography, University of Potsdam, Potsdam, Germany*

This chapter is published with different layout in:

*Scientific Reports* 12.20704, DOI: <https://doi.org/10.1038/s41598-022-24749-7>, 2022

**ABSTRACT.** Tillage erosion is a widely underestimated process initiating soil degradation especially in case of large agricultural fields located in rolling topography. It is often assumed that, conservation, non-inversion tillage causes less tillage erosion than conventional inversion tillage. In this study, tillage erosion was determined on three paired plots comparing non-inversion chisel versus inversion mouldboard tillage. The experiments were performed at three sites in Northeast Germany with gentle, moderate, and steep slope, while tillage depth (0.25 m) and speed ( $\approx 6 \text{ km h}^{-1}$ ) were kept constant during all experiments. The results indicate that non-inversion tillage produces significantly more soil movement compared to inversion tillage. The soil translocation distance was by a factor of 1.3-2.1 larger in case of chisel tillage. The largest difference in translocation distance and  $k_{til}$  was found on the gentle slope exhibiting the lowest soil cohesion. Our results together with an evaluation of tillage transport coefficient ( $k_{til}$ ) values derived from literature and standardised for 0.25 m tillage depth contradict the general assumption that non-inversion tillage reduces tillage erosion. In tillage erosion dominated areas, non-inversion tillage applied with high tillage speed and depth potentially increases tillage erosion and fails its purpose to serve as soil conservation measure.

### 3.1 INTRODUCTION

Soil erosion is a major threat for world's soils (Evans et al., 2020; Montgomery, 2007b) that critically endangers the supply of soil ecosystem services such as food production, biodiversity, carbon storage and water quality (Adhikari and Hartemink, 2016). Soil erosion due to water and wind occurs in natural and human-dominated environments, where especially arable management increases erosion processes due to prolonged times of bare soil following tillage operations. One very effective way of reducing soil erosion on arable land is to reduce tillage intensity and improve residue or mulch cover on soil surfaces (Gao et al., 2016; Klik and Rosner, 2020; Seitz et al., 2018). Typically, this is done via non-inversion mulch tillage (conservation tillage) or direct seeding without tillage (no-till) systems (Lal et al., 2007). At least in Europe no-till does not play a big role, while conservation tillage is increasingly applied due to economic (saving costs of labour and machinery) and ecological benefits (Mal et al., 2015) (e. g. in Germany: at 1 % and 37 % of the arable land no-till and conservation tillage are applied, respectively (Destatis, 2011).

On arable land, another important but less recognised erosion process is tillage erosion, causing substantial down-slope movement of soil. On global scale, it is estimated that tillage erosion equates a fifth of water erosion and twice as much as wind erosion (Quinton et al., 2010). In regions with limited erosive rainfall, tillage erosion can be the dominant soil degradation process (e. g. in Northeast Germany Wilken et al., 2020; Öttl et al., 2021), which takes place wherever soils are tilled on sloped land regardless of climatic conditions. In addition, progressive mechanisation of agriculture since the mid of the twentieth century leads to increasing tillage erosion rates (Van Oost et al., 2006a; Wilken et al., 2020; Winnige, 2004). Tillage erosion is related to slope gradient, where changes in gradient either lead to local soil loss or gain. Furthermore, tillage erosion is driven by the kind of tillage implement (type, shape, and tool size), operational conditions (tillage depth, speed, and direction), field parameters (field size and boundaries), and soil properties (soil texture, soil moisture, and bulk density) (Van Oost et al., 2006a).

As tillage erosion does not lead to off-site effects causing obvious damage in surrounding ecosystems by sediment deposition (along streets, in-streams, etc.) as it is the case for water and wind erosion, the latter receive much higher attention. Determining tillage erosion requires different measuring techniques compared to water and wind erosion, where sediment can be trapped at the 'outlet' of an area under study (Fiener et al., 2019). Assessing tillage erosion can be based on different monitoring techniques such as topographic change (Fiener et al., 2018; Kimaro et al., 2005; Sadowski and Sorge, 2005) or tracers. These tracers are either added before performing individual or a series

of tillage operations (Lobb et al., 1999; Turkelboom et al., 1997; Van Muysen et al., 2000; Zhang and Li, 2011) or in-situ tracers, e. g. fallout radionuclides (Heckrath et al., 2005; Quine et al., 1994; Wilken et al., 2020), are used to estimate long-term erosion rates, which in the latter case account for all erosion processes. An overview and comparison of methods for assessing tillage erosion is given in Fiener et al. (2018).

Compared to water and wind erosion there are hardly any targeted measures to reduce or avoid tillage erosion. No-till practice keeps the soil structure intact and causes minimum soil disruption and translocation (Carter, 2005), and is an effective measure combating water, wind and tillage erosion. However, for much more frequently applied non-inversion tillage, it is not clear if this practice has a reducing effect on tillage erosion. Overall, few studies assessed tillage erosion driven by non-inversion tillage compared to inversion tillage (Govers et al., 1994; Lobb et al., 1999; Marques da Silva and Alexandre, 2004; Mech and Free, 1942; Tiessen et al., 2007). Analysing the published differences in tillage erosion due to inversion tillage and non-inversion tillage indicates that the latter (mostly based on different chisel ploughs) tends to induce smaller erosion rates (Govers et al., 1994; Marques da Silva et al., 2004; Mech and Free, 1942). However, the smaller tillage erosion rate seemed to be often associated with smaller tillage depths in case of chisel plough systems compared to traditional mouldboard ploughing (Van Oost et al., 2006a). Moreover, it is important to note that there are also few studies (Lobb et al., 1999; Tiessen et al., 2007) indicating that non-inversion tillage has even higher tillage erosion rates as compared to inversion tillage, which might be related to higher tillage speeds that are sometimes applied to non-inversion implements (Kietzer, 2007; Lobb et al., 1999).

The aim of this study is to determine differences in tillage erosion intensity between a non-inversion chisel plough and an inversion mouldboard plough on different paired slopes, while keeping tillage speed and depth constant to ensure comparability. It is hypothesised that for the same tillage speed and depth, inversion and non-inversion tillage cause similar tillage erosion rates.

### 3.2 MATERIALS & METHODS

**RESEARCH AREA AND EXPERIMENTAL SITES.** The research area is the “AgroScapeLab Quillow” located approximately 100 km north of Berlin, Germany. It represents a typical ground moraine landscape formed after the retreat of the Weichselian glaciers (ca. 15 ka BP) in Northeast Germany (Lüthgens et al., 2011). The hummocky area is characterized by a hilly topography with short summit-footslope distances (on average 35 m). Due to its undulating topography (mean slope ca.  $7\% \pm 6\%$ ; 74 % of the area with a slope  $> 3\%$ ), large field sizes (mean field size  $13 \text{ ha} \pm 18 \text{ ha}$ ; 2-150 ha) and highly mechanized

arable farming, the region faces severe soil degradation by tillage erosion (Wilken et al., 2020; Öttl et al., 2021). Generally, extremely eroded A-C profiles (Calcaric Regosols) occur at convex knolls and steep slopes. Strongly eroded soils (Nudiargic Luvisols) cover upper slopes and non-eroded soils (Calcic Luvisols) dominate at lower mid-slopes. Footslope areas and closed depressions show colluvial soils (Colluvic Regosols), often influenced by near-surface groundwater (for illustration of soil profiles please refer to Wilken et al., 2020; Öttl et al., 2021). Overall, the spatial distribution of soil types is closely linked to soil redistribution processes and terrain position (Deumlich et al., 2010; Koszinski et al., 2013; Sommer et al., 2008). Soil texture of Ap horizons in the region ranges from loamy sand to sandy clay loam, depending on soils' erosion status. The climate is subcontinental with an average annual air temperature of 9.4 °C and a mean annual precipitation of 466 mm (20-year average 2001-2020, DWD meteorological station at Grünow DWD, 2018a, 2021).

Tillage experiments were performed at three experimental sites managed by the research station of the Leibniz Center for Agricultural Landscape Research (ZALF) in Dedelow (federal state of Brandenburg, Northeast Germany). The sites were selected following a topographic gradient with slopes of 3.5 %, 5.9 %, and 11.8 % (Figure 3.1), which in the following are referred to as gentle, moderate, and steep slope (*GeS*, *MoS*, and *StS*, respectively). Compared to *GeS* and *MoS*, the steepest slope *StS* showed a somewhat more variable soil texture following topography and erosion status. Overall, the topsoils of the *GeS* have a coarser texture ( $d_{50} = 0.093$  mm; 64 % sand, 29 % silt, 7 % clay) than those of the *MoS* ( $d_{50} = 0.077$  mm; 57 % sand, 30 % silt, 13 % clay) and *StS* ( $d_{50} = 0.079$  mm; 55 % sand, 29 % silt, 17 % clay).

**EXPERIMENTAL DESIGN.** The three experimental sites were subdivided in two paired plots with a width of 4 m each and equipped with tracers over a slope length of 50, 60, and 70 m at the *GeS*, *MoS*, and *StS*, respectively (Figure 3.1). To avoid cross-contamination with tracers between the plots, a buffer of 5 m was established between them. Radiofrequency identification transponder glass tags (RFIDs; Smartrac, Avery Dennison, US) with a frequency of 125 kHz, a diameter of 0.4 cm, a length of 2.2 cm, and a density of 2.3-2.5 g cm<sup>-3</sup> were placed regularly within the plots (Figure 3.1). The RFIDs were inserted in three rows per plot with a spacing of 2 m between the rows and 1 m between the RFIDs along the slope in a depth of 0.125 m (half of ploughing depth). This resulted in 150, 180, and 210 RFIDs per plot on the *GeS*, *MoS*, and *StS*, respectively.

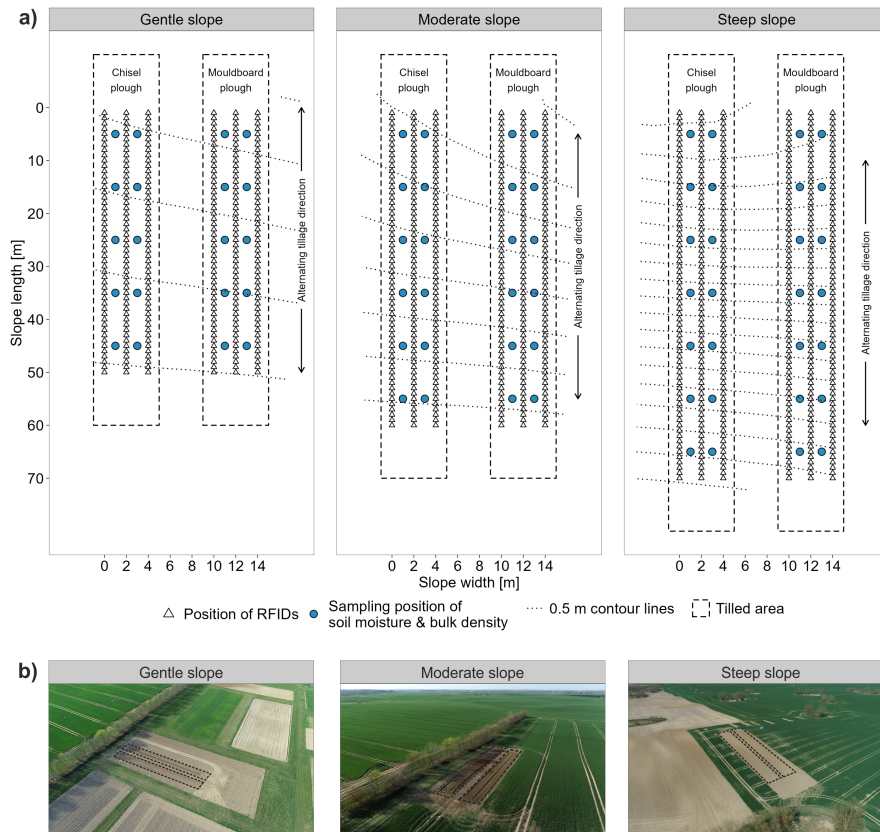


Figure 3.1: (a) Experimental design of the tillage experiments. Separate plots for chisel plough (left) and mouldboard plough (right) tillage next to each other at each of the three experimental sites with gentle, moderate, and steep slope. Three rows of RFIDs (triangles) for each plot with 2 m distance between the rows and 1 m between the RFIDs along the slope. Soil moisture and bulk density were measured in lines between the RFID rows starting after 5 m with 10 m increments (blue dots). Dotted lines indicate contour lines (0.5 m interval). Dashed boxes mark the tilled area, whereby tillage direction was alternating up- and down-slope. Please note the different plot lengths per site. (b) Aerial photos of the experimental sites (black dashed boxes) that are located at  $53.370546^{\circ}$  N  $13.800004^{\circ}$  E (gentle slope),  $53.374694^{\circ}$  N  $13.799799^{\circ}$  E (moderate slope), and  $53.421454^{\circ}$  N  $13.678403^{\circ}$  E (steep slope)

The experiment was carried out during the typical time of tillage in the region end of April 2021. For homogenous starting conditions, all three experimental slopes were prepared with a chisel plough (tillage depth 0.2 m). Tillage experiments on the paired plots were performed with a chisel and a mouldboard plough representing soil conserving, non-inversion and conventional, inversion tillage, respectively, whereby both tillage implements were always followed by a roller (Figure 3.2). Tillage depth was chosen to be 0.25 m for both implements as this is a typical tillage depth in the study area. Both implements tilled alternating five times up- and down-slope per plot (10 times in total). The translocation distance was retrieved from the difference in the coordinates and calculated for left, right, up- and

down-slope direction and the resulting net distance. Results are given in translocation distance per pass, i. e. the measured translocation distance divided by ten.

The compared implements utilised during the experiment are a chisel and mouldboard plough that were operated by tractors of 150 hp. The wing-shared chisel plough (Smaragd, Lemken, Germany; Figure 3.2 a) consists of seven duck feet followed by six discs for crumbling soil clods and a cage roller for re-compaction of the soil. The implement has a working width of 3 m and operated at a tillage speed of 6.4-7.0 km h<sup>-1</sup>. It took two passes next to each other in one direction to cover the full plot width of 4 m. The three-bladed mouldboard plough (Albatros, Raabe, Germany; Figure 3.2 b) has a working width of 1.5 m and was operated at a comparable tillage speed of 6.3-6.5 km h<sup>-1</sup>. It took four passes per direction to cover the full plot width of 4 m. After each complete up- or downward tillage pass over the full plot width a tooth packer roller (Amazone, Germany; Figure 3.2 c) was applied for soil re-compaction.



Figure 3.2: Implements used within tillage experiments: (a) chisel plough, (b) mouldboard plough, and (c) roller.

**DETERMINING SOIL PROPERTIES AND SOIL MOVEMENT.** Soil moisture and bulk density were measured in a regular grid at each of the six plots (Figure 3.1). Soil moisture was measured using a hand-held FDR (frequency domain reflectometry) soil moisture probe (Theta-Probe ML3 Delta-T Devices, UK) shortly before the tillage experiments started. At each measurement position, nine single measurements were taken and averaged. Soil samples for determining bulk density were taken with a liner sampler (set B, Eijkelkamp, Netherlands) that takes an undisturbed soil core of 0.037 m diameter and 0.2 m length. At each measurement position (Figure 3.1), a mixed soil sample of two samples was taken before and after the experiments. Before weighing the soil samples, they were oven dried at 105°C for at least 60 h.

Movement of RFID tags was measured with a detection antenna (Figure 3.3, Rolling Stone, TECTUS, Germany) with a diameter of 0.125 m and a soil penetration depth between 0.20 and 0.25 m. The attached RFID reader indicates a detected transponder via a sound signal and logs the ID number of the detected RFID together with detection time and coordinates. The location of the detected RFIDs is determined using RTK GNSS (real time kinetics global navigation satellite system)

correction. A geostationary base station (Reach RS+, Emlid, China) was set-up over fixed reference points at each slope. The base station sent real-time correction to the GNSS rover (Reach M+, Emlid, China; satellite constellation GPS and GALILEO, frequency 5 Hz) of the RFID detection system to achieve accuracies of about 0.05 m (Zhang et al., 2019). The uncertainty of the RFID position obtained by the GPS measurements was estimated via two approaches. One approach was to insert four RFID transponders per site at locations that are not affected by translocation during the tillage experiments (grass strips nearby each field corner). The position of those RFIDs was measured together with all other RFIDs before and after the experiments. The second approach compares the RTK GNSS coordinates of the RFID detection system against high accuracy total station measurements (TS06plus, Leica Geosystems AG, Switzerland). This comparison was exemplarily done at *MoS*. The comparison focused on potential geo-rectifications that go back to the RTK GNSS measurements. The major advantage of the RFID detection system is that it can be conducted by only one person alone compared to the use of a total station where at least 2 people are needed.

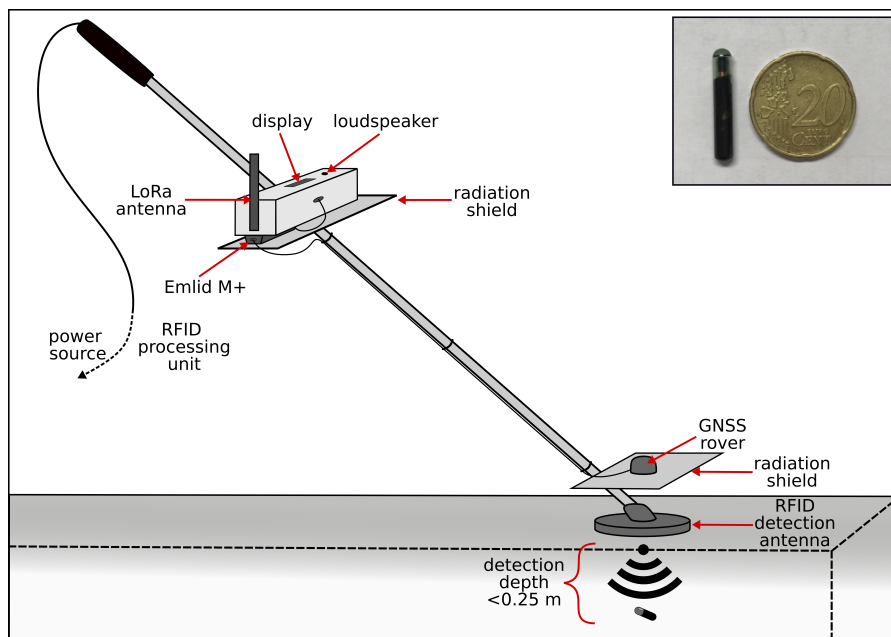


Figure 3.3: Schematic drawing of the RTK GNSS RFID (real time kinetic global navigation satellite system radiofrequency identification) detection and geolocation system. The lower part (direct proximity to soil surface) of the setup consists of an RFID and GNSS antenna, which are located above each other. The upper part consists of the processing unit for RFID identification and RTK GNSS module that communicates with a geostationary base station (not shown) via long-range radio (LoRa) to receive correction data. The inset frame contains a photo of an RFID tag next to a coin acting as scale.

**DATA ANALYSIS.** Initially, a coordinate transformation from UTM to a local coordinate system was applied where plot width is on the x-axis and plot length on the y-axis. Positive values indicate a translocation in upslope direction and negative values a down-slope movement relative to the starting position of the RFID, respectively. To calculate the tillage transport coefficient ( $k_{til}$ ) (as used in many models e. g. WaTEM/SEDEM, SPEROS-C) for all plots and tillage implements, the plots were subdivided into 10 m increments along down-slope direction. Subsequently, mean down-slope transport distances  $\bar{d}_n$  per pass were calculated based on RFID translocation within these segments. Based on the assumption that  $\bar{d}_n$  per segment is proportional to slope (Govers et al., 1994; Tiessen et al., 2007; Van Oost et al., 2006a),  $k_{til}$  was calculated per segment following Eqs. (3.1) and (3.2) according to Govers et al. (1994).

$$\bar{d}_n = bS_n \quad (3.1)$$

$$k_{til} = D\rho_b b \quad (3.2)$$

Thereby,  $b$  is the linear regression slope,  $S_n$  is slope tangent,  $D$  is tillage depth (0.25 m in the experiments), and  $\rho_b$  is bulk density, whereas the mean bulk density is used for all slope increments per slope.

An unpaired two-sample Wilcoxon rank sum test was performed to compare the mean transport distance  $d$  and the mean  $k_{til}$  between the plots. Moreover, this test was used to compare translocation directions (up- vs. downslope and up-/downslope vs. left/right) per implement and between the implements. This non-parametric test is an alternative to the unpaired two-sample t-test that is used when data is not normally distributed (Crawley, 2013). All figures showing data are generated with the R package ggplot2 (Wickham, 2016) and all analysis were performed in RStudio 2021.09.2 with R version 4.1.2 (R Core Team, 2021).

### 3.3 RESULTS

The positional uncertainty of the RFID detection system assessed by the geostationary RFIDs revealed a mean ( $\pm$  one standard deviation) positional error of  $0.1 \pm 0.2$  m, while the mean absolute net translocation distance over all fields was  $2.2 \pm 2.3$  m. A somewhat lower accuracy was shown for the GeS ( $0.17 \pm 0.17$  m), which is likely caused by disturbance originating from a nearby cell tower. For MoS and StS, the accuracy was  $0.05 \pm 0.03$  m and  $0.05 \pm 0.01$  m, respectively. At all test slopes the deviation between the repeated measurements of the geostationary RFIDs was randomly distributed in all spatial directions.

The mean recovery rate for all plots after ten tillage passes was  $66 \pm 11$  %. In general, the recovery rate of the RFIDs was higher for the chisel plough plots (67 %, 73 %, and 76 % for the *GeS*, *MoS*, and *StS*, respectively) compared to the plots tilled by mouldboard plough (53 %, 57 %, and 46 % for the *GeS*, *MoS*, and *StS*, respectively).

As expected, the dominant tillage translocation is in down-slope direction (p-value < 0.01 for the three test sites, respectively; Figures 3.4 and 3.5), whereas in case of the mouldboard plough the movement in tillage direction (up and downslope) is less pronounced due to a sideward movement during soil inversion (p-value < 0.1 for the three test sites, respectively). For all slopes, the variation in RFID transport distance is much higher for chisel plough compared to mouldboard plough (Figure 3.4), which indicates more pronounced soil mixing during tillage operations.

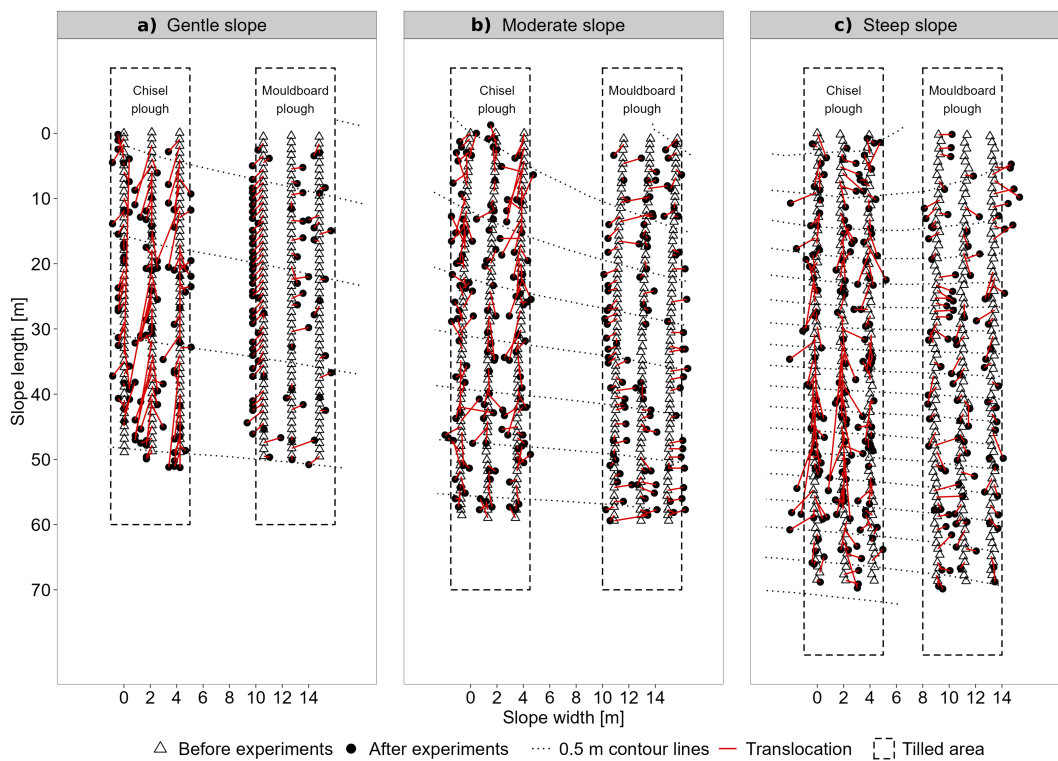


Figure 3.4: Spatial pattern of the position of the RFIDs before (triangles) and after the experiments (black dots) for the three experimental sites with (a) gentle, (b) moderate, and (c) steep slope. Tillage by chisel plough (left) and mouldboard plough (right), respectively. Red lines indicate the net movement of the individual RFID transponders. Dotted lines indicate contour lines (0.5 m interval) of the digital elevation model and dashed boxes mark the tilled area whereby tillage direction was alternating up- and downslope.

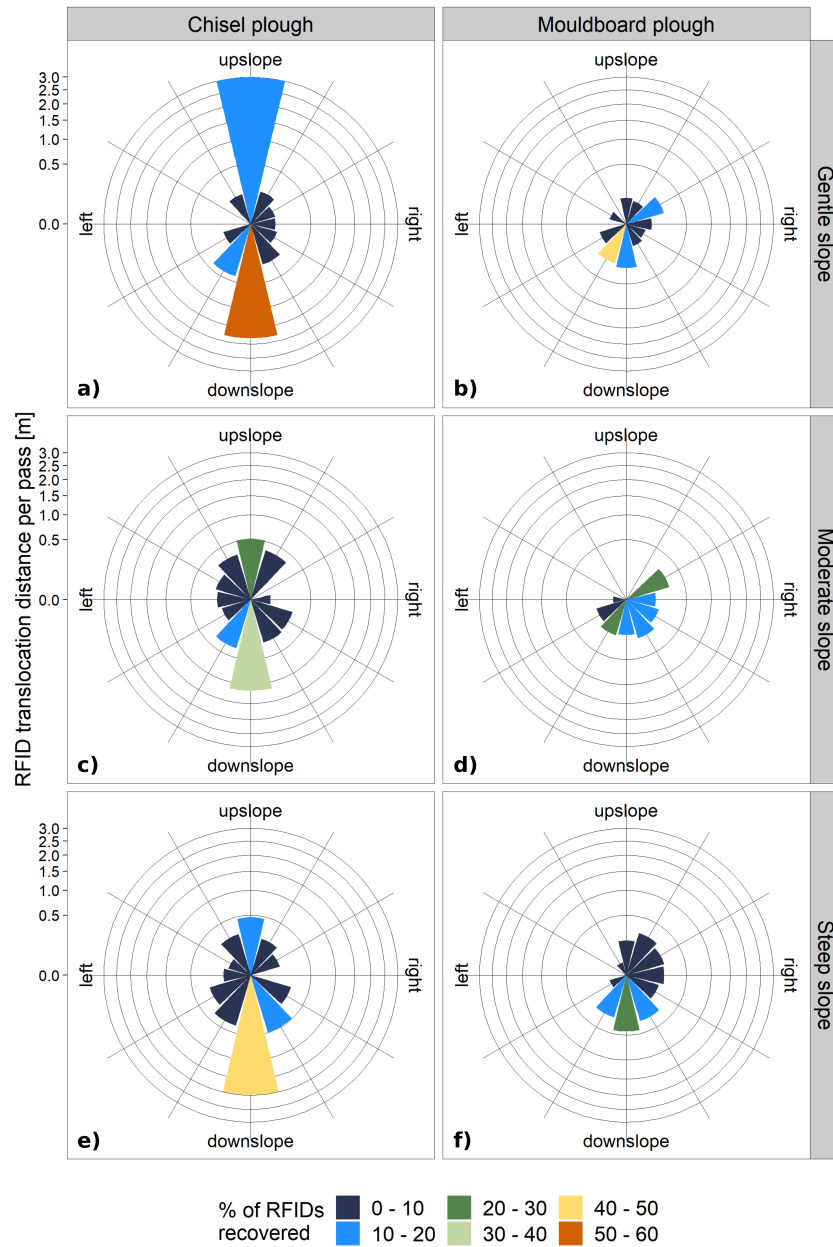


Figure 3.5: Direction and net translocation distance of the RFID translocation per pass [m] for the two tillage implements chisel and mouldboard plough (in columns) and the three experimental sites (a,b) gentle, (c,d) moderate, and (e,f) steep slope (in rows). Colours indicate the percentage of RFIDs from all inserted RFIDs per experimental plot (a-f) that were translocated in each direction (360° divided in 12 segments of 30° each). Direction of translocation is related to the field geometry. Please note that the y-axis is square root transformed, i. e. unequally sized space between axis breaks for a better comparison of chisel and mouldboard plough data.

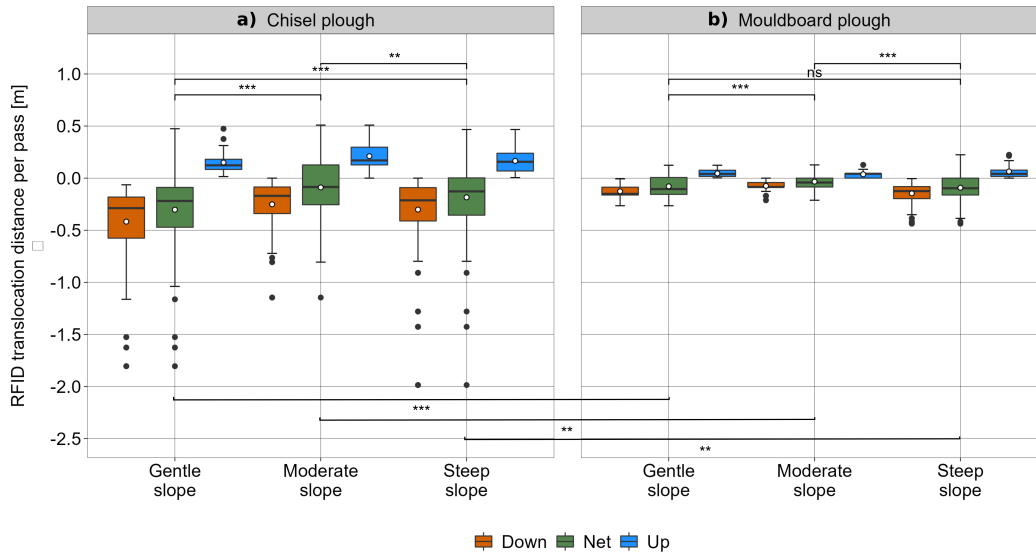


Figure 3.6: Boxplot of the RFID translocation distance per pass [m] for the three experimental sites with gentle, moderate, and steep slope. Comparison of the tillage implements (a) chisel plough and (b) mouldboard plough as well as down-slope (orange), up-slope (blue), and net translocation (green) of the RFIDs. Boxes indicate 1st quartile, median and 3rd quartile, whiskers indicate  $\pm 1.5$  times the inter-quartile range, while dots represent data beyond the end of the whiskers. White circles indicate mean values per boxplot. Stars denote significance levels of the Wilcoxon rank sum test for difference in means (ns: p-value > 0.05, \*: p value < 0.05, \*\*: p value < 0.01, \*\*\*: p value < 0.001).

The chisel plough led to a significantly larger mean down-slope soil translocation indicating a more pronounced tillage erosion effect (Figure 3.6). Overall, the chisel plough led to a 342 %, 270 %, and 200 % larger mean (207 %, 202 %, and 131 % median) net down-slope soil transport as compared to the mouldboard plough for the paired plots on *GeS*, *MoS*, and *StS*, respectively (Figure 3.6). It is interesting to note that differences between chisel plough and mouldboard plough decreased with increasing slope steepness.

Calculating mean  $k_{til}$  values for the different plots and treatments underlines a substantially higher erosion potential of using a chisel plough compared to a mouldboard plough if tillage depth and speed are kept constant (Figure 3.7). As  $k_{til}$  is supposed to be independent from slope (see Equations 3.1 and 3.2), differences for the same implement with similar tillage speed and depth result from differences in soil properties of the plots. Here it is important to note that sandier and especially drier soils at the *GeS* show a higher  $k_{til}$ , which indicates a higher erosion potential, particularly for non-inversion tillage (Table 3.1).

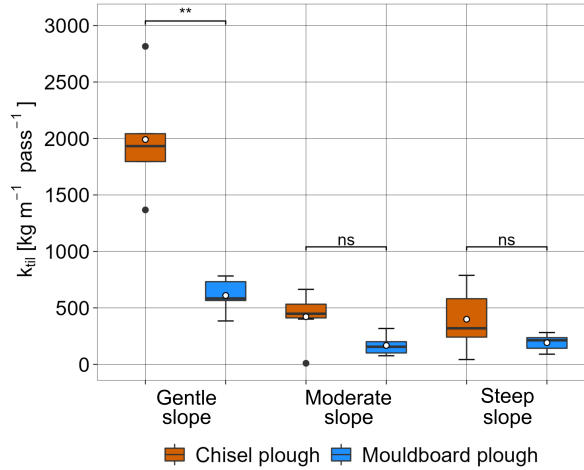


Figure 3.7: Boxplots of  $k_{til}$  [ $\text{kg m}^{-1} \text{ pass}^{-1}$ ] for the three experimental sites with gentle, moderate, and steep slope calculated based on slope segments. Boxes indicate 1st quartile, median and 3rd quartile, whiskers indicate  $\pm 1.5$  times the inter-quartile range, while dots represent data beyond the end of the whiskers. White circles indicate mean values per boxplot. Stars denote significance levels of the Wilcoxon rank sum test for difference in means (ns: p-value  $> 0.05$ , \*: p value  $< 0.05$ , \*\*: p value  $< 0.01$ , \*\*\*: p value  $< 0.001$ ).

Table 3.1: Soil moisture measured before starting the tillage experiments and bulk density measured before and after the experiments.

Experimental site	Sampling positions	Soil moisture per experiment [w-%]	Bulk density [ $\text{kg m}^{-3}$ ]	
Slope	n	Mean ( $\pm$ standard deviation)	Before experiments	After experiments
Gentle ( <i>GeS</i> )	10	11.8 $\pm$ 1.8	1140 $\pm$ 100	1250 $\pm$ 70
Moderate ( <i>MoS</i> )	12	15.8 $\pm$ 1.9	1210 $\pm$ 90	1260 $\pm$ 60
Steep ( <i>StS</i> )	14	16.3 $\pm$ 2.4	1120 $\pm$ 100	1160 $\pm$ 70

### 3.4 DISCUSSION

The direct comparison between inversion mouldboard versus non-inversion chisel tillage is subject to some uncertainties. The sensitivity of tillage speed is potentially higher for chisel plough compared to mouldboard plough due to the design and purpose of the implement. While a mouldboard plough inverts soil by cutting and moving soil perpendicular to the tillage direction, e. g. illustrated in De Alba (2001), chisel tillage induces soil disruption and mixture by stirring soil up and forming a wave-like soil flux. The height and corresponding translocation distance of this wave is controlled by tillage speed. The sensitivity of chisel tillage to speed is also indicated by Van Muysen

et al. (2000), reporting almost a doubling of tillage translocation due to a 20% increase of tillage speed (Table 3.2). To quantify the sensitivity of single tillage implements to tillage speed, a larger set of experiments including different implements, slopes, speeds and depths would be required. In this study, the up- and down-slope tillage speed and depth was kept constant for both implements at all sites (*GeS*, *MoS*, and *StS*). This enabled to focus solely on differences in tillage implements and slope gradients as well as to avoid artificially high down-slope movement. Nevertheless, at *StS*, a minor reduction of upslope tillage speed (upslope speed  $5.5 \text{ km h}^{-1}$  vs. mean speed of experiment  $5.9 \text{ km h}^{-1}$ ) for mouldboard plough was unavoidable due to power limitations of the pulling machinery. Hence, the down-slope translocation at *StS* for mouldboard plough might be slightly overestimated.

However, it is important to note that the speed of chisel tillage was lower compared to typical speeds applied in the region (approx.  $10 \text{ km h}^{-1}$  for mouldboard and  $12 \text{ km h}^{-1}$  for chisel tillage with commonly used big tractors; information from G. Verch, head of the research station). Hence, the differences between inversion and non-inversion tillage found in this study are rather conservative.

Based on the methodological comparison study by Fiener et al. (2018) it was demonstrated that RFID-based transport tracing is in agreement with established approaches based on different tracers (magnetic iron oxide, fluorescent sand, and RFIDs) and topographic change approaches (terrestrial laser scanning, unmanned aerial vehicle-based structure from motion approaches, and changes in soil depths over buried concrete flagstones). The RFIDs showed a similar transport behaviour compared to other macro-tracers like coloured stones (Tiessen et al., 2007) or metal cubes (Van Muysen and Govers, 2002a) used in several earlier studies determining tillage erosion. Hence, in general, the RFID approach is assumed to be suitable to determine soil movement.

The RFID detection system used in this study yielded similar recovery rates as shown in Fiener et al. (2018) for chisel plough (this study: 67-76%; Fiener et al. (2018): 75-79%). It is assumed that the somewhat lower recovery rates in our study are a result of a higher tillage depth, which is close to the detection limit of the antenna (penetrating between 0.20 and 0.25 m into the soil). One could speculate that this leads to a slight overestimation of transport distances as deeper layers of tilled soil horizons might be transported less, while RFIDs moving in these layers are more difficult to locate. However, Fiener et al. (2018) demonstrated that chisel tillage resulted in a mostly homogenous soil mixture within the plough layer based on fluorescent sand.

The mean positional error of the RFID detection system (0.1 m) is an order of magnitude smaller compared to the mean net translocation distance after 10 tillage passes (1.25 m). Although the measured RFID position error did not show any direction, it would result only in a

6.5 % reduction of translocation distances or 14 % reduction of  $k_{til}$ , in case the highest error measured on *GeS* (mean position error = 0.17 m) would have been exclusively occurred in slope direction. However, for translocation assessments of individual tillage passes, the positional accuracy of the RFID detection system might not be sufficient and the use of a total station for RFID positioning is more appropriate.

Table 3.2: Comparison of tillage erosion coefficients ( $k_{til}$ ) for inversion (mouldboard plough) vs. non-inversion (chisel plough) up- and down-slope tillage. The normalized  $k_{til}$  is calculated for a tillage depth of 0.25 m.

Study	Implement	Speed [km h <sup>-1</sup> ]	Depth [m]	$k_{til}$	Normalized $k_{til}$ [kg m <sup>-1</sup> per pass]
<b>Direct comparison of implements</b>					
Govers et al. (1994)	Mouldboard	4.5	0.28	234	209
	Chisel	4.5	0.15	111	185
Kietzer (2007)	Mouldboard	6.0	0.19	138	182
	Chisel	6.1	0.14	250	446
Lobb et al. (1999)	Mouldboard	6.2	0.23	364	396
	Chisel	9.6	0.17	275	404
Marques da Silva et al. (2004)	Mouldboard	3.7	0.39	770	494
	Chisel	3.6	0.11	75	170
	Chisel	3.4	0.19	27	36
Mech and Free (1942)	Mouldboard	3.6	0.08	24	75
	Chisel	3.6	0.06	13	54
Tiessen et al. (2007)	Mouldboard	7.0	0.175	43	62
	Chisel	7.0	0.175	64	92
<b>No direct comparison of implements</b>					
De Alba (2001)	Mouldboard	4.5	0.24	204	213
Gerontidis et al. (2001)	Mouldboard	4.5	0.2	153	191
	Mouldboard	4.5	0.3	383	319
	Mouldboard	4.5	0.4	670	419
Heckrath et al. (2005)	Mouldboard	4.9	0.25	200	200
	Mouldboard	6.3	0.26	335	322
Kosmas et al. (2001)	Mouldboard	4.5	0.18	63	88
	Mouldboard	4.5	0.25	160	160
Lindstrom et al. (1992)	Mouldboard	7.6	0.24	330	344
Lobb et al. (1995)	Mouldboard	4.0	0.15	184	307
Quine and Zhang (2004a)	Mouldboard	5.8	0.22	112	127
Quine et al. (2003)	Mouldboard	7.0	0.17	324	476
Revel and Guiesse (1995)	Mouldboard	6.5	0.27	263	244
Van Muysen and Govers (2002a)	Mouldboard	5.0	0.25	224	224

	Mouldboard	5.4	0.21	169	201
Van Muysen et al. (1999)	Mouldboard	1.8	0.33	245	186
	Mouldboard	2.7	0.15	70	117
Poesen et al. (1997)	Chisel	2.3	0.16	282	441
	Chisel	2.3	0.14	139	248
Quine et al. (1999a)	Chisel	2.2	0.19	657	864
Van Muysen et al. (2002)*	Chisel	5.8	0.15	225	375
	Chisel	7.2	0.2	545	681
Van Muysen and Govers (2002a)	Chisel	6.8	0.069	123	446
<b>Mouldboard</b>	Mean	5.0	0.1	214	342
	CV [%]	47	30	91	72
<b>This study</b>	Mouldboard	5.9	0.25		324
	Chisel	7.1	0.25		1037

Regarding the comparison of the two tillage implements, the hypothesis is falsified that non-inversion chisel plough results in similar tillage erosion as mouldboard ploughing as long as tillage depth and speed are kept constant. This study highlights that tillage erosion by non-inversion chisel tillage substantially exceeds conventional, inversion mouldboard tillage practices by a factor of 1.3-2.1 regarding soil erosion under similar tillage depth and speed. Site specific differences for *GeS*, *MoS*, and *StS* are even higher when  $k_{hil}$  values are compared (factor 2.9-3.5; Figure 3.7). Although the differences in tillage erosion between the implements are not significant at *MoS* and *StS*, especially the difference on the flattest slope (*GeS*) is astonishing (mean net translocation distance of -0.27 m for chisel and -0.08 m for mouldboard tillage). Comparing the  $k_{hil}$  values with literature data shows that  $k_{hil}$  derived for chisel plough is approximately 1.1 times larger as the highest reported values for comparable implements (864 kg m<sup>-1</sup> per pass in Quine et al. (1999a), normalised for 0.25 m tillage depth). The equations used to calculate  $k_{hil}$  (Equations 3.1, 3.2) assume a linear relation between slope and transport distance in case of up- and down-slope tillage (Govers et al., 1994; Lindstrom et al., 1990). However, as the measured transport distances in case of chisel and mouldboard plough on the *GeS* are as high as on the *StS*, they result in very high  $k_{hil}$  values for the *GeS* due to the small slope. In addition, the high translocation distances at the *GeS* are assumed to be driven by weak soil cohesion associated with sandy and dry soils (Kemper and Rosenau, 1984) during the experiment (Table 3.1). However, the effect of soil texture and soil moisture could not be quantified based on the experimental set-up of this study. Nevertheless, our results point at a potential need for further research on the effect of climate change conditions with

\* In the published paper Öttl et al. (2022) the wrong reference “Van Muysen and Govers (2002a)” is given but corrected for this thesis.

longer dry spells during times of tillage operations (Lüttger and Feike, 2018; Reiner mann et al., 2019).

As already mentioned above, in our study, the differences between chisel and mouldboard plough are much higher compared to other studies (Table 3.2). However, normalising the literature values to an equal tillage depth of 0.25 m (using Equation 3.2) leads to non-inversion tillage producing more tillage erosion (+ 42 %; Table 3.2) compared to inversion tillage. This challenges the general idea of non-inversion tillage as a tool for soil conservation, which is only valid as long as tillage depth is substantially lower compared to inversion tillage. Currently, non-inversion tillage becomes more common in agricultural practices (Madarász et al., 2016) due to rising awareness of soils as a limited resource that drives an increasing implementation of soil conservation measures. Among many others, a major benefit of non-inversion minimal tillage is water and wind erosion reduction (Gao et al., 2016; Seitz et al., 2018) as remaining plant residues form protective soil cover (Lal et al., 2007). This study demonstrates that non-inversion conservation tillage calls for substantially lower tillage depth to reduce tillage erosion. However, field sizes increased in developed countries globally over the last 60 years (Lowder et al., 2016), which fosters higher mechanisation that typically goes in hand with big farming structures for efficient, optimised cultivation (Napoli et al., 2020; Sommer et al., 2008). Thereby, powerful machinery allow higher speed and depth of tillage operations, which is increasingly applied to non-inversion tillage practices due to the much lower energy and time demand (larger working width and possible tillage speed; Dumanski et al., 2006; Lal et al., 2007; Madarász et al., 2016). However, the results of this study suggest a critical evaluation of the question if non-inversion tillage can serve as a soil protection measure against the background of individual agroecosystem conditions. It needs to be stressed that an application of non-inversion tillage with high speeds and high tillage depths cannot meet the goals of conservation tillage on rolling topography. In areas like Northeast Germany, where water erosion is about one order of magnitude lower than tillage erosion (Wilken et al., 2020) and non-inversion tillage is getting increasingly applied using big farming machines, the promotion of non-inversion tillage for soil conservation might result in large damage of precious soil systems.

### 3.5 CONCLUSIONS

In this study we determined tillage erosion on paired plots to compare non-inversion chisel versus inversion mouldboard tillage while keeping tillage depth and speed constant. The results indicate that against most literature results, non-inversion tillage produces significantly more soil movement compared to inversion tillage. For the three

tested slopes the translocation distance was by a factor of 1.3 to 2.1 larger in case of chisel tillage. The by far largest translocation distance and also  $k_{til}$  was found on the flattest slope, which showed low soil cohesion due to sandier and drier conditions during the experiment. This indicates an increasing climate sensitivity of tillage erosion in regions where dry soil conditions increase during spring season.

Our findings contradict the general assumption that non-inversion tillage reduces total erosion. This is supported by an analysis of standardised  $k_{til}$  values for different tillage implements of various studies. Especially in tillage erosion dominated areas with large-field farming using chisel tillage at high speeds and depths, calls for a critical evaluation if non-inversion tillage practices can still serve as soil conservation measure.



## TILLAGE EROSION AS AN IMPORTANT DRIVER OF IN-FIELD BIOMASS PATTERNS IN AN INTENSIVELY USED HUMMOCKY LANDSCAPE

---

LENA K. ÖTTL<sup>1</sup>, FLORIAN WILKEN<sup>1,2</sup>, KARL AUERSWALD<sup>3</sup>, MICHAEL SOMMER<sup>4,5</sup>, MARC WEHRHAN<sup>4</sup>, AND PETER FIENER<sup>1</sup>

<sup>1</sup> *Water and Soil Resource Research, Institute of Geography, University of Augsburg, Augsburg, Germany*

<sup>2</sup> *Department of Environmental Systems Science, ETH Zürich, Zürich, Switzerland*

<sup>3</sup> *Aquatic Systems Biology, Technical University of Munich, Freising, Germany*

<sup>4</sup> *Landscape Pedology Working Group, Leibniz Centre for Agricultural Landscape Research ZALF e. V., Müncheberg, Germany*

<sup>5</sup> *Institute of Environmental Science and Geography, University of Potsdam, Potsdam, Germany*

This chapter is published with different layout in:

*Land Degradation & Development* 32.10, pp. 3077-3091,

DOI: <https://doi.org/10.1002/ldr.3968>, 2021

**ABSTRACT.** Tillage erosion causes substantial soil redistribution that can exceed water erosion especially in hummocky landscapes under highly mechanized large field agriculture. Consequently, truncated soil profiles can be found on hill shoulders and top slopes, whereas colluvial material is accumulated at footslopes, in depressions, and along downslope field borders. We tested the hypothesis that soil erosion substantially affects in-field patterns of the enhanced vegetation index (EVI) of different crop types on landscape scale. The interrelation between the EVI (RAPIDEYE satellite data; 5 m spatial resolution) as a proxy for crop biomass and modeled total soil erosion (tillage and water erosion modeled using SPEROS-C) was analyzed for the Quillow catchment (size: 196 km<sup>2</sup>) in Northeast Germany in a wet versus normal year for four crop types (winter wheat, maize, winter rapeseed, winter barley). Our findings clearly indicate that eroded areas had the lowest EVI values, while the highest EVI values were found in depositional areas. The differences in the EVI between erosional and depositional sites are more pronounced in the analyzed normal year. The net effect of total erosion on the EVI compared to areas without pronounced erosion or deposition ranged from -10.2% for maize in the normal year to +3.7% for winter barley in the wet year. Tillage erosion has been identified as an important driver of soil

degradation affecting in-field crop biomass patterns in a hummocky ground moraine landscape. While soil erosion estimates are to be made, more attention should be given toward tillage erosion.

#### 4.1 INTRODUCTION

Soil erosion on arable land is one of the most destructive human perturbations to soil sustainability and food security (Amundson et al., 2015; Zhao et al., 2018). The effect of soil erosion on crop biomass and yields was investigated in a large number of studies (Bakker et al., 2004) that showed a wide range of yield reduction (Den Biggelaar et al., 2003). Even if the different experimental set-ups make it difficult to compare the results of different studies, more or less standardised desurfacing experiments from different continents underline the general tendency that eroded soils lose crop yield potential (Figure 5.1). As most of these artificial experiments were performed on soils without substantial (pre-)erosion, the reduction in crop yields would be even more pronounced in landscapes strongly affected by erosion at the beginning of such experiments.

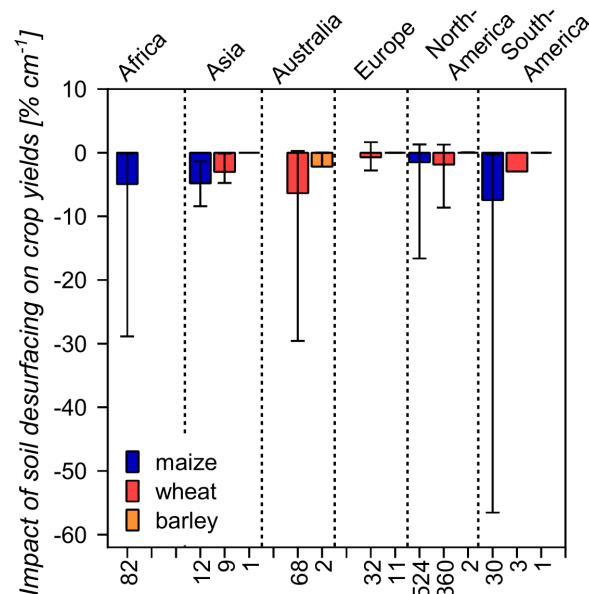


Figure 4.1: Impact of desurfacing on maize, wheat, and barley yields. Data from different continents. Erosion-induced yield effects were calculated relative to the yield of all treatments of the single experiments (18 to 30 cm of topsoil removed) following the methodology of Den Biggelaar et al. (2003). Numbers at x-axis indicate the number of records taken into account for each crop type per continent respectively. Data are taken from the review of Den Biggelaar et al. (2003) and expanded with data from a variety of sources (Allen et al., 2011; Gorji et al., 2008; Izaurralde et al., 2006; Larney et al., 2009; Sui et al., 2009).

The decline in yields at eroded soils can be mainly traced back to a reduction in soil depth and corresponding rooting depth, a reduction in nutrient availability and storage potential, and changes in soil physical properties like porosity, infiltration capacity, and water holding capacity (Den Biggelaar et al., 2001; Herbrich et al., 2018; Lal et al., 1999; Quinton et al., 2010). In contrast to the decrease in yields at eroding sites, the potential increase in yields at depositional sites is less intensively studied. However, several studies indicate that crop yields at depositional sites exceed those at erosional sites (Heckrath et al., 2005; Papiernik et al., 2005; Wehrhan et al., 2016).

In general, tillage leads to a truncation of soil profiles at convexities or upslope field borders, which results in shallower soils and subsequently in an incorporation of subsoil or parent material with poorer physical or chemical properties (De Alba et al., 2004; Gerke and Hierold, 2012). Moreover, subsoil of higher bulk density and missing continuous pore space can be a barrier for root growth (Chirinda et al., 2014; Herbrich et al., 2018; Singh et al., 2019) and, therefore, reduce water and nutrient accessibility. Modified soil properties (e. g. soil organic carbon, clay content, soil moisture) at erosional sites show the strongest effect on crop yields during dry years (Chi et al., 2009; Den Biggelaar et al., 2001; Kravchenko et al., 2005), resulting in a more pronounced in-field variation of crop growth and yields (Stadler et al., 2015; Taylor et al., 2003). The decline of yields at erosional sites is smaller or may even disappear in wet years, as water limitations are less important. In very wet years, yields at erosional sites may exceed those at depositional sites as high groundwater level and resulting oxygen deficiency in closed depressions and lower landscape positions will negatively affect crop growth conditions at depositional sites (Gerke et al., 2016; Kaspar et al., 2004; Martinez-Feria and Basso, 2020). However, this is not or only indirectly related to soil redistribution processes.

Although tillage-induced soil redistribution globally occurs in many areas, its deteriorating effect on soil properties especially affects areas with short summit-footslope distances and relatively shallow soils, which are faced with decreasing yields at hilltops. This has been recognized for the hummocky young moraine landscapes of northern America (Papiernik et al., 2005; Pennock, 2003; Thaler et al., 2021), northern Europe (Heckrath et al., 2005), and Russia (Olson et al., 2002).

Considering different erosion types, tillage erosion is still understudied compared to water and wind erosion (Fiener et al., 2018), although their rates are often in the same order of magnitude or even exceed those of other erosion types (Govers et al., 1996a; Lobb et al., 1995; Schimmack et al., 2002). Nevertheless, their spatial patterns are quite different: Tillage erosion exclusively leads to in-field soil redistribution without off-site damage (Van Oost et al., 2006b). Thereby, soil loss by tillage often occurs at landscape positions where water erosion

is minimal (at convexities, e. g. hilltops), while soil accumulation by tillage takes place at positions where water erosion is maximal (in concavities, e. g. hydrological depressions and thalwegs where overland flow concentrates) (Govers et al., 1999). Moreover, tillage erosion patterns are dominated by the field layouts with highest erosion at the upslope field borders and most deposition at the downslope field borders (Wilken et al., 2017b).

Compared to the large number of studies assessing the effect of erosion on field-scale crop yields (e. g. Lal et al., 2000; Larney et al., 2009), there are only few studies investigating a larger landscape-scale (e. g. Battiston et al., 1987; Thaler et al., 2021). For example, In the young morainic landscape of Ontario, Canada (study area: 90 km<sup>2</sup>), moderate to severely eroded soils (water and wind erosion) led to an average decline in maize yield of ca. 3.6 %, whereby the redistribution and deposition of the eroded material was not considered (Battiston et al., 1987). In the morainic landscape of the midwestern United States ('Corn Belt region'; study area: 210 km<sup>2</sup>), an annual crop yield reduction of  $6 \pm 2$  % due to A-horizon loss was found, which was mainly traced back to tillage erosion (Thaler et al., 2021). However, soil redistribution as a combination of erosion and deposition was not considered, although it is highly relevant for landscape-scale understanding of yield patterns as the negative effects of soil erosion may be partly compensated by positive effects at depositional sites (Govers et al., 2004).

For the comparison of the erosion and biomass patterns on landscape-scale, remote sensing products are required that provide a relatively high spatial resolution (< 10 m) (Wehrhan et al., 2016) and spectral bands that are suitable for crop biomass detection (red and near infrared, NIR) (Gao et al., 2000). Therefore, the spectral properties should be suitable for a rather linear representation of low and high biomass conditions (Huete et al., 2002). The Enhanced Vegetation Index (EVI) has been developed to optimize the sensitivity for the reflectance of high, green biomass and to reduce soil background and atmospheric influences (Huete et al., 1997). Imagery delivered by the RAPIDEYE satellite constellation (5 m spatial resolution; 5.5 day repetition cycle; 5 bands VIS-NIR) (Chander et al., 2013) has been proven to be useful for assessing crop variability (Reichenau et al., 2016; Shang et al., 2015), or to quantify vegetation cover (Rudolph et al., 2015; Shang et al., 2014).

To our knowledge, an investigation of the influence of soil redistribution on crop biomass on landscape scale in Europe has been little documented, although the young moraine landscape of central Europe is highly affected by combined tillage and water erosion (hereinafter referred to as total erosion) (Heinrich et al., 2018). In general, soils in loamy ground moraine landscapes are quite fertile (Sommer et al., 2008) and comprise important crop growth areas. Those soils that developed from glacial till are characterized by relatively shallow

development depths compared to the mostly studied water-erosion prone loess areas and, thus, are more susceptible to a reduction in crop biomass production.

The aims of our study are (a) to compare spatial patterns of modeled tillage and water erosion against the EVI in an intensively used hummocky landscape of North-East Germany, (b) to analyse the impact of soil redistribution on the EVI depending on crop type and differences in seasonal precipitation, and (c) determine the net effect of total soil redistribution on landscape-scale EVI as a proxy for crop biomass.

## 4.2 MATERIALS & METHODS

**STUDY SITE.** The study area is located at ZALF's landscape laboratory 'AgroScapeLab Quillow', which comprises a catchment of approximately 196 km<sup>2</sup> located about 100 km north of Berlin, Germany (Figure 5.2). It represents a typical ground moraine landscape formed after the retreat of the Weichselian glaciers (ca. 15 ka BP) in Northeast Germany (shaded area in Figure 5.2) (Lüthgens et al., 2011). The hummocky area is characterized by a hilly topography with short summit-footslope distances (on average 35 m). Typical for the landscape is the large number of kettle holes, which were formed by melting of dead ice (Anderson, 1998) and only drain via sub-surface flow. These kettle holes can still be filled by water or (degraded) peat. However, many of them are nowadays covered by colluvial material, which resulted from centennial land use as arable land (Van der Meij et al., 2019). The "AgroScapeLab Quillow" is not a typical catchment in a hydrological sense as a large part of the catchment drains into kettle holes, which are only connected to the river Quillow via complex ground water fluxes (Lischeid et al., 2017). The mean slope ( $\pm$  standard deviation) of the study area is about 7% ( $\pm$  6%) with a general west-east elevation gradient (from 165 to 15 m a.s.l.).

Land cover in this area is dominated by arable land and pasture (ca. 70%), followed by wetlands and lakes (ca. 16%), forest (ca. 11%), and settlements (ca. 3%) (Heinrich et al., 2018). Due to its fertile soils, large parts of the catchment are used for agricultural production since Neolithic times (Kappler et al., 2018; Sommer et al., 2008). Since the second half of the 20<sup>th</sup> century, agriculture was intensively mechanised and field sizes were substantially enlarged during the socialistic era of the German Democratic Republic (Bayerl, 2006). Today, the average field size is about 13 ha  $\pm$  18 ha\* (2 to 150 ha). Typical crop types are winter wheat (*Triticum aestivum* L.), winter barley (*Hordeum vulgare* L.), winter rapeseed (*Brassica napus* L.), and maize (*Zea mays* L.). The catchment is characterized by a subcontinental climate with an average annual air temperature of 9.3 °C and a mean annual precipitation of

\* In the published paper Öttl et al. (2021) average field size was given with 22 ha  $\pm$  20 ha, which was recently found to be erroneous and corrected for this thesis.

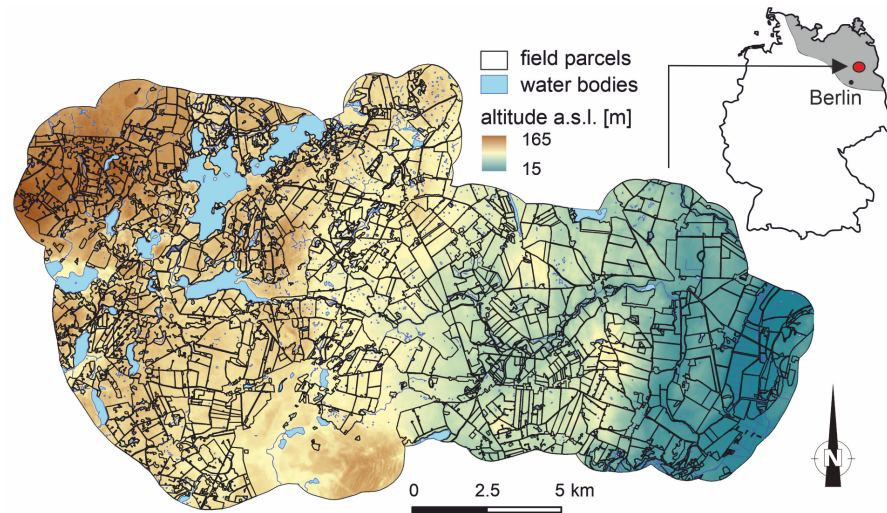


Figure 4.2: The study area 'AgroScapeLab Quillow' is located north of Berlin in the young moraine landscape of Northeast Germany (grey area of inset map).

468 mm (20-year average 1999-2018, DWD meteorological station at Grünow). The average precipitation during the main growing season for wheat and maize is approximately 284 mm (April to September 1999-2018) (DWD, 2018a,b).

The soil pattern of the region (Figure 5.3) is related to topography and the heterogeneity of Pleistocene deposits and has been strongly modified by soil erosion over the past centuries (Deumlich et al., 2010; Koszinski et al., 2013; Sommer et al., 2008). Recently, only 20 % of the arable land shows non-eroded soils (Calcic Luvisols) (IUSS Working Group WRB, 2015), mainly at lower midslopes. Extremely eroded soils (Calcaric Regosols) occur at hilltops, ridges and slope shoulders, while strongly eroded soils (Nudiargic Luvisols) reach from slope shoulders to upper midslopes. Footslopes and closed depressions also comprise approximately 20 % of the landscape. Here, groundwater-influenced colluvial soils (Gleyic-Colluvic Regosols, partly overlying peat) have developed. Generally, the soil landscape reveals strong local gradients in wetness (< 100 m distance) and the soil texture ranges from loamy sand (80 % sand, 15 % silt, 5 % clay) to sandy clay loam (50 % sand, 30 % silt, 20 % clay).

**PATTERNS OF CROP-SPECIFIC EVI/BIOMASS VARIABILITY.** RAPIDEYE satellite images were used to classify crop types and to determine in-field patterns of crop-specific EVI. The RAPIDEYE satellite system consists of five identical satellites and provides 5-band multispectral images on a basis of 5.5 days (at nadir) with a ground sample distance of 6.5 m. The five bands are visible blue (440-510 nm), green (520-590 nm), and red (630-685 nm), red edge (690-730 nm), and near infrared (760-850 nm) (Chander et al., 2013; Planet, 2016). In this



Figure 4.3: Erosion-affected soil pattern in the study area and corresponding exemplary soil profiles: Light colours at top slopes and hill shoulders indicate extremely eroded soils (a: Calcaric Regosols) by tillage erosion; brownish colours represent strongly eroded soils (b: Nudiargic Luvisols) affected by tillage and water erosion; brighter colours at lower midslopes indicate noneroded soils (c: Calcic Luvisols) and dark greyish areas indicate colluvial soils in closed depressions (d: Gleyic-Colluvic Regosols). Soil classification is according to IUSS Working Group WRB (2015).

study, the Level 3A product was used, which is radiometrically and geometrically sensor corrected and resampled to 5 m spatial resolution (Chander et al., 2013). The advantages of the RAPIDEYE satellite images are the relatively high spatial resolution, the short revisiting time and the band-combination that is well suited for crop detection (Kim and Yeom, 2012).

Preprocessing of the RAPIDEYE imagery included atmospheric correction with the algorithm FLAASH (Fast Line-of-sight Atmospheric Analysis of Spectral Hypercubes; Cooley et al., 2002) of the software ENVI. Three cloud-free images in 2010 and 2015 (DOY (day of year) 2010: 168, 192, 266; DOY 2015: 155, 188, 262) were classified in a multi-temporal maximum-likelihood approach with ERDAS Imagine to derive main crop types for further analysis (producer's accuracy in both years > 92.9%; user's accuracy > 86.4%) (ERDAS Inc., 2008; Tso and Mather, 2009). The four main crops used for further analysis accounted for approximately 80% of the arable land in both years. Their proportions in the year 2010 (2015) were 38 (36)% winter wheat, 21 (18)% winter rapeseed, 11 (14)% maize and 8 (9)% winter barley. The remaining area was covered by grassland, sugar beet (*Beta vulgaris* L.), and triticale (*x Triticosecale*) that are not further considered in this study.

To calculate the EVI of winter wheat, winter rapeseed, and maize, the July images from 2010 and 2015 were used (DOY 2010: 192, DOY 2015: 188). For winter barley, the June images were used (DOY 2010: 169, DOY 2015: 155) because it was already partly harvested in July. Both years exhibited a similar overall precipitation before and during the growing season (November 2009-July 2010: 323 mm; November 2014-July 2015: 266 mm; DWD meteorological station at Grünow).

However, there was a distinct difference in precipitation in the main growing season of the winter crops and maize (April – September; 405 mm in 2010; 211 mm in 2015) (DWD, 2018b), which had a substantial effect on crop biomass production in those years. Hence, we further refer to 2010 as a wet year and 2015 as a normal year, respectively.

The use of the EVI is preferred over the most commonly used vegetation index, namely the normalized difference vegetation index (NDVI), for two reasons: The EVI was found to be a good indicator for crop biomass (Jin et al., 2017; Wehrhan et al., 2016) and is more sensitive to high biomass than the NDVI (Huete et al., 2002; Matsushita et al., 2007). The calculation of the EVI (range from 0 ‘no vegetation vitality’ to 1 ‘very high vegetation vitality’) is shown in Equation 5.1 (Huete et al., 2002, 1997).

$$EVI = G \cdot \frac{(NIR - R)}{(NIR + C_1 \cdot R - C_2 \cdot B + L)} \quad (4.1)$$

Where: atmospherically corrected reflectance in the near infrared (NIR), red (R) and blue (B) spectral regions are combined. A gain factor ( $G = 2.5$ ) and empirically derived correction factors are included to remove the soil signal from the mixed soil-vegetation spectral signature ( $L = 1.0$ ) and atmospheric effects ( $C_1 = 6.0$  and  $C_2 = 7.5$ ) (Huete et al., 2002, 1997). As we did not carry out any biomass harvesting during the satellite overpasses, the EVI is used as a relative proxy variable for crop biomass.

The EVI was standardised to the mean and standard deviation of each agricultural field to remove the mean differences between fields and focus on in-field EVI variability (Equation 5.2).

$$EVI_z = \frac{EVI_i - \text{mean}(\sum_{i=1}^n EVI)}{sd(\sum_{i=1}^n EVI)} \quad (4.2)$$

Where: the standardised EVI ( $EVI_z$ ) is the difference of the EVI per grid cell  $i$  and the mean EVI of the grid cells  $n$  of the corresponding agricultural field divided by the standard deviation of the  $n$  EVI values of this field. All spatial analyses were performed using R version 3.6.1 (R Core Team, 2019) and ESRI ARCMAP version 10.5.1 (ESRI, 2017).

**PATTERNS OF SOIL EROSION.** To determine soil erosion patterns, we used the well-established soil erosion and carbon turnover model SPEROS-C that allows calculating spatially explicit soil redistribution due to tillage and water in an annual time-step (Van Oost et al., 2006b). It is important to note here that we focus on the actual erosion pattern and not on the quantification of long-term soil loss or gain due to centuries of erosion. Hence, the underlying assumption is that this pattern is a good proxy for soil erosion and deposition in a region,

which is under arable use for at least 500 years (Kappler et al., 2018; Sommer et al., 2008).

The tillage erosion pattern was calculated based on a diffusion-type equation developed by Govers et al. (1994) (Equation 4.3). The net flux due to tillage ( $Q_{til}$ ) can be written as

$$Q_{til} = -k_{til} \cdot s = -k_{til} \cdot \frac{\partial h}{\partial x} \quad (4.3)$$

Where:  $k_{til}$  is the tillage transport coefficient ( $\text{kg m}^{-1} \text{yr}^{-1}$ ),  $s$  is the local slope (%),  $h$  is the height at a given point of the hillslope (m), and  $x$  is the distance in horizontal direction (m) (Govers et al., 1994). The local tillage-induced erosion or deposition rate tillage-induced soil redistribution ( $E_{til}$ ) ( $\text{kg}^{-2} \text{yr}^{-1}$ ) has been calculated as

$$E_{til} = -\frac{\partial Q_{til}}{\partial x} = k_{til} \cdot \frac{\partial^2 h}{\partial x^2} \quad (4.4)$$

As tillage erosion is governed by the change in slope gradient and not by the slope gradient itself, erosion mainly takes place on convexities and soil accumulates in concavities (Govers et al., 1994; Van Oost et al., 2000). Moreover, erosion and deposition in the region are governed by the edge of kettle holes and, to a lesser extent, field borders (Wilken et al., 2017b).

The tillage transport coefficient  $k_{til}$  depends on the tillage implement, tillage speed, tillage depths, bulk density, texture, and soil moisture at time of tillage (Van Oost et al., 2006b). For our study, we used a constant  $k_{til}$  value of  $350 \text{ kg m}^{-1} \text{yr}^{-1}$ , which was recently determined for this region (Wilken et al., 2020). As tillage transport coefficient ( $k_{til}$ ) only determines the intensity of the calculated erosion rates, the parameterization of  $k_{til}$  is not sensitive to the spatial pattern of tillage translocation. Hence, the absolute erosion rates do not influence the results of the EVI correlation analysis carried out in this study.

The water erosion pattern was calculated according to a slightly modified approach of the Revised Universal Soil Loss Equation (RUSLE) (Renard et al., 1997) described in detail in Van Oost et al. (2000). Erosion, sediment transport, and deposition are based on the local transport capacity  $T_c$  ( $\text{kg m}^{-1} \text{yr}^{-1}$ ), which multiplies the RUSLE factors  $R$ ,  $C$ ,  $K$ ,  $P$  (see Renard et al., 1997), and  $LS_{2D}$  (Desmet and Govers, 1996) with a transport capacity coefficient ( $k_{tc}$ ; m) (Equation 4.5).

$$T_c = k_{tc} \cdot R \cdot C \cdot K \cdot LS_{2D} \cdot P \quad (4.5)$$

The parameterization of the water erosion module follows Wilken et al. (2020) with a  $k_{tc}$  value of 150 m,  $R$  factor of  $450 \text{ MJ mm ha}^{-1} \text{hr}^{-1} \text{yr}^{-1}$ ,  $K$  factor of  $0.027 \text{ Mg ha hr ha}^{-1} \text{MJ}^{-1} \text{mm}^{-1}$ , and  $P$  factor of 1.0 (i. e. no

erosion control practices). The C factor was calculated for a conventional small grain tillage crop rotation that is typical for the study region (Wilken et al., 2018, winter rapeseed – winter wheat – winter barley, cultivated without cover crops). Maize was not considered as it is only relevant in recent crop rotations (Gömann and Kreins, 2012; Vogel et al., 2016). Following the procedure of Schwertmann et al. (1987), this crop rotation resulted in a C factor of 0.081. The  $LS_{2D}$  is a grid cell-specific topographic factor calculated following Desmet and Govers (1996) using the digital elevation model (DEM; derived from airborne laserscanning; original spatial resolution of 1 m resampled to 5 m) (Landesamt für Umwelt & Landesvermessung und Geobasisinformation Brandenburg, 2012).

As most topsoil layers (Ap-horizons) of the study area show a sandy-loam soil texture (e. g. Deumlich et al., 2017), wind erosion is of minor importance (Deumlich et al., 2006). Hence, the spatial pattern of total erosion results from adding up tillage and water erosion per grid cell. In the following, the modeled tillage, water, and total erosion pattern based on SPEROS-C will be referred to as  $E_{til}$ , water-induced soil redistribution ( $E_{wat}$ ), and total soil redistribution due to tillage and water ( $E_{tot}$ ) respectively. To avoid misinterpretations due to mixed pixels along field borders, a 30 m buffer inside each field border was excluded from the analysis. For the same reason, a 15 m buffer around the kettle holes was removed from the data. Note that using buffers at field borders and around kettle holes also means that areas of potentially strong tillage erosion and deposition are excluded. Extremely high erosion or deposition rates of single grid cells often resulting from DEM artefacts or errors in land use classification were also excluded to reduce skewness and meet the requirements for regression analysis (erosion  $> 35$  and  $< -35$  Mg ha<sup>-1</sup>; ca. 0.01 % of the data).

**STATISTICAL ANALYSIS.** Three approaches were performed to analyze the potential effect of soil redistribution on crop biomass: (a) The EVI was related to  $E_{til}$ ,  $E_{wat}$ , and  $E_{tot}$  on a pixel-by-pixel basis for a single field (no. of pixels  $n = 9,290$ ). (b) The standardised EVI ( $EVI_z$ ) was related to  $E_{tot}$  for all fields with the same crop on a pixel-by-pixel basis (no. of pixels: barley  $n \approx 60,000$ , maize  $n \approx 150,000$ , winter rapeseed  $n \approx 220,000$ , winter wheat  $n \approx 800,000$ ). The standardisation was applied to focus on infield variability and reduce between-field variability. (c) To reduce small-scale scattering of the EVI and  $EVI_z$  caused by other influences than soil redistribution, all crop-specific EVI and  $EVI_z$  values were grouped into classes of  $E_{tot}$  and  $E_{til}$  (size of each class: 5 Mg ha<sup>-1</sup> yr<sup>-1</sup>). Subsequently, mean EVI values were calculated per  $E_{tot}$  and  $E_{til}$  class.

The strength of the interrelation between EVI and  $E_{til}$ ,  $E_{wat}$ , or  $E_{tot}$  was calculated using linear and nonlinear regression analysis (polynomials

degree = 1 or 2) and quantified by the adjusted coefficient of determination ( $R^2$ ). The wet and normal year were analyzed separately to identify potential effects of seasonal differences in rainfall on EVI and  $EVI_z$  patterns. Moreover, all analyses were performed for each crop separately. To determine whether two coefficients of determination (and hence slope) differed significantly, we used the test according to Hotelling (1931, 1940) in the case of overlapping pairs of variables (i. e. for the example field data) or according to Fisher (1921) in the case of independent samples (i. e. for the landscape-scale data).

To quantify the net effect of soil redistribution ( $E_{tot}$ ) on the EVI as proxy for biomass production on landscape scale, the differences of EVI at sites of little erosion (-5 to 5  $Mg\ ha^{-1}\ yr^{-1}$ ) taken as baseline and the EVI of all other sites were calculated and averaged per crop. The significance of the net effect was determined using Student's t test or alternatively Wilcoxon rank sum-test when the samples were not normally distributed. All statistical analyses were performed using R version 3.6.1 (R Core Team, 2019).

### 4.3 RESULTS

Analyzing an exemplary field (35 ha) cropped with winter wheat in both years illustrated the similarity between patterns of  $E_{tot}$  and EVI as a proxy for biomass (Figure 5.4). The lowest EVI values were found on hill shoulders and top slopes where most  $E_{til}$  and  $E_{tot}$  occurred, while the highest EVI values were found in the depositional areas (positive  $E_{til}$  and  $E_{tot}$  and partly positive  $E_{wat}$ ). No obvious similarity in pattern between  $E_{wat}$  and EVI can be found, partly because  $E_{wat}$  is substantially smaller than  $E_{til}$ .

Taking a closer look at the general behavior of the relation between EVI and  $E_{til}$ ,  $E_{wat}$ , or  $E_{tot}$  for the exemplary wheat field revealed that a pixel-by-pixel comparison resulted in a highly significant linear regression between EVI and  $E_{til}$  or  $E_{tot}$  in both years ( $R^2 = 0.15 \dots 0.19$ , p value  $< 0.001$ ; Figure 5.5 a,b). This indicated that 15-19 % of the total variation was due to soil redistribution, while the many other reasons for differences in EVI including error contributed 81-85 %. The coefficients of determination for  $E_{wat}$ , although very highly significant, are not given in Figure 5.5 due to the statistically unfavorable, highly skewed distribution of data that mainly resulted from former kettle holes that still caused depressions capturing large amount of sediments. However, the combination of  $E_{wat}$  and  $E_{til}$  in  $E_{tot}$ , which did not have this problem, always had a higher  $R^2$  than  $E_{til}$  alone. The difference, although small due to the much smaller  $E_{wat}$  than  $E_{til}$  rates, was even very highly significant in the wet year according to the Hotelling test. The patterns of  $E_{wat}$  and  $E_{til}$  were almost completely independent ( $R^2 = 0.008$ ) and thus contributed both independently to the EVI patterns. In the normal year, EVI showed much more variability due to soil

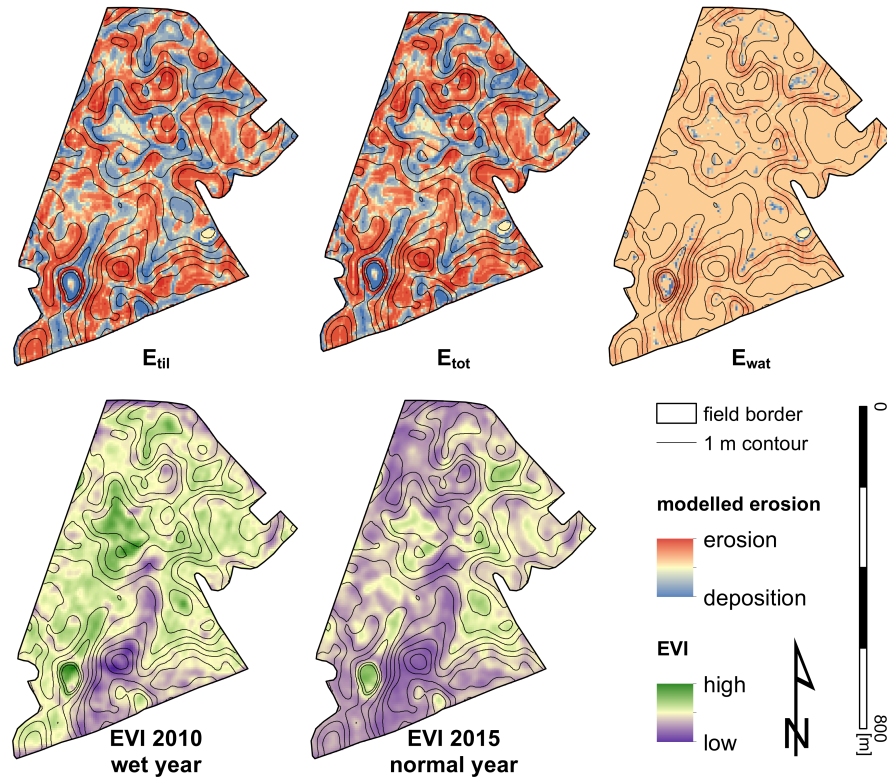


Figure 4.4: Spatial patterns of modeled tillage erosion ( $E_{til}$ ), total erosion ( $E_{tot}$ ), and water erosion ( $E_{wat}$ ) and enhanced vegetation index (EVI) for the wet year 2010 and the normal year 2015 with contour lines of 1 m derived from the digital elevation model (DEM). Results are shown for an exemplary winter wheat field (35 ha, 53.36° N, 13.66° E).

redistribution compared to the wet year, and the relations to  $E_{til}$  and  $E_{tot}$  were highly significantly steeper and closer (p value < 0.001).

Reducing the effects of other causes of EVI variability to extract the influence of  $E_{tot}$  by calculating mean values per soil redistribution classes (Figure 5.5 d,e) revealed that in the wet year, a reduction in the EVI mainly occurred at losses above 10 Mg ha<sup>-1</sup> yr<sup>-1</sup>, while in the normal year, any increase in erosion rate caused a decrease in EVI. In depositional areas, EVI only increased up to a deposition rate of 10 Mg ha<sup>-1</sup> yr<sup>-1</sup>, while higher rates did not increase EVI anymore. The increase in EVI explained by soil redistribution was small in the wet year (difference between the minimum and the flattening was about 0.13 for  $E_{til}$  and 0.15 for  $E_{tot}$ ), while in the normal year, it was substantial (about 0.22 for  $E_{til}$  and 0.26 for  $E_{tot}$ ). Remarkably, the within-field variation of EVI caused by soil redistribution was larger in the normal year than the difference between the wet and the normal year on sites with the lowest soil redistribution rates (0.15 for  $E_{til}$  and  $E_{tot}$ ).

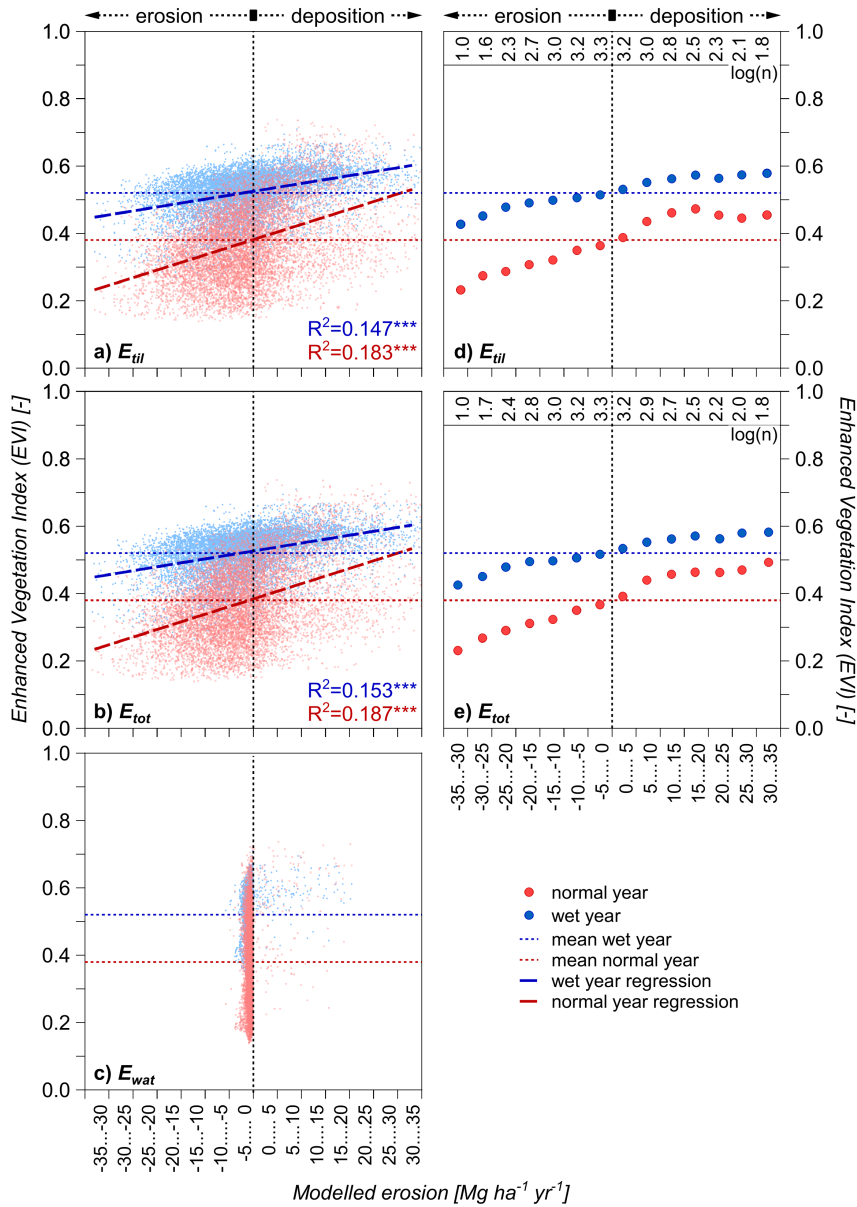


Figure 4.5: Enhanced vegetation index (EVI) versus modeled tillage erosion ( $E_{til}$ , a), total erosion ( $E_{tot}$ , b), and water erosion ( $E_{wat}$ , c) for a single exemplary winter wheat field (also shown in Figure 5.4) in the wet (blue) and normal year (red). The horizontal lines denote the mean EVI in the wet (blue line) and normal year (red line). Left: pixel-by-pixel comparison (no. of pixels  $n=9,290$ ) with dashed lines showing linear regression models. Stars denote the significance level of the adjusted coefficient of determination  $R^2$  (\*p value  $< 0.05$ , \*\*p value  $< 0.01$ , \*\*\*p value  $< 0.001$ ). Right: comparison of mean EVI for  $5 \text{ Mg ha}^{-1} \text{ yr}^{-1}$   $E_{til}$  (d) and  $E_{tot}$  classes (e). The number of values per class is given by the common logarithm of the respective number.

The general behavior of the relation between the EVI and  $E_{tot}$  as well as  $E_{til}$  did not only hold true for the exemplary winter wheat field (Figures 5.4 and 5.5) but was also found when the standardised

EVI ( $EVI_z$ ) of all fields of the entire study area was considered for the different crop types and years (Figure 4.6). As the standardisation removes differences between fields,  $EVI_z$  describes the in-field variability of the EVI. Based on the pixel-by-pixel comparison (Figure 4.6 a-d), the relation between  $E_{tot}$  and  $EVI_z$  could be fairly well described with first- or second-order polynomials. The winter rapeseed  $EVI_z$  had the strongest relation to  $E_{tot}$  ( $R^2 = 0.16$  and  $0.30$  in the wet and normal year, respectively), that is, erosion explained 16 % or even 30 % of the total variation that occurred within many ordinarily farmed fields belonging to different farmers with multiple reasons for variation. The strength of the relation decreased in the order winter wheat, maize, and winter barley. This order was true in the wet and in the normal year, but for winter barley, the effect became very small in the wet year.

Regarding the classified data (Figure 4.6 e-h), the functional relation was sigmoid for winter rapeseed and maize, indicating that very high erosion or deposition rates only caused small additional effects compared to lower rates. For winter wheat, the effect appeared to increase linearly over the entire range. In contrast to the example field shown in Figure 5.5, both years were not separated by a shift, which was an effect of normalizing the data. Nevertheless, the  $EVI_z$  at the erosional sites was significantly lower in the normal than in the wet year for all crops.

The net effect on the landscape scale that results from EVI gains on depositional sites and EVI losses on eroded sites was greatest for maize (based on no. of pixels  $n \approx 150,000$ ) with a reduction of -10.2 % in the wet and -8.5 % in the normal year compared to areas with more or less no erosion and deposition (Figure 4.7). In the wet year, there was nearly no change of the EVI related to  $E_{tot}$  for winter wheat (-1.4 %;  $n \approx 800,000$ ) and winter rapeseed (-0.6 %;  $n \approx 220,000$ ). In these cases, higher EVI values at depositional sites outweighed lower EVI values at erosional sites. However, in the normal year, significant reductions due to  $E_{tot}$  were observed for winter rapeseed (-4.5 %) and winter wheat (-6.4 %). Interestingly, there was a significant increase in the winter barley EVI in the wet year (+3.7 %;  $n \approx 60,000$ ), but no significant influence of  $E_{tot}$  in the normal year (+0.2 %).

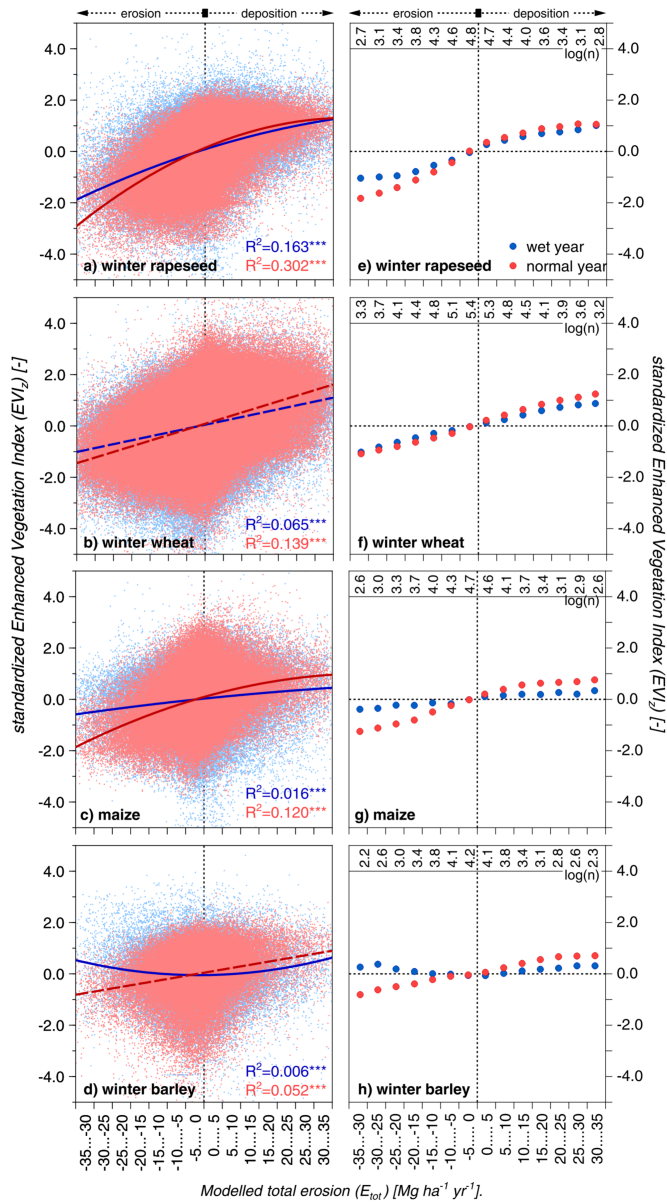


Figure 4.6: Standardized enhanced vegetation index ( $EVI_z$ ) versus modelled total erosion ( $E_{tot}$ ) for the four crop types winter rapeseed (a,  $n \approx 220,000$ ), winter wheat (b,  $n \approx 800,000$ ), maize (c,  $n \approx 150,000$ ), and winter barley (d,  $n \approx 60,000$ ) in the wet (blue) and normal year (red) for the entire study area. Left: pixel-by-pixel comparison with regression lines shown for first- (dashed lines) and second-degree polynomial models (solid lines). Stars denote the significance level of the adjusted coefficient of determination  $R^2$  (\*p value < 0.05, \*\*p value < 0.01, \*\*\*p value < 0.001). Right: comparison of mean  $EVI_z$  for  $5\ Mg\ ha^{-1}\ yr^{-1}$   $E_{tot}$  classes ([e] winter rapeseed, [f] winter wheat, [g] maize, [h] winter barley). The number of values per class is given by the common logarithm of the respective number.

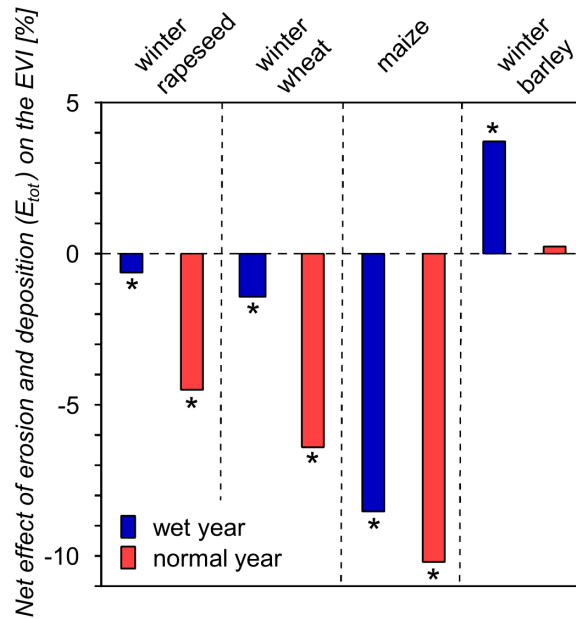


Figure 4.7: Net effect of soil redistribution (modeled total erosion  $E_{tot}$ ) on the enhanced vegetation index (EVI) of the four crop types winter rapeseed, winter wheat, maize, and winter barley in the wet and normal year. Stars denote the significance ( $p$  value  $< 0.001$ ) of the net effect of soil redistribution (zero line; class -5 to 5  $\text{Mg ha}^{-1} \text{yr}^{-1}$ ). Areas affected by soil redistribution vary among crops (45 % for winter wheat, 41 % for maize, 50 % for winter rapeseed, and 54 % for winter barley).

#### 4.4 DISCUSSION

The impact of soil erosion on crop biomass has already been investigated in a large number of studies on field-scale, which is exemplarily shown for more or less standardised desurfacing experiments (Figure 5.1). Although the results vary greatly, a clear decline in yields due to erosion can be seen. In comparison to desurfacing studies, our approach considered real soil redistribution that also included soil deposition on the large scale in the hummocky ground moraine landscape of Northeast Germany. Here, soil redistribution was found to be dominated by tillage erosion that led to in-field variation of the EVI and, hence, biomass patterns. All crops had a lower EVI on eroded sites. Taking depositional sites into account as well, a net reduction effect due to soil redistribution was confirmed for three out of four crop types (Figure 4.7).

**METHODOLOGICAL CONSIDERATIONS.** The regressions between EVI or  $\text{EVI}_z$  and  $E_{tot}$  on a pixel-by-pixel basis were highly significant but had, in some cases, little explanatory power (wet year in Figure 4.6 b-d). This was not surprising because due to the relatively high spatial resolution of the EVI and the calculated total erosion, many

effects influencing crop growth contribute to the total variation. The EVI contained existing small-scale differences in biomass, for example, due to tractor lanes or local differences in management (e. g. fertilization, varieties, pests, management mistakes) and is also sensitive to local environmental differences (e. g. windbreak, shadows, exposition). Other factors causing uneven crop growth are for example short-range (< 1 km) variation in rainfall (Fiener and Auerswald, 2009) and wind erosion. Although wind erosion is relevant for sandy topsoils across Germany, it is more or less negligible for our study area (Deumlich et al., 2006; Sommer et al., 2008). Besides these reasons of true variability, the pixel-by-pixel comparison of different high-resolution products is always confronted with some errors in geo-referencing, which inevitably result in an (unevenly distributed) offset of one or two pixels between the EVI and the DEM. Despite the manifold reasons for growth variability on fields managed by many farmers, it was remarkable that still up to 30 % of the total variability was explained by soil redistribution. This interpretation of a strong erosion effect deteriorating the water capacity of the soils is corroborated by the fact that, in wet years, the influence of erosion decreased.

We can safely assume that most of the erosion-related pattern of EVI was not caused by recent erosion (e. g. due to water losses by runoff) but related to long-term soil truncation and colluviation, which modify important soil properties influencing plant growth and crop biomass (e. g. rooting depth, bulk density, water and nutrient availability, etc.). Nevertheless, the modeled erosion patterns served well as proxy variables for long-term soil truncation or colluviation even though they were based on recent data of soil use valid for the last 60 years (Wilken et al., 2020). Most changes in erosion parameters like rain erosivity, cropping sequence, or tillage intensity, which might have happened, would not change the soil redistribution pattern but only the absolute amount. Thus, they cannot influence our analysis based on the patterns except for two exceptions: First, the relative contribution of water and tillage erosion may change with different parameter values. This influence can be regarded small, given the large absolute difference between both erosion types under recent management. Moreover, increasing tillage intensity also decreases soil cover and thus increases tillage and water erosion simultaneously. Second, the large fields that can be found nowadays were set into practice during the socialistic era and are only about 60 years old (Bayerl, 2006). Before, many more field borders existed, which particularly govern tillage erosion. The influence of historic field borders, as far as it still exists after 60 years, will contribute to the scatter at pixel resolution, while it is eliminated in the classified analysis.

Another pitfall of our proxies would be to neglect other processes that influence EVI and create a similar pattern like  $E_{til}$  and  $E_{wat}$  and, thus, would erroneously be attributed to soil redistribution. There are

mainly two processes that produce similar patterns. One is solifluction during the Pleistocene, which creates a similar pattern as  $E_{til}$ , because its driving principle is identical to that of tillage erosion: during frost, the soil is lifted parallel to the soil surface, but during thawing, it settles back vertically causing a net movement downslope. However, areal soil observations (e. g. Figure 5.3) indicate strong soil translocation and profile truncation, which must have happened after soil genesis and cannot be of Pleistocene origin. The other potential process creating a similar pattern is surface runoff (plus runoff infiltration) or interflow, which causes water deficit in upslope positions and a longer and better water supply in downslope positions. However, lateral water flow should be larger in wet years, while we observed consistently more pronounced patterns in the normal year. An often-used argument is that the potential effect of erosion on crop biomass or yields is just resulting from the coincidence of water erosion and soil moisture patterns modified by lateral fluxes (Heckrath et al., 2005; Moulin et al., 1994; Stone et al., 1985), which has a particular effect in dry years. This does not hold true within this study, as the low precipitation of only 211 mm during the vegetation period in the normal year is not sufficient to cause substantial lateral water flux.

Overall, our findings of tillage erosion being the dominant erosion process in the region are also confirmed by other local studies conducted in the young moraine landscape of Northeast Germany. The dramatic increase of sedimentation rates in kettle holes and at footslopes, which was dated on the second half of the 20<sup>th</sup> century, was related to increasing mechanization of tillage practices (Frielinghaus and Vahrson, 1998; Keller et al., 2019; Li et al., 2002; Van der Meij et al., 2019). Wilken et al. (2020) assessed soil redistribution by tillage and water in a small, representative sub-catchment (ca. 4.2 ha) in the centre of our study area using  $^{239+240}\text{Pu}$  and an inverse modeling analysis. The results showed that soil erosion by water is an order of magnitude lower compared to tillage erosion (Wilken et al., 2020) and, thus, support our findings that tillage erosion and the corresponding patterns in soil properties and plant growth conditions are dominant in this region.

It is important to note that in our study, EVI is only a proxy for crop biomass. However, EVI was already related to crop biomass in other studies. For example, a strong relationship between EVI and fresh biomass of lucerne (*Medicago sativa* L.) was found at a test site in our study area (Wehrhan et al., 2016) and between EVI and winter wheat biomass in China (Jin et al., 2017, 2015). Jin et al. (2015) found an exponential relation of EVI and biomass. Application of this relation to convert our winter wheat EVI (range from 0.2 to 0.7) into biomass would result in a more pronounced effect of total erosion on biomass compared to the effect on the EVI. Although a direct comparison of Jin et al. (2015) with this study is difficult, it indicates that the

relative reduction of the EVI due to soil redistribution is a conservative estimate of the potentially higher reduction of crop biomass.

**RESPONSE OF EVI TO SOIL EROSION PATTERNS.** In general, our analysis of the EVI and  $EVI_z$  revealed that erosion-induced truncation and accumulation had a larger influence on crop biomass in a normal year compared to a wet year. This might be traced back to water limitation due to lower water holding capacity of truncated soil profiles and improvements on colluvial soils. The sigmoidal behaviour at the lower end (high soil losses), which comprised about 2 % of our data, suggests that at this end, most of the soil has already been lost and crops already utilize the unweathered moraine sediments. Once the complete soil is lost, no further decrease in crop growth will occur as long as moraine sediments are still available. The flattening at the upper end (high accumulation rates), which again comprised about 2 % of our data, may indicate that the colluvial material already exceeds effective rooting depth of the crops and an increase did not have further positive effects. The almost linear response function of winter wheat may be caused by an especially large rooting depth (Araki and Iijima, 2001; Fan et al., 2016; Thorup-Kristensen et al., 2009). However, the interpretation of the response functions varying between the crops is difficult because we analyzed only one wet and one normal year. Within the denominations wet and normal, precipitation between months may vary considerably. Given that the temporal course of ontogenesis differs between crops, the specific rain distribution in 2010 or 2015 may have been more favourable for one crop than for the other. The fact that the response of winter rapeseed was strong in the normal and in the wet year, while the response of winter barley was small in both years, suggests that at least some of the differences are crop specific and not due to the specific distribution of precipitation in both years. It is also interesting to note that although winter rapeseed shows the highest in-field variation, maize seems to be the crop type most affected on landscape scale. This might be traced back to the already mentioned differences (e. g. regional precipitation patterns, management, etc.) leading to fields with generally low or high biomass. The underlying reasons for the different behaviour of the crop types are beyond the scope of this study and would require different data and an approach related to yield physiology.

Overall, our analysis showed highly significant relations between soil redistribution and EVI/biomass patterns in a hummocky ground moraine landscape. Similar results were found in the hummocky moraine landscape of Denmark (Heckrath et al., 2005), in the morainic area of Minnesota, North America (Papiernik et al., 2005) or in the young moraine landscape of Ontario, Canada (Battiston et al., 1987). Compared to Battiston et al. (1987) who quantified the yield decline at eroded areas to be -3.6 %, we even found a net effect including the

EVI gains on depositional sites to be -8.5 % in the wet and -10.2 % in the normal year for maize\*. In addition to the net effect, redistribution induces a pronounced heterogeneity that brings about management problems like uneven fertilizer demand or uneven ripening.

Soil redistribution was dominated by tillage, but the effect of water erosion was still detectable. This relation was tighter and steeper in the normal year. In the context of climate change, potentially introducing more dry spells in spring and early summer (Gerstengarbe et al., 2003; Heinrich et al., 2018), the negative effect of soil redistribution on crop biomass might become even more important, especially for winter wheat as the dominant crop type in the studied region. This also holds true for maize, which seems to be the crop type mostly affected by soil redistribution (Figure 4.7). This is particularly critical, as maize has become an important energy crop that is increasingly cultivated (Hoffmann et al., 2018; Peichl et al., 2018; Vogel et al., 2016). In this respect, it is also important to note that these hummocky landscapes, which are highly prone to tillage erosion, cover an area of approximately  $1.8 \times 10^6$  km<sup>2</sup> globally (comparable to the size of Libya or five times the size of Germany), whereby half of it is or was used as arable land (Sommer et al., 2004).

#### 4.5 CONCLUSIONS

Soil redistribution feedbacks on above-ground crop biomass of different crop types were investigated by the comparison of the EVI as a proxy for crop biomass with modeled tillage, water, and total erosion patterns in the hummocky ground moraine landscape of Northeast Germany. The differences in the EVI between erosional and depositional sites were more pronounced in the analyzed normal year compared to the wet year. On average, total erosion patterns explained 6 % of the within-field variation of EVI<sub>Z</sub> in a wet and 15 % in a normal year. It was shown that the erosion-related variation can be much higher for individual fields and for specific crops. Although soil redistribution can lead to beneficial soil properties at depositional areas and hence, to higher EVI/biomass, the net effect of erosion and deposition on the EVI resulted in an average change of -5 % for a normal year. As water erosion only contributed little to the patterns of total soil redistribution in this landscape, tillage erosion was found to be the dominant soil redistribution process in this region. This stresses an urgent need to consider tillage as major soil redistribution process affecting crop biomass production.

---

\* In the published paper Öttl et al. (2021) this sentence is erroneous and was corrected for this thesis. In the publication, the numbers that are visualised in Figure 4.7 were swapped: "... we even found a net effect including the EVI gains on depositional sites to be -10.2 % in the wet and -8.5 % in the normal year for maize."

## TILLAGE EXACERBATES THE VULNERABILITY OF CROPS TO DROUGHT

---

JOHN N. QUINTON<sup>1</sup>, LENA K. ÖTTL<sup>2</sup>, AND PETER FIENER<sup>2</sup>

<sup>1</sup> Lancaster Environment Centre, Lancaster University, Lancaster, UK

<sup>2</sup> Water and Soil Resource Research, Institute of Geography, University of Augsburg, Augsburg, Germany

This chapter is published with different layout in:

*Nature Food* 3, pp. 472-479, DOI: <https://doi.org/10.1038/s43016-022-00533-8>, 2022

**ABSTRACT.** Soils used for crop production cover 15.5 million km<sup>2</sup> and almost all have been tilled at some point in their history. However, it is unclear how the changes in soil depth and soil properties associated with tillage affect crop yields. Here we show that tillage on slopes thins soils and reduces wheat and maize yields. At the landscape scale, tillage erosion gradually reduces crop yields as the duration and intensity of tillage increase. Over the next 50-100 years, the overall yields are likely to further decline as modern mechanised agriculture accelerates the process of tillage erosion compared with centuries of non-mechanised tillage. Arresting this downward trend will require more widespread adoption of no-tillage practices and avoidance of down-slope cultivation. The downward pressure on landscape-scale yields due to tillage erosion is expected to be amplified by climate-change-induced increases in dry spells during crop growth.

### 5.1 INTRODUCTION

Tillage moves substantial amounts of soil down-slope, estimated to be approximately a fifth of that associated with water erosion and over twice the amount globally moved by wind erosion (Quinton et al., 2010). Soils used for crop production cover 15.5 million km<sup>2</sup> and almost all have been tilled at some point in their history, yet the role of tillage in reducing soil depth remains an under-recognized threat to plant production. We also know little about how the changes in soil depth and soil properties associated with tillage affect crop yields and threaten the delivery of the UN Sustainable Development Goals. On sloping land, tillage thins soils on slope convexities and causes soil accumulation in concavities (Figure 5.1, left). Tillage translocation

depends upon the speed and depths of tillage and the implements used, with inversion tillage tending to move more material than non-inversion cultivations (Van Oost et al., 2006a). Only no-tillage systems do not move substantial amounts of soil. Soil translocation by tillage is also affected by soil properties, soil status variables (for example, moisture, consolidation after preceding tillage) and slope gradient, with the greater movement occurring on steeper slopes and where there are changes in slope. In areas with a long history of cultivation, soil redistribution by tillage almost certainly started when the land was first cultivated for agriculture (Figure 5.1, left); however, rates of movement from hand tools and ploughs pulled by animals (Wildemeersch et al., 2014) are much lower than those associated with mechanised agriculture and these rates have accelerated in recent decades as agriculture has intensified and machinery has increased in size and power (Schjønning et al., 2015). As soils become thinner, and if the tillage depth is not reduced, material from the subsoil is mixed with the topsoil and over time the topsoil properties approach those of the subsoil (Figure 5.2). This leads to a reduction in the quality of the A horizon, which contains most of the soil nutrients and biological activity and stores a substantial amount of the water needed for plant growth. In some case soil horizons with physical or chemical properties that are inhospitable for plants approach the surface. Therefore, soils on convexities where soil is lost are shallower, and hence mostly hold less water, are depleted in nutrients and carbon, and have poorer chemical and physical properties. The contrary is true for the concavities where the soil translocated from upslopes is accumulated. Here soil accumulates and is mixed with the existing A horizon, leading to deeper soils that are enriched in nutrients and carbon and able to store greater amounts of plant-available water. However, prolonged landscape erosion might also result in a degradation of topsoils at depositional sites because over time subsoil exposed to the surface at eroded sites will be redistributed to depositional sites (Świtoniak, 2015) (Figure 5.2). Although the question of how erosion affects agricultural production has long been a research topic, there have been only isolated studies on the effects of tillage erosion (citepheckrath:2005). This is surprising because tillage erosion affects all hilly agricultural landscapes, not just those prone to water and wind erosion. Thus, estimates of how tillage erosion affects agricultural yields at the landscape scale, especially under increasing mechanization, are lacking. To illustrate the general problem of erosion and yield loss, we synthesize published information on the impacts of soil thinning on crop productivity. We then utilize soil redistribution and crop growth models to examine the effects of tillage over a landscape, where soils on the convexities lose and those in the concavities gain soil, to see whether the potential gains in crop production due to increased soil depth outweigh the losses due to thinning soils. Next, we examine the potential

future impacts of likely changes in tillage equipment on soils and crop production to 2100. Finally, we discuss the wider implications of these findings for the sustainability of crop production in arable landscapes.

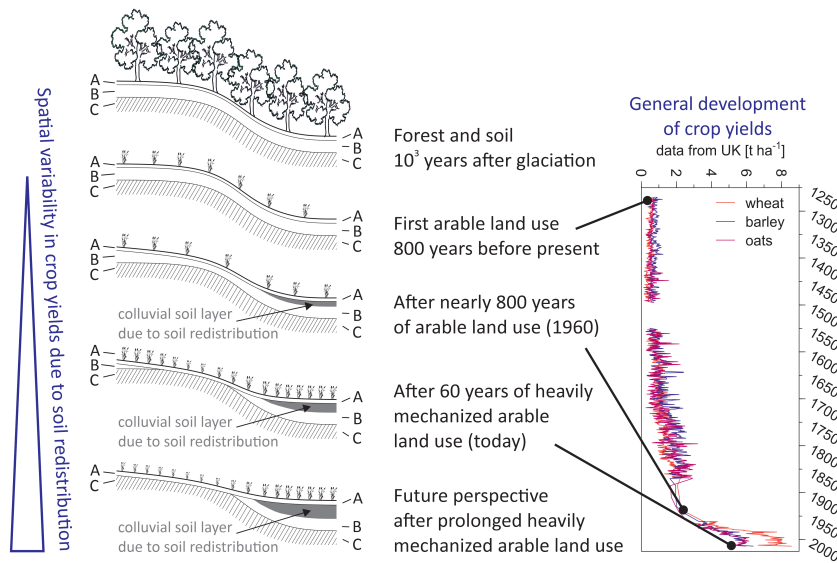


Figure 5.1: Changes in soil properties and crop yields. Schematic illustration of the increase in spatial heterogeneity in soil properties (indicated as change in A, B and C soil horizons) due to (tillage) erosion following conversion from forests to arable affecting heterogeneity in crop yields. The yield effect is masked at the field scale due to the large increase in yields within the later part of the last century. Data illustrating changes in annual yields in Europe are taken from the United Kingdom (Ritchie and Roser, 2013).

## 5.2 METHODS

**MEASURED SOIL LOSS AND YIELDS FROM PLOTS.** To identify relevant data on soil loss or soil truncation on biomass production and yields, we conducted a systematic search of the experimental erosion literature. We focused on soil surface removal plot experiments (often called desurfacing experiments), where yields on plots, typically of the order of a few tens of square metres, without artificial removal of surface soil are compared to treated plots. We used predefined search terms (desurfacing, soil removal, erosion and yield) in the ISI Web of Knowledge and Scopus databases. From the search results we identified two sets of plot studies: (1) studies containing plot data on the extent of desurfacing and its effects on wheat yields, which also contain fertilised and not fertilised areas, allowing a comparison of the effect of surface lowering on yields in high-input versus low-input agricultural systems (Figure 5.3) (Allen et al., 2011; Brunel et al., 2011;

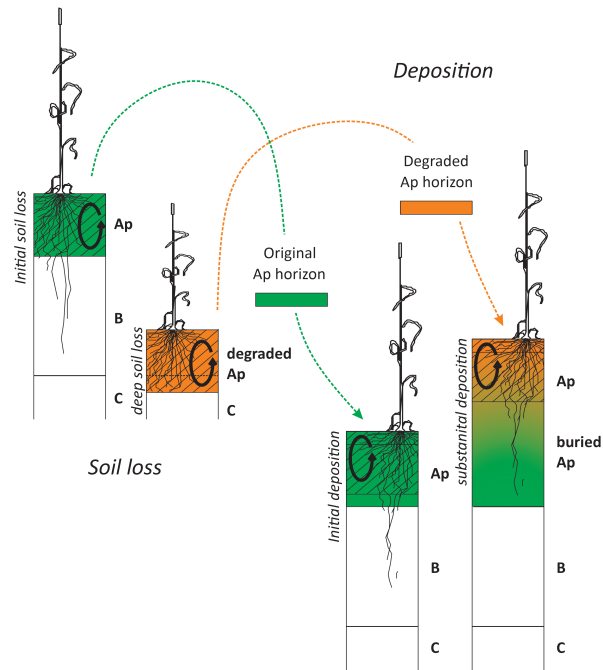


Figure 5.2: The effects of soil loss and deposition on topsoil properties. Schematic illustration of the effects of soil loss and deposition on topsoil properties following initial to long-term soil loss and deposition. Ap, plough horizon; B, mineral horizon; C, parent material of the systematic soil profiles.

Dormaar et al., 1986; Gorji et al., 2008; Izaurralde et al., 2006; Larney et al., 1995; Larney et al., 2009; Masee, 1990; Masee and Waggoner, 1985; Tanaka and Aese, 1989); (2) studies where the relative or absolute reduction of soil thickness was given - here only three studies (Gollany et al., 1992; Rejman et al., 2014; Swan et al., 1987) analysing maize and barley yields were identified.

**MODELLED SOIL REDISTRIBUTION AND BIOMASS FOR LANDSCAPES.** We used well-established modelling tools to illustrate the impact of long-term tillage on crop production in the Quillow catchment representing the Uckermark region (Supplementary Figure 5.8), an area of predominantly arable farming in northern Germany, following a three-step approach: (1) area-specific non-eroded soil profiles modified to represent soil truncation or colluvial deposition were used to model biomass production under different soil erosion conditions with AQUACROP (Steduto et al., 2009); (2) long-term landscape-scale soil redistribution due to tillage was modelled based on the spatially distributed model SPEROS-C (Fiener et al., 2015; Van Oost et al., 2005b); (3) profile-based modelled biomass and modelled spatially distributed soil thinning or thickening due to tillage erosion were then combined to determine overall impacts of soil redistribution by tillage

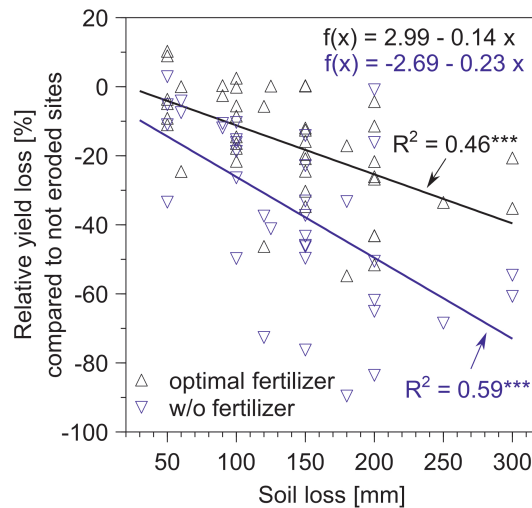


Figure 5.3: Effects of topsoil removal on yields. Effects of removing topsoil on wheat yields under optimal fertilization and no fertilization (Allen et al., 2011; Brunel et al., 2011; Dormaar et al., 1986; Gorji et al., 2008; Izaurrealde et al., 2006; Larney et al., 1995; Larney et al., 2009; Massee, 1990; Massee and Waggoner, 1985; Tanaka and Aese, 1989).

on biomass production on a landscape scale.

**Test catchment.** The Quillow test catchment (196 km<sup>2</sup>) is located about 100 km north of Berlin (Supplementary Figure 5.8). It represents a typical ground moraine landscape, formed after the retreat of the Weichselian glaciers (~15,000 years BP), typically found in large areas of northeastern Germany. The hilly area is characterized by small hummocks and a large number of kettle holes draining via groundwater. The mean slope of the catchment is about 7%. Land use is dominated by arable land (~70%). Due to its fertile soils large parts of the catchment have been used for agricultural production for over 1000 years and some areas since Neolithic times (Kappler et al., 2018; Sommer et al., 2008). Beginning in the 1960s, agriculture was intensively mechanised, and field sizes were substantially enlarged (current mean field size, 22 ha). Crops typically planted are winter wheat (*Triticum aestivum* L.), winter barley (*Hordeum vulgare* L.), rapeseed (*Brassica napus* L.) and maize (*Zea mays* L.). The catchment is characterized by a subcontinental climate with an average annual air temperature of 8.6 °C and a mean annual precipitation of about 500 mm (30 years average, 1981-2010). The average precipitation during the growing season (April-September) is approximately 350 mm (1989-2017) (meteorological data from the Dedelow Experimental Field Station of the Leibniz Centre for Agricultural Landscape Research (ZALF) (53° 36' N, 13° 80' E; Supplementary Figure 5.9). The primary soils developed from

glacial till are Luvisols (IUSS Working Group WRB, 2015), but typical sequences of erosion-affected soils can be found due to the long history of arable land use and the hilly terrain.

Daily soil temperature, global radiation, relative humidity, air temperature, potential evaporation and wind speed between 1992 and 2017 used for modelling were taken from climatic records from the Dedelow Experimental Field Station. Due to the 25 years record a wide range of annual and seasonal climatic variation (especially precipitation; Supplementary Figure 5.9) was used for the modelling. Data for the spatial distribution of the EVI, a proxy variable for biomass production, of winter wheat were derived from RAPIDEYE data in 2010 and 2015 taken from Öttl et al. (2021). Note that 2010 and 2015 represent a 'wet' and a 'normal-to-dry' year regarding precipitation during the growing season (Supplementary Figure 5.9). Topography for use in SPEROS-C is represented by a  $5\text{ m} \times 5\text{ m}$  Lidar-based digital elevation model (Landesamt für Umwelt & Landesvermessung und Geobasisinformation Brandenburg, 2012). Field boundaries are also important for modelling tillage erosion and are taken from an earlier study (Öttl et al., 2021) and represent the situation in 2010.

**Crop modelling.** We assumed that crops were not nutrient limited because farmers used inorganic fertilisers to manage crop nutrition. Therefore, we focused on the impact of soil redistribution on water availability. To simulate crop response to change in water availability in different soils the daily timestep FAO-AQUACROP model (Steduto et al., 2009) was used. The Food and Agriculture Organization offers a menu-driven version of the model and versions suitable for executing without a graphical interface. For this work we used a version of the model designed for use in a geographic information system (GIS) environment (AQUACROP GIS file builder and AQUACROP plugin v.4.0) which allowed multiple runs to be made quickly with different parameter sets. The model is described in detail in Steduto et al. (2009), but in brief it calculates transpiration which is translated into biomass. This is adapted to local conditions using the biomass productivity parameter which is normalized for evaporative demand and air  $\text{CO}_2$  concentration. The crops' response to water is simulated based on water stress and its effect on canopy expansion, stomatal control of transpiration, canopy senescence and the harvest index. Soil water availability is determined for up to five soil layers for which the user specifies characteristics. The model calculates a water balance for each time step based on infiltration, drainage, runoff, root uptake in different layers, deep percolation, evaporation, transpiration and capillary rise.

**Soil data.** The soil component of AQUACROP was parameterized based on three representative soil profiles unaffected by soil loss and

deposition drawn from the database of ZALF, Müncheberg, Germany (Supplementary Table 5.2). These profiles (Calcic Luvisols; IUSS Working Group WRB (2015)) represent about 20% of arable land, while in general the Uckermark soils have been greatly modified by soil erosion over the past centuries (Koszinski et al., 2013; Sommer et al., 2008). The profiles were then combined into one standard profile as follows. Almost all of the pedogenic horizons were the same for the three soils and only differed in their depth and slight textural variation. Therefore, the mean values of depth and sand and clay content were calculated for each horizon. A different approach was required for one of the profiles where two of its horizons did not exist in the other two soils (Bt<sub>3</sub> and Bt<sub>4</sub>). In this case the data for the Bt<sub>3</sub> and Bt<sub>4</sub> horizons were combined with the Bt<sub>2</sub> horizon for that soil to give a new average condition. The mean values for horizon depth and the hydraulic parameters for each horizon used in AQUACROP are given in Supplementary Table 5.3.

The response of crop yield to tillage erosion was simulated based on modifying the standard profiles (Supplementary Tables 5.3 and 5.3) as follows. In the case of deposition, the profile was grown by changing the Ap horizon depth. The properties of the new material were assumed to be the same as that of the existing Ap horizon. In the case of a profile losing soil, the soil was lost from the surface soil and the depth of each horizon, except that at the base of the profile, which extended into the horizon below by an amount corresponding to the eroded depth. The properties of each of the horizons were then recalculated by mixing in the relevant proportion of the horizon below. For example, the loss of 10 mm from the surface of a 100-mm-thick Ap horizon would mean that 10 mm of material from the B horizon was incorporated into the Ap and the properties of the Ap would reflect a mixture of 90% of the original Ap and 10% of the B horizon. New soil profiles representing 1 cm steps of soil thinning and thickening were created for a maximum soil loss and gain of 130 cm, which in case of soil loss would represent a total loss of the A and B horizon. Based on the changes in texture, soil organic carbon and thickness of the new profiles the hydraulic properties (Supplementary Table 5.3) of the new profiles are derived within AQUACROP using standard pedotransfer functions (Saxton et al., 1986). However, it is important to note that moisture content at field capacity and wilting point in the eroded profiles will be somewhat underestimated because the dynamic replacement of soil organic carbon is ignored at the newly created eroded profiles. This will affect plant-available water but not nutrient supply because we assume no nutrient limitation of any of the profiles. Overall, 260 new soil profiles representing different stages of soil thinning and thickening were created and used for modelling biomass production for the different climatic conditions. These new profiles and their crop yields were translated to the entire

test catchment using the modelled spatially distributed soil thinning or thickening based on SPEROS-C (see below).

Crop parameters were drawn from standard AQUACROP files for maize and winter wheat and modified for northern European conditions to reflect planting timings and plant growth curves. To check the performance of modelled crop biomass and yield for maize and winter wheat in the Uckermark, biomass was modelled for the average undisturbed soil profile for the years 1992-2017 and compared with the mean biomass for the region as given in agricultural statistics (see Supplementary Information for more detail). There was no significant difference in wheat yield between the simulated and measured data over the study period; however, simulated maize biomass was an average of 18% lower year-on-year. We concluded that the modelling approach was reasonable as an approach focusing on relative differences in biomass production at different landscape positions.

**Soil redistribution by tillage modelling.** Soil redistribution by tillage was modelled using a diffusion-type equation developed by Govers et al. (1994) as implemented in the spatially distributed model SPEROS-C. Tillage erosion is modelled using equations 5.1 and 5.2 in a spatial context.

$$Q_{til} = -k_{til} \cdot s = -k_{til} \cdot \frac{\partial h}{\partial x} \quad (5.1)$$

where  $Q_{til}$  is the net flux due to tillage,  $k_{til}$  is the tillage transport coefficient ( $\text{kg m}^{-2} \text{ years}^{-1}$ ),  $s$  is the tangent of the local slope gradient (-),  $h$  is the height at a given point of the hillslope (m) and  $x$  is the distance in the horizontal direction (m). The local tillage-induced erosion or deposition rate tillage-induced soil redistribution ( $E_{til}$ ) ( $\text{kg m}^{-2} \text{ years}^{-1}$ ) is been calculated as

$$E_{til} = -\frac{\partial Q_{til}}{\partial x} = k_{til} \cdot \frac{\partial^2 h}{\partial x^2} \quad (5.2)$$

The tillage transport coefficient ( $k_{til}$ ) depends on the tillage implement, tillage speed, tillage depths, bulk density, texture and soil moisture at the time of tillage (Van Oost et al., 2006a). The model calculates sediment redistribution within each field with a raster resolution of  $5 \text{ m} \times 5 \text{ m}$ , which results in data for roughly 5 million raster cells within the Quillow catchment.

While this tillage erosion approach generally leads to reasonable results over several decades as validated against tracer data (Wilken et al., 2020), the modelling over several centuries (necessary to address long-term soil loss and gain) in our test site is associated with large uncertainties. These are mostly associated with missing or only weak parameter values, especially for land use and land management over

such a long time span. Moreover, the change in topography over time is difficult to address. Although it is documented that arable land use started roughly 1000 years BP (Kappler et al., 2018) in the test region, we do not have detailed land-use change or field layout data, or detailed data concerning land management (crop rotations, tillage intensity, and so on) for that long period. Consequently, the uncertainties associated with these unknown details were addressed by taking a simplified approach to parameterization. Topography and field layout were not reconstructed. To avoid artificial results due to a stable digital elevation model, all modelled tillage erosion results were smoothed using a moving average in  $3 \times 3$  raster kernels. Potential erosion patterns associated with the field borders of smaller fields were ignored, as the soil loss and gain patterns along former field borders would be partly erased due to the use of heavy machinery from the 1960s onwards.

To robustly estimate the cumulative tillage erosion, which can be expressed as a cumulative  $k_{till}$  (see yearly  $k_{till}$  in equations 5.1 and 5.2), since cultivation started, we used two independent approaches.

- (1) Based on Kappler et al. (2018), we simply assume that tillage in the entire area used for agriculture today started 1000 years ago. To account for differences in tillage intensity during this long period the  $k_{till}$  value for different time periods was estimated based on (i) earlier erosion tracer ( $^{239+240}\text{Pu}$ ) measurements (Wilken et al., 2020) representing roughly the time from the 1960s to 2015, which were performed within the test site (see super test site in Supplementary Figure 5.8); or (ii) literature values for different kinds of tillage techniques ranging from horse-drawn to mechanised systems (Van Oost et al., 2006a) and the assumption that before 1850 no mechanised tillage occurred. This resulted in a cumulative  $k_{till}$  value of  $186,125 \text{ kg m}^{-1}$  (Supplementary Table 5.1). Assuming that SPEROS-C in general is able to reproduce tillage erosion patterns (Wilken et al., 2020) in the region, this should result in a reasonable soil truncation and colluviation, which, however is associated with relative large uncertainties due to the rough estimates of the model input parameters.
- (2) To achieve more confidence in these results we used a second independent approach using the current remote-sensing-based spatial distribution of biomass production of winter wheat in the test area, in combination with modelled soil loss/deposition-affected biomass. Based on Öttl et al. (2021), the raster cell-specific, EVI-derived, mean biomass of winter wheat for 2010 and 2015 (approximately  $5 \times 10^6$  raster cells) was determined, while using an EVI–biomass relation presented by Jin et al. (2017). The spatially distributed mean biomass was converted into spatially distrib-

uted soil loss and soil gain using the results of the winter wheat modelling for these specific years with AQUACROP, assuming different soil truncation and colluviation (Figure 5.4). Under the assumption that tillage erosion is one of the dominant processes in the variability in soil properties in the region (Van Loo et al., 2017; Wilken et al., 2020), the resulting soil loss and gain map was used to test and calibrate the outputs of SPEROS-C. This was done for eight different erosion and deposition classes by increasing the cumulative  $k_{til}$  in a stepwise fashion so that the number of raster cells per soil erosion class in SPEROS-C aligned with the class derived from the biomass/soil erosion map. The calibration was done for each of the soil erosion classes separately so that a mean optimal cumulative  $k_{til}$  and its standard deviation could be calculated. Keeping the simplified time periods with different  $k_{til}$  values as used in the first approach (Supplementary Table 5.1) with a constant  $k_{til}$  before 1850 ( $150 \text{ kg m}^{-1} \text{ years}^{-1}$ ), the mean time since tillage was introduced could be calculated to additionally test plausibility. Based on the calibration, it could be estimated that tillage started in the region  $\sim 1,073 \pm 299$  years BP (based on modelling from 2015 backwards). This compares well with the results of the first approach and our original assumption of 1000 years BP as the start date for tillage in the region and is in line with the geoarchaeological findings of (Kappler et al., 2018), indicating that substantial agriculturally induced soil erosion in the region did not occur before the beginning of the last millennium.

Given the challenges of modelling soil redistribution by tillage over 1000 years, the similar results of both approaches described give confidence in the robustness of the cumulative tillage erosion modelling. However, to account for at least some uncertainty in the cumulative tillage erosion, all modelled erosion results are always based on the mean calibrated cumulative  $k_{til}$  and its standard deviation (Supplementary Table 5.3). This results in a range of soil truncation and colluvial accumulation as given in Supplementary Figure 5.7.

**Combined biomass and tillage erosion modelling.** Results from tillage erosion and biomass modelling were combined in a GIS. Therefore, the soil loss or gain from the tillage erosion model was classified into 130 thinning and 130 thickening soil profiles as used to determine crop growth based on the modified standard soil profiles with AQUACROP. This resulted in a spatially distributed profile information in a  $5 \text{ m} \times 5 \text{ m}$  raster for the entire test region. For each of the 260 soil profiles the biomass was modelled for winter wheat and maize with AQUACROP for the different years. The results of the biomass modelling were then spatially distributed according to the profiles modelled with SPEROS-C. This coupling allowed the determination of the effects

of tillage erosion on biomass production at a landscape scale, while considering the effect of different seasonal weather conditions and crops. To determine the net effect on biomass production on all fields the results of the combined models were compared with the results from an AQUACROP modelling on the undisturbed standard soil profiles. This combined modelling also allowed the assessment of future effects of soil loss and gain on biomass production for different tillage scenarios for the next 50 and 100 years. These tillage scenarios use  $k_{til}$  values from other studies (Van Oost et al., 2006a) to address future reduced tillage ( $k_{til}=250\text{ kg m}^{-1}\text{ years}^{-1}$ ), intensified tillage ( $k_{til}=1000\text{ kg m}^{-1}\text{ years}^{-1}$ ) or a business-as-usual approach with a  $k_{til}$  of  $500\text{ kg m}^{-1}\text{ years}^{-1}$ . It is important to note that our scenarios are based on 'wet' and 'normal-to-dry' years for the relatively dry region. Hence, the scenarios are somewhat conservative regarding the effect of soil redistribution by tillage on yields because the effects we simulated would be amplified in the case of potentially reduced or more variable rainfall during the growing season.

### 5.3 RESULTS

**TILLAGE EROSION AND CROP PRODUCTIVITY.** Tillage results in reduced plant productivity in those parts of the landscape where the soil thins. Thinning soils have reduced water storage, and, where no fertilisers are applied, lower nutrient availability which leads to lower crop productivity. The negative relationship between soil loss and crop productivity determined at the plot scale by removing topsoil, so-called desurfacing experiments, is well documented and consolidated in several review papers (for example, Zhang et al. (2021)). The effect of soil loss upon biomass production or yield is significantly more pronounced in the case of zero or low fertiliser inputs (Figure 5.3) and therefore poses a significant problem in low-input, subsistence farming systems (Bakker et al., 2004). However, almost all these studies relate the change in crop yield to soil loss, but not to the change in soil depth, which has the potential to be a better predictor. The reduction in soil depth, and the associated ability of the soil to store and supply water to plants, is more important in high-input agricultural systems than the loss of nutrients, which can, at least in the short term, be replaced by fertilization (Larney et al., 2009). The loss of water storage capacity will be most important during prolonged dry spells or periods of drought during the cropping season. In the few experiments (Gollany et al., 1992; Rejman et al., 2014; Swan et al., 1987) which have mechanically removed soil and which have related soil depth to crop yield, there is an indication that the loss in yield is less pronounced than in those which have only measured soil depth reduction (Figure 5.3). However, the relationship is uncertain: the experiments do not encompass situations where, because of soil

thinning, only a little soil is left to be cultivated; nor do they include areas with pronounced drought during the growing period; moreover, the sample sizes are small, with crops limited to barley and maize. The relationship between soil depth and crop production is further complicated due to the properties of soil parent material, which may extend the rooting depth beyond the depth of the soil. For example, weakly consolidated and porous parent materials, such as loess, are penetrated by plant roots to access water. Although deposition of eroded material may cause soils to thicken, and thus, in periods of drought, have higher crop yields than comparable shallower soils there are no standardised plot studies to illustrate this.

At the landscape scale, the response of crop productivity to landscape positions is complex. In Denmark crop yields were lower on slope convexities and higher on concavities and were related to changes in soil phosphorous content (Heckrath et al., 2005), whereas in England the crop response was more complex with locations associated with tillage erosion displaying nutrient depletion and low rates of crop production; however, there were also areas of low production associated with aggrading areas, and no consideration was given to changes in soil depth or to trade-offs between yields where soils are thinning and where they are thickening.

**TILLAGE-INDUCED SOIL REDISTRIBUTION AND LANDSCAPE-SCALE RESPONSE OF CROP PRODUCTIVITY.** To understand the landscape-scale impacts of soil truncation and colluviation due to tillage on biomass production we coupled the well-established crop model AQUACROP (Steduto et al., 2009) and the tillage erosion component of the model SPEROS-C (Fiener et al., 2015). We then applied the model for both wheat and maize in a test region of approximately 200 km<sup>2</sup> in the Uckermark, 100 km north of Berlin, Germany (Supplementary Figure 5.8). This test region was chosen because: (1) it has been used for crop production over the last millennia, with intensive mechanization of agriculture and substantially enlarged field sizes since the 1960s under the German Democratic Republic; (2) it represents a typical ground moraine landscape, found in large areas of Europe and North America, dominated by a rolling topography and soils developed on glacial tills, a highly compacted and difficult-to-root parent material; (3) soil truncation due to tillage erosion is known to be widespread in the area (Wilken et al., 2020; Öttl et al., 2021); and (4) results from earlier studies in the region dealing with different erosion processes (Wilken et al., 2020) and erosion/biomass interactions can be utilized (Öttl et al., 2021).

A series of biomass/soil-depth responses for the period 1964-2017 were produced using the AQUACROP model driven by soil properties generated by mixing an average non-eroded profile from the region

(soil depths to C horizon, 1.4 m) following the loss or gain of soil at the surface and measured climate data.

There was a strong interaction between climate and the yield/soil-depth response. In wet years, when plant water is plentiful, there is a smaller difference in biomass production between shallow and deeper soils (Figure 5.4, left) than in a dry year, when crops rely on water stored in the soil profile and the difference in biomass production between thinning and thickening soils is amplified (Figure 5.4, left). Modelled reduction in yield started earlier with soil truncation in the case of winter wheat as compared to maize, but maize biomass immediately fell if soil thickness dropped below about 0.75 m. At depositional sites modelled winter wheat biomass profited from deeper soils, while this was not the case for maize. This general behaviour was also found when comparing remote-sensing-derived biomass proxy variables (Enhanced Vegetation Index, EVI) with patterns of modelled tillage erosion classes (Figure 5.4, right).

The yield information resulting from the AQUACROP modelling of different soil profiles was extended across the landscape using SPEROS-C to model the spatially distributed tillage-induced soil thinning and thickening for about the last 1000 years. To achieve this, low values of tillage intensity for the first 940 years and much higher values for the last approximately 60 years were assumed, and the latter were calibrated against soil redistribution patterns derived from radio-nuclide data of a small sub-catchment (Wilken et al., 2020) (Supplementary Figure 5.8). Soil redistribution due to tillage lowered overall simulated biomass production in a 'normal-to-dry' year (Figure 5.4) from 215,000 t to 202,000 t for wheat, and from 276,000 t to 269,000 t for maize. In a wetter year yield reductions were lower with 317,000 t of wheat and 415,000 t of maize reduced to 308,000 t or 411,000 t, respectively (Figure 5.5).

**FUTURE PRODUCTION.** Agricultural production has been possible in the Uckermark for at least 1000 years. Our modelling results suggest that by continuing to till the Uckermark soils, mean yields on the landscape scale will continue to decline and that this decline increases with tillage intensity and reduced water availability (Figure 5.5). In 50 years, we expect reductions in normal-to-dry years winter wheat biomass of between 6.6 % and 7.1 %, depending on the intensity of tillage (see Figure 5.5 for scenarios). These differences increase to between 8 % and 10 % at 100 years. Maize biomass was less affected in normal-to-dry years, with reductions of between 3.1 % and 4.0 % for the 50 years time horizon and 3.9 % to 5.9 % at 100 years in the future. In wet years reductions were smaller at between 3.3 % and 4.4 % for wheat and between 1.1 % and 1.9 % for maize for the 50 years scenario, whereas for the 100 years scenarios, reductions are between 4.3 % and 5.9 % for wheat and between 1.9 % and 3.2 % for maize.

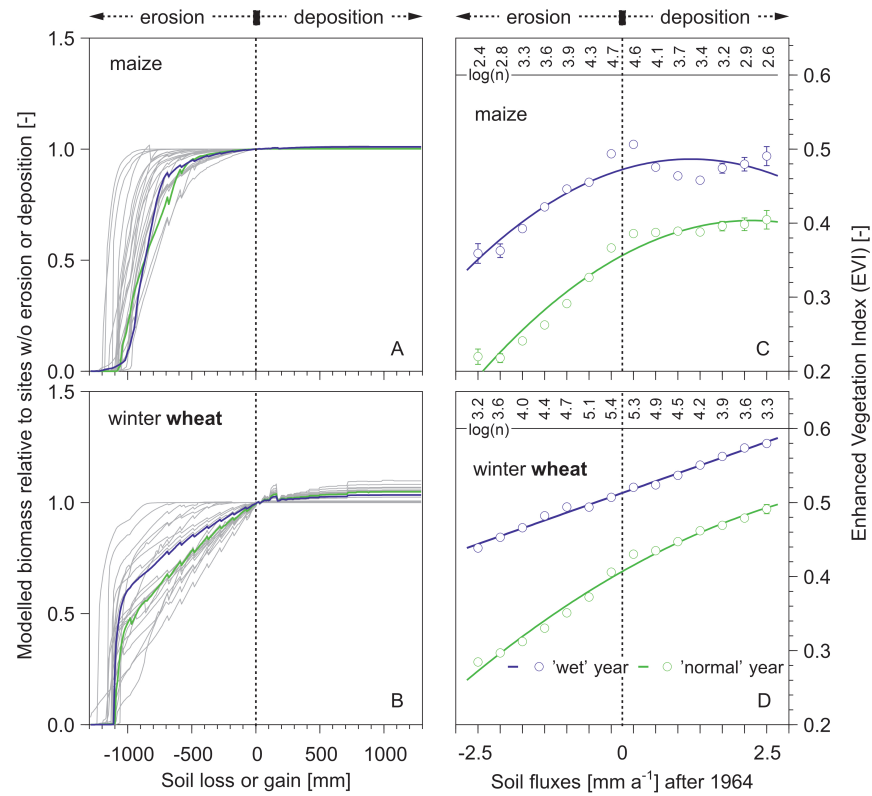


Figure 5.4: Modelled biomass production and EVI. a,b, AQUACROP-modelled biomass production of maize (a) and winter wheat (b) depending on soil loss and gain. Grey lines result from the different climate between 1992 and 2017, while the blue and green lines represent a 'wet' and 'normal to dry' year used for further analysis. Data are given as relative biomass from profiles with no soil erosion or deposition as 1. c,d, Mean EVI as a proxy variable for biomass in different classes of modelled tillage-erosion-induced soil fluxes for maize (c) and winter wheat (d). The EVI was derived from RAPIDEYE satellite images from 2010 and 2015 (bands in the visible–near infrared spectrum; resolution,  $5 \times 5 \text{ m}^2$ ). The tillage erosion modelling and the EVI analysis are described in detail in Öttl et al. (2021). Note that the modelled soil fluxes are aggregated in classes and are only indicators of soil truncation and/or colluvial deposition because the duration of tillage erosion was not analysed.  $n$ , number of pixels analysed per soil erosion class; error bars indicate 95 % confidence intervals of EVI within each class.

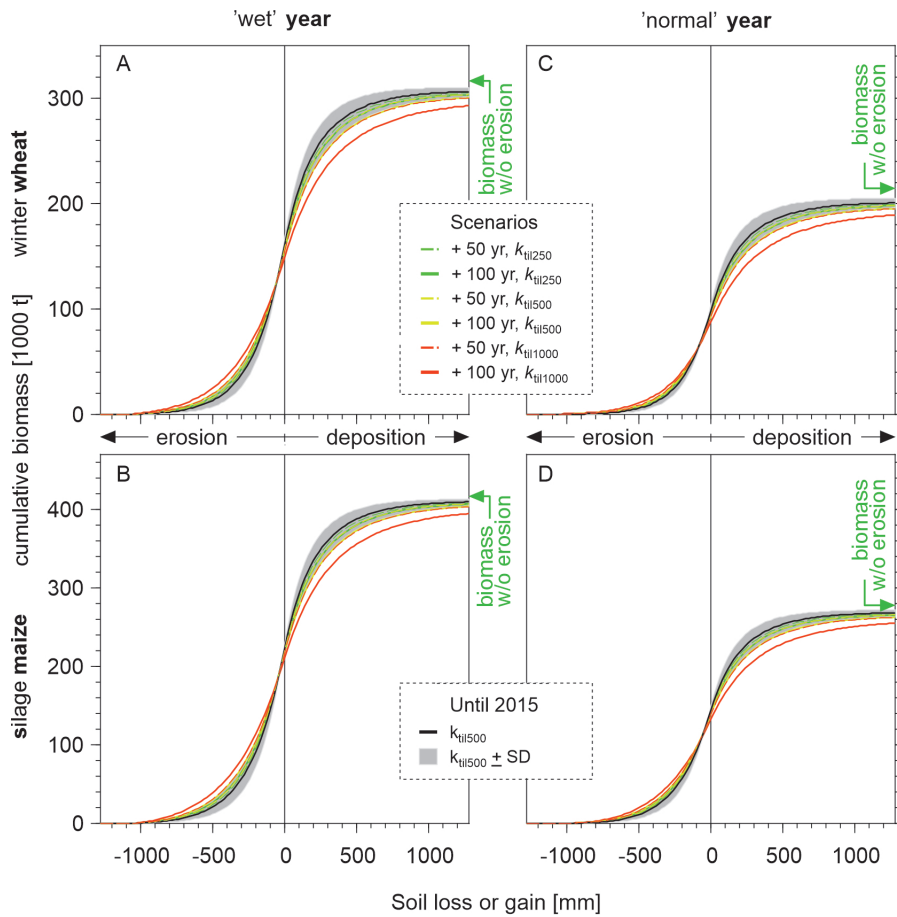


Figure 5.5: Changes in modelled cumulative landscape-scale biomass production. a-d, Changes in modelled cumulative landscape-scale biomass production for different tillage scenarios for 'wet' (a,b) and 'normal-to-dry' years (c,d) for winter wheat (a,c) and silage maize (b,d). Definitions of years are given in the Supplementary Information. The bold black lines indicate the actual mean with grey shaded areas giving the uncertainty of the results ( $\pm 1$  s.d. of modelled mean soil loss or gain). The coloured lines indicate six scenarios for 50 and 100 years of additional tillage, with reduced tillage (green), tillage equal to the mean of the last 50 years (yellow), and increased tillage representing the use of heavier and faster machines (red). The tillage intensity of the different scenarios is given as the tillage coefficient  $k_{til}$  of 250, 500, and 1000 used in SPEROS-C. The green arrows on the right side of the panels indicate modelled cumulative biomass without soil loss or deposition. Note: increasing soil loss leads to decreasing biomass production but the cumulative biomass production of erosional sites (as given in the figure) increases as the area affected by soil loss is increasing.

#### 5.4 DISCUSSION

The reviewed desurfacing experiments illustrated, as expected, the negative effect of soil loss on crop yields (Figure 5.3). Experiments that add topsoil to plots to test potential positive yield effects (Masse and Waggoner, 1985) are much rarer. Therefore, even if these plot experiments give a first indication, it is difficult to use them to understand the effect of soil redistribution on crop yields at the landscape scale. To overcome this, studies have determined soil loss and deposition using radionuclide erosion tracers, such as  $^{137}\text{Cs}$ , associated with atomic weapons testing, and compared them with yield data (Heckrath et al., 2005; Yang et al., 2019). However, such tracer-based approaches miss the long-term effect associated with centuries to millennia of soil loss and gain as they only focus on the last approximately 70 years to explain spatial distributed yield effects. They are also, mostly, limited to small test sites as the effort required for soil sampling and analysis is substantial. Our modelling approach allows a much longer perspective, focusing on soil loss or gain since start of cultivation in the test region roughly 1000 years ago. Obviously, modelling land management over such a long time span is challenging and model parameterization requires a number of assumptions, such as the historical tillage intensity (see Supplementary Information for a discussion of uncertainty). However, as we were interested in relative changes in spatial variability of crop biomass production following soil redistribution, which we know to be important for the test area (Öttl et al., 2021), we are confident that our parsimonious model system is robust enough to illustrate the general problem associated with tillage erosion in regions only slightly affected by other erosion processes (Wilken et al., 2020).

Our modelled landscape-scale yield losses suggest that deeper soils in depositional environments at least partly compensate for yield losses in erosional settings and that agricultural production is likely to continue in the Uckermark. Tillage erosion reduced landscape-scale yield potential, but yields did not collapse. As in other empirical studies focusing on erosion since the 1960s (Heckrath et al., 2005), the significant differences in soil properties in eroded or depositional environments resulted in differences in crop yield, with the lowest yields on the hillslopes and the highest in the valley bottoms. The lack of a major decline on yields may be because the area with more than 0.3 m soil loss, resulting in a substantial yield loss (Figure 5.4, left), is relatively small in our test region. Our findings are similar to results from a smaller catchment in Turkey (Van Loo et al., 2017). In that study soil truncation was modelled along with its potential yield effects on winter barley for a mountainous catchment in the Mediterranean region over a period of 4,000 years, with catchment-scale crop yields estimated to drop by 22 % from  $2.80 \text{ t ha}^{-1} \text{ year}^{-1}$  before widespread

deforestation to  $2.19 \text{ t ha}^{-1} \text{ year}^{-1}$  at present, whereas deeper soils in the valley bottoms at least partly compensated for substantial yield losses on the hillslopes. An additional factor that may explain the larger differences in the Turkish study (Van Loo et al., 2017) is that the work focuses on areas of substantial water erosion (Yang et al., 2019) representing environments with steep slopes and heavy rainfall events, where water erosion is well-recognized to be an important soil threat. In contrast, in the Uckermark water erosion plays only a minor role (Wilken et al., 2020).

A more substantial overall relative yield effect was modelled for winter wheat versus maize (Figure 5.5). Comparing the remote-sensing-based biomass proxy with the modelled biomass based on soil loss and gain (Figure 5.4) gives an indication why the modelled maize yield effect following landscape-scale soil redistribution is somewhat underestimated. While modelled winter wheat yields immediately react to soil truncation (Figure 5.4 a), this is not the case for maize, which does not react to soil thinning of less than approximately 0.3 m (Figure 5.4 a). The modelled response reflects the parameterization of the crop model, which produces a higher water-use efficiency of maize over winter wheat, meaning that the maize produces more biomass per litre of water than the wheat and therefore is less prone, in the model realization, to a reduction in water availability due to soil thinning. This is in agreement with results from the Berlin area (Mueller et al., 2005), but not all studies concur. Europe-wide modelling suggests that in Europe maize is more substantially affected by droughts than wheat (Webber et al., 2018) which is supported by findings (Öttl et al., 2021) based on remote sensing of our study area (see also Figure 5.4, right) that slightly larger landscape-scale yield effects can be expected in the case of maize. Therefore, it is likely that our modelled yield effects are conservative for maize.

Based on the reference soil profiles from the Uckermark, we can identify a threshold of approximately 0.3 m of soil loss beyond which affected soils contribute little biomass (Figure 5.4). In our future scenarios, the area of soil in this class (soil thinning,  $> 0.3 \text{ m}$ ) increases up to 100%. The increase in the area of soils that are non-productive highlights the need for urgent action to reduce soil thinning due to tillage.

In our scenarios we addressed different potential trajectories of future tillage practice (Figure 5.5), but we did not use future climate scenarios, which indicate longer dry spells or phases of droughts during the growing period in the region (Reinermann et al., 2019). However, our analysis comparing a normal-to-dry year with a wet year clearly indicates that the downward landscape-scale effect of tillage erosion on crop yields in the region is more pronounced in case of drier conditions during the growing season (Figures 5.4 and 5.5). Hence, there is clear evidence that projected future climate conditions

will amplify the downward landscape-scale yield effect. Moreover, we ignored the potential effects of soil quality loss due to deposition of depleted topsoil material coming from strongly eroded sites (Figure 5.2). This will also strengthen the negative yield effect which might foster future adaptations of management towards irrigation in this already dry region of northern Germany.

The increasing mechanization of agriculture, with significant innovations in agricultural machinery during the 1950s and 1960s increasing the size, weight and speed of tractors and cultivators, has played a significant role in accelerating tillage erosion. For example, the front and rear axle loads of tractors in Illinois (United States) have increased since 1960 by a factor of four and two, respectively (Schjønning et al., 2015). It is hard to find measurements of pre-mechanization tillage speeds, but contemporary measurements of horse-drawn ploughs in Ethiopia place speeds at between 3.2 and 4.7 km h<sup>-1</sup> (Fentahun et al., 2014), or between 1.0 and 1.8 km h<sup>-1</sup> in the case of ox-drawn mouldboard ploughing in Cuba (Wildemeersch et al., 2014). By 1925, with the introduction of the tractor, a plough would typically be pulled through the soil at 4–6.4 km h<sup>-1</sup> (Keen, 1925) and ploughing speeds are now in the range of 6.4–11.3 km h<sup>-1</sup> (Helsel, 2007), or even higher in case of non-inversion tillage (personal communication with farmers from the test site). Such an increase in tillage speeds accelerates tillage erosion (Van Oost et al., 2006a) and hastens the thinning and thickening of soils in sloping landscapes. There is some indication that the rate of tillage translocation in mechanised agriculture may be slowing. In recent decades there have been substantial shifts in the types of machinery used to cultivate soils. At one time, mechanised cereal production was dominated by the mouldboard plough as a primary cultivation tool. Although, still widely used, there has been a shift towards non-inversion tillage and no-tillage systems. However, non-inversion systems utilizing chisel ploughs in combination with powerful tractors have been demonstrated to move as much, if not more, soil than plough-based systems (Lobb, 2011) due to high tillage speeds. No-tillage systems, where seeds are sown directly into undisturbed soil, translocate an order of magnitude less soil than conventional tillage systems (Li et al., 2007) and therefore represent the best option for reducing the translocation of soil in agricultural landscapes.

As our results suggest that tillage erosion rates accelerated during phases of intensified agricultural mechanization, it is clear that the most pronounced future changes in tillage erosion can be expected in those regions where agricultural mechanization is still minimal. The region with the largest mechanization gap, and hence largest potential for accelerating tillage erosion, is Africa. Tractor use in sub-Saharan Africa was 1.3 tractors per 1000 ha in 2002 (the last date for which the Food and Agriculture Organization (FAO, 2020) holds data on farm

machinery for much of the world) compared with 9.1 tractors per 1000 ha in South Asia and 10.4 tractors per 1000 ha in Latin America for the same year (Pingali, 2007). With increasing areas of land coming into cultivation (FAO (2020) and gross national per-capita income rising across sub-Saharan Africa (The World Bank, 2020), it can be assumed that agricultural mechanization may also increase in the region (Sims and Kienzle, 2016), presenting a risk to the soils of the continent and highlighting the need to develop no-tillage systems adapted to the regional socioeconomic and environmental conditions.

Tackling the impact of tillage erosion is problematic. In cases, such as the Uckermark, where redistribution may have already gone too far, the only option is to relocate soil from the base of the slope to the top of slope in an attempt to rebuild soils. Anecdotally, farmers have been doing this for generations (D. Lobb, personal communication) and it has been demonstrated experimentally that adding 10 cm of topsoil to severely thinned hillcrests in Manitoba, Canada led to significantly greater yields than on those sites with no soil additions (Papiernik et al., 2009). Clearly, the best option is to prevent tillage erosion altogether and the adoption of practices that have virtually eliminated soil redistribution has taken place at scale. Large tracts of arable land in South America are managed using no-tillage systems that minimize soil disturbance (Derpsch et al., 2010) and are one of the central platforms of conservation agriculture. In addition, soil conservation practices that seek to reduce the effective slope of the land, for example, terracing or the use of contour grass strips, force farmers to cultivate parallel to the contour, reducing tillage erosion rates.

Further work is needed to adapt the principles of no-tillage and/or at least to take tillage erosion into account. This could include using precision agriculture to manage tillage speeds and depths in sloping agricultural land to arrest the redistribution of soils in agricultural landscapes. In addition, we need to understand better how soil redistribution impacts on soil carbon, nitrogen and phosphorus cycles and water availability in contrasting arable landscapes and how these changes impact on biomass production. This understanding should lead to the development of models which will allow us to assess the future sustainability of agricultural production in response to climate, land-use and technological change.

## 5.5 SUPPLEMENTARY INFORMATION

### 5.5.1 *Structure of supplementary material*

The supplementary material contains two major parts: In a first part, a short paragraph discusses the quality and limitations of the coupled tillage erosion (SPEROS-C) and crop growth model (AQUACROP). Here, figures and tables regarding the comparison of the model with measured data (Figure 5.6), calibration results (Table 5.1) and modelling outputs (Figure 5.7) are given. In the second part, figures and tables supplementing the modelling methods are collected (Figure 5.8 & 5.9, and Table 5.2 & 5.3) and presented with extended captions.

### 5.5.2 *Model quality and limitations*

Our modelling approach suffers from epistemic uncertainty associated with a number of sources. Parameter values for the tillage erosion model when simulating approximately 1000 years of cultivation can only be estimated, since we do not know the precise date that the land was cleared, nor the precise land and tool use history of the area. Moreover, the soil profiles we used were reconstructed using measured profiles, but with properties altered by the tillage erosion model, creating new soil profiles (see Figure 5.7) which were used for the crop modelling. In addition, the parameterisation of the crop model relied on the use of standard parameter sets with the model tested against regional data (see supplementary information). However, as we were mostly interested in relative changes in spatial variability of crop biomass production following soil redistribution, which has been shown to be important for the test area in a remote sensing analysis (Öttl et al., 2021), we are confident that our parsimonious model system is robust enough to illustrate the general problem associated with tillage erosion in regions only slightly affected by other erosion processes (Wilken et al., 2020).

Since our objective was to simulate relative regional changes in crop production, we tested the AQUACROP model against regional data sets. As no specific data for the Uckermark was available for fodder maize, we used fodder maize biomass data from the German Agricultural Statistics yearbook for the Brandenburg region, of which the Uckermark is a part (Destatis, 2021). For winter wheat we were able to obtain subregional data specifically related to the region (Anonymous, 2019). Simulated fodder maize biomass (Figure 5.6 A) was lower than the measured data and had a significantly lower variance ( $F = 2.97$ ;  $P < 0.05$ ). However, there was a reasonable relationship between the measured and observed time series (Figure 5.6 B), albeit with the observed values that were 18% higher than the simulated values. Overall simulated winter wheat yields were similar to measured data with

no difference between the variance of the two data sets ( $F = 1.49$ ) (Figure 5.6 C), however, the correlation between the two time series was weaker (Figure 5.6 D) than that for fodder maize. We attributed the lower simulated maize biomass to the more generalised Brandenburg data used for model testing. The soils of the Uckermark are predominantly sandy loams, whereas in the wider Brandenburg region there is a mix of textures including more fertile soil which is likely to have produced higher biomass of fodder maize. Given that we were interested in relative differences in crop production, we were satisfied that the AQUACROP model provided a basis for simulating the impact of soil depth changes on crop production.

Table 5.1: Cumulative  $k_{til}$  estimated from literature values and calibrated using recent winter wheat biomass and the effect of soil truncation as modelled with AQUACROP.

From	To	Duration (yr)	$k_{til}$	Cumulative $k_{til}$ ( $\text{kg m}^{-1}$ )		Reference
				Estimated	Calibrated	
2015	1964	51	475	24225	24225	Wilken et al. (2020) and Van Oost et al. (2006a)
1963	1920	43	350	15050	15050	Van Oost et al. (2006a)
1919	1850	69	250	17250	17250	Van Oost et al. (2006a)
1849	985	864	150	129600		Van Oost et al. (2006a)
1849	942	907	150		136094	calibrated
				<b>186125</b>	<b>192619 <math>\pm</math> 44894<sup>§</sup></b>	

<sup>§</sup> mean  $\pm$  standard deviation

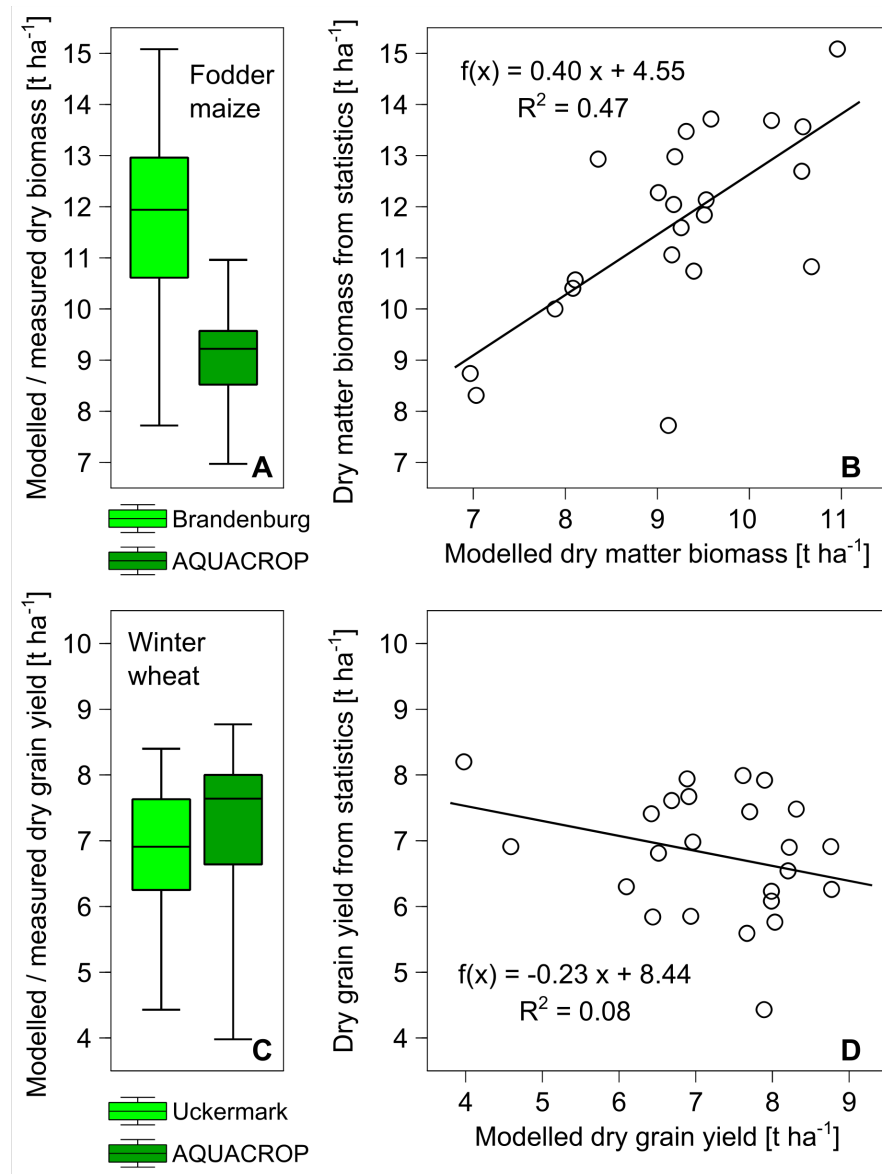


Figure 5.6: A,B: Comparison of AQUACROP with agricultural statistics from the entire state of Brandenburg (area approx. 29,500 km<sup>2</sup>) for 1993 to 2014. B,C: Comparison of AQUACROP with agricultural statistics from the Uckermark rural district (area approx. 3,000 km<sup>2</sup>) within the federal state of Brandenburg for 1993 to 2017. The boxplots (Figure 5.6) indicate the mean, the 1. and 3. quartile as well as the minimum and maximum biomass.

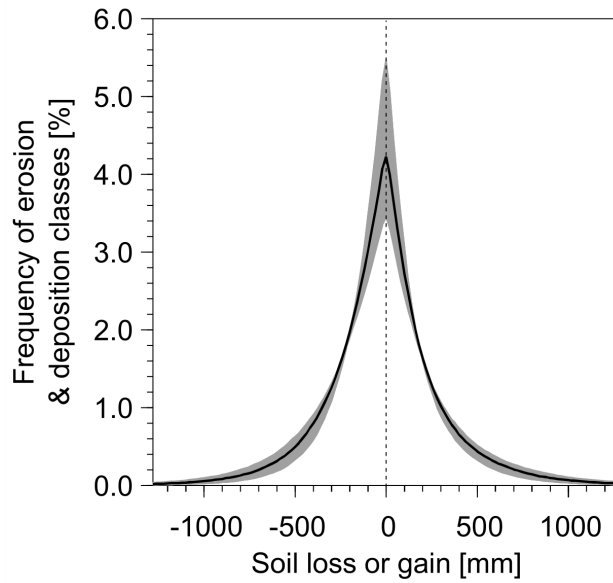


Figure 5.7: Modelled soil loss and gain based on best fit between tillage erosion modelling and the combined AQUACROP / remote sensing approach. Data are given in 130 erosion classes and their relative contribution to the entire fields in the catchment (based on approximately  $5 \times 10^6$  raster cells). The grey shaded area indicates the potential tillage erosion variability due to uncertainties in the calibrated cumulative mean  $k_{til}$  and represent the standard deviation of this mean.

## 5.5.3 Figures and tables related to methods

Table 5.2: Soil properties of references Calcic Luvisols used to represent soils without erosion and deposition; location within the catchment see Figure 5.8.

Upper depth	Lower depth	Soil horizon German classification	Bulk density	> 2 mm Sand	Silt	Clay	CaCO <sub>3</sub>	SOC	N <sub>total</sub>	C/N	ph (CaCl <sub>2</sub> )	
m	m		g cm <sup>-3</sup>	weight-%								
0.00	0.29	Ap	1.51	2	62	31	7	0	0.62	0.077	8	7.1
0.29	0.55	Al	1.61	3	58	31	11	0	0.22	0.035	6	6.1
0.55	0.8	Bt1	1.72	2	50	37	14	0	0.21	0.037	6	6.5
0.8	1.15	Bt2	1.68	2	45	32	23	0	0.18	0.036	5	7.1
1.15	1.5	elCcv	1.74	3	48	37	15	10	0.12	0.021	6	7.8
0.00	0.31	Ap	1.54	2	72	21	7	0	0.78	0.093	8	7.0
0.31	0.44	Al	1.62	3	66	28	6	0	0.25	0.020	12	7.0
0.44	0.60	Bvt1	1.65	2	71	19	11	0	0.21	0.025	8	7.1
0.60	1.07	Bvt2	1.72	2	70	19	11	0	0.21	0.025	8	7.1
1.07	1.40	elCcv	1.75	2	64	27	10	5	0.09	0.015	6	7.6
0.00	0.33	Ap	1.61	3	69	21	10	0	0.82	0.089	9	6.8
0.33	0.45	Al	1.71	3	72	21	7	0	0.34	0.034	10	6.8
0.45	0.79	Bt1	1.72	2	64	20	16	0	0.24	0.028	9	6.3
0.79	1.17	Bt2	1.74	2	59	21	20	0	0.24	0.019	13	7.1
1.17	1.34	Bt3	1.71	3	62	21	17	0	0.21	0.019	11	7.2
1.34	1.48	Bt4	1.70	2	63	22	16	0	0.21	0.018	12	7.7
1.48	1.60	elCcv	1.79	3	63	23	14	8	0.08	0.012	7	7.7

Table 5.3: Hydraulic properties of undisturbed soil (from AQUACROP input file) as derived from the soil properties in Table 5.2.

Horizon No.	1	2	3	4	5
Thickness (cm)	31	17	25	30	27
Saturation moisture content (%-vol.)	40	41	43	45	44
Field capacity moisture content (%-vol.)	29	29	29	29	30
Wilting point moisture content (%-vol.)	13	13	14	15	10
Saturated hydraulic conductivity (mm day <sup>-1</sup> )	868	745	416	258	809

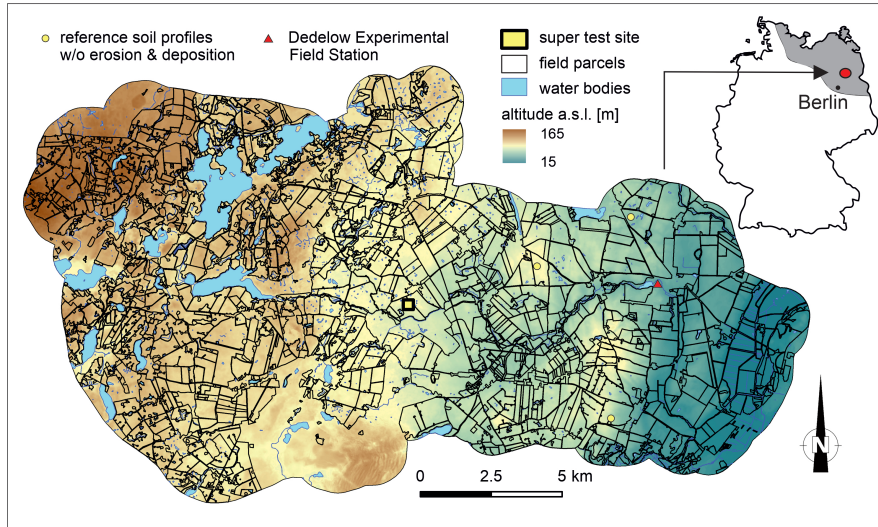


Figure 5.8: Topography and arable fields in the test area the Quillow catchment as used in Öttl et al. (2021); Note the super test site is the area where Wilken et al. (2020) used an inverse modelling approach to determine the parameters for the tillage erosion model which, with a slight adaption, represent tillage erosion within the last 50 years. The grey shaded area in the map of Germany indicates the area of ground moraines which the Quillow catchment typifies and the red oval the location of the Quillow catchment.

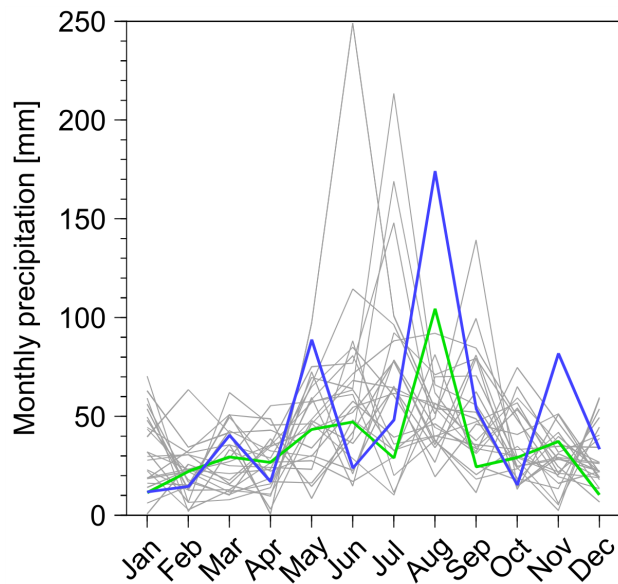


Figure 5.9: Monthly precipitation at the station Dedelow (for location see Figure 5.8) between 1992 and 2017. The years 2010 and 2015, used for the illustrative modelling to represent a 'wet' and a 'normal' year, are given in blue and green, respectively.



## A MILLENNIUM OF ARABLE LAND USE – THE LONG-TERM IMPACT OF WATER AND TILLAGE EROSION ON LANDSCAPE-SCALE CARBON DYNAMICS

---

LENA K. ÖRTL<sup>1</sup>, FLORIAN WILKEN<sup>1</sup>, ANNA JUŘICOVÁ<sup>2,3</sup>, PEDRO BATISTA<sup>1</sup>, AND PETER FIENER<sup>1</sup>

<sup>1</sup> *Water and Soil Resource Research, Institute of Geography, University of Augsburg, Augsburg, Germany*

<sup>2</sup> *Department of Physical Geography and Geoecology, Charles University, Prague, Czech Republic*

<sup>3</sup> *Remote Sensing and Pedometrics Laboratory, Soil Survey, Research Institute for Soil and Water Conservation, Prague, Czech Republic*

This chapter is submitted to *Soil*.

**ABSTRACT.** In the last decades, soils and their agricultural management have received great scientific and political attention due to their associated potential to act as a sink of atmospheric carbon dioxide (CO<sub>2</sub>). It is questioned if soil redistribution processes affect this potential CO<sub>2</sub> sink function, as agricultural management has a strong potential to accelerate soil redistribution. Most studies analysing the effect of soil redistribution upon soil organic carbon (SOC) dynamics focus on water erosion, analyse only relatively small catchments and relatively short timespans of several years to decades. The aim of this study is to widen the perspective by including tillage erosion as another important driver of soil redistribution and performing a model-based analysis in a 200 km<sup>2</sup>-sized arable region of north-eastern Germany for the period since the conversion from forest to arable land (approx. 1000 years ago). Therefore, a modified version of the spatially explicit soil redistribution and carbon (C) turnover model SPEROS-C was applied to simulate lateral soil and SOC redistribution and SOC turnover (spatial resolution 5 m × 5 m). The model parameterisation uncertainty was estimated by simulating different realisations of the development of agricultural management over the past millennium. The results indicate that in young moraine areas, which are relatively dry but intensively used for agriculture for centuries, SOC patterns and dynamics are substantially affected by tillage-induced soil redistribution processes. To understand the landscape scale effect of these

redistribution processes on SOC dynamics it is essential to account for long-term changes following land conversion, as typical soil-erosion induced processes, e. g. dynamic replacement, only take place after former forest soils reach a new equilibrium following conversion. Overall, it was estimated that after 1000 years of arable land use, SOC redistribution by tillage and water erosion results in a landscape-scale C sink of up to 0.66 ‰ per year.

## 6.1 INTRODUCTION

Soils play an important role in the global carbon (C) cycle (Bellamy et al., 2005; Berhe et al., 2008; Lal, 2004) and have received great scientific (e. g. Amelung et al., 2020; Bellassen et al., 2022; Van Oost et al., 2007) and political attention as one of the cornerstones to tackle climate change, e. g. 4 ‰ initiative (Minasny et al., 2017), Article 3.4 of the Kyoto Protocol (UNFCCC, 1998), and special report of the IPCC (IPCC, 2019).

A substantial loss of soil organic carbon (SOC) to the atmosphere before industrialisation is generally associated to the conversion of (natural) forest sites to cropland (Lal, 2019; Le Quéré et al., 2016; Sanderman et al., 2017). However, tillage operations and water erosion lead to an accelerated lateral redistribution of SOC within agricultural landscapes (Montgomery, 2007b). In consequence, the spatial variability of SOC within soils of arable landscapes increase, but this also creates complex interactions between changing SOC profiles, site-specific C mineralisation and sequestration, and potential losses to aquatic ecosystems (Doetterl et al., 2016). In a nutshell, (i) the removal of SOC-rich topsoil at erosional areas stimulates dynamic replacement of C via fresh photosynthates and the uplift of more reactive subsoil minerals (Harden et al., 1999; Stallard, 1998). (ii) During transport by different erosion agents, some SOC might be mineralised due to erosion-induced aggregate breakdown (Doetterl et al., 2016); however, this has a relatively short-lived effect, due to the episodic nature of erosion processes (Van Oost and Six, 2023). (iii) At depositional sites, SOC is buried in deeper soil layers and hence is protected from fast mineralisation (Berhe et al., 2008; Rumpel and Kögel-Knabner, 2011; Stallard, 1998). (iv) In case of water erosion, SOC will also partly enter aquatic ecosystems, where it is either buried in sedimentary deposits or mineralised during fluvial transport (Aufdenkampe et al., 2011; Battin et al., 2009).

The impact of soil redistribution on C dynamics has been assessed in various studies as reviewed in e. g. Doetterl et al. (2016), Kirkels et al. (2014), and Van Oost and Six (2023). Such studies have often benefited from a strong modelling component, which has been explored by both process-oriented models and more conceptual approaches. Most process-oriented studies focused on water-erosion prone micro-

catchments where field surveys regarding spatial patterns of SOC and erosion, or general erosion monitoring, can be used for model development and testing (e. g. Doetterl et al., 2012; Van Oost et al., 2005a; Wilken et al., 2017a). The focus on small erosion-prone catchments has several implications: (i) results can only be partially generalised, as these small-scale water erosion studies tend to be located in steeper areas; (ii) water erosion studies are often associated with loess-burden soils (e. g. Dlugoß et al., 2012; Li et al., 2007; Wilken et al., 2017a), which, although highly erodible, are also deep and display a low sensitivity to soil truncation regarding crop productivity; and (iii) the focus on water erosion makes it difficult to close the C balance, as the fate of SOC after leaving the micro-catchment is open to debate (Aufdenkampe et al., 2011; Battin et al., 2009; Van Oost and Six, 2023). Apart from these process-oriented studies, there are also regional (Lugato et al., 2018; Nadeu et al., 2015) and even global (Naipal et al., 2018; Van Oost et al., 2007) model-based estimates of the effect of soil redistribution on SOC stocks, which are based on coupled conceptual soil erosion and C turnover models. These (water erosion) modelling studies give valuable insights for large areas but are mostly focused on current erosion and C turnover (e. g. Nadeu et al., 2015; Van Oost et al., 2007), while long-term effects of erosion-induced C dynamics after centuries or even millennia of land management are ignored. In consequence, model results might overestimate the effect of intensive modern agriculture, as they typically only take the last 50 to 100 years into account (e. g. Dlugoß et al., 2012; Nadeu et al., 2015; Wilken et al., 2017b). Only a few of these regional studies addressed longer time scales (e. g. Bouchoms et al., 2017; Wang et al., 2017), which is a prerequisite to compare today's SOC soil profiles with model outputs in regions with a long agricultural land use history.

However, such long-term regional erosion and C turnover modelling is obviously challenged through the rapid decline in data accessibility and quality when moving back for centuries or even millennia. Apart from natural factors (e. g. climate, topography, soil cover, soil development, etc.) it is most challenging to reconstruct factors governed by agricultural practices (e. g. crop rotations, productivity, modification of soil cover, tillage methods, etc.). Moreover, estimates of initial (undisturbed) soil conditions (especially SOC stock profiles) are required to initiate long-term modelling. The existing long-term modelling studies (Bouchoms et al., 2017; Wang et al., 2017) used undisturbed soil profiles from long-term arable land, while to our knowledge studies accounting for the decline of SOC following conversion from forest to arable land in combination with erosion-induced C fluxes have not been carried out. Moreover, tillage erosion has been shown to be the main soil redistribution process in different parts of the world (e. g. Gerontidis et al., 2001; Lobb et al., 1995; Van Oost et al., 2003) and

ignoring its effects on long-term C dynamics might lead to spurious conclusions.

Any large-scale and long-term study faces the challenge of assumption-based input data. Hence, the aim of large-scale and long-term modelling must be to simulate plausible patterns instead of process-based reconstruction. The aims of this study are (i) to simulate long-term changes (1000 years) in soil profiles in an agricultural landscape heavily affected by tillage erosion and less affected by water erosion; (ii) to perform a model-based soil redistribution and SOC turnover analysis for a larger area (about 200 km<sup>2</sup>), in order to avoid a systematic bias typically found in small-scale studies focussing on erosion processes in steep areas; and (iii) to model the long-term effect of soil redistribution when moving from a SOC-rich forest soil to a heavily eroded arable soil after 1000 years of cultivation.

## 6.2 MATERIALS AND METHODS

### 6.2.1 *Study area*

The study area covers an area of 196 km<sup>2</sup> and is located in the Quillow river catchment about 100 km north of Berlin in north-eastern Germany (Figure 6.1). It represents a typical ground moraine landscape formed after the retreat of the Weichselian glaciers ca. 15,000 years ago (shaded area in Figure 6.1; Lüthgens et al., 2011). The area is characterized by a hilly topography with short summit-footslope distances (on average 35 m) and a mean slope ( $\pm$  standard deviation) of ca. 4.4%  $\pm$  3.7%. A large number of kettle holes that were formed by the delayed melting of bigger ice blocks (Anderson, 1998) are typical landscape elements. Drainage is only possible via sub-surface flow from the kettle holes (Lischeid et al., 2017). The kettle holes can be filled with water, (degraded) peat or are covered by colluvial material resulting from arable land use over centuries (Van der Meij et al., 2019).

The land cover of the study area is dominated by arable land and pasture (ca. 70%), followed by wetlands and lakes (ca. 16%), while only a small part is made up by forest (ca. 11%) and settlements (ca. 3%; Heinrich et al., 2018). Some parts of the study area have been used for agriculture since Neolithic times (ca. 5500 BCE; Behre, 2008), while it is assumed that agricultural land use became widespread approximately in 1000 CE (Behre, 2008; Herrmann, 1985). Intensive mechanisation of agriculture started in the second half of the 20<sup>th</sup> century. This was accompanied by a substantial increase of field sizes during the socialistic era of the German Democratic Republic (Bayerl, 2006), resulting in recent average field sizes of 21 ha ( $\pm$  20 ha). The region is characterized by a relatively dry subcontinental climate with an average annual air temperature of 9.4 °C and a mean annual pre-

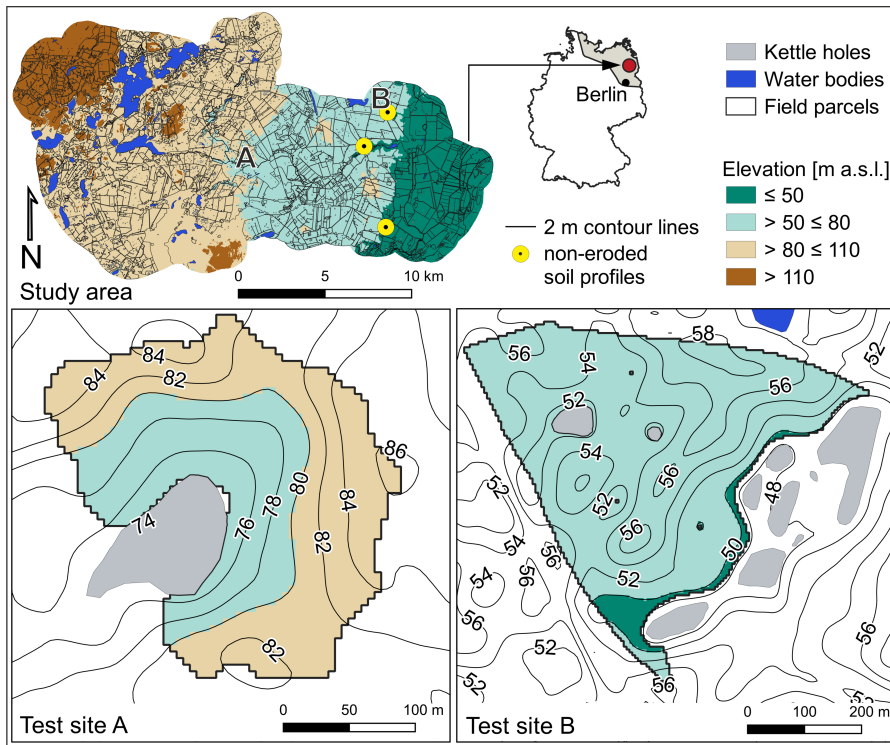


Figure 6.1: The study area is located north of Berlin in the young moraine landscape of north-eastern Germany indicated by the grey area of the inset map (upper panel). Location of the two test sites A and B (black letters) as well as of the four non-eroded soil profiles used for calibration (yellow circles) within the study area. Thereby, the yellow circle close to test site B represents two profiles. Topography and kettle holes of test site A (lower left panel) and B (lower right panel) with 2 m contour lines (black lines). The elevation of the test sites is shown by using the colour scheme of the upper panel.

precipitation of 466 mm (20-year average 2001-2020, DWD meteorological station at Grünow; DWD, 2018a, 2021).

The soil pattern of the region follows the heterogeneity of Pleistocene deposits and has been strongly modified by soil redistribution over the past centuries (Deumlich et al., 2010; Koszinski et al., 2013; Sommer et al., 2008). Nowadays, non-eroded soils can only be found at ca. 20% of the arable land, mainly at lower midslopes or flat plateaus. Thereby, extremely eroded soils occur at hilltops, ridges, and slope shoulders, while strongly eroded soils are found from slope shoulders to upper midslopes. Groundwater-influenced colluvial soils have developed at footslopes of closed depressions, which are often covering fossil peat (see more details in Öttl et al., 2021).

Within the Quillow study area two agricultural fields (Figure 6.1) were chosen to test the plausibility of the modelling results (i. e. current estimates of SOC stocks and patterns). They were selected because of existing SOC data from previous studies (e. g. Wehrhan and Sommer, 2021; Wilken et al., 2020). Test site A is located approximately in the centre of the study area ( $53.3550^{\circ}$  N,  $13.6643^{\circ}$  E), has a size of ca. 4.4 ha

and a mean slope of  $8.7\% \pm 3.9\%$ . Test site B is in the northeast of the study area ( $53.3836^\circ$  N,  $13.7818^\circ$  E), has an area of ca. 20.5 ha and a mean slope of  $5.5\% \pm 2.9\%$ .

### 6.2.2 Modelling approach

A modified version of the spatially explicit soil redistribution and C turnover model SPEROS-C (Dlugoß et al., 2012; Fiener et al., 2015; Van Oost et al., 2005a) was applied for modelling tillage- (TIL) and water-induced (WAT) soil redistribution in the mesoscale study catchment over the past millennium. Thereby, lateral soil and SOC redistribution, SOC turnover, and vertical mixing within the profile (spatial and vertical resolution  $5\text{ m} \times 5\text{ m}$  and  $10 \times 0.1\text{ m}$  soil depth increments, respectively) were simulated. To isolate C fluxes that occur solely due to total soil redistribution (TOT is the sum of TIL and WAT), a reference run simulating C fluxes without soil redistribution was calculated. Modelling soil redistribution and C dynamics required estimating and calibrating model input parameters and their uncertainty, as well as evaluating the model outputs. The single steps are described in detail in the following section.

**MODELLING SOIL REDISTRIBUTION AND SOC DYNAMICS.**  
**Tillage-induced soil redistribution.** TIL is calculated based on a diffusion-type equation developed by Govers et al. (1994) (Eq. 6.1). The net soil flux due to tillage  $Q_{til}$  ( $\text{kg m}^{-1} \text{ yr}^{-1}$ ) can be written as

$$Q_{til} = -k_{til} \cdot s = -k_{til} \cdot \frac{\delta h}{\delta x}, \quad (6.1)$$

whereby tillage transport coefficient ( $k_{til}$ ) is the tillage transport coefficient ( $\text{kg m}^{-1} \text{ yr}^{-1}$ ),  $s$  is the local slope (%),  $h$  is the height at a given point of the hillslope (m), and  $x$  is the soil translocation distance in horizontal direction (m). The local tillage-induced soil redistribution rate tillage-induced soil redistribution ( $E_{til}$ ) ( $\text{kg m}^{-1} \text{ yr}^{-1}$ ) is calculated as

$$E_{til} = -\frac{\delta Q_{til}}{\delta x} = -k_{til} \cdot \frac{\delta^2 h}{\delta x^2}. \quad (6.2)$$

Thereby, the intensity of the calculated erosion rates is determined by the  $k_{til}$  and the change in slope gradient determines the spatial pattern of tillage-induced soil redistribution.

**Water-induced soil redistribution.** WAT is calculated according to a slightly modified approach of the Revised Universal Soil Loss Equation (Revised Universal Soil Loss Equation (RUSLE); Renard et al., 1997), which is described in detail in Van Oost et al. (2000). A local transport

capacity  $T_c$  ( $\text{kg m}^{-1} \text{yr}^{-1}$ ; Eq. 6.3) determines whether erosion, sediment transport, or deposition occurs. If the sediment inflow is higher than  $T_c$  the excess is deposited, while the  $T_c$  is further routed downstream.

$$T_c = k_{tc} \cdot P \cdot C \cdot K \cdot R \cdot LS_{2D}, \quad (6.3)$$

whereby  $k_{tc}$  is the transport capacity coefficient (m),  $P$ ,  $C$ ,  $K$ , and  $R$  are the RUSLE factors, and  $LS_{2D}$  is a grid-cell specific topographic factor calculated following Desmet and Govers (1996).

**SOC turnover model.** SOC stocks are modelled for a soil profile with 10 soil layers of 0.1 m. The model equations describing the SOC depth profile and SOC decay are based on the Introductory Carbon Balance Model (Introductory Carbon Balance Model (ICBM); Andrén and Kätterer, 1997; Kätterer and Andrén, 1999). ICBM considers a young ( $Y$ ) and old ( $O$ ) C pool with different turnover rates ( $k_Y = 0.8 \text{ yr}^{-1}$ ,  $k_O = 0.006 \text{ yr}^{-1}$ ). The fraction of the annual flux from  $Y$  to  $O$  is determined by the humification coefficient  $h$ . External environmental factors from climate and soils are combined in the factor  $r$  and the mean annual C input to the soil is represented by the parameter  $i$  (Andrén and Kätterer, 1997). The dynamics of the two SOC pools are described by the following differential equations (Andrén and Kätterer, 1997):

$$\frac{\delta Y}{\delta t} = i - k_y \cdot r \cdot Y, \quad (6.4)$$

$$\frac{\delta O}{\delta t} = h \cdot k_y \cdot r \cdot Y - k_O \cdot r \cdot O, \quad (6.5)$$

SOC turnover rates are assumed to decrease exponentially with depth due to a decreasing influence of environmental conditions (Eq. 6.6; Rosenbloom et al., 2001).

$$k_{Y/Oz} = k_{Y/Oz} \cdot e^{(-u \cdot z)} \quad (6.6)$$

Annual C input  $i$  ( $\text{g C m}^{-2} \text{yr}^{-1}$ ) is derived from crops ( $i_c$ ) and manure ( $i_m$ ; Eq. 6.7). Thereby,  $i_c$  is made up by an above- and a belowground component. Crop residues are determined by the residue to aboveground biomass (AGBM) ratio ( $Res$ ). The fraction of C input from roots and rhizodeposition ( $p_z$ ) at a given soil depth  $z$  (m) is defined by the root to AGBM ratio ( $RS$ ). For  $i_c$ , a C content ( $C_{cont}$ ) of 0.45 is used (Eq. 6.8; Tum and Günther, 2011).

$$i = i_c + i_m \quad (6.7)$$

$$i_c = C_{cont} \cdot [(Res \cdot AGBM) + (p_z \cdot RS \cdot AGBM)] \quad (6.8)$$

The C input into the soil is modelled by assuming an exponential root density profile (Gerwitz and Page, 1974; Van Oost et al., 2005a), while manure input is only assigned to the plough layer (or layers). The allocation of total root dry matter to each soil layer  $z$  (m) was calculated according to a reference soil depth  $z_r = 0.25$  m (Van Oost et al., 2005a) and a constant  $c$  that determines the proportion of the roots per soil layer ( $p_z$ ; Eq. 6.9).

$$\begin{aligned} \text{for } z \leq z_r : p_z &= \frac{z}{z_r + \frac{1 - e^{-c(1-z_r)}}{c}} \\ \text{for } z > z_r : p_z &= \frac{z_r + (1 - e^{-c(z-z_r)})/c}{z_r + (1 - e^{-c(1-z_r)})/c} \end{aligned} \quad (6.9)$$

The humification coefficient  $h$  is weighted according to the proportion of the source of  $i$  and depends on clay content  $cp$  (%) (Eq. 6.10; Kätterer and Andrén, 1999).

$$h = \frac{i_c \cdot h_c + i_m \cdot h_m}{i} \cdot e^{0.0112 \cdot (cp - 36.5)} \quad (6.10)$$

The temperature response factor  $r$  that accounts for the environmental influence on SOC decay is calculated with the following exponential  $Q_{10}$  function (Kätterer et al., 1998; Van Oost et al., 2005a):

$$r = Q_{10} \frac{T - 5.4}{10}. \quad (6.11)$$

Thereby,  $r$  is estimated with a  $Q_{10}$  value of 2.07 (Kätterer et al., 1998), a temperature  $T$  (°C) calibrated for this study (as described below), and by correcting temperature by the annual mean temperature of central Sweden (+5.4 °C) (Andrén and Kätterer, 1997).

**Soil profile update.** After every time step the SOC profile is updated considering yearly soil loss and gain due to water and tillage erosion. At eroding sites, a fraction of SOC from the first subsoil layer equal to the thickness of the eroded layer is incorporated into the plough layer. At depositional sites, a fraction of the SOC from the plough layer is shifted downwards into a buried plough layer. The underlying subsoil layers are further buried according to the depth of the soil deposition in that time step (Dlugosz et al., 2012; Van Oost et al., 2005a).

To account for the development of tillage implements and practices (Figure 6.2 a, Table 6.3), plough depth was updated with time, but kept constant through periods without significant changes in historical

plough development. Based on a literature review, we changed plough depth from 0.1 m for the first 800 years of the model simulations to 0.2 m for 1800-1900 CE and to 0.3 m for 1900-2000 CE (Figure 6.2 c). The yearly vertical C fluxes are then calculated following the profile update.

**MODEL IMPLEMENTATION.** One of the major challenges in performing a model-based analysis of the impacts of 1000 years of soil erosion upon C fluxes in an area of 200 km<sup>2</sup> is to estimate reasonable model inputs and to determine appropriate model parameters. Obviously, this is associated with large uncertainties and requires substantial simplifications. It is important to note that the model allows a reasonable analysis of the importance of soil redistribution for the C balance of the entire study area, but it is not expected to exactly mimic the current observational data.

**Model realisations.** Due to the uncertainties in the main model input parameters for the erosion modelling and to account for a varying importance of TIL and WAT, we created nine model realisations (R1 - R9). The realisations were simulated by a combination of a low, medium, and high water erosion pathway indicated by the minimum, the mean and the maximum values of the  $C$ ,  $K$ , and  $R$  factors as shown in Figure 6.2 b, with a low, medium, and high tillage erosion pathway using the different  $k_{til}$  values from Figure 6.2 a. The theoretical background that led to the erosion pathways is explained in detail in the next paragraphs. It is important to note that the variation in TIL and WAT is set to the relative importance of tillage and water erosion in the region as determined in earlier studies (Wilken et al., 2020; Öttl et al., 2021). The nine realisations are: (R1) low TIL, low WAT; (R2) low TIL, medium WAT; (R3) low TIL, high WAT; (R4) medium TIL, low WAT; (R5) medium TIL, medium WAT; (R6) medium TIL, high WAT; (R7) high TIL, low WAT; (R8) high TIL, medium WAT; and (R9) high TIL, high WAT. Due to the large computing requirements in simulating 1000 years for roughly  $8 \times 10^6$  raster cells of the entire study area, we only modelled the different realisations for the test fields (Figure 6.1, together roughly  $10 \times 10^3$  raster cells). The most plausible realisation (as defined below) was later on used to model the entire study area.

**Tillage-induced soil redistribution.** A comprehensive literature review (comprising 47 original publications representing 137  $k_{til}$  values; Table 6.3) was performed to assess tillage erosion intensity of different soil cultivation techniques. According to the land use history of the study region, the model period was subdivided into five periods representing different soil cultivation techniques.

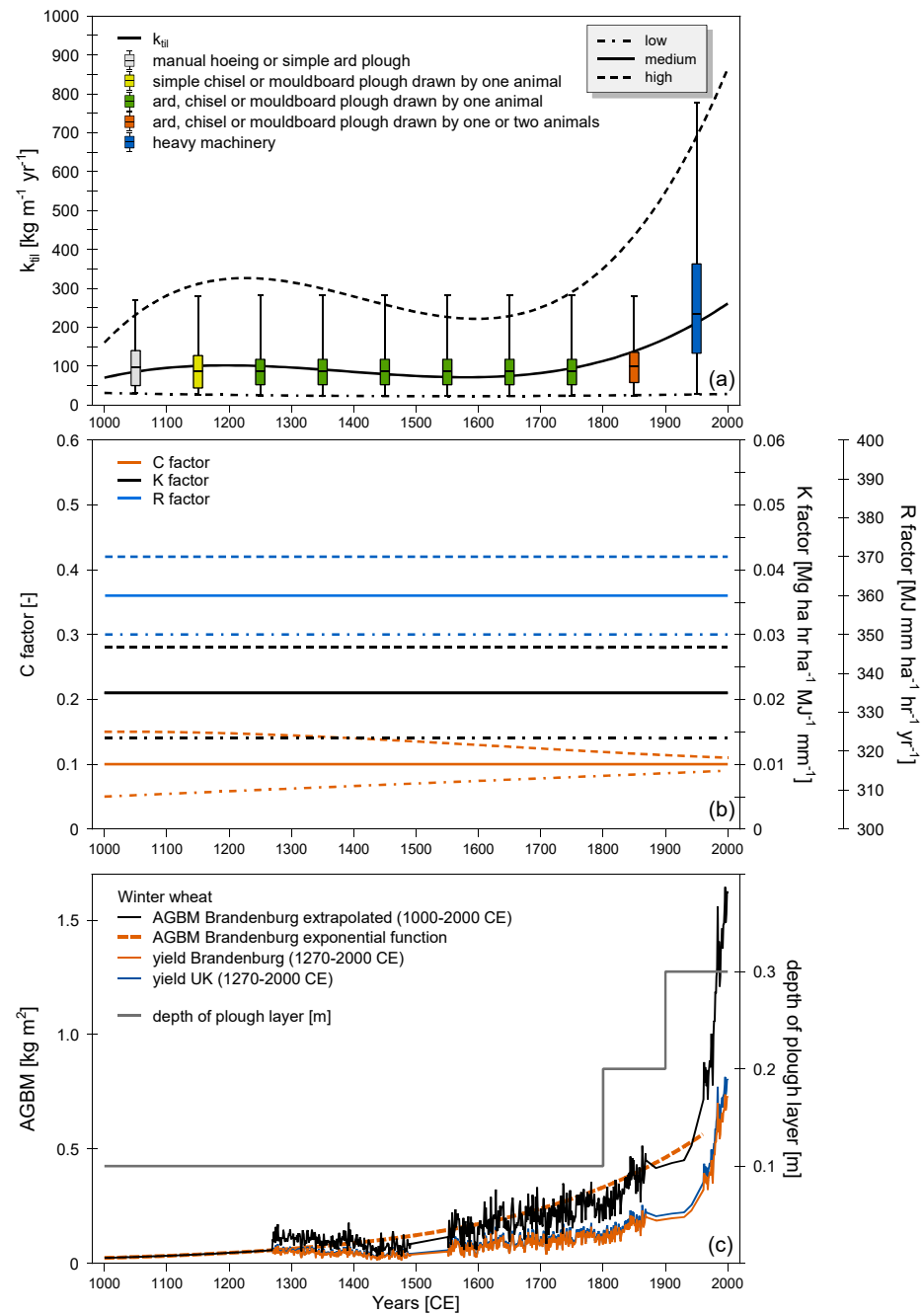


Figure 6.2: Range of reasonable input parameters for modelling tillage- (a) and water-induced soil redistribution (b), and SOC dynamics (c) for the model period of 1000 years. The range of parameters in (a) and (b) (dashed-dotted for the lower and dashed lines for the upper range, respectively; solid line represents the mean) is used in the different model realisations. Please notice the different scales of the y-axes. Abbreviations:  $k_{til}$  = tillage transport coefficient,  $AGBM$  = aboveground biomass;  $C$ ,  $R$ , and  $K$  factor = factors of the RUSLE (Eq. 6.3). Information on data sources and explanation of the parameters can be found in the text.

For the first period (1000-1100 CE), the median  $k_{til}$  of  $98 \text{ kg m}^{-1}$  (min.  $9 \text{ kg m}^{-1}$ , max.  $300 \text{ kg m}^{-1}$ ) was calculated from 23  $k_{til}$  values for manual hoeing or the use of a simple ard (Table 6.3). Although the medieval mouldboard plough was already invented around 200-900 CE (Van der Meij et al., 2019), it was assumed that the majority of the farmers still practiced manual hoeing or used the simple ard plough in the first period (Behre, 2008; Herrmann, 1985).

For the second period (1100-1800 CE) it was assumed that an increasing number of farmers used a rudimentary chisel or mouldboard plough drawn by an animal, as the turning plough was introduced around 1000 CE (Behre, 2008; Herrmann, 1985). As not much further information is available until the end of the 18<sup>th</sup> century, we used a set of 30  $k_{til}$  literature values representing ard, chisel or mouldboard plough drawn by a single animal. The median  $k_{til}$  of these studies is  $88 \text{ kg m}^{-1}$  (min.  $14 \text{ kg m}^{-1}$ , max.  $300 \text{ kg m}^{-1}$ ; Table 6.3).

The fourth period (1800-1900 CE) was characterised by the industrial revolution that tremendously changed the way land was managed. From 1800 onwards the so-called "Ruchadlo", a steep turning tipping plough (Herrmann, 1985), and the "Mecklenburgischer Haken" for seedbed preparation were used (Behre, 2008). Both implements were pulled by animals (oxen or horses). A median  $k_{til}$  of  $100 \text{ kg m}^{-1}$  (min.  $14 \text{ kg m}^{-1}$ , max.  $300 \text{ kg m}^{-1}$ ) was calculated from 15  $k_{til}$  values for an ard, chisel or mouldboard plough pulled by one or two animals (Table 6.3).

The last period (1900-2000 CE) is characterized by the introduction of automotive tractors that were able to pull heavy implements and in consequence the ploughing depths increased to 20 - 40 cm (Behre, 2008; Bork et al., 1998; Van der Meij et al., 2019). The median  $k_{til}$  of  $234 \text{ kg m}^{-1}$  (min.  $13 \text{ kg m}^{-1}$ , max.  $900 \text{ kg m}^{-1}$ ) was calculated from 69  $k_{til}$  values for tractor-pulled heavy machinery (early and recent chisel and mouldboard plough, harrow, cultivator, tandem disc, etc.; Table 6.3).

**Water-induced soil redistribution.** A range of C factor values was estimated to represent the changes in crop cover/management throughout the simulation period (Figure 6.2 b). As such, two different conditions were assumed: for the upper limit of the parameter space it is assumed that the crop cover was low (i.e. high C factor) at the beginning of the simulation period due to relatively lower yields and high row spacing. For the lower limit it is assumed that a much lower historic C factor might be reasonable due to a high vegetation cover related to a high proportion of weeds and grasses between the crops, which decreased over time due to improved weeding methods. To account for this uncertainty over time, we assumed that at 1000 CE the C factor might be either 50% higher or lower than the current mean value. This range decreased according to a polynomial function (degree = 3) until reaching  $\pm 10\%$  of the current value in 2000 CE. The current mean C factor of 0.1 was calculated assuming a small-

grain crop rotation (e. g. winter wheat – winter wheat – winter barley – winter rapeseed) typically applied under today's conditions (Deumlich et al., 2002; Schwertmann et al., 1987; Öttl et al., 2021).

The soil erodibility factor  $K$  was assumed to remain constant throughout the simulation period and was calculated based on a soil group map (Bundesministerium der Finanzen, 2007; Rust, 2006), following the approach as described in DIN ISO (19708:2017-08). The area-weighted mean  $K$  factor of  $0.021 \text{ Mg ha hr ha}^{-1} \text{ MJ}^{-1} \text{ mm}^{-1}$  was used as medium realisation (Figure 6.2 b). The lower and upper parameter values used for creating the model realisations are the area-weighted mean plus-minus the standard deviation of the  $K$  factor, respectively ( $0.021 \pm 0.007 \text{ Mg ha hr ha}^{-1} \text{ MJ}^{-1} \text{ mm}^{-1}$ ).

The rainfall erosivity factor  $R$  was calculated based on a long-term precipitation reconstruction for Europe (1500-2000 CE; Pauling et al., 2005) and an approach of Diodato et al. (2017) developed to estimate long-term erosion changes from historic precipitation data. As no precipitation data was available for the period 1000-1500 CE, the mean  $R$  factor of the available data ( $362 \text{ MJ mm ha}^{-1} \text{ hr}^{-1} \text{ yr}^{-1}$  for 1500-2000 CE) was used as mean for the whole modelling period (Figure 6.2 b). To address a potential range in the  $R$  factor we used the mean  $\pm 95\%$  confidence interval ( $362 \pm 8.3 \text{ MJ mm ha}^{-1} \text{ hr}^{-1} \text{ yr}^{-1}$ ; Figure 6.2 b).

For this study, a constant transport capacity coefficient  $k_{tc}$  of 150 m was used as this value was found to be suitable for cropland and a grid resolution of  $5 \text{ m} \times 5 \text{ m}$  (Dlugoß et al., 2012; Van Oost et al., 2003). The grid cell-specific topographic factor  $LS_{2D}$  was calculated based on a digital elevation model (digital elevation model (DEM); derived from airborne laser scanning; original spatial resolution of 1 m resampled to 5 m; Landesamt für Umwelt & Landesvermessung und Geobasisinformation Brandenburg, 2012). The support practice factor  $P$  is 1.0 for all realisations for the whole modelling period as no erosion control practices are assumed.

Both water and tillage erosion are sensitive to field sizes and layouts, which according to historic maps and later aerial photographs substantially changed over time. As we could not reconstruct field layout over one millennium for the entire test area, it was decided to use recent field layouts. However, as the recent fields are very large this leads to an underestimation of potential field border effects.

**SOC turnover and C balancing.** To model SOC dynamics over 1000 years, SPEROS-C needs yearly estimates of C inputs based on *AGBM* as well as estimates of ploughing depths (Figure 6.2 c), as these variables change the C incorporation into the soil. To calculate the temporal evolution of *AGBM* (Figure 6.2 c), yield data for the federal state of Brandenburg from 1950 until 2018 CE (Federal Statistical Office, 1990-2018; Staatliche Zentralverwaltung für Statistik, 1956-1990) was combined with a long-term winter wheat yield dataset of the UK

(1270-2014 CE; Ritchie and Roser, 2013). Yield was converted to *AGBM* by multiplying with the harvest index (*HI*; Donald and Hamblin, 1976), which determines the proportion of yield to total biomass for specific crop species. The *HI* was calculated with winter wheat grain and straw data from Brandenburg (mean *HI* = 0.449; KTBL, 1951, 1970, 1980, 1993, 2005). We assumed that for every third year of the simulation the *AGBM* would not be harvested, in order to account for the so-called “three-field economy” (Rösener, 1985; Volkert, 1991), i. e. a crop rotation regime commonly used in Germany since medieval times and in which a field was left fallow every third year.

While changes in *AGBM* and ploughing depths can be reasonably estimated based on existing data, it is hardly possible to estimate the temporal (or even spatial) variability of other model parameters, e. g. root:shoot ratio, manure application etc., used in ICBM. Therefore, we used SOC depth distributions from four standard soil profiles representing undisturbed (i. e. non-eroded) arable soils in the study area (soil database of ZALF e.V. and Sommer et al. (2020)) and values from the literature as initial model parameters (Table 6.1).

Table 6.1: Model input parameters for modelling SOC dynamics in agricultural soils determined by Monte Carlo simulations ( $n = 1000$ ). The initial values are varied by  $\pm 10\%$  for sampling and the final value is the parameter set that yielded the highest Nash Sutcliffe model efficiency. The references proof that the initial values and their ranges are valid assumptions.

Calibrated parameter	Abbreviations used in the text	Unit	Initial value	Final value	Reference for initial value
Clay percentage	<i>cp</i>	%	13.0	14.0	Sommer et al. (2020)
Constant that defines root growth	<i>c</i>	–	4.0	3.62	Van Oost et al. (2005a)
Decomposition depth attenuation	<i>u</i>	–	3.0	2.99	Van Oost et al. (2005a)
Manure input	<i>m</i>	kg m <sup>-2</sup>	0.05	0.05	Verch (2020)
Root:shoot ratio	<i>RS</i>	–	0.16	0.16	Herbrich et al. (2018)
Reference soil depth	<i>z<sub>r</sub></i>	m	0.25		Van Oost et al. (2005a)
Residue to <i>AGBM</i> ratio	<i>Res</i>	–	0.1	0.11	Dlugoß et al. (2012)
Temperature	<i>T</i>	°C	8.0	7.9	DWD (2018a)
Depth of plough horizon	–	m	0.3		Behre (2008) and Herrmann (1985)

These were later optimised to derive a model parameter set used for the entire modelling period. That is, first we varied the literature parameter values one-at-time until they matched the observation data (i. e. combination of the four non-eroded SOC depth profiles; orange line in Figure 6.3). Second, the obtained representative initial values for the observed SOC profile were used in a Monte Carlo simulation

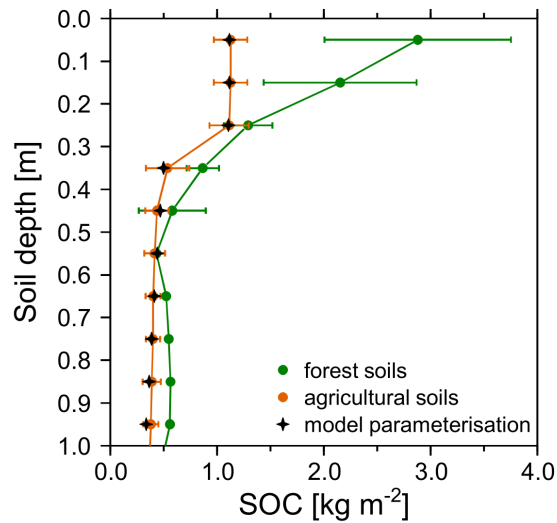


Figure 6.3: Depth profile of the mean observed SOC stocks for the forest (green) and agricultural soils (orange) with error bars of  $\pm$  one standard deviation. The forest soils are used as initial soil condition, while the calibration of the agricultural soils is used as parameterisation for modelling the 1000 years (black stars).

( $n = 1000$ ). Each parameter was sampled from a uniform distribution in a range of  $\pm 10\%$  around its initial value, which resulted in 1000 different modelled SOC-depth profiles. Hence, not only the direct influence of each parameter on the model output was considered but also the joint influence due to interactions between the parameters (Pianosi et al., 2016). The parameter set which yielded the highest Nash-Sutcliffe model efficiency (Nash and Sutcliffe, 1970) was selected for the final modelling (black stars in Figure 6.3).

**Model evaluation.** A straightforward, traditional model-testing approach of the correspondence between observational data and model outputs after simulating 1000 years of soil redistribution and C turnover in a study area of about 200 km<sup>2</sup> is obviously hardly possible. There are neither commensurate quantitative measurements of erosion available at this spatiotemporal scale, nor is it appropriate to directly compare soil truncation or SOC patterns of individual fields with a model output based on a parameterisation for the entire study area. As such, we focused on an investigative model evaluation approach (Baker, 2017), in which two independent datasets were used to evaluate the model's capability to consistently represent the long-term erosion-induced C balance for the study area.

The first independent data used for model evaluation was derived from a remote sensing approach for identifying spatial patterns of severe soil erosion and soil truncation. Typical features in the study



Figure 6.4: Exemplary aerial photos of the study area showing eroded hilltops indicated by the lighter soil colours. Notice that the aerial photo to the left was taken in 1953 (© ZALF e.V.), while the one to the right is from 06/09/2016 (© Google).

area are signs of soil truncation at hilltops, which most likely result from prolonged tillage erosion (Deumlich et al., 2010; Sommer et al., 2008). The heavily eroded hilltops are visible in remote sensing data due to their brighter colours resulting from an exposure of the subsoil horizon partly consisting of glacial till (Figure 6.4).

Heavily eroded areas can be straightforwardly detected by using remote sensing data for the entire catchment area. Therefore, 24 multispectral Sentinel-2 satellite images (ESA, 2015) acquired during bare soil conditions were classified (support vector machine tool; ArcGIS version 10.7.1). As the classification can only be performed for fields with bare soil conditions at the time of satellite image acquisition, about 21 % of the study area (ca.  $1.7 \times 10^6$  raster cells) was classified, whereby 6 % of the study area were classified as heavily eroded (ca.  $4.2 \times 10^5$  raster cells). As hilltop erosion might also lead to a movement of the surface-exposed subsoil into the surrounding areas not affected by erosion, a buffer of -5 m was created to the inside of the area resulting in 5.2 km<sup>2</sup> or  $2.1 \times 10^5$  raster cells classified as heavily eroded. These raster cells are used to evaluate the consistency of the modelled erosion patterns, which have been shown to be dominated by tillage erosion in a previous study (Wilken et al., 2020).

The second source of independent model-evaluation data was derived from measured SOC stocks for two different test sites in the study area. For test site A (Figure 6.1), plough layer SOC stocks are available from a nested sampling design (20 m × 20 m; see Wilken et al., 2020) carried out in 2018. The data were geostatistically interpolated using a kriging approach to a regular grid with 5 m × 5 m resolution. At test site B (Figure 6.1), the topsoil SOC stocks were derived from a regression analysis of ground truth SOC measurements (first 0.15 m) against multispectral images taken by a remotely piloted aircraft system (Wehrhan and Sommer, 2021). Both observed SOC patterns were compared to model outputs.

### 6.3 RESULTS

#### 6.3.1 Model evaluation

A comparison between modelled and remotely sensed soil redistribution patterns (Table 6.2) indicated that the most severely eroded sites were associated with tillage induced (TIL) and total soil redistribution (TOT). Overall, about 81 % of the areas classified as heavily eroded according to the remote sensing approach correspond to the modelled erosion class. On average those areas show a modelled soil loss of  $-0.23 \text{ mm yr}^{-1}$  (R4), most of which was caused by tillage erosion (Table 6.2).

Table 6.2: Agreement between modelled WAT, TIL and TOT erosion classes and remote-sensing derived erosion classification. Note that a threshold of  $-0.05 \text{ mm}$  erosion per year was used to exclude areas with minimal erosion after modelling 1000 years of soil redistribution. The area classified from the remote sensing data represents about 21 % of the entire study area. Within the classified area, about 28 % is heavily eroded (about  $4.7 \times 10^5$  raster cells).

Erosion type	Agreement [%]	Mean erosion rate [m] $\pm$ one standard deviation
Total erosion (TOT)	81.21	$-0.23 \pm 0.14$
Tillage erosion (TIL)	76.00	$-0.22 \pm 0.13$
Water erosion (WAT)	11.63	$-0.08 \pm 0.03$

A visual comparison of modelled erosion against observed topsoil SOC patterns of the two test fields (A and B; Figure 6.5) shows an obvious relation between the observed SOC patterns and tillage erosion. This finding is further supported by a comparison of modelled topsoil SOC stocks based on the nine model realisations, which underlines that the quality of the results is mostly determined by the differences in tillage erosion intensity (Figure 6.6). Best results in respect of the used goodness-of-fit parameters can be reached for the medium (R4-R6) and high tillage erosion realisations (R7-9), whereas the medium and high TIL realisation fits better for test site A and B, respectively (Figure 6.6). In contrast, WAT plays only a minor role in explaining the spatial distribution of SOC. It is important to note that especially in case of test site B, where topsoil SOC stocks are estimated with a remote sensing approach, the model substantially underestimates the SOC contents. Taking this into consideration, while also trying to perform a somewhat conservative estimate of the extent of tillage erosion, we used realisation R4 (medium TIL, low WAT) for the following model analysis of the entire study area.

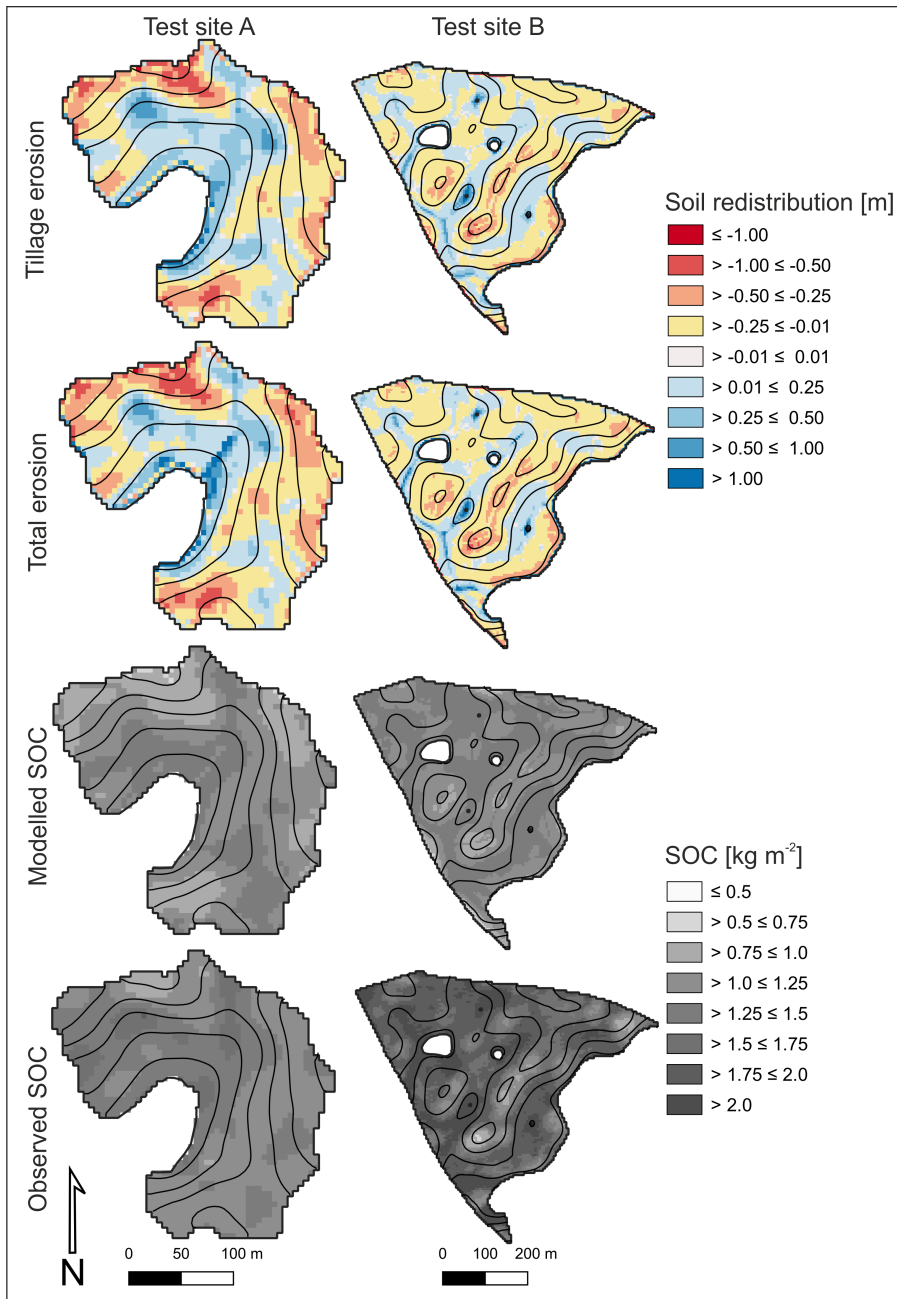


Figure 6.5: Modelled spatial patterns of tillage-induced (first row) and total soil redistribution (second row) at the end of the 1000 years simulation period. Modelled (third row) and observed topsoil (first 0.1 m) SOC (last row). For the two test sites A (left) and B (right). Model results are produced with realisation R4 (medium TIL and low WAT). Black lines indicate 2 m contour intervals.

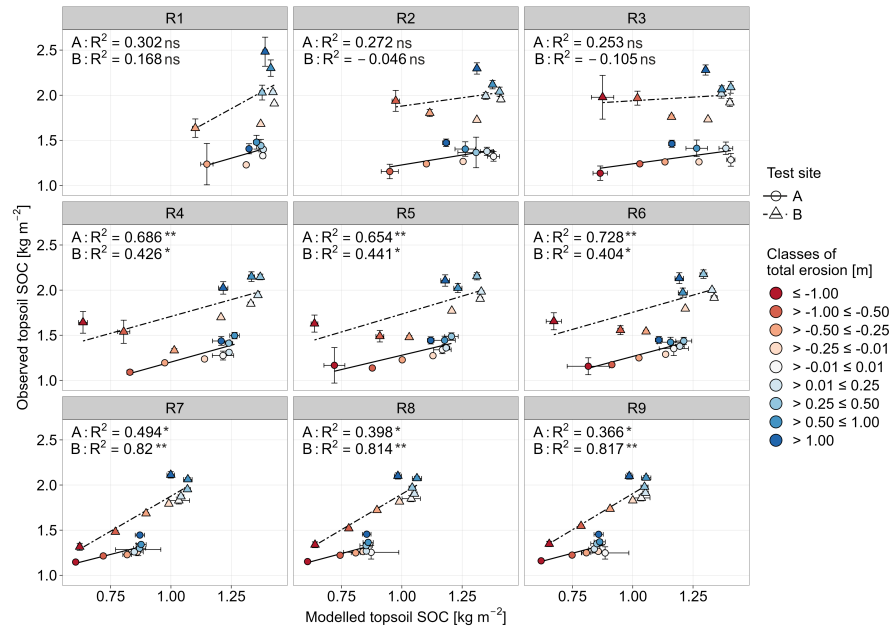


Figure 6.6: Modelled versus observed topsoil (first 0.1 m) SOC stocks for the two test sites A (circles) and B (triangles) and the nine realisations (in panels). Data is grouped into classes of total soil redistribution ranging from extreme erosion ( $\leq -1$  m, red) to high deposition ( $\geq 1$  m, blue). Error bars indicate the 95 % confidence interval of the mean per class. Black lines show the regression of the classified data (solid for A, dashed for B) with the respective adjusted coefficient of determination ( $R^2$ ; ns =  $p$ -value  $\geq 0.05$ , \* =  $p$ -value  $< 0.05$  and  $\geq 0.01$ , \*\* =  $p$ -value  $< 0.01$ ).

### 6.3.2 Results of modelling erosion-induced C-flux dynamics for 1000 years

The modelled C fluxes without soil redistribution indicated a C loss to the atmosphere following conversion to arable land for about the first 800 years of the simulation (Figure 6.7 a, b; *w/o soil redistribution*), with some interannual variability of vertical C fluxes due to the three-field economy (i. e. crops left on the field every third year). The resulting decrease in SOC stocks (Figure 6.7 e) was more pronounced for the first 500 years, nearly reaching a new equilibrium around 1700 CE. Soils turned into a slight C sink in the beginning of the 19<sup>th</sup> century, after an abrupt change in modelled plough depth from 0.1 to 0.2 m. This changed again at the beginning of the 20<sup>th</sup> century after the modelled plough depth was increased to 0.3 m and especially after the end of the three-field economy, which substantially reduced the modelled soil C input (Figure 6.7 a, b; *w/o soil redistribution*). Finally, soils turned into a C sink again after 1950 due to the extremely increasing yields (associated with a substantial increase in soil-C input) following the end of the Second World War (Figure 6.2 c).

Based on the model simulations with the representation of lateral soil redistribution processes, we found that at erosional sites (Figure 6.7 a) the C loss to the atmosphere was less pronounced compared

to sites without soil redistribution, and from about 1550 CE onwards eroded soils became a C sink. From this time onwards the C sink function steadily increased until 1900 CE, when it dropped due to changes in soil C input (i. e. end of the three field economy). The C sink function at eroding positions increased more pronouncedly again in the 20<sup>th</sup> century compared to sites without soil redistribution until the end of the modelling period.

Moreover, the simulations considering lateral soil redistribution processes revealed a decrease in vertical C fluxes in depositional sites, compared to the simulations without soil redistribution (Figure 6.7 b). Such differences became more pronounced over time, as increasingly more C was stored in colluvial soils. It is important to note that deep C burial (> 1 m soil depths) did successively become more important for the vertical C fluxes over time (Figure 6.7 b), whereas the increase in C mineralisation in the upper 1 m of depositional sites (first order kinetics) was reduced by deep burial. This is especially important in case of prolonged severe deposition, as more and more C-rich former topsoil is moving to depths below 1 m.

The simulated lateral C export due to water erosion (Figure 6.7 d;  $exp_{tot}$ ) in the test region was very small, especially since a new SOC equilibrium under arable land is reached. For approximately the first 200 years of the simulation, the C export steadily decreased as the SOC content of the topsoil being eroded substantially declined following land-use conversion. For about the next 600 years the modelled export steadily increased due to rising water erosion rates, as we assumed an increase in the C factor for the period in the low water erosion pathway (Figure 6.7 b; R4) used to analyse the entire study area. At the beginning of the 19<sup>th</sup> and 20<sup>th</sup> century, respectively, the increase in ploughing depth led to a reduction of the topsoil SOC content and hence less C export via water erosion.

Based on the conservative assumption that all lateral C fluxes leaving arable land were lost to the atmosphere (Figure 6.7 d;  $vf-exp_{tot}$ ), soil redistribution resulted in a steadily increasing C sink of about  $3 \text{ g C m}^{-2} \text{ yr}^{-1}$  at the end of the modelling period. This sink function is only slightly more pronounced if we assume that most C exported from arable land into neighbouring land uses or into kettle holes was stored and not mineralised, while only the proportion entering the stream network was lost to the atmosphere (Figure 6.7 d;  $vf-exp_{rest}$ ). Especially in the last two centuries of the simulation, deep C burial became more important for the entire soil redistribution-induced C balance of the study area (Figure 6.7 d;  $vf \text{ w/o deep C burial}$ ).

The sum of all C fluxes with and without lateral soil redistribution is also mirrored in the changes of the mean SOC stocks of the study area (Figure 6.7 e). Here it is interesting to note that for about the first 300 years after conversion to arable land, soil redistribution led to a faster decline in SOC stocks compared to the system without

soil redistribution. After about 500 years the reverse was simulated, leading to a mean difference between mean SOC stocks with and without redistribution of about  $0.42 \text{ kg C m}^{-2}$  (8.7%).

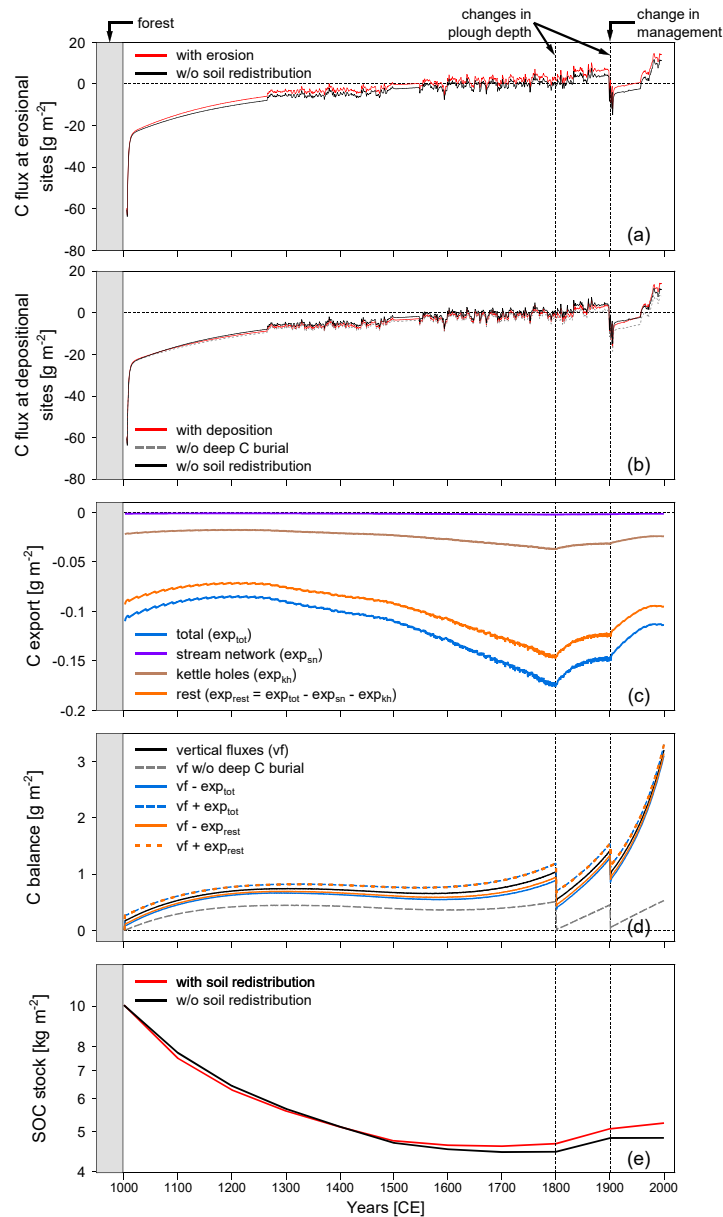


Figure 6.7: Temporal variation (1000 years) of annual vertical C fluxes, lateral C export, C balance, and SOC stocks modelled for the study region (R4) following conversion from forest to agricultural land (grey boxes). Plough depth was increased from 0.1 to 0.2 m and to 0.3 m in year 1800 and 1900, respectively (vertical dotted lines). Until 1900, *AGBM* was left on the field every third year. Vertical C fluxes at erosional (a) and depositional sites (b), total lateral C export (c), soil redistribution-induced C balance of all modelled fluxes (d), and mean soil SOC stocks of the entire study area (e; log-scaled y-axis). Notice that negative vertical C fluxes indicate a loss of C to the atmosphere, while positive C fluxes indicate a gain in soil C.

## 6.4 DISCUSSION

### 6.4.1 *Challenge of long-term soil redistribution and C turnover modelling*

Understanding current agricultural soil-landscape relations requires to consider the long-term soil change, as today's soil and SOC patterns cannot be explained via the short-term soil redistribution history. The importance of long-term soil redistribution processes in agricultural landscapes is particularly obvious in the Quillow catchment, as our results have demonstrated. Although soil redistribution in the study area increased with the intensive agricultural mechanisation since the 1960s (Frielinghaus and Vahrson, 1998), this does not explain the observed erosion rates and patterns in the area (Wilken et al., 2020), especially at slope shoulders, where signs of tillage erosion are clearly visible in aerial photographs from the 1950s (Figure 6.4, left). A comparison between our results with typical soil truncation and accumulation rates for the study area (Van der Meij et al., 2017) shows that it is necessary to consider the past millennium (i. e. since the beginning of agricultural management) to understand the landscape C dynamics.

However, any long-term and particularly landscape-scale modelling approaches are subject to considerable uncertainties. Here we did not intend to mimic detailed observational data of lateral soil fluxes (which are in any case not available at a commensurate temporal resolution to our model outputs) from individual sites of the 200 km<sup>2</sup> study area with a high degree of accuracy and precision. On the contrary, our investigative model evaluation approach was focused on testing the model's consistency for simulating long-term, landscape-scale spatial patterns of soil truncation and SOC stocks, while partially representing the uncertainties associated with parameter estimation in such an ambitious modelling experiment. As such, a set of model realisations (Figure 6.2; Figure 6.6) that combined different soil-redistribution assumptions were considered. The entire study area was ultimately analysed following the model realisation R<sub>4</sub> (i. e. medium tillage and low water erosion), which could explain 69% and 43% (see R<sup>2</sup> in Figure 6.6) of the current spatial pattern of SOC stocks in test sites A and B (Figure 6.1; Figure 6.5). This leads to an underestimation of the mean SOC stocks by 40% and 20% in the topsoil of test site A (50 cm soil depth) and B (plough layer), respectively. Importantly, the model outputs displayed a high agreement (81%) with independent data used for estimating areas of severe soil truncation.

Overall, these results are encouraging, considering that (i) we only calibrated C-turnover parameters, while the tillage and water erosion components of the model were applied 'blindly' to derive a set of plausible realisations for the whole study area; (ii) the model was parameterised to represent the average conditions in the entire study

area, not accounting for the anyway unknown specific land use and management history of the individual test sites; and that (iii) in the relatively rare cases in which soil erosion models have been tested against independent spatial data, results have generally shown a poor agreement with observational data (Batista et al., 2019). As such, our modelling outputs are consistent with independent lines of evidence of related phenomena and with our current understanding of long-term soil- and SOC-redistribution processes at landscape scale. This corroborates the usefulness of the employed modelling approach for elucidating soil redistribution and C dynamics in the study area over the last 1000 years.

#### 6.4.2 *Long-term soil redistribution and C dynamics*

This model-based analysis of the long-term, landscape-scale effects of soil redistribution following land conversion from forest to arable land upon C dynamics extends previous studies that mostly combine soil redistribution with SOC turnover over shorter time periods, smaller areas, and were based on soils that are already in C equilibrium due to long-term arable use (e. g. Dlugoß et al., 2012; Nadeu et al., 2015; Wilken et al., 2017b). Taking the conversion from forest to arable land into account clearly indicates that time since conversion is essential for the understanding of soil redistribution-induced C fluxes, which was to the best of our knowledge not included in previous long-term modelling studies (e. g. Bouchoms et al., 2017; Wang et al., 2017). Our results demonstrate that there is no dynamic replacement at erosional sites as long as topsoil soils still lose C following conversion from SOC-rich forest to SOC-depleted arable soils. This is particularly important as dynamic replacement is assumed to be one of the key processes for a potential C sink function of soil erosion (Doetterl et al., 2016; Harden et al., 1999). Within our simulation it took about 500 years until eroded soils in the study region started to act as C sink (Figure 6.7 a). This period would be substantially shorter in smaller, more erosion-prone catchments where SOC-rich topsoil from former forested areas is lost faster (Dlugoß et al., 2012; Juřicová et al., submitted to Soil & Tillage Research; Wilken et al., 2017b). This result underlines that it is essential to model entire landscapes instead of upscaling conclusions from small-scale studies.

Erosion-induced SOC loss and its partial deposition is most pronounced shortly after land conversion as the topsoil is still rich in SOC. Therefore, results from studies in regions where arable land was established centuries ago (e. g. Dlugoß et al., 2012; Juřicová et al., submitted to Soil & Tillage Research; Nadeu et al., 2015) might not allow to draw general conclusions for regions where land conversion happened recently. This corroborates the argument from Van Oost and Six (2023) that our understanding of coupled erosion and C turnover

processes is strongly biased towards humid/temperate settings, where land conversion mostly occurred centuries ago, while little is known for regions with on-going land conversion often located in tropical regions (Song et al., 2018).

#### 6.4.3 *Tillage-induced soil redistribution and C dynamics*

**TILLAGE AS THE MAIN DRIVER OF THE EROSION-INDUCED C PUMP.** Within our study area, tillage erosion was demonstrated to be a critically important process dominating the catchment's C balance and the C sink function induced by soil redistribution. Water erosion cannot be neglected due to extreme events that are responsible for crop losses, high sedimentation rates, and off-site damage (Frielinghaus and Schmidt, 1993; Frielinghaus et al., 1992). However, as illustrated by the historical aerial photograph in Figure 6.4, tillage-induced soil redistribution in this area is dominating and not only important since the introduction of heavy machinery 70 years ago (Van der Meij et al., 2017; Wilken et al., 2020; Winnige et al., 2003). In addition, tillage is known to further increase the susceptibility of arable soils to water erosion (Lobb et al., 1995) due to its effect on soil microporosity and changes in surface roughness (Poesen and Govers, 1985). The impact of tillage outcompetes soil redistribution by water due to specific conditions in the study area. The farming structures in the post-socialistic study area (large field sizes) perform tillage on a high optimisation level. Within a typical 5-year crop rotation (rapeseed – winter wheat – maize – winter wheat – winter barley) inversion tillage is only applied once between two small-grain cereals, while chisel plough is applied in all other years. The rationale is that chisel ploughing can be applied faster and requires less mechanical force (i. e. kinetic energy) compared to inversion ploughing, which reduces the time effort and fuel consumption, respectively (Dumanski et al., 2006; Hessel, 2007). Furthermore, the hummocky topography of the young morainic study area shows a short summit-foot slope distance that benefits tillage erosion, which does not increase with slope length such as water erosion. This characteristic topography also leads to large depositional areas (41 % of the study area; in comparison to  $25 \pm 7\%$  in a global estimate of Van Oost et al., 2007) that favours C burial and sequestration. In addition, there is a low hydrological and sedimentological connectivity to the river system in the study area. Only  $5 \times 10^{-4} \text{ t ha}^{-1}$  of eroded soil are exported by water to the river system, while ca. 20 times more C ( $0.1 \text{ t ha}^{-1}$ ) are buried in kettle holes. Even if this limited hydrological connectivity benefits the water-redistribution-induced C sink function, tillage erosion is still dominant as erosive rainfall appears only on a relatively low frequency in this region (Deumlich, 1999; Wilken et al., 2018).

RECENT DEVELOPMENTS IN TILLAGE-INDUCED SOIL REDISTRIBUTION. Tillage erosivity partly decreased due to the introduction of pesticides for weed control which reduced the relevance of inversion tillage over the past decades (Lobb et al., 2007). Also in our study area, non-inversion conservation tillage receives more attention and is already applied to 47% of the cropland area (44% conventional tillage and 0.06% no-till; Destatis, 2017). Nevertheless, it needs to be mentioned that conservation tillage focuses on water erosion mitigation, while tillage erosion is not accounted for. A recent study demonstrated that soil tillage by chisel plough leads to substantially more tillage erosion than inversion implements (Öttl et al., 2022). Hence, tillage practices show high spatiotemporal variation, which is fused to a large sensitivity of tillage erosion predictions. The sensitivity is reflected in the erosion pathways, whereby the difference between the C balance of the low and high tillage erosion pathways (C balance  $R_8 - R_2$ ) is higher than the difference in the C balance without and with consideration of deep v burial, respectively. Hence, the C balance and corresponding sequestration potential of agricultural soil systems is mainly driven by individual farmers' decisions.

#### 6.4.4 *The way ahead for long-term and large-scale soil redistribution and C dynamics modelling*

It is evident that long-term and large-scale simulations are needed to gain understanding of C dynamics, not only for scientific purposes but also to find adapted management strategies to increase soil C sequestration. From our perspective, the implementation of the following three processes would substantially increase the simulation quality of coupled soil redistribution and C turnover models.

KEEPING TRACK OF TOPOGRAPHIC CHANGE BY SOIL REDISTRIBUTION. The model does not account for topographic change related to soil redistribution (i. e. DEM update). For shorter temporal scales (ca. 50-100 years; e. g. Dlugoß et al., 2012; Nadeu et al., 2015; Wilken et al., 2017b), the topographic change has a limited impact, but for a modelling period of 1000 years, neglecting DEM update affects lateral and vertical C dynamics. In a tillage-erosion dominated study area like the Quillow river catchment, both erosion and deposition processes will be substantially overestimated at individual raster cells (erosion: slope shoulders; deposition: footslopes and field borders). This is due to a constant erosion and deposition pattern, which becomes more relevant towards the end of the simulation period. This means that severe erosion is simulated for a smaller spatial area than it would take place in reality. As a result, at erosional sites substantial dynamic replacement is calculated for a limited number of raster cells and SOC is buried more likely below 1 m at severe depositional

sites. The latter is especially critical if the modelled deposition is large enough that deposited C-rich topsoil reaches soil layers below 1 m, where it is assumed that SOC is stable in time (Rumpel and Kögel-Knabner, 2011). Hence, taking the topographic change corresponding to soil redistribution into account would be an important step forward to improve the quality of soil patterns.

**PLANT FEEDBACK ON SOIL DEGRADATION.** Coupling the impact of soil redistribution against plant growth would be a great step towards a better representation of C dynamics in disturbed landscapes. A cornerstone for a landscape to function as a C sink is dynamic replacement of eroded C by fresh biomass C due to the uplift of unsaturated reactive minerals (Doetterl et al., 2016; Harden et al., 1999). However, this calls for constantly high yields and corresponding C input at eroding landscape positions (Doetterl et al., 2016; Van Oost and Six, 2023). As severe long-term soil erosion typically causes declining yields (e.g. Bakker et al., 2004; Den Biggelaar et al., 2001; Herbrich et al., 2018), which was also demonstrated in the study area (Öttl et al., 2021), C input is overestimated at erosional areas. On the other hand, C input is underestimated at depositional areas due to more favourable growing conditions (Heckrath et al., 2005; Papiernik et al., 2005; Öttl et al., 2021), which attenuates overstating the C sink term (Quinton et al., 2022; Öttl et al., 2021).

**SOC BURIAL IN DEEPER SOIL LAYERS (< 1 M).** Long-term soil redistribution following land conversion from natural forest to arable land leads to deep burial of SOC (< 1 m; Hoffmann et al., 2013). In our modelling approach the assumptions regarding the stability of SOC buried below 1 m are of tremendous importance in the range of soil-redistribution induced C fluxes (Figure 6.7 d). Assuming that all SOC allocated below 1 m would be immediately mineralised, the overall soil-redistribution induced C sink would be only 0.11 ‰ of mean SOC stocks per year, while it would be 0.66 ‰ if all SOC stocks would be stabilised. However, long-term modelling of SOC turnover in these deep layers is challenging due to the generally limited knowledge of SOC turnover in deep soils (Rumpel and Kögel-Knabner, 2011) and the fluctuating stagnic soil conditions partly associated with landscape positions where soil is deposited.

## 6.5 CONCLUSION

In this study, the long-term (1000 years) effect of soil redistribution upon C fluxes and SOC stocks was modelled in a study region of 200 km<sup>2</sup> in north-eastern Germany. Different to earlier studies focussing on erosion-induced C fluxes we included the change in SOC stocks following conversion from a natural forest to arable land and accounted for changes in agricultural practises and production over time.

The modelling results from a study area representing ground moraine landscapes as typically found in northern Europe, Asia, and North America indicate that soil redistribution in such regions is resulting in a slight C sink, increasing the landscape-scale SOC stocks by 0.66 ‰ per year as compared to an area without erosion. This sink function mostly results from tillage-induced soil redistribution, while soil redistribution by water only plays a minor role, which is also quite typical for more continental climatic conditions. Modelling a representative segment of a larger landscape instead of focussing on a small (water) erosion prone area with steeper slopes indicates that the C sink function is less pronounced at this scale. The study also underlines the importance of addressing the soil-redistribution induced C fluxes starting with forest-related SOC stocks before conversion to arable land, because focusing only on the phase of arable soil use alone overestimates the erosion-induced sink function.

## 6.6 SUPPLEMENTARY MATERIAL

Table 6.3: Literature review as basis for the temporal variation of the  $k_{fit}$  values shown in Figure 6.2 a sorted by period. “Original reference” is the publication where the experiment is described which does not necessarily include the calculated  $k_{fit}$ -value. “Reference  $k_{fit}$ -value” is the publication that refers to the original reference but includes the  $k_{fit}$ -value. Abbreviations: CP = chisel plough, MP = mouldboard plough, TE = tillage implements, D = downslope, UD = alternating up- and downslope, C = contour-parallel, EXP = experiment, SIM = simulation.

Original reference	Reference $k_{fit}$ -value	$k_{fit}$ -value [ $\text{kg m}^{-1}$ ]	Country	Implement	Period	Slope [%]	Tillage speed [ $\text{km h}^{-1}$ ]	Tillage depth [m]	Bulk density [ $\text{kg m}^{-3}$ ]	Tillage direction	Method
Dupin et al. (2009)	Dupin et al. (2009)	9.59	Laos	manual (hoe)	P1	30-90	1.11	0.02	900	C	EXP
Kimaro et al. (2005)	Kimaro et al. (2005)	96	Tanzania	manual (hoe)	P1	31-67	-	0.05	1200	UD	EXP
Su and Zhang (2010)	Su and Zhang (2010)	118	China	manual (hoe)	P1	14-28	-	-	-	UD	Sim
Turkelboom et al. (1999)	Turkelboom et al. (1999)	43.2	Thailand	manual (hoe)	P1	17-82	-	0.09	1100	UD	EXP
Turkelboom et al. (1999)	Turkelboom et al. (1999)	45.1	Thailand	manual (hoe)	P1	17-82	-	0.09	1100	UD	EXP
Turkelboom et al. (1999)	Turkelboom et al. (1999)	48.2	Thailand	manual (hoe)	P1	17-82	-	0.09	1100	UD	EXP
Turkelboom et al. (1999)	Turkelboom et al. (1999)	52.4	Thailand	manual (hoe)	P1	17-82	-	0.09	1100	UD	EXP
Turkelboom et al. (1999)	Van Muysen et al. (2000)	77	Thailand	manual (hoe)	P1	17-82	-	0.09	1100	UD	EXP
Turkelboom et al. (1999)	Turkelboom et al. (1999)	98.7	Thailand	manual (hoe)	P1	17-82	-	0.09	1100	UD	EXP
Wang et al. (2021)	Wang et al. (2021)	108.2	China	manual (hoe)	P1	6-50	-	0.18	1404	D	EXP
Wassmer, 1981	Kimaro et al. (2005)	173	Rwanda	manual (hoe)	P1	60	-	-	-	-	EXP
Zhang et al. (2004b)	Zhang et al. (2004b)	139	China	manual (hoe)	P1	4-47	-	-	-	UD	EXP
Zhang et al. (2004a)	Van Oost et al. (2006a)	141	China	manual (hoe)	P1	4-48	-	0.22	1310	UD	EXP
Zhang et al. (2004a)	Zhang et al. (2004a)	153	China	manual (hoe)	P1	4-48	-	-	-	UD	EXP
Zhang et al. (2009)	Zhang et al. (2009)	35	China	manual (hoe)	P1	8-65	-	0.19	1391	C	EXP

Original reference	Reference $k_{HI}$ -value	$k_{HI}$ -value [kg m <sup>-1</sup> ]	Country	Implement	Period	Slope [%]	Tillage speed [km h <sup>-1</sup> ]	Tillage depth [m]	Bulk density [kg m <sup>-3</sup> ]	Tillage direction	Method
Quine et al. (1999c)	Van Oost et al. (2006a)	31	China	manual and/or animal-pulled plough	P <sub>1,2</sub>	-	-	0.17	1300	C	EXP
Quine et al. (1999c)	Van Oost et al. (2006a)	250	China	manual and/or animal-pulled plough	P <sub>1,2</sub>	-	-	0.17	1300	UD	SIM
Nyssen et al. (2000)	Nyssen et al. (2000)	68	Ethiopia	animal pulled ard plough	P <sub>1,2,3,4</sub>	3	1.1	0.08	1143	C	SIM
Nyssen et al. (2000)	Nyssen et al. (2000)	272	Ethiopia	animal pulled ard plough	P <sub>1,2,3,4</sub>	48	1.1	0.08	1143	C	EXP
Dercon et al. (2007)	Dercon et al. (2007)	100	Ecuador	animal pulled ard plough	P <sub>1,2,3,4</sub>	18-36	-	-	-	C	EXP
Dercon et al. (2007)	Dercon et al. (2007)	300	Ecuador	animal pulled ard plough	P <sub>1,2,3,4</sub>	18-36	-	-	-	-	EXP
Quine et al. (1999b)	Quine et al. (1999b)	108	China	animal pulled CP	P <sub>2,3,4</sub>	11	-	0.2	1350	-	EXP
Quine et al. (1999b)	Quine et al. (1999b)	113	Zimbabwe	animal pulled CP	P <sub>2,3,4</sub>	6	-	0.2	1350	-	SIM
Barneveld et al. (2009)	Barneveld et al. (2009)	14.3	Syria	animal pulled CP	P <sub>2,3,4</sub>	2-43	-	-	1120	C	EXP
Barneveld et al. (2009)	Barneveld et al. (2009)	34.1	Syria	animal pulled CP	P <sub>2,3,4</sub>	2-43	-	-	1120	UD	EXP
Barneveld et al. (2009)	Barneveld et al. (2009)	47.4	Syria	animal pulled CP	P <sub>2,3,4</sub>	2-43	-	-	1120	UD	EXP
Rymshaw et al. (1997)	Van Oost et al. (2006a)	29	Venezuela	animal pulled CP	P <sub>2,3,4</sub>	33-78	-	0.2	1270	C	EXP

Original reference	Reference $k_{til}$ -value	$k_{til}$ -value [kg m <sup>-1</sup> ]	Country	Implement	Period	Slope [%]	Tillage speed [km h <sup>-1</sup> ]	Tillage depth [m]	Bulk density [kg m <sup>-3</sup> ]	Tillage direction	Method
Thapa et al. (1999a)	Van Oost et al. (2006a)	76	Philippines	animal pulled	P2, 3, 4	25-36	-	0.2	730	C	EXP
				MP							
Thapa et al. (1999b)	Van Oost et al. (2006a)	119	Philippines	animal pulled	P2, 3, 4	16-22	-	0.2	1000	C	EXP
				MP							
Thapa et al. (1999b)	Van Oost et al. (2006a)	152	Philippines	animal pulled	P2, 3, 4	16-22	-	0.2	1000	UD	EXP
				MP							
Quine et al. (1999b)	Quine et al. (1999b)	243	Lesotho	animal pulled	P4	7	-	0.15	1350	-	SIM
				MP (2 animals)							
Govers et al. (1994)	Govers et al. (1994)	111	Belgium	CP	P5	max. 25	4.5	0.15	1350	-	EXP
Lobb et al. (1999)	Van Muysen et al. (2000)	275	Canada	CP	P5	—	9.6	0.17	1580	-	EXP
Marques da Silva and Alexandre (2004)	Van Oost et al. (2006a)	27	Portugal	CP	P5	14-26	3-4	0.19	1600	-	EXP
Marques da Silva and Alexandre (2004)	Van Oost et al. (2006a)	75	Portugal	CP	P5	14-26	3.6	0.11	1600	-	EXP
Poesen et al. (1997)	Van Oost et al. (2006a)	282	Spain	CP	P5	2-41	2-3	0.16	1582	-	EXP
Quine et al. (1999a)	Quine et al. (1999a)	657	Spain	CP	P5	-	2.2	0.19	1382	UD	EXP
Tiessen et al. (2007)	Tiessen et al. (2007)	444-66	Canada	CP	P5	2-35	6.9	0.16	1367	-	EXP
Van Muysen and Govers (2002b)	Van Muysen and Govers (2002b)	123	Belgium	CP	P5	0-15	7.92	0.07	1130	UD	EXP
Van Muysen et al. (2000)	Van Muysen et al. (2000)	225	Belgium	CP	P5	max. 30	5.8	0.15	1560	-	EXP
Van Muysen et al. (2000)	Van Muysen et al. (2000)	545	Belgium	CP	P5	max. 30	7.2	0.2	1250	-	EXP
Mech and Free (1942)	Van Oost et al. (2006a)	13	USA	CP	P5	0-20	3.6	0.06	1155	-	-
				(before 1960)							

Original reference	Reference $k_{eff}$ -value	$k_{eff}$ -value [kg m <sup>-1</sup> ]	Country	Implement	Period	Slope [%]	Tillage speed [km h <sup>-1</sup> ]	Tillage depth [m]	Bulk density [kg m <sup>-3</sup> ]	Tillage direction	Method	
Mech and Free (1942)	Van Oost et al. (2006a)	28	USA	cultivator shovel	P5	10-20	-	0.08	-	-	UD	-
Marques da Silva and Alexandre (2004)	Marques da Silva and Alexandre (2004)	183	Portugal	harrow	P5	14-26	-	-	-	-	-	EXP
Mech and Free (1942)	Van Oost et al. (2006a)	78	USA	harrow	P5	-	-	0.12	-	-	UD	-
Tiessen et al. (2010)	Tiessen et al. (2010)	232.93	Costa Rica	harrow	P5	10	4.2	0.28	683	U	EXP	
Tiessen et al. (2010)	Tiessen et al. (2010)	468.75	Costa Rica	harrow	P5	10	5.3	0.29	663	UD	EXP	
Tiessen et al. (2010)	Tiessen et al. (2010)	788.89	Costa Rica	harrow	P5	10	6.4	0.3	642	D	EXP	
De Alba (2001)	Van Oost et al. (2006a)	164	Spain	MP	P5	15-35	4.5	0.24	1370	C	-	
De Alba (2001)	Van Oost et al. (2006a)	204	Spain	MP	P5	15-35	4.5	0.24	1370	UD	-	
Gerontidis et al. (2001)	Van Oost et al. (2006a)	134	Greece	MP	P5	6-22	4.5	0.2	1420	C	EXP	
Gerontidis et al. (2001)	Van Oost et al. (2006a)	252	Greece	MP	P5	6-22	4.5	0.3	1420	C	EXP	
Gerontidis et al. (2001)	Van Oost et al. (2006a)	360	Greece	MP	P5	6-22	4.5	0.4	1420	C	EXP	
Gerontidis et al. (2001)	Van Oost et al. (2006a)	383	Greece	MP	P5	6-22	4.5	0.3	1420	UD	EXP	
Gerontidis et al. (2001)	Van Oost et al. (2006a)	670	Greece	MP	P5	6-22	4.5	0.4	1420	UD	EXP	
Govers et al. (1994)	Govers et al. (1994)	234	Belgium	MP	P5	max 25	4.5	0.28	1350	UD	EXP	
Heckrath et al. (2006)	Van Oost et al. (2006a)	49	Denmark	MP	P5	-	4.9	0.23	1529	C	EXP	
Heckrath et al. (2006)	Van Oost et al. (2006a)	132	Denmark	MP	P5	-	4	0.26	1490	C	EXP	
Heckrath et al. (2006)	Van Oost et al. (2006a)	137	Denmark	MP	P5	-	4.1	0.22	1423	S	EXP	
Heckrath et al. (2006)	Van Oost et al. (2006a)	200	Denmark	MP	P5	-	4.9	0.25	1517	UD	EXP	
Heckrath et al. (2006)	Van Oost et al. (2006a)	239	Denmark	MP	P5	-	4.1	0.24	1449	S	EXP	
Heckrath et al. (2006)	Van Oost et al. (2006a)	281	Denmark	MP	P5	-	4.9	0.24	1555	S	EXP	
Heckrath et al. (2006)	Van Oost et al. (2006a)	335	Denmark	MP	P5	-	6.3	0.26	1507	UD	EXP	

Original reference	Reference $k_{HI}$ -value	$k_{HI}$ -value [kg m <sup>-1</sup> ]	Country	Implement	Period	Slope [%]	Tillage speed [km h <sup>-1</sup> ]	Tillage depth [m]	Bulk density [kg m <sup>-3</sup> ]	Tillage direction	Method
Kosmas et al. (2001)	Van Oost et al. (2006a)	63	Greece	MP	P5	14-21	4.5	0.18	1598	UD	EXP
Kosmas et al. (2001)	Van Oost et al. (2006a)	159.8	Greece	MP	P5	14-21	4.5	0.25	1598	UD	EXP
Lindstrom et al. (1992)	Van Oost et al. (2006a)	330	USA	MP	P5	1-14	7.6	0.24	1350	UD	EXP
Lindstrom et al. (1992)	Van Oost et al. (2006a)	363	USA	MP	P5	1-14	7.6	0.24	1350	C	EXP
Lobb et al. (1995)	Van Oost et al. (2006a)	184	Canada	MP	P5	-	4	0.15	1350	UD	EXP
Lobb et al. (1999)	Van Muysen et al. (2000)	346	Canada	MP	P5	-	6.2	0.23	1350	UD	EXP
Marques da Silva and Alexandre (2004)	Marques da Silva and Alexandre (2004)	770	Portugal	MP	P5	14-26	3.7	0.39	1680	UD	EXP
Montgomery et al. (1999)	Montgomery et al. (1999)	110	USA	MP	P5	7-31	3.6	0.23	1310	C	EXP
Quine and Zhang (2004b)	Van Oost et al. (2006a)	101	UK	MP	P5	-	5.9	0.21	1374	UD	EXP
Quine and Zhang (2004b)	Quine and Zhang (2004b)	112	UK	MP	P5	-	5.76	0.22	1420	UD	EXP
Quine et al. (2003)	Van Oost et al. (2006a)	324	New Zealand	MP	P5	5-10	7	0.17	1350	UD	EXP
Revel and Guirese (1995)	Van Oost et al. (2006a)	263	France	MP	P5	-	6.5	0.27	1350	UD	-
Tiessen et al. (2007)	Tiessen et al. (2007)	269.77	Canada	MP	P5	2-35	6.3	0.17	1367	-	EXP
Tsara et al. (2001)	Tsara et al. (2001)	793	Greece	MP	P5	5-25	-	0.3	1430	C	EXP
Van Muysen et al. (1999)	Van Muysen et al. 1999	70	Spain	MP	P5	max. 25	2.7	0.15	1650	UD	EXP
Van Muysen et al. (1999)	Van Muysen et al. 1999	254	Spain	MP	P5	max. 25	1.8	0.33	1070	UD	EXP
Van Muysen and Gov-ers (2002b)	Van Muysen and Gov-ers (2002b)	169	Belgium	MP	P5	max. 30	5.54	0.21	1561	UD	EXP

Original reference	Reference $k_{HI}$ -value	$k_{HI}$ -value [kg m <sup>-1</sup> ]	Country	Implement	Period	Slope [%]	Tillage speed [km h <sup>-1</sup> ]	Tillage depth [m]	Bulk density [kg m <sup>-3</sup> ]	Tillage direction	Method
Van Muysen and Govers (2002b)	Van Muysen and Govers (2002b)	224	Belgium	MP	P5	max. 30	5.22	0.25	1498	UD	EXP
Mech and Free (1942)	Van Oost et al. (2006a)	24	USA	MP (before 1960)	P5	10-20	3.6	0.08	1155	UD	-
Petersen, 1960	Van Oost et al. (2006a)	64	USA	MP (before 1960)	P5	-	3.6	0.16	1239	C	-
Govers et al. (1994)	Van Muysen et al. (2006)	133	Belgium	series of TE	P5	max. 25	-	-	-	UD	EXP
Govers et al. (1994)	Govers et al. (1994)	400	Belgium	series of TE	P5	max. 25	4.5	0.28	1350	UD	EXP
Govers et al. (1994)	Govers et al. (1994)	600	Belgium	series of TE	P5	max. 25	4.5	0.28	1350	UD	EXP
Govers et al. (1996b)	Govers et al. (1996b)	348	UK	series of TE	P5	5	-	-	-	-	SIM
Govers et al. (1996b)	Govers et al. (1996b)	397	UK	series of TE	P5	5	-	-	-	-	SIM
Quine et al. (1994)	Quine et al. (1994)	550	Belgium	series of TE	P5	-	-	-	-	UD	-
Van Muysen et al. (2006)	Van Muysen et al. (2006)	781	Belgium	series of TE	P5	0-17	-	-	-	UD	experiment
Wilken et al. (2020)	Wilken et al. (2020)	350	Germany	series of TE	P5	0-18	-	-	-	UD	SIM
Van Muysen et al. (2006)	Van Muysen et al. (2006)	167	Belgium	series of TE	P5	0-17	-	-	-	UD	EXP
Van Oost et al. (2000)	Van Oost et al. (2000)	900	Belgium	series of TE	P5	-	-	-	-	UD	-
Lobb et al. (1999)	Van Muysen et al. (2000)	369	Canada	tandem disc	P5	-	3.02	0.17	1105	UD	EXP

## GENERAL DISCUSSION AND CONCLUSION

---

### 7.1 SUMMARY AND GENERAL DISCUSSION

Soil erosion has been a major threat since the onset of settled agriculture and thus, has controlled the rise and fall of early civilisations (Lal et al., 2007; Montgomery, 2007a). The impact of soil redistribution by tillage and water on crop yields as well as on soil organic carbon (SOC) translocation and dynamics is studied at a relatively large spatial (ca. 200 km<sup>2</sup>) and temporal scale (1000 years) taking into account the history of agricultural management. All chapters of this thesis deal with the same study area, namely the catchment of the River Quillow located in the Uckermark region in Northeast Germany. The results might be transferable to other hummocky young moraine landscapes in the world (e. g. in Canada, Denmark, Russia, Sweden, the USA) that are agriculturally used (approximately  $0.9 \times 10^6$  km<sup>2</sup>; Sommer et al., 2004). The main innovations of this thesis and its contributions to the scientific community are as follows:

- 1) This thesis comprises the first study that assesses the spatial patterns of crop biomass in the Uckermark region and clearly attributes them to tillage-induced soil redistribution.
- 2) Soil redistribution leads to an overall reduction in mean crop yields at landscape scale, especially in relatively dry years. The soil redistribution-induced yield losses at erosional areas are to some extent outweighed by increased yields at depositional areas in wet-to-normal years.
- 3) Chisel tillage induces larger soil redistribution than mouldboard ploughing when it is used with the same tillage depth and speed on sloping land, thereby questioning its usefulness as soil conservation implement.
- 4) Tillage-dominated soil redistribution contains the potential to increase SOC sequestration and even compensate carbon (C) losses due to land conversion when the time since the onset of widespread agriculture is considered and the impact of erosion as well as deposition are considered.

### 7.1.1 *Effect of soil redistribution on the yield potential of agricultural landscapes*

Several approaches have been applied to assess the impact of soil redistribution on the agronomic productivity at the landscape scale. First, the interrelation between the Enhanced Vegetation Index (EVI) and total soil redistribution modelled with SPEROS-C was analysed for a normal and a dry year (Chapter 4). Thereby, the EVI served as a proxy for crop biomass or yield of four different crop types (maize, winter barley, winter rapeseed, and winter wheat). Second, biomass production of maize and winter wheat was modelled under different soil redistribution conditions with AQUACROP (Chapter 5). It was then combined with long-term (1000 years) tillage-induced soil redistribution modelled with SPEROS-C. Third, a systematic literature review was conducted on soil surface removal plot experiments (so-called *desurfacing experiments*; Chapter 5). It enables a comparison of the effect of surface lowering on crop yields in agricultural systems with high versus low fertiliser input.

The results of Chapters 4 and 5 agreed on the conclusion that tillage on slopes thins soils and reduces crop yields. Eroded areas show the lowest EVI values, while the highest EVI values are found in depositional areas (Chapter 4). The differences in the EVI between erosional and depositional sites were more pronounced in the analysed normal-to-dry year. The net effect at the landscape scale that results from EVI reductions at erosional sites and increased EVI at depositional sites compared to areas without pronounced erosion or deposition ranges from -10.2 % for maize in the normal-to-dry year to +3.4 % for winter barley in the wet year. For winter rapeseed and winter wheat the net effect was nearly zero, which indicates that depositional areas outweighed the reduction at erosional sites.

Modelling the feedback of soil redistribution and crop yields for the next 50 - 100 years shows that the overall yields are likely to further decline, especially with increased tillage intensity and reduced water availability (Chapter 5). In 50 (100) years, winter wheat biomass is expected to decline between 6.6 and 7.1 % (8 - 10 %) depending on tillage intensity in normal-to-dry years and 3.3 to 4.4 % (4.3 - 5.9 %) in wet years. Maize biomass is expected to be less affected in the next 50 (100) years, with reductions of 3.1 to 4.0 % (3.9 - 5.9 %) in normal-to-dry years and between 1.1 and 1.9 % (1.9 - 3.2 %) in wet years.

The effect of soil loss upon crop yield is more pronounced in case of zero or low fertiliser inputs (Chapter 5). In agricultural systems with high fertiliser inputs the reduction in soil depth and the accompanied reduced ability of the soil to store and supply water to the plants is more important than the loss of nutrients.

The methodological approach used in Chapter 4 would have been even more meaningful if the remote sensing signal of the EVI was

converted into yield information. Therefore, field measurements of aboveground biomass (AGBM) are required that are taken at the time of the satellite overpass. Regarding the methodology of Chapter 5, the model setup could be expanded to other crop types as they showed quite different behaviour in the first approach. Moreover, model assumptions could be refined by detailed information on land use history for modelling a longer time span (e. g. tillage intensity, percentage of cropland, crop rotations, etc.). The necessary data for improving the approaches of both chapters were not available for this thesis. However, both modelling studies were able to illustrate the general problem of crop yield reduction due to tillage-dominated soil redistribution.

To sum up, tillage erosion is an important driver of in-field variation of soil patterns affecting crop biomass production. However, some crop types are more sensitive to soil thinning than others (e. g. maize is more affected than winter wheat). Tillage was already found to increase landscape heterogeneity through the redistribution of soil from upland positions to depressions in other studies. However, these studies only considered smaller spatial scales (plot to field scale, e. g. Papiernik et al., 2005; Stadler et al., 2015; Taylor et al., 2003), smaller temporal scales (tracer studies capturing the last 45 - 60 years, e. g. Heckrath et al., 2005; Yang et al., 2019) or only one crop type (maize for 300 km<sup>2</sup> and 5.52 km<sup>2</sup>, respectively; Battiston et al., 1987; Yang et al., 2019). The strong interaction between climate and the yield/soil-depth response indicates that this problem will be even more severe in the future taking into account climate projections that prognose increasing summer temperatures and more dry spells in summer for the study region (Gerstengarbe et al., 2003; Heinrich et al., 2018). The main findings do not only have implications for the future but also for regions or agricultural systems that are faced with low fertiliser availability as well as shallow soils and thus, are assumed to suffer more in case of land degradation due to soil redistribution by tillage.

### 7.1.2 *Dominance of tillage erosion*

Tillage-induced soil redistribution was found to be the dominant erosion agent in the study area due to various characteristics of the region (Chapters 4 and 6). In general, it is located in a hummocky young moraine landscape that has a specific undulating morphometry with a high relief energy (Winnige et al., 2003). The short summit-footslope distances (on average 35 m) and thus, immediate changes between convex and concave landscape positions, lead to a high susceptibility to tillage erosion, which mainly depends on slope curvature (Deumlich et al., 2006; Van Oost et al., 2006a).

Nowadays, the most prominent property facilitating soil redistribution by tillage is the relatively large average field size of 22 ha (0.4

to 50 ha; 5<sup>th</sup> and 95<sup>th</sup> percentile, respectively). Only approximately 20 % of agricultural fields in Germany meet the category of *large* fields ( $> 16 \leq 100$  ha), while 52 % are classified as *medium* ( $> 2.56 \leq 16$  ha; Lesiv et al., 2019). There are regions in Europe that are characterised by much smaller mean field sizes, e. g. landscapes in Lower Franconia, Germany, with ca. 2 ha and in Scania, southern Sweden, with mean field sizes around 12 ha (Clough et al., 2020). However, in North America and Europe a high proportion of the fields are even larger (45 and 32 % are *very large* fields  $> 100$  ha, respectively) and one third are in the same category as the fields in the study area (31 and 30 % are *large* fields  $> 16 \leq 100$  ha, respectively). Depending on the specific properties of these regions, the large field sizes are not only problematic regarding tillage erosion due to the possibility of using large machinery but also regarding an enhanced sedimentological and hydrological connectivity between landscape elements (Baartman et al., 2020). This means that water and wind erosion can be increased due to high slope lengths and the lack of structural elements, respectively (Bakker et al., 2008; Devátý et al., 2019; Ouyang et al., 2010).

Another characteristic favouring the dominance of tillage-induced soil redistribution in the study region is the relatively low precipitation rate. The mean annual precipitation is just a little more than half of Germany's long-term rainfall (466 mm vs. 781 mm; 20-year average 2001 - 2020; DWD, 2021; UBA, 2022). Moreover, the study region is characterised by a relative small number of erosive rainfall events (7 - 11 days per year; Deumlich, 1999)<sup>†</sup>. In other areas of Germany, this number can reach ca. 20 - 40 days per year (Deumlich and Gericke, 2020)<sup>††</sup>.

Furthermore, the soils of the study region have a relatively low susceptibility to water erosion due to the typical soil texture ranging from loamy sand (80 % sand, 15 % silt, 5 % clay) to sandy clay loam (50 % sand, 30 % silt, 20 % clay; Chapter 4). Analysis of available soil data resulted in a soil erodibility factor  $K$  of  $0.014 - 0.028 \text{ Mg ha hr ha}^{-1} \text{ MJ}^{-1} \text{ mm}^{-1}$  (Chapters 4 and 6). This is at the lower end of the range of the mean  $\pm$  one standard deviation  $K$  factor for Europe ( $0.032 \pm 0.009 \text{ Mg ha hr ha}^{-1} \text{ MJ}^{-1} \text{ mm}^{-1}$ ; Panagos et al., 2014). Compared to that, Luvisols in West Germany ( $K$  factor of 0.058 to 0.061; Dlugoß et al., 2012) and the loess-derived soils in Czech Republik and Belgium have a much higher susceptibility to water erosion ( $K$  factor of 0.04 and  $0.041 \text{ Mg ha hr ha}^{-1} \text{ MJ}^{-1} \text{ mm}^{-1}$ , respectively; Bouchoms et al., 2017; Juřicová et al., submitted to Soil & Tillage Research).

The evidence of tillage as an important or even dominant erosion agent in the study region is quite new. Until the end of the 1990s, water erosion was still assumed to be the dominant driver of soil

<sup>†</sup> heavy rainfall event defined as daily precipitation  $\geq 10$  mm or a maximum 30-minute rainfall intensity  $I_{30} \geq 10$  mm

<sup>††</sup> heavy rainfall event defined as daily precipitation  $\geq 20$  mm.

redistribution due to the large deposition rates in kettle holes after single heavy rain events (Frielinghaus and Vahrson, 1998). At the beginning of the 21<sup>st</sup> century, indicators such as the typical erosion pattern of eroded hilltops and slope shoulders led to first experiments to assess tillage erosion rates (Winnige, 2004; Winnige et al., 2003). Only recently, a first field-scale study gave evidence on the dominance of tillage erosion (Wilken et al., 2020). Hence, the landscape-scale modelling approach of this thesis strengthens the previous findings by showing that crop biomass patterns as well as topsoil SOC pattern mostly follow the pattern of soil redistribution by tillage and only have low similarities with that by water (Chapters 4 and 6). However, recent data analysing the last 20 years show a trend of more intense erosive rainfalls and an increase in the *R factor* leading to the presumption of rising water erosion rates in Germany in the near future (Auerswald et al., 2019; Deumlich and Gericke, 2020).

To conclude, the dominance of tillage erosion highlights the importance of land management and farmers' decisions regarding soil redistribution by tillage (e. g. size and power of the tractors used, erosivity of the tillage implement, field size, etc.) and water (e. g. cover crops, landscape structure, slope length, etc.).

### 7.1.3 *Impact of agricultural management on soil redistribution*

An extensive literature review was conducted to reconstruct the historical development of tillage practices and their erosive power (Chapter 6). In total, 95 studies assessing soil redistribution rates by different tillage implements in 24 countries were included (see Supplementary Information in Section 6.6). In some of the countries manual hoeing or the use of traditional wooden ploughs pulled by animals are still common due to environmental or social circumstances (slopes are too steep for machines and/or low development status; e. g. Nyssen et al., 2000; Zhang et al., 2009).

Reconstructing the historical development of tillage implements in the study region over the past 1000 years by using the literature-derived tillage transport coefficient ( $k_{til}$ ) values (Chapter 6) shows that manual hoeing conducted on slopes has a substantial impact on soil movement (median  $k_{til}$  of  $98 \text{ kg m}^{-1} \text{ yr}^{-1}$ ; Chapter 6). Reasons are that it is nearly always carried out in downslope direction (non-alternating) and thus, soil movement follows gravity (e. g. Turkelboom et al., 1999; Zhang et al., 2009). It has to be noted that those experiments were conducted at slopes that are too steep to use machinery and higher than the slopes of the study region, which means that the  $k_{til}$  values might be slightly overestimated (mean slopes  $\pm$  one standard deviation of  $27\% \pm 14\%$  compared to  $4\% \pm 4\%$  in the study region; Chapter 6). However, it becomes obvious that not only tillage by mouldboard ploughs causes soil erosion but *all* tillage implements contribute to

soil redistribution. Hand-held tools even lead to net downslope soil translocation when they are conducted upslope, contour parallel or at terraces (Kimaro et al., 2005; Su and Zhang, 2010; Zhang et al., 2004a). Furthermore, the literature data show the expected increase of the erosivity of tillage implements with time, especially since the onset of intense mechanisation of agriculture in the 20<sup>th</sup> century.

Nowadays, non-inversion chisel ploughs are assumed to have a lower impact on soil redistribution rates than soil-inverting mouldboard ploughs and are often used as conservation tillage implements (e. g. Lal et al., 2007; Zikeli and Gruber, 2017). This general notion is confirmed by comparing soil redistribution rates of modern mouldboard and chisel ploughs (Table 3.2). However, when the literature values are normalised to the same tillage depth, the tillage erosion coefficients of chisel tillage exceed those of mouldboard tillage on average (Table 3.2). To assess soil redistribution rates by the two contrasting tillage implements in the study area of this thesis, tillage experiments were carried out at three different slopes. When tillage speed and depth is kept constant for both implements and all slopes, the non-inversion chisel plough leads to more than three times higher soil redistribution rates compared to the inversion plough (Table 3.2).

This leads to the conclusion that non-inversion tillage alone is not sufficient for acting as a soil conservation tool. For reducing tillage erosion it is necessary to decrease tillage speed and depth as well. To meet the standards of conservation agriculture, additional measures are required, e. g. leaving crop residues on the field so that at least 30 % of the soil are covered by a vegetative mulch (CTIC, 2017; Zikeli and Gruber, 2017).

The great diversity of conservation tillage systems ensures the applicability to all soil types and farming systems (Carter, 2004; Huggins and Reganold, 2008; Zikeli and Gruber, 2017). Reasons for adoption of conservation agriculture are not only a reduction in soil degradation by tillage, water, and wind but also several economic and environmental incentives that are already mentioned in Chapter 2. The review of Zikeli and Gruber (2017) reveals that the main motive of German organic farmers for adopting reduced and no-tillage is the maintenance of soil quality. However, the dominance of conventional tillage, not only in Germany but also globally (see numbers in Chapter 2), shows that the risk of changing to conservation agriculture for farmers is still too high (Huggins and Reganold, 2008). Yield limiting factors such as weed pressure and reduced nitrogen availability highly influence their level of acceptance (Zikeli and Gruber, 2017). However, there is a strong need to enhance sustainability of agricultural production systems while improving the quality of soils and the environment (Lal et al., 2007).

#### 7.1.4 *Impact of soil redistribution on the carbon (C) balance*

Modelling a millennium of soil redistribution by tillage and water as well as accompanied SOC redistribution and C turnover on a regional scale (ca. 200 km<sup>2</sup>) enabled the assessment of soil redistribution on the C balance of the study region (Chapter 6). The focus lies on the impact of agricultural practices on land-atmosphere exchange of carbon dioxide (CO<sub>2</sub>). Therefore, the spatially-explicit soil redistribution and SOC turnover model SPEROS-C was fed with varying input variables according to different realisations of the development of agricultural management as well as rain erosivity over the past millennium. The historical development and erosive power of agricultural practices in the study region is based on the literature review already discussed above (Section 7.1.3). The results of the model realisations were compared to two test sites in the study region for evaluating the model results (size of test sites: 4.4 ha and 20.5 ha).

This is (to my knowledge) the first modelling study of coupled soil redistribution and SOC turnover that starts with forest soils as steady-state condition, thereby taking C fluxes due to conversion from forest to agriculture into account. Starting the modelling approach 1000 years ago with homogeneously distributed forest soil conditions is much closer to reality than most other approaches. Studies that assess the impact of soil redistribution by tillage (and water) since the onset of mechanised agriculture in the 20<sup>th</sup> century usually start with homogeneous, non-eroded agricultural soils (e. g. Dlugoß et al., 2012; Nadeu et al., 2015; Van Oost et al., 2005a). However, it is known that the recent, typical tillage erosion pattern in the study region cannot be the result of the last approximately 60 to 70 years of tillage (Wilken et al., 2020). Van Oost et al. (2005a) recognise that this is an implausible initial condition that is used due to the lack of data to determine the actual starting condition.

Starting with forest soils and thus, higher SOC stocks than in present-day agricultural soils means that in the first centuries a relatively large amount of C is mineralised by soil organisms and lost to the atmosphere as CO<sub>2</sub>. The reason is that early agricultural management was not able to provide enough C input by crops, crop residues, and manure, the soils are in disequilibrium and constitute a C source. This is the case until sufficient C input is available and C sequestration is as high or higher than C mineralisation. According to our modelling approach, it takes approximately 500 years until the combined processes of dynamic replacement and deep C burial are able to offset lateral SOC losses due to soil redistribution as well as vertical C losses due to mineralisation in the study region. After modelling a millennium of tillage and water erosion, the landscape-scale SOC stocks increase by 0.66 % as compared to an area without erosion.

The study of Bouchoms et al. (2017) is, to my knowledge, the first and only model approach that assesses the long-term (1000 years) SOC dynamics under the impact of land cover change and soil redistribution at a regional scale (591 km<sup>2</sup>). However, the parameterisation of the land cover classes (forest, cropland, grassland, and built area) follows non-eroded soils of today that are already in C equilibrium due to long-term arable use. Additionally, tillage-induced soil redistribution was not considered.

Although the results of this thesis show that it is essential to model a long time scale and a larger spatial scale (e.g. regional scale) for understanding SOC dynamics, such a modelling approach is subject to considerable uncertainties. Some part of the uncertainty is related to the topic of deep C burial. In general, relatively little is known about SOC in subsoil layers (below 0.3 m; Doetterl et al., 2016; Rumpel and Kögel-Knabner, 2011). It has been suggested that unfavourable edaphic conditions regarding temperature, nutrients, oxygen, and energy in subsoils limit the degradation of SOC contained in these soil horizons (Fontaine et al., 2007; Rumpel and Kögel-Knabner, 2011) but microbial activity might be present to some extent (Sagova-Mareckova et al., 2016). In the tillage-erosion dominated study region, soil material is mainly translocated within single fields, the majority of the eroded (often C-rich) topsoil material is deposited, and no transport related mineralisation of SOC occurs (Doetterl et al., 2016; Van Oost et al., 2004b). Moreover, eroded soil material is often deposited in drainless kettle holes that act as sediment traps. In the model approach of this thesis, SOC below 1 m is assumed to be inert. As a large amount of the eroded soil is deeply buried in the typical kettle holes of the study region, which are often layered with peat or filled with groundwater, this assumption is seen as reasonable.

Besides the limited biogeochemical understanding of deep C burial, the representation of the process of deep C burial should be improved in future long-term modelling studies. In reality, the soil surface would change due to soil profile truncation and accumulation resulting from ongoing soil redistribution. Hence, consecutive erosion and deposition would take place at different landscape positions as before, leading to a smoothed distribution and sedimentation of deposited material (in case of tillage-dominated soil redistribution). The model SPEROS-C is not able yet to update the soil surface, which leads to an uncertainty regarding the spatial distribution of erosional and depositional sites as well as SOC stocks. However, it was not the intention of the modelling approach to realistically represent observational data but to test the model's capability to simulate long-term, landscape-scale spatial patterns of soil truncation and SOC stocks. In this regard, the model results are encouraging as they displayed a high agreement (81 %) with independent data used for estimating areas of severe soil truncation.

Another improvement of the modelling approach would be necessary regarding a coupling of the impact of soil redistribution against plant growth. A prerequisite for a landscape to function as a C sink is dynamic replacement of eroded C by fresh C from crops or crop residues, which requires constantly high yields and corresponding C input (Doetterl et al., 2016; Harden et al., 1999). As already stated in Section 7.1.1, long-term soil erosion causes declining yields and thus, an overestimation of C inputs at erosional zones. However, the underestimation of C input at depositional zones due to more favourable growing conditions and hence higher yields is assumed to attenuate overstating the C sink term (Chapter 4 and 5).

In contrast to the homogeneous spatial distribution of crop yields, the temporal development of agricultural management is varied over the long term. Thereby, agricultural management is characterised by the combination of crop yields, crop residues left on the field, and tillage depth. Its temporal variation creates a more dynamic C balance than it was shown in previous studies, where only single parameters were varied, e. g. crop rotations *or* tillage intensity (Dlugoß et al., 2012; Wilken et al., 2017b). The approach used in this thesis might not only be closer to reality but one can also learn from the reaction of the model to the combination of assumptions.

To sum up, the effect of soil redistribution by tillage and water turns the study region into a slight C sink when the conversion from forest to crop land as well as tillage-induced soil redistribution is considered. As the C balance showed a high sensitivity to soil redistribution by tillage, this highlights the potential of land management influencing C dynamics.

## 7.2 CONCLUDING REMARKS AND OUTLOOK

“Following the American dustbowl of the 1930s, Franklin D. Roosevelt famously said, *‘the Nation that destroys its soil destroys itself’* (Roosevelt, 1937).

Eight decades later we might paraphrase his famous statement in a global context and say, *‘the world that secures its soil will sustain itself.’*”

— Koch et al. (2013)

The fact that soil science links SOC with soil functions not only as a potential mechanism for climate change mitigation but also with fundamental ecosystem services, such as provision of food, fiber, water and biodiversity, provides insight into a far broader set of environmental, economic and social outcomes for the planet (Koch et al., 2013). This emphasises the necessity to reduce soil losses due to the many benefits it brings for soil quality and the delivery of the mentioned ecosystems services.

Selecting management practices that help controlling erosion can not only improve productivity and promote sustained production but also help to maintain, or possibly increase, the storage of C in soils (Gregorich et al., 1998). However, cultural and scientific challenges suggest that proposals such as the *4 %-initiative* are overly optimistic. This initiative is considered critically because to achieve its full objective, it must be implemented immediately on all lands on Earth, and the practices must be sustained without change for decades (Amundson and Biardeau, 2018).

Nevertheless, it was already questioned more than 20 years ago, why the problems of erosion have not attracted more attention from politics and why preventive measures have not been widely employed although there is fundamental evidence of the deteriorating impact of soil degradation and of a clear economic benefit of its reduction (Pimentel, 2000). Future agricultural management needs to adapt the principles of no-tillage as well as precision agriculture to manage tillage speeds and depths in sloping agricultural land. This requires as much support as possible to farmers - from scientific and political side.

Although the overview of previous studies and the research results of this thesis show that soils are apparently unlikely to help us mitigating climate change, their preservation is essential for our survival (Amundson and Biardeau, 2018).

At the end of this thesis, for me the question remains on how long we can plough our soils until the whole soil system collapses and global food safety is jeopardised?

## BIBLIOGRAPHY

---

- Adhikari, K. and A. E. Hartemink (2016). 'Linking soils to ecosystem services – A global review'. In: *Geoderma* 262, pp. 101–111.
- Allen, Brett L., Verlan L. Cochran, TheCan Caesar and Donald L. Tanaka (2011). 'Long-term effects of topsoil removal on soil productivity factors, wheat yield and protein content'. In: *Archives of Agronomy and Soil Science* 57.3, pp. 293–303.
- Amelung, W., D. Bossio, W. de Vries, I. Kögel-Knabner, J. Lehmann, R. Amundson, R. Bol, C. Collins, R. Lal, J. Leifeld, B. Minasny, G. Pan, K. Paustian, C. Rumpel, J. Sanderman, J. W. van Groenigen, S. Mooney, B. van Wesemael, M. Wander and A. Chabbi (2020). 'Towards a global-scale soil climate mitigation strategy'. In: *Nat Commun* 11.1, p. 5427.
- Amundson, R., A. A. Berhe, J. W. Hopmans, C. Olson, A. E. Sztein and D. L. Sparks (2015). 'Soil and human security in the 21<sup>st</sup> century'. In: *Science* 348.6235.
- Amundson, R. and L. Biardeau (2018). 'Soil carbon sequestration is an elusive climate mitigation tool'. In: *Proceedings of the National Academy of Sciences of the United States of America* 115.46, pp. 11652–11656.
- Anderson, G. (1998). 'Genesis of hummocky moraine in the Bolmen area, southwestern Sweden'. In: *Boreas* 27, pp. 55–67.
- Andrén, O. and T. Kätterer (1997). 'ICBM: The introductory carbon balance model for exploration of soil carbon balances'. In: *Ecological Applications* 7.4, pp. 1226–1236.
- Anonymous (2019). *Statistical winter wheat yield data from the rural district of the Uckermark*.
- Araki, H. and M. Iijima (2001). 'Deep rooting in winter wheat: rooting nodes of deep roots in two cultivars with deep and shallow root systems'. In: *Plant Production Science* 4.3, pp. 215–9.
- Auerswald, K., P. Fiener and R. Dikau (2009). 'Rates of sheet and rill erosion in Germany – A meta-analysis'. In: *Geomorphology* 111.3-4, pp. 182–193.
- Auerswald, K., P. Fiener, W. Martin and D. Elhaus (2016). 'Corrigendum to "Use and misuse of the K factor equation in soil erosion modeling" [Catena 118 (2014) 220-225]'. In: *Catena* 139.271.
- Auerswald, K., F. K. Fischer, T. Winterrath and R. Brandhuber (2019). 'Rain erosivity map for Germany derived from contiguous radar rain data'. In: *Hydrology and Earth System Sciences* 23.4, pp. 1819–1832.

- Aufdenkampe, A. K., E. Mayorga, P. A. Raymond, J. M. Melack, S. C. Doney, S. R. Alin, R. E. Aalto and K. Yoo (2011). 'Riverine coupling of biogeochemical cycles between land, oceans, and atmosphere'. In: *Frontiers in Ecology and the Environment* 9.1, pp. 53–60.
- Baartman, J. E. M., J. P. Nunes, R. Masselink, F. Darboux, C. Biëlders, A. Degré, V. Cantreul, O. Cerdan, T. Grangeon, P. Fiener, F. Wilken, M. Schindewolf and J. Wainwright (2020). 'What do models tell us about water and sediment connectivity?' In: *Geomorphology* 367.
- Baker, V. R. (2017). 'Debates - Hypothesis testing in hydrology: Pursuing certainty versus pursuing uberty'. In: *Water Resources Research* 53.3, pp. 1770–1778.
- Bakker, M. M., G. Govers, A. van Doorn, F. Quetier, D. Chouvardas and M. D. A. Rounsevell (2008). 'The response of soil erosion and sediment export to land-use change in four areas of Europe: The importance of landscape pattern'. In: *Geomorphology* 98.3-4, pp. 213–226.
- Bakker, M. M., G. Govers and M. D. A. Rounsevell (2004). 'The crop productivity-erosion relationship: an analysis based on experimental work'. In: *Catena* 57.1, pp. 55–76.
- Barneveld, R. J., A. Bruggeman, G. Sterk and F. Turkelboom (2009). 'Comparison of two methods for quantification of tillage erosion rates in olive orchards of north-west Syria'. In: *Soil & Tillage Research* 103.1, pp. 105–112.
- Batista, P. V. G., J. A. C. Davies, M. L. N. Silva and J. N. Quinton (2019). 'On the evaluation of soil erosion models: Are we doing enough?' In: *Earth-Science Reviews* 197.
- Batista, P. V. G., D. L. Evans, B. M. Cândido and P. Fiener (2023). 'Does soil thinning change soil erodibility? An exploration of long-term erosion feedback systems'. In: *Soil* 9.1, pp. 71–88.
- Battin, Tom J., Sebastiaan Luyssaert, Louis A. Kaplan, Anthony K. Aufdenkampe, Andreas Richter and Lars J. Tranvik (2009). 'The boundless carbon cycle'. In: *Nature Geoscience* 2.9, pp. 598–600.
- Battiston, L. A., M. H. Miller and I. J. Shelton (1987). 'Soil erosion and corn yield in Ontario. I. Field evaluation'. In: *Canadian Journal of Soil Science* 67, pp. 731–745.
- Bayerl, G. (2006). *Geschichte der Landnutzung in der Region Barnim-Uckermark*.
- Behre, K.-E. (2008). *Landschaftsgeschichte Norddeutschlands. Umwelt und Siedlung von der Steinzeit bis zur Gegenwart*. Neumünster: Wachholtz Verlag.
- Bellamy, P. H., P. J. Loveland, R. I. Bradley, R. M. Lark and G. J. Kirk (2005). 'Carbon losses from all soils across England and Wales 1978-2003'. In: *Nature* 437.7056, pp. 245–248.

- Bellassen, V., D. A. Angers, T. Kowalczewski and A. Olesen (2022). 'Soil carbon is the blind spot of European national GHG inventories'. In: *Nature Climate Change* 12.4, pp. 324–331.
- Beranová, M. and A. Kubačák (2010). 'Dějiny zemědělství v Čechách, na Moravě a ve Slezsku (in Czech)'. PhD thesis.
- Berhe, A. A., C. Arnold, E. Stacy, R. Lever, E. McCorkle and S. N. Araya (2014). 'Soil erosion controls on biogeochemical cycling of carbon and nitrogen'. In: *Nature Education Knowledge* 5.8, p. 2.
- Berhe, A. A., J. W. Harden, M. S. Torn and J. Harte (2008). 'Linking soil organic matter dynamics and erosion-induced terrestrial carbon sequestration at different landform positions'. In: *Journal of Geophysical Research: Biogeosciences* 113.G4.
- Berhe, A. A., J. W. Harden, M. S. Torn, M. Kleber, S. D. Burton and J. Harte (2012). 'Persistence of soil organic matter in eroding versus depositional landform positions'. In: *Journal of Geophysical Research: Biogeosciences* 117.G2.
- Berhe, A. A., J. Harte, J. W. Harden and M. S. Torn (2007). 'The significance of the erosion-induced terrestrial carbon sink'. In: *BioScience* 57.4.
- Berhe, A. A. and M. Kleber (2013). 'Erosion, deposition, and the persistence of soil organic matter: Mechanistic considerations and problems with terminology'. In: *Earth Surface Processes and Landforms* 38.8, pp. 908–912.
- Blanco-Canqui, H. and R. Lal (2010). *Principles of soil conservation and management*. Dordrecht: Springer.
- Blum, W. E. H. (2005). 'Functions of soil for society and the environment'. In: *Reviews in Environmental Science and Bio/Technology* 4.3, pp. 75–79.
- Blum, W. E. H. and H. Eswaran (2004). 'Soils for sustaining global food production'. In: *Journal of Food Science* 69.2, pp. 37–42.
- Boardman, J. (1998). 'An average soil erosion rate for Europe: Myth or reality?' In: *Journal of Soil and Water Conservation* 53.1, pp. 46–50.
- Boardman, J. and J. Poesen (2006). 'Soil erosion in Europe: Major processes, causes and consequences'. In: *Soil erosion in Europe*. Ed. by J. Boardman and J. Poesen. Chichester, West Sussex, England: John Wiley & Sons, p. 839.
- Boardman, J., K. Vandaele, R. Evans, I. D. L. Foster and M. Aitkenhead (2019). 'Off-site impacts of soil erosion and runoff: Why connectivity is more important than erosion rates'. In: *Soil Use and Management* 35.2, pp. 245–256.
- Bolinder, M. A., D. A. Angers, G. Bélanger, R. Michaud and M. R. Laverdière (2002). 'Root biomass and shoot to root ratios of perennial forage crops in eastern Canada'. In: *Canadian Journal of Plant Science* 82.4, pp. 731–737.

- Bolinder, M. A., D. A. Angers, M. Giroux and M. R. Laverdière (1999). 'Estimating C inputs retained as soil organic matter from corn (*Zea Mays* L.)' In: *Plant and Soil* 215, pp. 85–91.
- Bolinder, M. A., A. J. VandenBygaart, E. G. Gregorich, D. A. Angers and H. H. Janzen (2006). 'Modelling soil organic carbon stock change for estimating whole-farm greenhouse gas emissions'. In: *Canadian Journal of Soil Science* 86.3, pp. 419–429.
- Bork, H. R., C. Dalchow, M. Dotterweich, T. Schatz and G. Schmidtchen (1998). 'Die Entwicklung der Landschaften Brandenburgs in den vergangenen Jahrtausenden'. In: *Geschichte der Landwirtschaft in Brandenburg*. Ed. by V. Klemm, G. Darkow and H. R. Bork. Budapest: Verlag Mezogazda, pp. 237–258.
- Borrelli, P., D. A. Robinson, L. R. Fleischer, E. Lugato, C. Ballabio, C. Alewell, K. Meusburger, S. Modugno, B. Schutt, V. Ferro, V. Bagarello, K. Van Oost, L. Montanarella and P. Panagos (2017). 'An assessment of the global impact of 21<sup>st</sup> century land use change on soil erosion'. In: *Nature Communications* 8.1, p. 2013.
- Bouchoms, S., Z. Wang, V. Vanacker, S. Doetterl and K. Van Oost (2017). 'Modelling long-term soil organic carbon dynamics under the impact of land cover change and soil redistribution'. In: *Catena* 151, pp. 63–73.
- Brunel, N., F. Meza, R. Ros and F. Santibáñez (2011). 'Effects of topsoil loss on wheat productivity in dryland zones of Chile'. In: *Journal of Soil Science and Plant Nutrition* 11.4, pp. 129–137.
- Buckwell, A., E. Nadeu and A. Williams (2022). *Sustainable Agricultural Soil Management in the EU: What's stopping it? How can it be enabled?* Tech. rep. RISE Foundation.
- Carter, M. R. (2004). 'Conservation tillage'. In: *Encyclopedia of soils in the environment*. Ed. by D. Hillel, J. L. Hatfield, D. S. Powlson, C. Rosenzweig, K. Scow, M. J. Singer and D. L. Sparks. Vol. 1. Cambridge, MA, USA: Academic Press, pp. 306–311.
- (2005). 'Conservation tillage'. In: *Encyclopedia of Soils in the Environment*, pp. 306–311.
- Chabbi, A., I. Kögel-Knabner and C. Rumpel (2009). 'Stabilised carbon in subsoil horizons is located in spatially distinct parts of the soil profile'. In: *Soil Biology and Biochemistry* 41.2, pp. 256–261.
- Chabbi, A., J. Lehmann, P. Ciais, H. W. Loescher, M. F. Cotrufo, A. Don, M. SanClements, L. Schipper, J. Six, P. Smith and C. Rumpel (2017). 'Aligning agriculture and climate policy'. In: *Nature Climate Change* 7.5, pp. 307–309.
- Chander, G., M. O. Haque, A. Sampath, A. Brunn, G. Trosset, D. Hoffmann, S. Roloff, M. Thiele and C. Anderson (2013). 'Radiometric and geometric assessment of data from the RapidEye constellation of

- satellites'. In: *International Journal of Remote Sensing* 34.16, pp. 5905–5925.
- Chappell, A., J. Baldock and J. Sanderman (2016). 'The global significance of omitting soil erosion from soil organic carbon cycling schemes'. In: *Nature Climate Change* 6.2, pp. 187–191.
- Chi, Bao-Liang, Cheng-Si Bing, F. Walley and T. Yates (2009). 'Topographic indices and yield variability in a rolling landscape of western Canada'. In: *Pedosphere* 19.3, pp. 362–370.
- Chirinda, N., S. D. Roncossek, G. Heckrath, L. Elsgaard, I. K. Thomsen and J. E. Olesen (2014). 'Root and soil carbon distribution at shoulderslope and footslope positions of temperate toposequences cropped to winter wheat'. In: *Catena* 123, pp. 99–105.
- Chlupáč, I., R. Brzobohatý, J. Kovanda and Z. Straník (2002). 'Geologická minulost České republiky [Geological history of the Czech Republic]'. PhD thesis.
- Clough, Y., S. Kirchweger and J. Kantelhardt (2020). 'Field sizes and the future of farmland biodiversity in European landscapes'. In: *Conservation Letters* 13.e12752.
- Coleman, K. and D. S. Jenkinson (2014). *RothC – A model for the turnover of C in soil. Model description and users guide*. Tech. rep.
- Conservation Technology Information Center (CTIC) (2017). *Tillage Type Definitions*. Tech. rep. URL: <https://www.mssoy.org/uploads/files/ctic.pdf>.
- Cooley, T., G. P. Anderson, G. W. Felde, M. L. Hoke, A. J. Ratkowski, J. H. Chetwynd, J. A. Gardner, S. M. Adler-Golden, M. W. Matthew, A. Berk, L. S. Bernstein, P. K. Acharya, D. Miller and P. Lewis (2002). 'FLAASH, a MODTRAN<sub>4</sub>-based atmospheric correction algorithm, its application and validation'. In: *IEEE International Geoscience and Remote Sensing Symposium*. Toronto, Ontario, Canada: IEEE.
- Crawley, M. J. (2013). *The R book*. 2<sup>nd</sup>. West Sussex, UK: Wiley.
- Czech Hydrometeorological Institute (2022). *Historical data*. URL: <https://www.chmi.cz/historicka-data/pocasi/zakladni-informace>.
- DIN ISO (19708:2017-08). *Bodenbeschaffenheit – Ermittlung der Erosionsgefährdung von Böden durch Wasser mit Hilfe der ABAG*.
- DWD Climate Data Center (CDC) (2018a). *Historical hourly station observations of 2m air temperature and humidity for Germany, version v006*.
- (2018b). *Historical hourly station observations of precipitation for Germany, version v21.3*.
- (2021). *Historical hourly station observations of precipitation for Germany, version v21.3*.
- De Alba, S. (2001). 'Modelling the effects of complex topography and patterns of tillage on soil translocation by tillage with mouldboard plough'. In: *Journal of Soil and Water Conservation* 56, pp. 335–345.

- De Alba, S., M. Lindstrom, T. E. Schumacher and D. D. Malo (2004). 'Soil landscape evolution due to soil redistribution by tillage: a new conceptual model of soil catena evolution in agricultural landscapes'. In: *Catena* 58.1, pp. 77–100.
- De Roo, A. P. J., C. G. Wesseling and C. J. Ritsema (1996). 'LISEM: A single-event physically based hydrological and soil erosion model for drainage basins. I: Theory, Input and Output'. In: *Hydrological Processes* 10.8, pp. 1107–1117.
- Den Biggelaar, C., R. Lal, K. Wiebe and V. Breneman (2001). 'The impact of soil erosion on crop yields in North America'. In: *Advances in agronomy*. Ed. by D. L. Sparks. Vol. 72. Massachusetts: Academic Press, pp. 1–52.
- (2003). 'The global impact of soil erosion on productivity I: absolute and relative erosion-induced yield losses'. In: *Advances in Agronomy*. Vol. 81. Advances in Agronomy. Massachusetts: Academic press, pp. 1–48.
- Dercon, G., G. Govers, J. Poesen, H. Sánchez, K. Rombaut, E. Vandebroek, G. Loaiza and J. Deckers (2007). 'Animal-powered tillage erosion assessment in the southern Andes region of Ecuador'. In: *Geomorphology* 87.1-2, pp. 4–15.
- Derpsch, R., T. Friedrich, A. Kassam and L. Hongwen (2010). 'Current status of adoption of no-till farming in the world and some of its main benefits'. In: *International Journal of Agriculture and Biological Engineering* 3, pp. 1–25.
- Desmet, P. J. J. and G. Govers (1996). 'A GIS procedure for automatically calculating the USLE LS factor on topographically complex landscape units'. In: *Journal of Soil and Water Conservation* 51.5, pp. 427–433.
- Deumlich, D. (1999). 'Erosive Niederschläge und ihre Eintrittswahrscheinlichkeit im Nordosten Deutschlands – Erosive rainstorms and their probability in Northeast Germany'. In: *Meteorologische Zeitschrift* 8.5, pp. 155–161.
- Deumlich, D., R. Funk, Mo. Frielinghaus, W.-A. Schmidt and O. Nitzsche (2006). 'Basics of effective erosion control in German agriculture'. In: *Journal of Plant Nutrition and Soil Science* 169.3, pp. 370–381.
- Deumlich, D. and A. Gericke (2020). 'Frequency trend analysis of heavy rainfall days for Germany'. In: *Water* 12.7.
- Deumlich, D., W. Mioduszeowski and A. Kocmit (2002). 'Analysis of sediment and nutrient loads due to soil erosion in rivers in the Odra catchment'. In: *Agricultural effects on ground and surface waters: Research at the edge of science and society*. Vol. 273. Wageningen, the Netherlands: IAHS Publication.

- Deumlich, D., H. Rogasik, W. Hierold, I. Onasch, L. Völker and M. Sommer (2017). 'The CarboZALF-D manipulation experiment – experimental design and SOC patterns'. In: *International Journal of Environmental & Agriculture Research* 3.1, pp. 40–50.
- Deumlich, D., R. Schmidt and M. Sommer (2010). 'A multiscale soil-landform relationship in the glacial-drift area based on digital terrain analysis and soil attributes'. In: *Journal of Plant Nutrition and Soil Science* 173.6, pp. 843–851.
- Devátý, J., T. Dostál, R. Hösl, J. Krása and P. Strauss (2019). 'Effects of historical land use and land pattern changes on soil erosion – Case studies from Lower Austria and Central Bohemia'. In: *Land Use Policy* 82, pp. 674–685.
- Diepenbrock, W. (2000). 'Yield analysis of winter oilseed rape (*Brassica Napus* L.): A review'. In: *Field Crops Research* 67.1, pp. 35–49.
- Diodato, N., P. Borrelli, P. Fiener, G. Bellocchi and N. Romano (2017). 'Discovering historical rainfall erosivity with a parsimonious approach: A case study in Western Germany'. In: *Journal of Hydrology* 544, pp. 1–9.
- Dlugoš, V., P. Fiener, K. Van Oost and K. Schneider (2012). 'Model based analysis of lateral and vertical soil carbon fluxes induced by soil redistribution processes in a small agricultural catchment'. In: *Earth Surface Processes and Landforms* 37.2, pp. 193–208.
- Doetterl, S., A. A. Berhe, E. Nadeu, Z. Wang, M. Sommer and P. Fiener (2016). 'Erosion, deposition and soil carbon: A review of process-level controls, experimental tools and models to address C cycling in dynamic landscapes'. In: *Earth-Science Reviews* 154, pp. 102–122.
- Doetterl, S., J. Six, B. Van Wesemael and K. Van Oost (2012). 'Carbon cycling in eroding landscapes: geomorphic controls on soil organic C pool composition and C stabilization'. In: *Global Change Biology* 18.7, pp. 2218–2232.
- Donald, C. M. and J. Hamblin (1976). 'The biological yield and harvest index of cereals as agronomic and plant breeding criteria'. In: *Advances in Agronomy*. Ed. by N. C. Brady. Vol. 28. Academic Press, pp. 361–405.
- Dormaar, J. F., C. W. Lindwall and G. C. Kozub (1986). 'Restoring productivity to an artificially eroded dark brown chernozemic soil under dryland conditions'. In: *Canadian Journal of Soil Science* 66, pp. 273–285.
- Dumanski, J., R. Peiretti, J. R. Benites, D. McGarry and C. Pieri (2006). 'The paradigm of conservation agriculture'. In: *Proceedings of World Association of Soil and Water Conservation* P1, pp. 58–64.
- Dupin, B., A. de Rouw, K. B. Phantahvong and C. Valentin (2009). 'Assessment of tillage erosion rates on steep slopes in northern Laos'. In: *Soil & Tillage Research* 103.1, pp. 119–126.

- ERDAS Inc. (2008). *Erdas Field Guide*.
- ESA (2015). *Sentinel-2 user handbook*. Tech. rep. URL: [https://sentinels.copernicus.eu/documents/247904/685211/Sentinel-2\\_User\\_Handbook](https://sentinels.copernicus.eu/documents/247904/685211/Sentinel-2_User_Handbook).
- ESRI (2017). *ArcMap Desktop version 10.5.1*. Environmental Systems Research Institute.
- Eck, N. J. van and L. Waltman (2010). 'Software survey: VOSviewer, a computer program for bibliometric mapping'. In: *Scientometrics* 84, pp. 523–538.
- Ehlers, W. and W. Claupein (2017). 'Approaches toward conservation tillage in Germany'. In: *Conservation tillage in temperate agroecosystems*. Ed. by M. R. Carter. Boca Raton, FL, USA: CRC Press, pp. 141–165.
- Evans, D. L., J. N. Quinton, J. A. C. Davies, J. Zhao and G. Govers (2020). 'Soil lifespans and how they can be extended by land use and management change'. In: *Environmental Research Letters* 15.9.
- Evans, D. L., J. N. Quinton, A. M. Tye, Á. Rodés, J. A. C. Davies, S. M. Mudd and T. A. Quine (2019). 'Arable soil formation and erosion: a hillslope-based cosmogenic nuclide study in the United Kingdom'. In: *Soil* 5.2, pp. 253–263.
- Fan, J., B. G. McConkey, H. Wang and H. H. Janzen (2016). 'Root distribution by depth for temperate agricultural crops'. In: *Field Crops Research* 189, pp. 68–74.
- Federal Statistical Office (1990–2018). *Statistical yearbook [year] for the Federal Republic of Germany*.
- Fentahun, T., A. Dagninet and A. Merkuze (2014). 'Evaluation of single yoke implement, harnessed and drawn by horse for cultivation of farm lands in north-western Ethiopia'. In: *Journal of Agricultural Research* 2.3, pp. 38–46.
- Fiener, P. and K. Auerswald (2009). 'Spatial variability of rainfall on a sub-kilometre scale'. In: *Earth Surface Processes and Landforms* 34.6, pp. 848–859.
- Fiener, P., V. Dlugoš and K. Van Oost (2015). 'Erosion-induced carbon redistribution, burial and mineralisation. Is the episodic nature of erosion processes important?' In: *Catena* 133, pp. 282–292.
- Fiener, P., F. Wilken, E. Aldana-Jague, D. Deumlich, J. A. Gómez, G. Guzmán, R. A. Hardy, J. N. Quinton, M. Sommer, K. Van Oost and R. Wexler (2018). 'Uncertainties in assessing tillage erosion – How appropriate are our measuring techniques?' In: *Geomorphology* 304, pp. 214–225.
- Fiener, P., F. Wilken and K. Auerswald (2019). 'Filling the gap between plot and landscape scale – eight years of soil erosion monitoring in 14 adjacent watersheds under soil conservation at Scheyern, Southern Germany'. In: *Advances in Geosciences* 48, pp. 31–48.

- Fisher, R. A. (1921). 'On the "probable error" of a coefficient of correlation deduced from a small sample'. In: *Metron* 1, pp. 3–32.
- Fontaine, S., S. Barot, P. Barre, N. Bdioui, B. Mary and C. Rumpel (2007). 'Stability of organic carbon in deep soil layers controlled by fresh carbon supply'. In: *Nature* 450.7167, pp. 277–80.
- Food and Agriculture Organization of the United Nations (2001). *The economics of conservation agriculture*. Tech. rep. Food and Agriculture Organization of the United Nations.
- (2019). *Soil erosion: The greatest challenge to sustainable soil management*. Tech. rep. Food and Agriculture Organization of the United Nations.
- (2020). *FAOSTAT*.
- Forster, T., F. Heller, M. E. Evans and P. Havlíček (1996). 'Loess in the Czech Republic: Magnetic properties and paleoclimate'. In: *Studia Geophysica et Geodaetica* 40, pp. 243–261.
- Franzluebbers, A. J. (2010). 'Achieving soil organic carbon sequestration with conservation agricultural systems in the Southeastern United States'. In: *Soil Science Society of America Journal* 74.2, pp. 347–357.
- Frielinghaus, M. and R. Schmidt (1993). 'On-site and off-site damages by erosion in landscapes of East Germany'. In: *Farm land erosion in temperate plains environment and hills. Proceedings of the international symposium on farm land erosion*. Ed. by S. Wicherek. Paris, France: Elsevier.
- Frielinghaus, Ma. and W.-G. Vahrson (1998). 'Soil translocation by water erosion from agricultural cropland into wet depressions (morainic kettle holes)'. In: *Soil & Tillage Research* 46, pp. 23–30.
- Frielinghaus, Mo., H. Petelkau and R. Schmidt (1992). 'Wassererosion im norddeutschen Jungmoränengebiet'. In: *Zeitschrift für Kulturtechnik und Landentwicklung* 33, pp. 22–33.
- Gao, X., A. R. Huete, W. Ni and T. Miura (2000). 'Optical-biophysical relationships of vegetation spectra without background contamination'. In: *Remote Sensing of Environment* 74, pp. 609–620.
- Gao, Y., X. Dang, Y. Yu, Y. Li, Y. Liu and J. Wang (2016). 'Effects of tillage methods on soil carbon and wind erosion'. In: *Land Degradation & Development* 27.3, pp. 583–591.
- Gerke, H. H. and W. Hierold (2012). 'Vertical bulk density distribution in C-horizons from marley till as indicator for erosion history in a hummocky post-glacial soil landscape'. In: *Soil & Tillage Research* 125, pp. 116–122.
- Gerke, H. H., H. Rieckh and M. Sommer (2016). 'Interactions between crop, water, and dissolved organic and inorganic carbon in a hummocky landscape with erosion-affected pedogenesis'. In: *Soil & Tillage Research* 156, pp. 230–244.

- Gerontidis, D. V. St., C. Kosmas, B. Detsis, M. Marathianou, T. Zafirious and M. Tsara (2001). 'The effect of moldboard plow on tillage erosion along a hillslope'. In: *Journal of Soil and Water Conservation* 56.2, pp. 147–152.
- Gerstengarbe, F.-W., F. Badeck, F. Hattermann, V. Krysanova, W. Lahmer, P. Lasch, M. Stock, F. Suckow, W. Wechsung and P. C. Werner (2003). *Studie zur klimatischen Entwicklung im Land Brandenburg bis 2055 und deren Auswirkungen auf den Wasserhaushalt, die Forst- und Landwirtschaft sowie die Ableitung erster Perspektiven*. Potsdam Institute for Climate Impact Research (PIK).
- Gerwitz, A. and E. R. Page (1974). 'An empirical mathematical model to describe plant root systems'. In: *Journal of Applied Ecology* 11.2, pp. 773–781.
- Gömann, H. and P. Kreins (2012). 'Landnutzungsänderungen in Deutschlands Landwirtschaft. Rückläufige Anbaudiversität hat viele Ursachen'. In: *Mais* 39.3, pp. 118–122.
- Gobin, A. (2010). 'Modelling climate impacts on crop yields in Belgium'. In: *Climate Research* 44.1, pp. 55–68.
- Gollany, H. T., T. E. Schumacher, M. J. Lindstrom, P. D. Evenson and G. D. Lemme (1992). 'Topsoil depth and desurfacing effects on properties and productivity'. In: *Soil Science Society of America Journal* 56, pp. 220–225.
- Gorji, M., H. Rafahi and S. Shahoe (2008). 'Effects of surface soil removal (simulated erosion) and fertilizer application on wheat yield'. In: *Journal of Agricultural Science and Technology* 10.4, pp. 317–323.
- Govers, G., D. A. Lobb and T. A. Quine (1999). 'Preface – Tillage erosion and translocation: emergence of a new paradigm in soil erosion research'. In: *Soil & Tillage Research* 51.3-4, pp. 167–174.
- Govers, G., J. Poesen and Dirk Goossens (2004). 'Soil erosion – processes, damages and countermeasures'. In: *Managing soil quality – challenges in modern agriculture*. Ed. by P. Schjønning, S. Elmholt and B. T. Christensen. Oxon, UK: CABI Publishing, pp. 199–217.
- Govers, G., T. A. Quine, P. J. J. Desmet and D. E. Walling (1996a). 'The relative contribution of soil tillage and overland flow erosion to soil redistribution on agricultural land'. In: *Earth Surface Processes and Landforms* 21, pp. 929–946.
- (1996b). 'The relative contribution of soil tillage and overland flow erosion to soil redistribution on agricultural land'. In: *Earth Surface Processes and Landforms* 21, pp. 929–946.
- Govers, G., T. A. Quine and D. E. Walling (1993). 'The effect of water erosion and tillage movement on hillslope profile development: A comparison of field observations and model results'. In: *Farm Land Erosion*. Ed. by S. Wicherek. Amsterdam: Elsevier, pp. 285–300.

- Govers, G., K. Vandaele, P. Desmet, J. Poesen and K. Bunte (1994). 'The role of tillage in soil redistribution on hillslopes'. In: *European Journal of Soil Science* 45.4, pp. 469–478.
- Graves, A. R., J. Morris, L. K. Deeks, R. J. Rickson, M. G. Kibblewhite, J. A. Harris, T. S. Farewell and I. Truckle (2015). 'The total costs of soil degradation in England and Wales'. In: *Ecological Economics* 119, pp. 399–413.
- Gregorich, E. G., K. J. Greer, D. W. Anderson and B. C. Liang (1998). 'Carbon distribution and losses: Erosion and deposition effects'. In: *Soil & Tillage Research* 47, pp. 291–302.
- Harden, J. W., J. M. Sharpe, W. J. Parton, D. S. Ojima, T. L. Fries, T. G. Huntington and S. M. Dabney (1999). 'Dynamic replacement and loss of soil carbon on eroding cropland'. In: *Global Biogeochemical Cycles* 13.4, pp. 885–901.
- Heckrath, G., J. Djurhuus, T. A. Quine, K. Van Oost, G. Govers and Y. Zhang (2005). 'Tillage erosion and its effect on soil properties and crop yield in Denmark'. In: *Journal of Environmental Quality* 34.1, pp. 312–324.
- Heckrath, G., U. Halekoh, J. Djurhuus and G. Govers (2006). 'The effect of tillage direction on soil redistribution by mouldboard ploughing on complex slopes'. In: *Soil & Tillage Research* 88.1-2, pp. 225–241.
- Heinrich, I. et al. (2018). 'Interdisciplinary geo-ecological research across time scales in the Northeast German lowland observatory (TERENO-NE)'. In: *Vadose Zone Journal* 17.180116.
- Helsel, Z. R. (2007). *Fuel requirements and energy savings tips for field operations*. Tech. rep. Rutgers Cooperative Extension.
- Herbrich, M., H. H. Gerke and M. Sommer (2018). 'Root development of winter wheat in erosion-affected soils depending on the position in a hummocky ground moraine soil landscape'. In: *Journal of Plant Nutrition and Soil Science* 181.2, pp. 147–157.
- Herrmann, K. (1985). *Pflügen, Säen, Ernten. Landarbeit und Landtechnik in der Geschichte*. Deutsches Museum, Rowohlt.
- Hoffmann, M., M. Pohl, N. Jurisch, A. K. Prescher, E. Mendez Campa, U. Hagemann, R. Remus, G. Verch, M. Sommer and J. Augustin (2018). 'Maize carbon dynamics are driven by soil erosion state and plant phenology rather than nitrogen fertilization form'. In: *Soil & Tillage Research* 175, pp. 255–266.
- Hoffmann, T., M. Schlummer, B. Notebaert, G. Verstraeten and O. Korup (2013). 'Carbon burial in soil sediments from Holocene agricultural erosion, Central Europe'. In: *Global Biogeochemical Cycles* 27.3, pp. 828–835.
- Hotelling, H. (1931). 'The generalization of student's ratio'. In: *The Annals of Mathematical Statistics* 2.3, pp. 360–378.

- Hotelling, H. (1940). 'The teaching of statistics'. In: *The Annals of Mathematical Statistics* 11.4, pp. 457–470.
- Hrabalíková, M., P. Huislová, J. Ureš, O. Holubík, D. Žížala and J. Kumhálová (2016). 'Assessment of changes in topsoil depth redistribution in relation to different tillage technologies'. In: *Proceedings of the 3<sup>rd</sup> WASWAC Conference*. Belgrade, Serbia, pp. 22–26.
- Huete, A., K. Didan, T. Miura, E. P. Rodriguez, X. Gao and L. G. Ferreira (2002). 'Overview of the radiometric and biophysical performance of the MODIS vegetation indices'. In: *Remote Sensing of Environment* 83.1-2, pp. 195–213.
- Huete, A., H. Q. Liu, K. Batchily and W. Van Leeuwen (1997). 'A comparison of vegetation indices over a global set of TM images for EOS-MODIS'. In: *Remote Sensing of Environment* 59, pp. 440–451.
- Huggins, D. R. and J. P. Reganold (2008). 'No-till: The quiet revolution'. In: *Scientific American Inc.*, pp. 70–77.
- IUSS Working Group WRB (2015). *World Reference Base for Soil Resources 2014, update 2015. International soil classification system for naming soils and creating legends for soil maps*. FAO.
- Intergovernmental Panel on Climate Change (IPCC) (2019). *Climate Change and Land: An IPCC Special Report on climate change, desertification, land degradation, sustainable land management, food security, and greenhouse gas fluxes in terrestrial ecosystems*. Tech. rep.
- International Organization for Standardization (ISO) (1995). *Soil quality – Determination of carbonate content – volumetric method (Standard No. 10693)*. URL: <https://www.iso.org/standard/18781.html>.
- (1998). *Soil quality – Determination of organic carbon by sulfochromic oxidation (Standard No. 14235)*. URL: <https://www.iso.org/standard/23140.html>.
- (2009). *Soil quality – Determination of particle size distribution in mineral soil material – Method by sieving and sedimentation (Standard No. 11277)*. URL: <https://www.iso.org/standard/54151.html>.
- Izaurrealde, R. C., S. S. Malhi, M. Nyborg, E. D. Solberg and M. C. Quiroga Jakas (2006). 'Crop performance and soil properties in two artificially eroded soils in north-central Alberta'. In: *Agronomy Journal* 98.5, pp. 1298–1311.
- Jacinthe, P. A. and R. Lal (2001). 'A mass balance approach to assess carbon dioxide evolution during erosional events'. In: *Land Degradation & Development* 12.4, pp. 329–339.
- Jacinthe, P. A., R. Lal and J. M. Kimble (2002). 'Carbon dioxide evolution in runoff from simulated rainfall on long-term no-till and plowed soils in southwestern Ohio'. In: *Soil & Tillage Research* 66.1, pp. 23–33.
- Jin, Xiuliang, Zhenhai Li, Guijun Yang, Hao Yang, Haikuan Feng, Xingang Xu, Jihua Wang, Xinchuan Li and Juhua Luo (2017). 'Winter

- wheat yield estimation based on multi-source medium resolution optical and radar imaging data and the AquaCrop model using the particle swarm optimization algorithm'. In: *ISPRS Journal of Photogrammetry and Remote Sensing* 126, pp. 24–37.
- Jin, Xiuliang, Guijun Yang, Xingang Xu, Hao Yang, Haikuan Feng, Zhenhai Li, Jiaxiao Shen, Yubin Lan and Chunjiang Zhao (2015). 'Combined multi-temporal optical and radar parameters for estimating LAI and biomass in winter wheat using HJ and RADARSAR-2 data'. In: *Remote Sensing* 7.10, pp. 13251–13272.
- Juřicová, A., T. Chuman and D. Žížala (2022). 'Soil organic carbon content and stock change after half a century of intensive cultivation in a chernozem area'. In: *Catena* 211.
- Juřicová, A., L. K. Öttl, F. Wilken, T. Chuman, D. Žížala, R. Minařík and P. Fiener (submitted to Soil & Tillage Research). *Tillage erosion as an underestimated driver of carbon dynamics*.
- Kappler, C., K. Kaiser, M. Küster, A. Nicolay, A. Fülling, O. Bens and T. Raab (2019). 'Late Pleistocene and Holocene terrestrial geomorphodynamics and soil formation in northeastern Germany: A review of geochronological data'. In: *Physical Geography* 40.5, pp. 405–432.
- Kappler, C., K. Kaiser, P. Tanski, F. Klos, A. Fülling, A. Mrotzek, M. Sommer and O. Bens (2018). 'Stratigraphy and age of colluvial deposits indicating Late Holocene soil erosion in northeastern Germany'. In: *Catena* 170, pp. 224–245.
- Kaspar, T. C., D. J. Pulido, T. E. Fenton, T. S. Colvin, D. L. Karlen, D. B. Jaynes and D. W. Meek (2004). 'Relationship of corn and soybean yield to soil and terrain properties'. In: *Agronomy Journal* 96.3, pp. 700–709.
- Kassam, A., T. Friedrich and R. Derpsch (2019). 'Global spread of conservation agriculture'. In: *International Journal of Environmental Studies* 76.1, pp. 29–51.
- Keen, B. A. (1925). 'Physics in agriculture'. In: *Nature* 116, pp. 905–907.
- Keller, T., M. Sandin, T. Colombi, R. Horn and D. Or (2019). 'Historical increase in agricultural machinery weights enhanced soil stress levels and adversely affected soil functioning'. In: *Soil & Tillage Research* 194.
- Kemper, W. D. and R. C. Rosenau (1984). 'Soil cohesion as affected by time and water content'. In: *Soil Science Society of America Journal* 48, pp. 1001–1006.
- Kietzer, B. (2007). 'Aufklärung der Bodenverlagerung durch Bearbeitungserosion in Jungmoränenlandschaften'. PhD thesis. Technische Universität Berlin.
- Kim, Hyun Ok and Jong Min Yeom (2012). 'Multi-temporal spectral analysis of rice fields in South Korea using MODIS and RapidEye

- satellite imagery'. In: *Journal of Astronomy and Space Sciences* 29.4, pp. 407–411.
- Kimaro, D. N., J. A. Deckers, J. Poesen, M. Kilasara and B. M. Msanya (2005). 'Short and medium term assessment of tillage erosion in the Uluguru Mountains, Tanzania'. In: *Soil & Tillage Research* 81.1, pp. 97–108.
- Kirkels, F. M. S. A., L. H. Cammeraat and N. J. Kuhn (2014). 'The fate of soil organic carbon upon erosion, transport and deposition in agricultural landscapes. A review of different concepts'. In: *Geomorphology* 226, pp. 94–105.
- Klik, A. and J. Rosner (2020). 'Long-term experience with conservation tillage practices in Austria: Impacts on soil erosion processes'. In: *Soil & Tillage Research* 203.
- Koch, A. et al. (2013). 'Soil Security: Solving the global soil crisis'. In: *Global Policy* 4.4, pp. 434–441.
- Kosmas, C., S. Gerontidis, M. Marathianou, B. Detsis, T. Zafiriou, W. N. Muysen, G. Govers, T. Quine and K. Van Oost (2001). 'The effects of tillage displaced soil on soil properties and wheat biomass'. In: *Soil & Tillage Research* 58.1-2, pp. 31–44.
- Koszinski, S., H. H. Gerke, W. Hierold and M. Sommer (2013). 'Geophysical based modeling of a kettle hole catchment of the morainic soil landscape'. In: *Vadose Zone Journal* 12.4.
- Kravchenko, A. N., G. P. Robertson, K. D. Thelen and R. R. Harwood (2005). 'Management, topographical, and weather effects of spatial variability of crop grain yields'. In: *Agronomy Journal* 97, pp. 514–523.
- Kráska, J., T. Dostál, B. Jáchymová, M. Bauer and J. Devátý (2019). 'Soil erosion as a source of sediment and phosphorus in rivers and reservoirs – Watershed analyses using WaTEM/SEDEM'. In: *Environ Res* 171, pp. 470–483.
- Kätterer, T. and O. Andrén (1999). 'Long-term agricultural field experiments in Northern Europe: Analysis of the influence of management on soil carbon stocks using the ICBM model'. In: *Agriculture, Ecosystems & Environment* 72, pp. 165–179.
- Kätterer, T., M. Reichstein, O. Andrén and A. Lomander (1998). 'Temperature dependence of organic matter decomposition: a critical review using literature data analyzed with different models'. In: *Biology and Fertility of Soils* 27, pp. 258–262.
- Kuhwald, M., F. Busche, P. Saggau and R. Duttmann (2022). 'Is soil loss due to crop harvesting the most disregarded soil erosion process? A review of harvest erosion'. In: *Soil & Tillage Research* 215.
- Kuratorium für Technik und Bauwesen in der Landwirtschaft e. V. (KTBL) (1951, 1970, 1980, 1993, 2005). *Faustzahlen für die Landwirtschaft*. Darmstadt, Germany.

- Kuzyakov, Y. and G. Domanski (2000). 'Carbon input by plants into the soil. Review'. In: *Journal of Plant Nutrition and Soil Science* 163, pp. 421–431.
- Lal, R. (1998). 'Soil erosion impact on agronomic productivity and environment quality'. In: *Critical Reviews in Plant Sciences* 17.4, pp. 319–464.
- (2001). 'Soil degradation by erosion'. In: *Land Degradation & Development* 12.6, pp. 519–539.
  - (2003). 'Soil erosion and the global carbon budget'. In: *Environment International* 29.4, pp. 437–450.
  - (2004). 'Soil carbon sequestration to mitigate climate change'. In: *Geoderma* 123.1-2, pp. 1–22.
  - (2005). 'Soil erosion and carbon dynamics'. In: *Soil & Tillage Research* 81.2, pp. 137–142.
  - (2018). 'Digging deeper: A holistic perspective of factors affecting soil organic carbon sequestration in agroecosystems'. In: *Global Change Biology* 24.8, pp. 3285–3301.
  - (2019). 'Accelerated soil erosion as a source of atmospheric CO<sub>2</sub>'. In: *Soil & Tillage Research* 188, pp. 35–40.
- Lal, R., M. Ahmadi and R. M. Bajracharya (2000). 'Erosional impacts on soil properties and corn yield on Alfisols in Central Ohio'. In: *Land Degradation & Development* 11, pp. 575–585.
- Lal, R., M. Griffin, J. Apt, L. Lave and M. G. Morgan (2004). 'Managing soil carbon'. In: *Science* 304.5669, p. 393.
- Lal, R., D. Mokma and B. Lowery (1999). 'Relation between soil quality and erosion'. In: *Soil quality and soil erosion*. Ed. by R. Lal. Boca Raton, Florida: CRC Press, pp. 237–258.
- Lal, R., D. C. Reicosky and J. D. Hanson (2007). 'Evolution of the plow over 10,000 years and the rationale for no-till farming'. In: *Soil & Tillage Research* 93.1, pp. 1–12.
- Landesamt für Umwelt, Gesundheit und Verbraucherschutz Brandenburg & Landesvermessung und Geobasisinformation Brandenburg (2012). *Digital elevation model with a grid size of 1 m (DEM<sub>1</sub>) derived from laser scan data*.
- Lang, A. and H. R. Bork (2006). 'Past soil erosion in Europe'. In: *Soil erosion in Europe*. Ed. by J. Boardman and J. Poesen. Chichester, UK: John Wiley & Sons, pp. 465–476.
- Larney, F. J., R. C. Izaurralde, H. Henry Janzen, Barry M. Olson, E. D. Solberg, C. W. Lindwall and M. Nyborg (1995). 'Soil erosion - crop productivity relationships for six Alberta soils'. In: *Journal of Soil and Water Conservation* 50.1, pp. 87–91.
- Larney, Francis J., H. Henry Janzen, Barry M. Olson and Andrew F. Olson (2009). 'Erosion-productivity-soil amendment relationships for wheat over 16 years'. In: *Soil & Tillage Research* 103.1, pp. 73–83.

- Le Quéré, C. et al. (2016). 'Global carbon budget 2016'. In: *Earth System Science Data* 8.2, pp. 605–649.
- Leser, P. (1931). *Entstehung und Verbreitung des Pfluges*. Münster, Germany: Aschendorff.
- Lesiv, M. et al. (2019). 'Estimating the global distribution of field size using crowdsourcing'. In: *Global Change Biology* 25.1, pp. 174–186.
- Li, S., D. A. Lobb and M. J. Lindstrom (2007). 'Tillage translocation and tillage erosion in cereal-based production in Manitoba, Canada'. In: *Soil & Tillage Research* 94.1, pp. 164–182.
- Li, Y., M. Frielinghaus, H. R. Bork, E. M. Friedland, U. K. Schkade, M. Naumann and H. Schäfer (2002). 'Slope basis deposits linked to long-term land use in NE-Germany'. In: *Archives of Agronomy and Soil Science* 48.4, pp. 335–342.
- Lindstrom, M. J., W. W. Nelson and T. E. Schumacher (1992). 'Quantifying tillage erosion rates due to moldboard plowing'. In: *Soil & Tillage Research* 24.3, pp. 243–255.
- Lindstrom, M. J., W. W. Nelson, T. E. Schumacher and G. D. Lemme (1990). 'Soil movement by tillage as affected by slope'. In: *Soil & Tillage Research* 17.3-4, pp. 255–264.
- Lipský, Z. (1995). 'The changing face of the Czech rurallandscape'. In: *Landscape and Urban Planning* 31, pp. 39–45.
- Lischeid, G., D. Balla, R. Dannowski, O. Dietrich, T. Kalettka, C. Merz, U. Schindler and J. Steidl (2017). 'Forensic hydrology: what function tells about structure in complex settings'. In: *Environmental Earth Sciences* 76.40, pp. 1–15.
- Liu, S., N. Bliss, E. Sundquist and T. G. Huntington (2003). 'Modeling carbon dynamics in vegetation and soil under the impact of soil erosion and deposition'. In: *Global Biogeochemical Cycles* 17.2, pp. 1–24.
- Lüning, J. (1997). *Deutsche Agrargeschichte, Vor- und Frühgeschichte*. Stuttgart, Germany: Ulmer.
- Lobb, D. A. (2011). 'Understanding and managing the causes of soil variability'. In: *Journal of Soil and Water Conservation* 66.6, pp. 175–179.
- Lobb, D. A., E. Huffman and D. C. Reicosky (2007). 'Importance of information on tillage practices in the modelling of environmental processes and in the use of environmental indicators'. In: *Journal of Environmental Management* 82.3, pp. 377–87.
- Lobb, D. A. and R. G. Kachanoski (1999). 'Modelling tillage erosion in the topographically complex landscapes of southwestern Ontario, Canada'. In: *Soil & Tillage Research* 51, pp. 261–277.
- Lobb, D. A., R. G. Kachanoski and M. H. Miller (1995). 'Tillage translocation and tillage erosion on shoulder slope landscape positions

- measured using Cs-137 as a tracer'. In: *Canadian Journal of Soil Science* 75.2, pp. 211–218.
- (1999). 'Tillage translocation and tillage erosion in the complex upland landscapes of southwestern Ontario, Canada'. In: *Soil & Tillage Research* 51.
- Lowder, S. K., J. Scoet and T. Raney (2016). 'The number, size, and distribution of farms, smallholder farms, and family farms worldwide'. In: *World Development* 87, pp. 16–29.
- Lüthgens, C., M. Böse and F. Preusser (2011). 'Age of the Pomeranian ice-marginal position in northeastern Germany determined by Optically Stimulated Luminescence (OSL) dating of glaciofluvial sediments'. In: *Boreas* 40.4, pp. 598–615.
- Lüttger, A. B. and T. Feike (2018). 'Development of heat and drought related extreme weather events and their effect on winter wheat yields in Germany'. In: *Theoretical and Applied Climatology* 132, pp. 15–29.
- Lugato, E., P. Smith, P. Borrelli, P. Panagos, C. Ballabio, A. Orgiazzi, O. Fernandez-Ugalde, L. Montanarella and A. Jones (2018). 'Soil erosion is unlikely to drive a future carbon sink in Europe'. In: *Science Advances* 4.
- Madarász, B., G. Jakab, Z. Szalai, K. Juhos, Z. Kotroczó, A. Tóth and M. Ladányi (2021). 'Long-term effects of conservation tillage on soil erosion in Central Europe: A random forest-based approach'. In: *Soil & Tillage Research* 209.104959.
- Madarász, B., K. Juhos, Z. Ruzsokiczay-Rüdiger, S. Benke, G. Jakab and Z. Szalai (2016). 'Conservation tillage vs. conventional tillage: long-term effects on yields in continental, sub-humid Central Europe, Hungary'. In: *International Journal of Agricultural Sustainability* 14.4, pp. 408–427.
- Mal, P., M. Schmitz and J. W. Hesse (2015). 'Economic and environmental effects of conservation tillage with glyphosate use: a case study of Germany'. In: *Outlooks on Pest Management* 26.1, pp. 24–27.
- Marques da Silva, J. R. and C. Alexandre (2004). 'Soil carbonation processes as evidence of tillage-induced erosion'. In: *Soil & Tillage Research* 78.2, pp. 217–224.
- Marques da Silva, J. R., J. M. C. N. Soares and D. L. Karlen (2004). 'Implement and soil condition effects on tillage-induced erosion'. In: *Soil & Tillage Research* 78.2, pp. 207–216.
- Martinez-Feria, R. A. and B. Basso (2020). 'Unstable crop yields reveal opportunities for site-specific adaptations to climate variability'. In: *Sci Rep* 10.1, p. 2885.
- Massee, T. W. (1990). 'Simulated erosion and fertilizer effects on winter wheat cropping intermountain dryland area'. In: *Soil Science Society of America Journal* 54, pp. 1720–1725.

- Massee, T. W. and H. O. Waggoner (1985). 'Productivity losses from soil erosion on dry cropland in the intermountain area'. In: *Journal of Soil and Water Conservation* 40, pp. 447–450.
- Matsushita, B., W. Yang, J. Chen, Y. Onda and G. Y. Qiu (2007). 'Sensitivity of the Enhanced Vegetation Index (EVI) and Normalized Difference Vegetation Index (NDVI) to topographic effects: a case study in high-density cypress forest'. In: *Sensors* 7.11, pp. 2636–2651.
- McCarty, G. W. and J. C. Ritchie (2002). 'Impact of soil movement on carbon sequestration in agricultural ecosystems'. In: *Environmental Pollution* 116, pp. 423–430.
- Mech, S. J. and G. R. Free (1942). 'Movement of soil during tillage operations'. In: *Agricultural Engineering* 23, pp. 379–382.
- Miller, M. P., M. J. Singer and D. R. Nielsen (1988). 'Spatial variability of wheat yield and soil properties on complex hills'. In: *Soil Science Society of America Journal*.
- Minasny, B. and A. B. McBratney (2006). 'A conditioned Latin hypercube method for sampling in the presence of ancillary information'. In: *Computers & Geosciences* 32.9, pp. 1378–1388.
- Minasny, B. et al. (2017). 'Soil carbon 4 per mille'. In: *Geoderma* 292, pp. 59–86.
- Montgomery, D. R. (2007a). *Dirt: The erosion of civilizations*. Oakland, CA, USA: University of California Press.
- (2007b). 'Soil erosion and agricultural sustainability'. In: *Proceedings of the National Academy of Sciences of the United States of America* 104.33, pp. 13268–13272.
- Montgomery, J. A., D. K. McCool, A. J. Busacca and B. E. Frazier (1999). 'Quantifying tillage translocation and deposition rates due to moldboard plowing in the Palouse region of the Pacific Northwest, USA'. In: *Soil & Tillage Research* 51, pp. 175–187.
- Moulin, A. P., D. W. Anderson and M. Mellinger (1994). 'Spatial variability of wheat yield, soil properties and erosion in hummocky terrain'. In: *Canadian Journal of Soil Science* 74.2, pp. 219–228.
- Mueller, L., A. Behrendt, G. Schalitz and U. Schindler (2005). 'Above ground biomass and water use efficiency of crops at shallow water tables in a temperate climate'. In: *Agricultural Water Management* 75.2, pp. 117–136.
- Nadeu, E., A. Gobin, P. Fiener, B. Van Wesemael and K. Van Oost (2015). 'Modelling the impact of agricultural management on soil carbon stocks at the regional scale: The role of lateral fluxes'. In: *Global Change Biology* 21.8, pp. 3181–92.
- Naipal, V., P. Ciais, Y. Wang, R. Lauerwald, B. Guenet and K. Van Oost (2018). 'Global soil organic carbon removal by water erosion under climate change and land use change during AD 1850–2005'. In: *Biogeosciences* 15.14, pp. 4459–4480.

- Napoli, M., F. Altobelli and S. Orlandini (2020). 'Effect of land set up systems on soil losses'. In: *Italian Journal of Agronomy* 15.4, pp. 306–314.
- Nash, J. E. and J. V. Sutcliffe (1970). 'River flow forecasting through conceptual models. Part I: A discussion of principles'. In: *Journal of Hydrology* 10, pp. 282–290.
- Nearing, M. A. (1989). 'A process-based soil erosion model for USDA-water erosion prediction project technology'. In: *Transactions of the ASABE* 32, pp. 1587–1593.
- Nyssen, J., J. Poesen, M. Haile, J. Moeyersons and J. Deckers (2000). 'Tillage erosion on slopes with soil conservation structures in the Ethiopian highlands'. In: *Soil & Tillage Research* 57.3, pp. 115–127.
- Oldeman, L. R. (1992). 'Global extent of soil degradation'. In: *ISRIC Bi-annual report 1991-1992*, pp. 19–36.
- Olson, K. R., A. N. Gennadiyev, R. L. Jones and S. Chernyanskii (2002). 'Erosion patterns on cultivated and reforested hillslopes in Moscow Region, Russia'. In: *Soil Science Society of America Journal* 66.1, pp. 193–201.
- OpenStreetMap contributors (2017). *Planet dump retrieved from <https://planet.osm.org>*. <https://www.openstreetmap.org>.
- Ouyang, W., A. K. Skidmore, F. Hao and T. Wang (2010). 'Soil erosion dynamics response to landscape pattern'. In: *Science of the Total Environment* 408.6, pp. 1358–66.
- Panagos, P., P. Borrelli, J. Poesen, C. Ballabio, E. Lugato, K. Meusburger, L. Montanarella and C. Alewell (2015). 'The new assessment of soil loss by water erosion in Europe'. In: *Environmental Science & Policy* 54, pp. 438–447.
- Panagos, P., K. Meusburger, C. Ballabio, P. Borrelli and C. Alewell (2014). 'Soil erodibility in Europe: A high-resolution dataset based on LUCAS'. In: *Science of The Total Environment* 479-480, pp. 189–200.
- Panagos, P., G. Standardi, P. Borrelli, E. Lugato, L. Montanarella and F. Bosello (2018). 'Cost of agricultural productivity loss due to soil erosion in the European Union: From direct cost evaluation approaches to the use of macroeconomic models'. In: *Land Degradation & Development* 29.3, pp. 471–484.
- Papiernik, S. K., M. J. Lindstrom, J. A. Schumacher, A. Farenhorst, K. D. Stephens, T. E. Schumacher and D. A. Lobb (2005). 'Variation in soil properties and crop yield across an eroded prairie landscape'. In: *Journal of Soil and Water Conservation* 60.6, pp. 388–395.
- Papiernik, S. K., T. E. Schumacher, D. A. Lobb, M. J. Lindstrom, M. Lieser, A. Eynard and J. A. Schumacher (2009). 'Soil properties and productivity as affected by topsoil movement within an eroded landform'. In: *Soil & Tillage Research* 102.1, pp. 67–77.

- Parton, W. J., D. S. Schimel, C. V. Cole and D. S. Ojima (1987). 'Analysis of factors controlling soil organic matter levels in Great Plains grasslands'. In: *Soil Science Society of America Journal* 51, pp. 1173–1179.
- Pauling, A., J. Luterbacher, C. Casty and H. Wanner (2005). 'Five hundred years of gridded high-resolution precipitation reconstructions over Europe and the connection to large-scale circulation'. In: *Climate Dynamics* 26.4, pp. 387–405.
- Paustian, K., O. Andr en, H. H. Janzen, R. Lal, P. Smith, G. Tian, H. Tiessen, M. Van Noordwijk and P. L. Woomer (1997). 'Agricultural soils as a sink to mitigate CO<sub>2</sub> emissions'. In: *Soil Use and Management* 13, pp. 230–244.
- Paustian, K., J. Lehmann, S. Ogle, D. Reay, G. P. Robertson and P. Smith (2016). 'Climate-smart soils'. In: *Nature* 532.7597, pp. 49–57.
- Paustian, K., J. Six, E. T. Elliott and H. W. Hunt (2000). 'Management options for reducing CO<sub>2</sub> emissions from agricultural soils'. In: *Biogeochemistry* 48, pp. 147–163.
- Peichl, M., S. Thober, V. Meyer and L. Samaniego (2018). 'The effect of soil moisture anomalies on maize yield in Germany'. In: *Natural Hazards and Earth System Sciences* 18.3, pp. 889–906.
- Pennock, D. J. (2003). 'Terrain attributes, landform segmentation, and soil redistribution'. In: *Soil & Tillage Research* 69.1-2, pp. 15–26.
- Pianosi, F., K. Beven, J. Freer, J. W. Hall, J. Rougier, D. B. Stephenson and T. Wagener (2016). 'Sensitivity analysis of environmental models: A systematic review with practical workflow'. In: *Environmental Modelling & Software* 79, pp. 214–232.
- Pimentel, D. (2000). 'Soil erosion and the threat to food security and the environment'. In: *Ecosystem Health* 6, pp. 221–226.
- Pimentel, D. and M. Burgess (2013). 'Soil erosion threatens food production'. In: *Agriculture* 3.3, pp. 443–463.
- Pingali, P. (2007). 'Handbook of Agricultural Economics'. In: ed. by R. Evenson and P. Pingali. Vol. 3. Elsevier, pp. 2779–2805.
- Planet Team (2016). *RapidEye imagery product specifications*.
- Poesen, J. and G. Govers (1985). 'A field-scale study on surface sealing and compaction on loam and sandy loam soils. Part II. Impact of soil surface sealing and compaction on water erosion processes'. In: *Assessment of soil surface sealing and crusting*. Ed. by F. Callebaut, D. Gabriels and M. De Broodt. Ghent, Belgium, pp. 183–193.
- (1986). 'A field-scale study on surface sealing and compaction on loam and sandy loam soils. Part II. Impact of soil surface sealing and compaction on water erosion processes'. In: *International symposium on the assessment of soil surface sealing and crusting*, pp. 183–193.
- Poesen, J., B. Van Wesemael, G. Govers, J. Martinez-Fernandez, P. Desmet, K. Vandaele, T. Quine and G. Degraer (1997). 'Patterns of

- rock fragment cover generated by tillage erosion'. In: *Geomorphology* 18, pp. 183–197.
- Prince, S. D., J. Haskett, M. Steininger, H. Strand and R. Wright (2001). 'Net primary production of U.S. Midwest croplands from agricultural harvest yield data'. In: *Ecological Applications* 11.4, pp. 1194–1205.
- QGIS Development Team (2022). *QGIS Geographic Information System. Open Source Geospatial Foundation Project*. URL: <http://www.qgis.org/>.
- Quine, T. A., L. R. Basher and A. P. Nicholas (2003). 'Tillage erosion intensity in the South Canterbury Downlands, New Zealand'. In: *Australian Journal of Soil Research* 41, pp. 789–807.
- Quine, T. A., P. J. J. Desmet, G. Govers, K. Vandaele and D. E. Walling (1994). 'A comparison of the roles of tillage and water erosion in landform development and sediment export on agricultural land near Leuven, Belgium'. In: *Variability in Stream Erosion and Sediment Transport* 224, pp. 77–86.
- Quine, T. A., G. Govers, J. Poesen, D. Walling, B. Van Wesemael and J. Martinez-Fernandez (1999a). 'Fine-earth translocation by tillage in stony soils in the Guadalentin, south-east Spain: An investigation using caesium-134'. In: *Soil & Tillage Research* 51, pp. 279–301.
- Quine, T. A., D. E. Walling, Q. K. Chakela, O. T. Mandiringana and X. Zhang (1999b). 'Rates and patterns of tillage and water erosion on terraces and contour strips: evidence from caesium-137 measurements'. In: *Catena* 36, pp. 115–142.
- Quine, T. A., D. E. Walling and X. Zhang (1999c). 'Tillage erosion, water erosion and soil quality on cultivated terraces near Xifeng in the loess plateau, China'. In: *Land Degradation & Development* 10, pp. 251–274.
- Quine, T. A. and Y. Zhang (2004a). 'Re-defining tillage erosion: quantifying intensity–direction relationships for complex terrain. 1. Derivation of an adirectional soil transport coefficient'. In: *Soil Use and Management* 20.2, pp. 114–123.
- (2004b). 'Re-defining tillage erosion: quantifying intensity–direction relationships for complex terrain. 2. Revised mouldboard erosion model'. In: *Soil Use and Management* 20.2, pp. 124–132.
- Quinton, J. N., J. A. Catt, G. A. Wood and J. Steer (2006). 'Soil carbon losses by water erosion: Experimentation and modeling at field and national scales in the UK'. In: *Agriculture, Ecosystems & Environment* 112.1, pp. 87–102.
- Quinton, J. N., G. Govers, K. Van Oost and R. D. Bardgett (2010). 'The impact of agricultural soil erosion on biogeochemical cycling'. In: *Nature Geoscience* 3.5, pp. 311–314.

- Quinton, J. N., L. K. Öttl and P. Fiener (2022). 'Tillage exacerbates the vulnerability of cereal crops to drought'. In: *Nature Food* 3.6, pp. 472–479.
- R Core Team (2019). *A language and environment for statistical computing*.  
 – (2021). *A language and environment for statistical computing*.  
 – (2022). *A language and environment for statistical computing*.
- Reichenau, T. G., W. Korres, C. Montzka, P. Fiener, F. Wilken, A. Stadler, G. Waldhoff and K. Schneider (2016). 'Spatial heterogeneity of Leaf Area Index (LAI) and its temporal course on arable land: Combining field measurements, remote sensing and simulation in a Comprehensive Data Analysis Approach (CDAA)'. In: *PLoS One* 11.7.
- Reinermann, S., U. Gessner, S. Asam, C. Kuenzer and S. Dech (2019). 'The effect of droughts on vegetation condition in Germany: An analysis based on two decades of satellite earth observation time series and crop yield statistics'. In: *Remote Sensing* 11.15.
- Rejman, J., I. Iglík, J. Paluszczek and J. Rodzik (2014). 'Soil redistribution and crop productivity in loess areas (Lublin Upland, Poland)'. In: *Soil & Tillage Research* 143, pp. 77–84.
- Renard, K. G., G. R. Foster, G. A. Weesies, D. K. McCool and D. C. Yoder (1997). *Predicting soil erosion by water: A guide to conservation planning with the Revised Universal Soil Loss Equation (RUSLE)*. USDA-ARS.
- Renwick, W. H., S. V. Smith, R. O. Sleezer and R. W. Buddemeier (2004). 'Comment on "Managing soil carbon" (II)'. In: *Science* 305.5690, pp. 1567–1567.
- Research Institute for Soil and Water Conservation (RISWC) (2018). *Soil Erosion Control Calculator – manual (in Czech)*. URL: <https://kalkulacka.vumop.cz/docs/manual.pdf>.
- Revel, J. C. and M. Guirresse (1995). 'Erosion due to cultivation of calcareous clay soils on the hillsides of south west France. I. Effect of former farming practices'. In: *Soil & Tillage Research* 35, pp. 147–155.
- Ritchie, H. and M. Roser (2013). *Crop yields*. URL: <https://ourworldindata.org/>.
- Rosenbloom, N. A., S. C. Doney and D. S. Schimel (2001). 'Geomorphic evolution of soil texture and organic matter in eroding landscapes'. In: *Global Biogeochemical Cycles* 15.2, pp. 365–381.
- Rösener, W. (1985). 'Arbeitsgerät, Bodennutzung und agrarwirtschaftlicher Fortschritt'. In: *Bauern im Mittelalter*. Ed. by W. Rösener. Munich: C. H. Beck'sche Verlagsbuchhandlung, pp. 118–133.
- Rudolph, S., J. van der Kruk, C. von Hebel, M. Ali, M. Herbst, C. Montzka, S. Pätzold, D. A. Robinson, H. Vereecken and L. Weihermüller (2015). 'Linking satellite derived LAI patterns with subsoil

- heterogeneity using large-scale ground-based electromagnetic induction measurements'. In: *Geoderma* 241-242, pp. 262-271.
- Rumpel, C. and I. Kögel-Knabner (2011). 'Deep soil organic matter – A key but poorly understood component of terrestrial C cycle'. In: *Plant and Soil* 338.1-2, pp. 143-158.
- Ruysschaert, G., J. Poesen, G. Verstraeten and G. Govers (2004). 'Soil loss due to crop harvesting: Significance and determining factors'. In: *Progress in Physical Geography* 28, pp. 467-501.
- Rymshaw, E., M. F. Walter and A. Van Wambeke (1997). 'Processes of soil movement on steep cultivated hill slopes in the Venezuelan Andes'. In: *Soil & Tillage Research* 44, pp. 265-272.
- Sadowski, H. and B. Sorge (2005). 'Der Normalhöhenpunkt von 1912 – Datumspunkt des DHHN 2012?' In: *Vermessung Brandenburg* 2.
- Sagova-Mareckova, M., T. Zadorova, V. Penizek, M. Omelka, V. Tejnecky, P. Pruchova, T. Chuman, O. Drabek, A. Buresova, A. Vanek and J. Kopecky (2016). 'The structure of bacterial communities along two vertical profiles of a deep colluvial soil'. In: *Soil Biology and Biochemistry* 101, pp. 65-73.
- Sanderman, J., T. Hengl and G. J. Fiske (2017). 'Soil carbon debt of 12,000 years of human land use'. In: *Proceedings of the National Academy of Sciences* 114.36, pp. 9575-9580.
- Saxton, K. E., W. J. Rawls, J. S. Romberger and R. I. Papendick (1986). 'Estimating generalized soil-water characteristics from texture'. In: *Soil Science Society of America Journal* 50, pp. 1031-1036.
- Schimmack, W., K. Auerswald and K. Bunzl (2002). 'Estimation of soil erosion and deposition rates at an agricultural site in Bavaria, Germany, as derived from fallout radiocesium and plutonium as tracers'. In: *Naturwissenschaften* 89.1, pp. 43-6.
- Schjønning, P., J. J. H. van den Akker, T. Keller, M. H. Greve, M. Lamandé, A. Simojoki, M. Stettler, J. Arvidsson and H. Breuning-Madsen (2015). 'Driver-Pressure-State-Impact-Response (DPSIR) analysis and risk assessment for soil compaction – a European perspective'. In: *Advances in Agronomy*, pp. 183-237.
- Schmidt, J., M. von Werner and A. Michael (1999). 'Application of the EROSION 3D model to the CATSOP watershed, the Netherlands'. In: *Catena* 37, pp. 449-456.
- Schwertmann, U., W. Vogl and M. Kainz (1987). *Bodenerosion durch Wasser. Vorhersage des Bodenabtrags und Bewertung von Gegenmaßnahmen*. Stuttgart: Ulmer Verlag.
- Seitz, S., P. Goebes, V. L. Puerta, E. I. P.I. Pereira, R. Wittwer, J. Six, M. G. A. van der Heijden and T. Scholten (2018). 'Conservation tillage and organic farming reduce soil erosion'. In: *Agronomy for Sustainable Development* 39.1.

- Shang, J., J. Liu, T. Huffman, B. Qian, E. Pattey, J. Wang, T. Zhao, X. Geng, D. Kroetsch, T. Dong and N. Lantz (2014). 'Estimating plant area index for monitoring crop growth dynamics using Landsat-8 and RapidEye images'. In: *Journal of Applied Remote Sensing* 8.1.
- Shang, J., J. Liu, B. Ma, T. Zhao, X. Jiao, X. Geng, T. Huffman, J. M. Kovacs and D. Walters (2015). 'Mapping spatial variability of crop growth conditions using RapidEye data in Northern Ontario, Canada'. In: *Remote Sensing of Environment* 168, pp. 113–125.
- Sims, B. and J. Kienzle (2016). 'Making mechanization accessible to smallholder farmers in Sub-Saharan Africa'. In: *Environments* 3.4.
- Singh, K., O. P. Choudhary, H. P. Singh, A. Singh and S. K. Mishra (2019). 'Sub-soiling improves productivity and economic returns of cotton-wheat cropping system'. In: *Soil & Tillage Research* 189, pp. 131–139.
- Smith, P., P. Falloon and W. L. Kutsch (2009). 'The role of soils in the Kyoto Protocol'. In: *Soil carbon dynamics. An integrated methodology*. Ed. by W. L. Kutsch, M. Bahn and A. Heinemeyer. Cambridge, UK: Cambridge University Press, pp. 245–256.
- Smith, P., J. U. Smith, D. S. Powlson, McGill W. B., J. R. M. Arah, O. G. Chertov, K. Coleman, U. Franko, S. Frolking, D. S. Jenkinson, L. S. Jensen, R. H. Kelly, H. Klein-Gunnewiek, A. S. Komarow, C. Li, J. A. E. Molina, T. Mueller, W. J. Parton, J. H. M. Thornley and A. P. Whitmore (1997). 'A comparison of the performance of nine soil organic matter models using datasets from seven long-term experiments'. In: *Geoderma* 81, pp. 153–225.
- Soil Science Society of America (2008). *Glossary of Soil Science Terms*. Madison, Wisconsin, USA: Soil Science Society of America.
- Sommer, M., S. Fiedler, S. Glatzel and M. Kleber (2004). 'First estimates of regional (Allgäu, Germany) and global CH<sub>4</sub> fluxes from wet colluvial margins of closed depressions in glacial drift areas'. In: *Agriculture, Ecosystems & Environment* 103.1, pp. 251–257.
- Sommer, M., H. H. Gerke and D. Deumlich (2008). 'Modelling soil landscape genesis. A "time split" approach for hummocky agricultural landscapes'. In: *Geoderma* 145.3-4, pp. 480–493.
- Sommer, M., M. Hoffmann, H. H. Gerke and K. Meier (2020). *Multi-year soil, plant, weather and treatment data from an erosion-affected soil landscape in the Uckermark region*.
- Song, X. P., M. C. Hansen, S. V. Stehman, P. V. Potapov, A. Tyukavina, E. F. Vermote and J. R. Townshend (2018). 'Global land change from 1982 to 2016'. In: *Nature* 560.7720, pp. 639–643.
- Staatliche Zentralverwaltung für Statistik (1956-1990). *Statistisches Jahrbuch der Deutschen Demokratischen Republik [year]*.
- Stadler, A., S. Rudolph, M. Kupisch, M. Langensiepen, J. van der Kruk and F. Ewert (2015). 'Quantifying the effects of soil variability on

- crop growth using apparent soil electrical conductivity measurements'. In: *European Journal of Agronomy* 64, pp. 8–20.
- Stallard, R. F. (1998). 'Terrestrial sedimentation and the carbon cycle: Coupling weathering and erosion to carbon burial'. In: *Global Biogeochemical Cycles* 12.2, pp. 231–257.
- Statistisches Bundesamt (Destatis) (2011). *Land- und Forstwirtschaft, Fischerei. Bodenbearbeitung, Bewässerung, Landschaftselemente. Erhebung über landwirtschaftliche Produktionsmethoden (ELPM). 2010.*
- (2015-2019). *Statistisches Jahrbuch. Deutschland und Internationales.*
- (2017). *Land- und Forstwirtschaft, Fischerei. Bodenbearbeitung, Erosionsschutz, Fruchtwechsel / Agrarstrukturerhebung 2016.*
- (2021). *DESTATIS. Statistical data from Brandenburg.* URL: [https://www.statistischebibliothek.de/mir/receive/DESerie\\_mods\\_00000498](https://www.statistischebibliothek.de/mir/receive/DESerie_mods_00000498).
- Steduto, P., T. C. Hsiao, D. Raes and E. Fereres (2009). 'AquaCrop – The FAO crop model to simulate yield response to water: I. Concepts and underlying principles'. In: *Agronomy Journal* 101.3, pp. 426–437.
- Stockmann, U. et al. (2013). 'The knowns, known unknowns and unknowns of sequestration of soil organic carbon'. In: *Agriculture, Ecosystems & Environment* 164, pp. 80–99.
- Stone, J. R., J. W. Gilliam, D. K. Cassel, R. B. Daniels, L. A. Nelson and H. J. Kleiss (1985). 'Effect of erosion and landscape position on the productivity of Piedmont soils'. In: *Soil Science Society of America Journal* 49, pp. 987–991.
- Su, Z. A. and J. H. Zhang (2010). 'Effects of tillage erosion on soil redistribution in a purple soil with steep sloping terraces'. In: *IEEE*.
- Sui, Yueyu, Xiaobing Liu, Jian Jin, Shaoliang Zhang, Xingyi Zhang, Stephen J. Herbert and Guangwei Ding (2009). 'Differentiating the early impacts of topsoil removal and soil amendments on crop performance/productivity of corn and soybean in eroded farmland of Chinese Mollisols'. In: *Field Crops Research* 111.3, pp. 276–283.
- Swan, J. B., M. J. Shaffer, W. H. Paulson and A. E. Peterson (1987). 'Simulating the effects of soil depth and climatic factors on corn yield'. In: *Soil Science Society of America Journal* 51, pp. 1025–1032.
- Tanaka, D. L. and J. K. Aese (1989). 'Influence of topsoil removal and fertilizer application on spring wheat yields'. In: *Soil Science Society of America Journal* 53, pp. 228–232.
- Taylor, J. C., G. A. Wood, R. Earl and R. J. Godwin (2003). 'Soil factors and their influence on within-field crop variability, part II: Spatial analysis and determination of management zones'. In: *Biosystems Engineering* 84.4, pp. 441–453.
- Thaler, E. A., I. J. Larsen and Q. Yu (2021). 'The extent of soil loss across the US Corn Belt'. In: *Proceedings of the National Academy of Sciences* 118.8.

- Thapa, B. B., D. K. Cassel and D. P. Garrity (1999a). 'Assessment of tillage erosion rates on steepland Oxisols in the humid tropics using granite rocks'. In: *Soil & Tillage Research* 51, pp. 233–243.
- (1999b). 'Ridge tillage and contour natural grass barrier strips reduce tillage erosion'. In: *Soil & Tillage Research* 51, pp. 341–356.
- Thorup-Kristensen, K., M. Salmerón Cortasa and R. Loges (2009). 'Winter wheat roots grow twice as deep as spring wheat roots, is this important for N uptake and N leaching losses?' In: *Plant and Soil* 322.1-2, pp. 101–114.
- Tiessen, K. H. D., G. R. Mehuys, D. A. Lobb and H. W. Rees (2007). 'Tillage erosion within potato production systems in Atlantic Canada: I. Measurement of tillage translocation by implements used in seedbed preparation'. In: *Soil & Tillage Research* 95.1-2, pp. 308–319.
- Tiessen, K. H. D., F. M. Sancho, D. A. Lobb and G. R. Mehuys (2010). 'Assessment of tillage translocation and erosion by the disk plow on steepland Andisols in Costa Rica'. In: *Journal of Soil and Water Conservation* 65.5, pp. 316–328.
- Tsara, M., S. Gerontidis, M. Marathianou and C. Kosmas (2001). 'The long-term effect of tillage on soil displacement of hilly areas used for growing wheat in Greece'. In: *Soil Use and Management* 17, pp. 113–120.
- Tso, B. and P. Mather (2009). *Classification methods for remotely sensed data*. Vol. 2. Boca Raton, FL, USA: CRC Press.
- Tum, M. and K. P. Günther (2011). 'Validating modelled NPP using statistical yield data'. In: *Biomass and Bioenergy* 35.11, pp. 4665–4674.
- Turkelboom, F., J. Poesen, I. Ohler and S. Ongprasert (1999). 'Reassessment of tillage erosion rates by manual tillage on steep slopes in northern Thailand'. In: *Soil & Tillage Research* 51, pp. 245–259.
- Turkelboom, F., J. Poesen, I. Ohler, K. Van Keer, S. Ongprasert and K. Vlassak (1997). 'Assessment of tillage erosion rates on steep slopes in northern Thailand'. In: *Catena* 29, pp. 29–44.
- Umweltbundesamt (UBA) (2022). 'Trends der Niederschlagshöhe'. In: URL: <https://plato.stanford.edu/archives/sum2017/entries/relativism>.
- United Nations Framework Convention on Climate Change (UNFCCC) (1998). *Kyoto Protocol to the United Nations Framework Convention on Climate Change*. Tech. rep.
- (2015). *Paris agreement*. Tech. rep.
- Vahrson, W.-G. and M. Frielinghaus (1998). 'Bodenverlagerung durch Ackerbau in einer Jungmoränenlandschaft Nordostdeutschlands'. In: *Beiträge für Forstwirtschaft und Landschaftsökologie* 32.3.
- Van Hemelryck, H., P. Fiener, K. Van Oost, G. Govers and R. Merckx (2010). 'The effect of soil redistribution on soil organic carbon: An experimental study'. In: *Biogeosciences* 7.12, pp. 3971–3986.

- Van Hemelryck, H., G. Govers, K. Van Oost and R. Merckx (2011). 'Evaluating the impact of soil redistribution on the in situ mineralization of soil organic carbon'. In: *Earth Surface Processes and Landforms* 36.4, pp. 427–438.
- Van Loo, M., B. Duser, G. Verstraeten, H. Renssen, B. Notebaert, K. D'Haen and J. Bakker (2017). 'Human induced soil erosion and the implications on crop yield in a small mountainous Mediterranean catchment (SW-Turkey)'. In: *Catena* 149, pp. 491–504.
- Van Muysen, W. and G. Govers (2002a). 'Soil displacement and tillage erosion during secondary tillage operations: The case of rotary harrow and seeding equipment'. In: *Soil & Tillage Research* 65, pp. 185–191.
- (2002b). 'Soil displacement and tillage erosion during secondary tillage operations: the case of rotary harrow and seeding equipment'. In: *Soil & Tillage Research* 65, pp. 185–191.
- Van Muysen, W., G. Govers, G. Bergkamp, M. Roxo and J. Poesen (1999). 'Measurement and modelling of the effects of initial soil conditions and slope gradient on soil translocation by tillage'. In: *Soil & Tillage Research* 51, pp. 303–316.
- Van Muysen, W., G. Govers and K. Van Oost (2002). 'Identification of important factors in the process of tillage erosion: The case of mouldboard tillage'. In: *Soil & Tillage Research* 65, pp. 77–93.
- Van Muysen, W., G. Govers, K. Van Oost and A. Van Rompaey (2000). 'The effect of tillage depth, tillage speed, and soil condition on chisel tillage erosivity'. In: *Journal of Soil and Water Conservation* 55.3, pp. 355–364.
- Van Muysen, W., K. Van Oost and G. Govers (2006). 'Soil translocation resulting from multiple passes of tillage under normal field operating conditions'. In: *Soil & Tillage Research* 87.2, pp. 218–230.
- Van Oost, K. and M. M. Bakker (2012). 'Soil erosion and productivity'. In: *Soil ecology and ecosystem services*. Ed. by D. H. Wall, R. D. Bardgett, V. Behan-Pelletier, J. E. Herrick, T. H. Jones, K. Ritz, J. Six, D. R. Strong and W. H. van der Putten. Oxford, UK: Oxford University Press, pp. 301–314.
- Van Oost, K., L. Beuselinck, P. B. Hairsine and G. Govers (2004a). 'Spatial evaluation of a multi-class sediment transport and deposition model'. In: *Earth Surface Processes and Landforms* 29.8, pp. 1027–1044.
- Van Oost, K., O. Cerdan and T. A. Quine (2009a). 'Accelerated sediment fluxes by water and tillage erosion on European agricultural land'. In: *Earth Surface Processes and Landforms* 34.12, pp. 1625–1634.
- Van Oost, K. and G. Govers (2006). 'Tillage erosion'. In: *Soil Erosion in Europe*. Ed. by J. Boardman and J. Poesen. Chichester, West Sussex, England: John Wiley & Sons, p. 839.

- Van Oost, K., G. Govers, S. De Alba and T. A. Quine (2006a). 'Tillage erosion: A review of controlling factors and implications for soil quality'. In: *Progress in Physical Geography* 30.4, pp. 443–466.
- Van Oost, K., G. Govers and P. Desmet (2000). 'Evaluating the effects of changes in landscape structure on soil erosion by water and tillage'. In: *Landscape Ecology* 15, pp. 577–589.
- Van Oost, K., G. Govers, T. A. Quine and G. Heckrath (2004b). 'Comment on "Managing soil carbon" (I)'. In: *Science* 305.5690, pp. 1567–1567.
- Van Oost, K., G. Govers, T. A. Quine, G. Heckrath, J. E. Olesen, S. De Gryze and R. Merckx (2005a). 'Landscape-scale modeling of carbon cycling under the impact of soil redistribution: The role of tillage erosion'. In: *Global Biogeochemical Cycles* 19.4.
- Van Oost, K., G. Govers and W. Van Muysen (2003). 'A process-based conversion model for caesium-137 derived erosion rates on agricultural land: an integrated spatial approach'. In: *Earth Surface Processes and Landforms* 28.2, pp. 187–207.
- Van Oost, K., T. A. Quine, G. Govers, S. De Gryze, J. Six, J. W. Harden, J. C. Ritchie, G. W. McCarty, G. Heckrath, C. Kosmas, J. V. Giraldez, J. R. Marques da Silva and R. Merckx (2007). 'The impact of agricultural soil erosion on the global carbon cycle'. In: *Science* 318.5150, pp. 626–629.
- Van Oost, K., T. A. Quine, G. Govers and G. Heckrath (2006b). 'Modeling soil erosion induced carbon fluxes between soil and atmosphere on agricultural land using SPEROS-C'. In: *Advances in soil science. Soil erosion and carbon dynamics*. Ed. by E. J. Roose, R. Lal, C. Feller, B. Barthes and B. A. Stewart. Boca Raton, FL, USA: CRS Press, pp. 37–51.
- Van Oost, K., T. Quine, G. Govers and G. Heckrath (2005b). 'Modeling soil erosion induced carbon fluxes between soil and atmosphere on agricultural land using SPEROS-C'. In: *Advances in Soil Science. Soil Erosion and Carbon Dynamics*. Ed. by E. J. Roose, R. Lal, C. Feller, B. Barthes and B. A. Stewart. Boca Raton, FL: CRC Press, pp. 37–51.
- Van Oost, K. and J. Six (2023). 'Reconciling the paradox of soil organic carbon erosion by water'. In: *Biogeosciences* 20.3, pp. 635–646.
- Van Oost, K., H. Van Hemelryck and J. W. Harden (2009b). 'Erosion of soil organic carbon: Implications for carbon sequestration'. In: *Carbon sequestration and its role in the global carbon cycle*. Ed. by B. J. McPherson and E. T. Sundquist. Washington, DC: American Geophysical Union, pp. 189–202.
- Van Oost, K., G. Verstraeten, S. Doetterl, B. Notebaert, F. Wiaux, N. Broothaerts and J. Six (2012). 'Legacy of human-induced C erosion and burial on soil-atmosphere C exchange'. In: *Proceedings of the National Academy of Sciences* 109.47, pp. 19492–7.

- Van Rompaey, A. J. J., G. Verstraeten, K. Van Oost, G. Govers and J. Poesen (2001). 'Modelling mean annual sediment yield using a distributed approach'. In: *Earth Surface Processes and Landforms* 26.11, pp. 1221–1236.
- Van der Meij, W. M., T. Reimann, V. K. Vornehm, A. J. A. M. Temme, J. Wallinga, R. Beek and M. Sommer (2019). 'Reconstructing rates and patterns of colluvial soil redistribution in agrarian (hummocky) landscapes'. In: *Earth Surface Processes and Landforms*.
- Van der Meij, W. M., A. J. A. M. Temme, J. Wallinga, W. Hierold and M. Sommer (2017). 'Topography reconstruction of eroding landscapes. A case study from a hummocky ground moraine (CarboZALF-D)'. In: *Geomorphology* 295, pp. 758–772.
- VandenBygaart, A. J., E. G. Gregorich and B. L. Helgason (2015). 'Cropland C erosion and burial: Is buried soil organic matter biodegradable?' In: *Geoderma* 239-240, pp. 240–249.
- Verch, G. (2020). *Longterm effects of different mineral and organic fertilizer and soil cultivation on the yield in a crop rotation (Northeast Germany)*.
- Verstraeten, G., K. Van Oost, A. J. J. Van Rompaey, J. Poesen and G. Govers (2002). 'Evaluating an integrated approach to catchment management to reduce soil loss and sediment pollution through modelling'. In: *Soil Use and Management* 19, pp. 386–394.
- Vogel, E., D. Deumlich and M. Kaupenjohann (2016). 'Bioenergy maize and soil erosion – Risk assessment and erosion control concepts'. In: *Geoderma* 261, pp. 80–92.
- Volkert, W. (1991). 'Dreifelderwirtschaft'. In: *Adel bis Zunft. Ein Lexikon des Mittelalters*. Ed. by W. Volkert. Munich: C. H. Beck'sche Verlagsbuchhandlung, p. 49.
- Wang, Y., Z. Zhang, J. Zhang, X. Liang, X. Liu and Y. Zeng (2021). 'Effect of surface rills on soil redistribution by tillage erosion on a steep hillslope'. In: *Geomorphology* 380.
- Wang, Z., T. Hoffmann, J. Six, J. O. Kaplan, G. Govers, S. Doetterl and K. Van Oost (2017). 'Human-induced erosion has offset one-third of carbon emissions from land cover change'. In: *Nature Climate Change* 7.5, pp. 345–349.
- Webber, H. et al. (2018). 'Diverging importance of drought stress for maize and winter wheat in Europe'. In: *Nature Communications* 9.1, p. 4249.
- Wehrhan, M., P. Rauneker and M. Sommer (2016). 'UAV-based estimation of carbon exports from heterogeneous soil landscapes. A case study from the CarboZALF experimental area'. In: *Sensors* 16.2, p. 255.
- Wehrhan, M. and M. Sommer (2021). 'A parsimonious approach to estimate soil organic carbon applying unmanned aerial system

- (UAS) multispectral imagery and the topographic position index in a heterogeneous soil landscape'. In: *Remote Sensing* 13.18.
- Weil, R. R. and N. C. Brady (2017). *The nature and properties of soil*. Harlow, Essex, England: Pearson Education Limited.
- Wickham, H. (2016). 'ggplot2: Elegant graphics for data analysis'. In: *Springer, New York*.
- Wildemeersch, J. C. J., J. Vermang, W. M. Cornelis, J. Diaz, D. Gabriels and M.-E. Ruiz (2014). 'Tillage erosion and controlling factors in traditional farming systems in Pinar del Río, Cuba'. In: *Catena* 121, pp. 344–353.
- Wilken, F., M. Baur, M. Sommer, D. Deumlich, O. Bens and P. Fiener (2018). 'Uncertainties in rainfall kinetic energy-intensity relations for soil erosion modelling'. In: *Catena* 171, pp. 234–244.
- Wilken, F., P. Fiener and K. Van Oost (2017a). 'Modelling a century of soil redistribution processes and carbon delivery from small watersheds using a multi-class sediment transport model'. In: *Earth Surface Dynamics* 5.1, pp. 113–124.
- Wilken, F., M. Ketterer, S. Koszinski, M. Sommer and P. Fiener (2020). 'Understanding the role of water and tillage erosion from  $^{239} + ^{240}\text{Pu}$  tracer measurements using inverse modelling'. In: *Soil* 6.2, pp. 549–564.
- Wilken, F., M. Sommer, K. Van Oost, O. Bens and P. Fiener (2017b). 'Process-oriented modelling to identify main drivers of erosion-induced carbon fluxes'. In: *Soil* 3.2, pp. 83–94.
- Winnige, B. (2004). 'Ergebnisse zur Bodenverlagerung durch Bearbeitungserosion in der Jungmoränenlandschaft Nordostdeutschlands – Investigations of soil movement by tillage as a type of soil erosion in the young moraine soil landscape of Northeast Germany'. In: *Archives of Agronomy and Soil Science* 50.3, pp. 319–327.
- Winnige, B., M. Frielinghaus and Y. Li (2003). 'Bedeutung der Bearbeitungserosion im Jungmoränengebiet'. In: *Mitteilungen der Deutschen Bodenkundlichen Gesellschaft*. Vol. 101, pp. 93–94.
- Wischmeier, W. H. and D. D. Smith (1978). *Predicting rainfall erosion losses: A guide to conservation planning*. Vol. 537. Agriculture Handbook. Washington, D.C.: United States Department for Agriculture.
- Yadav, V. and G. P. Malanson (2009). 'Modeling impacts of erosion and deposition on soil organic carbon in the Big Creek Basin of southern Illinois'. In: *Geomorphology* 106.3-4, pp. 304–314.
- Yang, W., X. Zhang, W. Gong, Y. Ye and Y. Yang (2019). 'Soil erosion and corn yield in a cultivated catchment of the Chinese Mollisol region'. In: *PLoS One* 14.10, e0221553.
- Zádorová, T. and V. Penížek (2018). 'Formation, morphology and classification of colluvial soils: A review'. In: *European Journal of Soil Science* 69.4, pp. 577–591.

- Zádorová, T., V. Penížek, R. Vašát, D. Žížala, T. Chuman and A. Vaněk (2015). 'Colluvial soils as a soil organic carbon pool in different soil regions'. In: *Geoderma* 253-254, pp. 122–134.
- Zádorová, T., V. Penížek, L. Šefrna, O. Drábek, M. Mihaljevič, Š. Volf and T. Chuman (2013). 'Identification of Neolithic to Modern erosion-sedimentation phases using geochemical approach in a loess covered sub-catchment of South Moravia, Czech Republic'. In: *Geoderma* 195-196, pp. 56–69.
- Zádorová, T., V. Penížek, L. Šefrna, M. Rohošková and L. Borůvka (2011). 'Spatial delineation of organic carbon-rich Colluvial soils in Chernozem regions by terrain analysis and fuzzy classification'. In: *Catena* 85.1, pp. 22–33.
- Zhang, H., E. Aldana-Jague, F. Clapuyt, F. Wilken, V. Vanacker and K. Van Oost (2019). 'Evaluating the potential of post-processing kinematic (PPK) georeferencing for UAV-based structure-from-motion (SfM) photogrammetry and surface change detection'. In: *Earth Surface Dynamics* 7.3, pp. 807–827.
- Zhang, J. H., M. Frielinghaus, G. Tian and D. A. Lobb (2004a). 'Ridge and contour tillage effects on soil erosion from steep hillslopes in the Sichuan Basin, China'. In: *Journal of Soil and Water Conservation* 59.4, pp. 277–284.
- Zhang, J. H. and F. C. Li (2011). 'An appraisal of two tracer methods for estimating tillage erosion rates under hoeing tillage'. In: *Procedia Environmental Sciences* 11, pp. 1227–1233.
- Zhang, J. H., Z. A. Su and X. J. Nie (2009). 'An investigation of soil translocation and erosion by conservation hoeing tillage on steep lands using a magnetic tracer'. In: *Soil & Tillage Research* 105.2, pp. 177–183.
- Zhang, J., D. A. Lobb, Y. Li and G. C. Liu (2004b). 'Assessment of tillage translocation and tillage erosion by hoeing on the steep land in hilly areas of Sichuan, China'. In: *Soil & Tillage Research* 75.2, pp. 99–107.
- Zhang, L., Y. Huang, L. Rong, X. Duan, R. Zhang, Y. Li and J. Guan (2021). 'Effect of soil erosion depth on crop yield based on topsoil removal method: A meta-analysis'. In: *Agronomy for Sustainable Development* 41.5.
- Zhao, P., S. Li, E. Wang, X. Chen, J. Deng and Y. Zhao (2018). 'Tillage erosion and its effect on spatial variations of soil organic carbon in the black soil region of China'. In: *Soil & Tillage Research* 178, pp. 72–81.
- Zikeli, S. and S. Gruber (2017). 'Reduced tillage and no-till in organic farming systems, Germany – Status quo, potentials and challenges'. In: *Agriculture* 7.4.

- Žížala, D., T. Zádorová and J. Kapička (2017). 'Assessment of soil degradation by erosion based on analysis of soil properties using aerial hyperspectral images and ancillary data, Czech Republic'. In: *Remote Sensing* 9.1.
- Öttl, L. K., F. Wilken, K. Auerswald, M. Sommer, M. Wehrhan and P. Fiener (2021). 'Tillage erosion as an important driver of in-field biomass patterns in an intensively used hummocky landscape'. In: *Land Degradation & Development* 32.10, pp. 3077–3091.
- Öttl, L. K., F. Wilken, A. Hupfer, M. Sommer and P. Fiener (2022). 'Non-inversion conservation tillage as an underestimated driver of tillage erosion'. In: *Scientific Reports* 12.20704.
- Öttl, L. K., F. Wilken, A. Juřicová, P. V. G. Batista and P. Fiener (submitted to Soil). *A millennium of arable land use - the long-term impact of water and tillage erosion on landscape-scale carbon dynamics*.
- Świtoniak, M. (2015). 'Issues relating to classification of colluvial soils in young morainic areas (Chełmno and Brodnica Lake District, northern Poland)'. In: *Soil Science Annual* 66.2, pp. 57–66.

## TILLAGE EROSION AS AN UNDERESTIMATED DRIVER OF CARBON DYNAMICS

---

ANNA JUŘICOVÁ<sup>1,2</sup>, LENA K. ÖTTL<sup>3</sup>, FLORIAN WILKEN<sup>3</sup>, TOMÁŠ CHUMAN<sup>1</sup>, DANIEL ŽÍŽALA<sup>2</sup>, ROBERT MINAŘÍK<sup>2,4</sup>, AND PETER FIENER<sup>3</sup>

<sup>1</sup> *Department of Physical Geography and Geocology, Faculty of Science, Charles University, Prague, Czech Republic*

<sup>2</sup> *Remote Sensing and Pedometrics Laboratory, Soil Survey, Research Institute for Soil and Water Conservation, Prague, Czech Republic* <sup>3</sup> *Water and Soil Resource Research, Institute of Geography, University of Augsburg, Augsburg, Germany* <sup>4</sup> *OpenGeoHub Foundation, Wageningen, The Netherlands*

This chapter is submitted to *Soil & Tillage Research*.

**ABSTRACT.** Arable soils may play an important role in climate mitigation actions as soil management directly affects soil carbon (C) sequestration and mineralisation. To evaluate the C sequestration potential in hilly terrain it is essential that not only changes in vertical C fluxes (more C input and/or reduced mineralisation), but also lateral soil organic carbon (SOC) redistribution due to erosion processes are considered. Soil redistribution due to tillage has been identified as an important contributor to soil redistribution processes and modulator of SOC dynamics. Nevertheless, the focus of most studies dealing with SOC redistribution still lies on water erosion. This study assesses the impact of tillage redistribution on C fluxes in an intensively cultivated loess region (200 ha) in the Czech Republic. Therefore, the coupled water and tillage redistribution and C turnover model SPEROS-C was used to analyse the effect of six decades of erosion upon C fluxes, whereas a specific focus was set to the analysis of the importance of tillage erosion processes. The results indicate that tillage redistribution (TIL) is an important driver of C dynamics in the study area, especially at slope shoulders where a substantial decline in SOC was modelled and monitored. Even if water erosion (WAT) is the more dominant process in the region, the model results reveal that TIL increased the cumulative, erosion-induced SOC sequestration potential by about 37%. Moreover, it was interesting to note that TIL reduced the total sediment delivery from the monitoring site via a change in topsoil SOC patterns and hence, water erosion induced sediment transport. Overall, we could show that tillage erosion in the highly productive

loess region of the Czech Republic led to a substantial SOC sink since agricultural mechanisation substantially increased about six decades ago. This indicates that climate mitigation measures based on adapted agricultural management to increase SOC sequestration, which are often in-line with soil conservation measures, might be less effective as the erosion-induced C sink effect declines.

**Keywords:** tillage erosion, water erosion, carbon dynamics, spatial modelling

#### A.1 INTRODUCTION

There are growing efforts to increase SOC sequestration to mitigate climate change, as prominently fostered in the 4 per 1000 initiative (Lima Paris Action Agenda: 4 per 1000 initiative). The aim attempts to increase C storage in the topsoil by 0.4 % every year by transforming agricultural management using the SOC sequestration potential of arable soils. However, to understand SOC sequestration in undulating arable landscapes, it is essential to account for different lateral soil redistribution processes (primarily due to water, wind, and tillage). Soil redistribution processes affect SOC dynamics and substantially alter the overall C balance of the entire agroecosystems (vannoost:2022; e.g. Berhe et al., 2007; Lal, 2003). The effect of soil redistribution on C fluxes on arable landscapes has been quantified in a number of regional studies (e.g. Dlugoš et al., 2012; Nadeu et al., 2015; Van Oost et al., 2012), while on a global scale there is still a considerable uncertainty if redistribution leads to a net source or sink of carbon dioxide (CO<sub>2</sub>) (summarised in Doetterl et al., 2016). The majority of studies that deal with the effect of soil redistribution on SOC patterns on arable land are solely considering soil redistribution processes by water (e.g. Jacinthe et al., 2002; Lal et al., 2004; Quinton et al., 2006), while processes of tillage are often ignored.

Tillage was originally only studied as a contributor to soil sensitivity for other erosion agents (mainly water erosion; Govers et al., 1994) as it substantially alters the soil macroporosity and surface roughness (Poesen and Govers, 1986). However, ongoing research identified tillage as a critically important soil redistribution process (e.g. Govers et al., 1993, 1994; Lindstrom et al., 1990; Lobb et al., 1995) and as one of the most important drivers of soil degradation (Miller et al., 1988; Moulin et al., 1994). This impact even increased in the past 70 years due to the development of mechanised agricultural soil cultivation (Lobb et al., 2007; Zádorová et al., 2013). The impact of tillage as erosion agent was also identified as critically important for biogeochemical cycles, such as the C cycle (Quinton et al., 2010; Van Oost et al., 2007).

Depending on the water erosion magnitude driven by differences in climate and crop management, tillage erosion was found to be in the same range (e. g. Govers et al., 1993; Quine et al., 1994; Van Oost et al., 2009a, 2000) or even larger in many areas (e. g. Van Oost et al., 2003; Wilken et al., 2020; Öttl et al., 2021). In comparison to water erosion, recognised after individual large events resulting in visible erosion rills and off-site damages, the physical effects and visibility of tillage within the field appear after decades (Govers et al., 1999). On sloping landscapes, tillage erosion predominantly transfers soil from convex hilltops to thalweg positions (Van Oost et al., 2006a). This is in contrast to water erosion, which takes place on steepest slopes and along the thalwegs (e. g. Van Oost et al., 2000).

The objective of this study is to assess the contribution of tillage to total soil redistribution on arable land, and to analyse its corresponding impact on SOC stocks and C fluxes using the coupled water and tillage redistribution and C turnover model SPEROS-C. Thereby, we hypothesize that: (i) Despite the fact that the study region is characterised by severe water redistribution, tillage redistribution substantially alters SOC patterns. (ii) Tillage redistribution strengthens the C sink function of soil redistribution processes in the study region, as SOC is not delivered from arable land to adjacent ecosystems.

## A.2 MATERIALS AND METHODS

### A.2.1 *Study site*

The study area is located in south Moravia, Czech Republic, a region characterised by intensive agricultural use and an undulating topography (Figure A.1). Due to the fertile soils in the region, cultivation has started about 1000 years ago (Beranová and Kubačák, 2010). Historically, narrow (< 15 m) and long fields (up to 150 - 200 m) and were typically arranged along the contours. This field layout was fundamentally changed into large homogenous fields during the collectivisation of agricultural land in the second half of the 20<sup>th</sup> century (Lipský, 1995). The absence of field boundaries that previously acted as sediment traps led to a substantial acceleration of water erosion (Devátý et al., 2019).

Since the 19<sup>th</sup> century the typical crops of the study area consist of cereals (*Triticum aestivum*, *Hordeum vulgare*), oilseed rape (*Brassica napus subsp. napus*), and corn (*Zea mays*). With changing the field layouts in the second half of the 20<sup>th</sup> century also new crop rotations were established which included potatoes (*Solanum tuberosum*) or sugar beet (*Beta vulgaris*). This again changed since 1990 and potatoes and sugar beet can hardly be found in today's rotations.

The study was conducted on four fields with a total area of 200 ha (mean field size of 47 ha). The study site is characterised by long

hillslopes (mean slope length of 130 m) and a varying topography with slopes ranging from  $1^{\circ}$  to  $20^{\circ}$  (mean slope of  $6.8^{\circ}$ ). Pleistocene loess deposits cover the undulating relief (Chlupáč et al., 2002; Forster et al., 1996). The climate is dominated by continental conditions with a 30-year (1961-1990) mean annual precipitation of 543 mm and temperature of  $8.3^{\circ}\text{C}$ . For the period 1981-2010 the mean annual precipitation slightly increased to 559 mm, and temperature increased to  $8.9^{\circ}\text{C}$  (Czech Hydrometeorological Institute, 2022). Initially, the dominant soil unit of the study area is Calcic Chernozem (IUSS Working Group WRB, 2015) which is altered by intensive redistribution processes. Hence, steep slopes and slope shoulders are nowadays mostly covered by Haplic Calcisols (Zádorová et al., 2011), while at footslopes, deep colluvial soils have been developed (Zádorová et al., 2015, 2011).

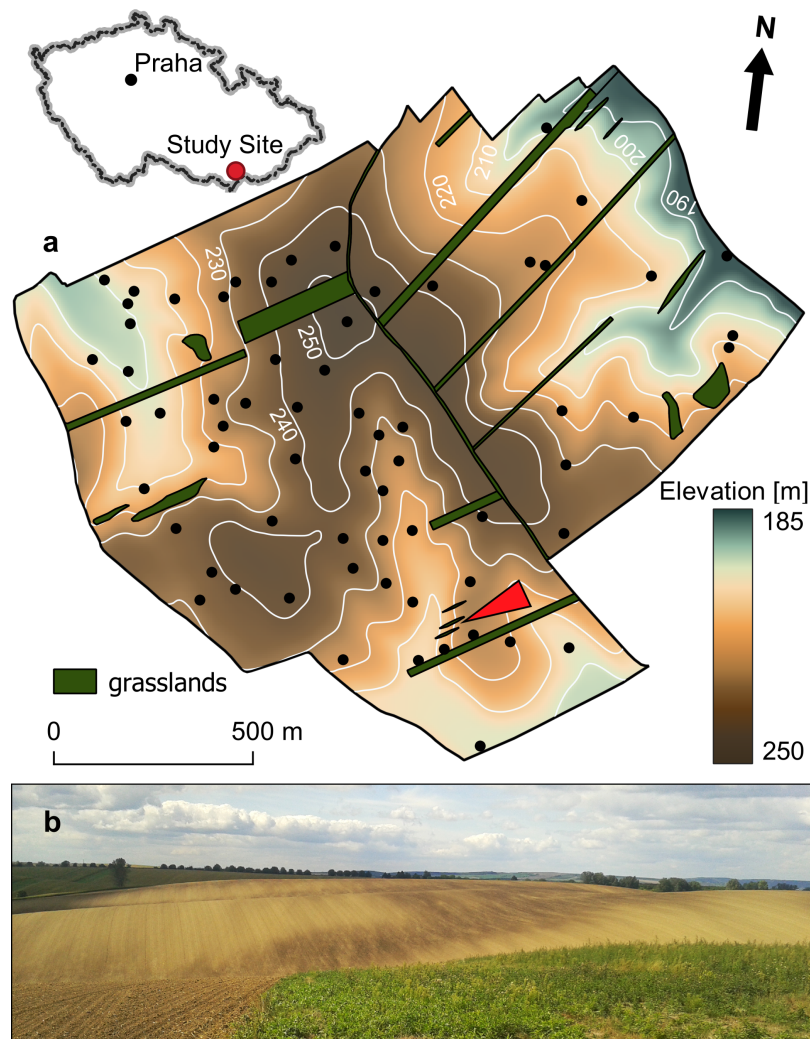


Figure A.1: (a) Study site with the position of the soil profiles (black dots). The red arrow in (a) indicates the direction of the photo view (b) over one of the thalwegs, showing a typical erosion pattern.

### A.2.2 *Field data collection*

During a field campaign in the study area, soil samples were taken to analyse the SOC content, soil texture, and bulk density from the plough layer (0–0.3 m) at 65 locations randomly sampled based on a Conditioned Latin Hypercube sampling strategy (Minasny and McBratney, 2006). For 37 out of the 65 locations, soil samples were taken from the whole humic horizon at 0.2 m intervals (up to a soil depth of 1 m, if applicable). To record the total depth of the humic horizon the soil was sampled by using a 1 m hand auger. The latter was used to classify each soil profile into either erosion ( $\leq 60$  cm of humic horizon; 44 soil profiles) or deposition ( $\geq 60$  cm of humic horizon; 21 soil profiles). Soil texture was determined using the sieve-pipette method (ISO, 2009). Bulk density ( $\text{kg m}^{-3}$ ) was measured gravimetrically from the volumes and masses of oven-dried soil using samples taken with Kopecky's cylinders. SOC content ( $\text{g kg}^{-1}$ ) was determined as the total oxidised C and was measured by wet oxidation with dichromate according to the Tjurin method (ISO, 1998). The C content was converted to SOC stocks ( $\text{kg m}^{-3}$ ) with a bulk density of  $1260 \text{ kg m}^{-3}$ . Carbonate ( $\text{CaCO}_3$ ) content was evaluated volumetrically (ISO, 1995). Stone content was not measured as Chernozems developed from loess are naturally free of stones.

To calibrate the C turnover parameters in SPEROS-C based on an inverse modelling approach, we used data from 26 nearby soil profiles located in a flat area without erosion and deposition that has a similar land management history and soil properties (detailed description in Juřicová et al., 2022).

### A.2.3 *Coupled soil redistribution and SOC turnover modelling*

The spatially explicit erosion and C turnover model SPEROS-C (Fiener et al., 2015; Van Oost et al., 2005b) was used to simulate soil and SOC redistribution due to water and tillage and associated C turnover dynamics. The erosion and sediment transport component of the model is based on the Water and Tillage Erosion Model/Sediment Delivery Model (WaTEM/SEDEM; Van Oost et al., 2000; Van Rompaey et al., 2001; Verstraeten et al., 2002), while the C turnover component is based on the Introductory Carbon Balance Model (ICBM) (Andrén and Kätterer, 1997). SPEROS-C is one of few tools available to address C dynamics associated with the combination of soil redistribution due to water and tillage.

**SOIL REDISTRIBUTION BY TILLAGE.** Soil redistribution via tillage is calculated with a diffusion-type equation originally developed by Govers et al. (1994). The rate of soil mass translocation ( $Q_s$  in  $\text{kg m}^{-2}$ ) is usually written as:

$$Q_s = D \cdot \rho_b \cdot b \cdot S = -k_{til} \cdot \frac{\partial h}{\partial x} \quad (\text{A.1})$$

$$k_{til} = -D \cdot \rho_b \cdot b \quad (\text{A.2})$$

where  $D$  is the tillage depth (m),  $\rho_b$  is the soil bulk density ( $\text{kg m}^{-3}$ ),  $S$  is the slope,  $b$  is the empirically obtained regression coefficient from the relationship between slope gradient and mean displacement of soil particles,  $h$  is the elevation of a given point,  $x$  is the direction of tillage operation, and  $k_{til}$  is the tillage transport coefficient ( $\text{kg m}^{-2}$ ). The local erosion or deposition rate ( $E$  in  $\text{kg m}^{-2} \text{yr}^{-1}$ ) is then described as:

$$E = \rho_b \cdot \frac{\partial h}{\partial t} = -\frac{\partial Q_s}{\partial x} = k_{til} \cdot \frac{\partial^2 h}{\partial x^2} \quad (\text{A.3})$$

where  $t$  is time. Due to the dependence on the change in slope gradient, redistribution by tillage operations mainly occurs on slope convexities, whereas soil accumulation prevails in concavities (Govers et al., 1994; Van Oost et al., 2000). To obtain tillage transport coefficient ( $k_{til}$ ) we used the non-linear relationship developed by Van Oost et al. (2006a) based on a regression analysis of available  $k_{til}$  data:

$$k_{til} = a \cdot \rho_b \cdot D^\alpha \cdot V^\beta \cdot X^\gamma \quad (\text{A.4})$$

where  $\rho_b$  is the soil bulk density ( $\text{kg m}^{-3}$ ),  $D$  is the tillage depth,  $V$  is the velocity of the tillage operation, and  $X$  symbolises the direction of the tillage operation (a value of 1 is used for contour tillage and a value of 2 for alternating up- and downslope tillage). The coefficients  $a$ ,  $\alpha$ ,  $\beta$ , and  $\gamma$  are the regression coefficients of Van Oost et al. (2006a). The corresponding values for mouldboard tillage for the study area are  $a = 0.97$ ,  $\alpha = 2.21$ ,  $\beta = 0.57$ , and  $\gamma = 0.67$ , respectively.

**SOIL REDISTRIBUTION BY WATER.** In order to represent spatially distributed redistribution processes by water, SPEROS-C routes sediments along hydrological networks. Water redistribution is calculated using a modified version of the widely used Revised Universal Soil Loss Equation (RUSLE) (Renard et al., 1997). The model distinguishes between erosion and deposition processes based on the local transport capacity ( $TC$  in  $\text{kg m}^{-1} \text{yr}^{-1}$ ; Van Oost et al., 2005b):

$$TC = k_{tc} \cdot (R \cdot K \cdot LS_{2D} \cdot C - (R \cdot K \cdot C \cdot 5.0 \cdot S_g^{0.8})) \cdot P_{con} \quad (\text{A.5})$$

where  $k_{tc}$  (m) is the transport capacity coefficient,  $R$  is the rain-fall erosivity factor ( $\text{MJ mm m}^{-2} \text{h}^{-1} \text{yr}^{-1}$ ),  $C$  is the cover-management factor (-),  $K$  is the soil erodibility factor ( $\text{kg m}^2 \text{h m}^{-2} \text{MJ}^{-1} \text{mm}^{-1}$ ),  $LS_{2D}$  a topographic factor (-) calculated according to Desmet and Govers (1996), and  $S$  is the slope gradient ( $\text{m m}^{-1}$ ). Parcel connectivity  $P_{con}$  (0-1) determines the proportion of sediment that is trapped at field borders, whereby 0 and 1 mean that 100% and 0% of the sediment is trapped at field borders, respectively.

**SOC DYNAMICS.** In SPEROS-C, the turnover of SOC is calculated based on ICBM (Andrén and Kätterer, 1997). SPEROS-C was already used several times to simulate SOC dynamics affected by lateral soil redistribution due to water and tillage (e. g. Dlugoß et al., 2012; Fiener et al., 2015; Nadeu et al., 2015).

ICBM represents C dynamics of two state variables, the young ( $Y$ ) and old C pool ( $O$ ), that are subject to four types of C fluxes (C input from crops and manure, mineralisation and humification; Andrén and Kätterer, 1997):

$$\frac{dY}{dt} = i - k_Y \cdot r \cdot Y \quad (\text{A.6})$$

$$\frac{dO}{dt} = h \cdot k_Y \cdot r \cdot Y - k_O \cdot r \cdot O \quad (\text{A.7})$$

where  $i$  represents C inputs by crops (here assumed as residues and roots) and manure, constants  $k_y$  and  $k_o$  determine the decomposition rates of  $Y$  and  $O$ , respectively,  $h$  is the humification coefficient, and  $r$  is a climate coefficient that depends on temperature  $T$ , which is assumed to be spatially homogenous:

$$r = 2.07 \cdot \frac{T - 5.4}{10} \quad (\text{A.8})$$

The humification coefficient ( $h$ ), which controls the C flux from  $Y$  to  $O$ , primarily depends on soil clay content ( $cl$  in %) and overall C input ( $\text{g m}^{-2} \text{yr}^{-1}$ ) from crops ( $i_c$ ) and manure ( $i_m$ ) and their respective humification coefficients ( $h_c$  and  $h_m$ ; Kätterer and Andrén, 1999):

$$h = \frac{i_c \cdot h_c + i_m \cdot h_m}{i} \cdot e^{0.0112 \cdot (cl - 36.5)} \quad (\text{A.9})$$

C inputs from crops are calculated from dry aboveground biomass (AGBM) that can be obtained from annual dry yield divided by crop-specific harvest index (HI) (Nadeu et al., 2015).

An exponential root density profile (Gerwitz and Page, 1974; Van Oost et al., 2005b) is used to model the C input into the soil. The allocation of total root dry matter to each soil layer  $z_z$  (m) is calculated based on a reference soil depth  $z_r = 0.25$  m (Van Oost et al., 2005b). A constant  $c$  determines the proportion of the roots per soil layer ( $p_z$ ).

$$\text{for } z \leq z_r: p_z = \frac{z}{z_r + \frac{1 - e^{-c \cdot (1 - z_r)}}{c}} \quad (\text{A.10})$$

$$\text{for } z > z_r: p_z = \frac{z_r + (1 - e^{-c \cdot (z - z_r)})/c}{z_r + (1 - e^{-c \cdot (1 - z_r)})/c} \quad (\text{A.11})$$

The exponential decrease of the turnover rates of the young and old pool with soil depth is expressed as follows (Rosenbloom et al., 2001):

$$k_{Y/Oz} = k_{Y/Os} \cdot e^{(-u \cdot z)} \quad (\text{A.12})$$

where  $k_{Y/Oz}$  and  $k_{Y/Os}$  are the turnover rates ( $\text{yr}^{-1}$ ) at soil depth  $z$  (m) and at the soil surface, respectively, and  $u$  (dimensionless) is the attenuation of SOC decomposition with soil depth.

A full description of the C turnover model implemented in SPEROS-C can be found in Van Oost et al. (2005b).

#### A.2.4 Model implementation and calibration

Based on the significant change in landscape structure in the Czech Republic in the middle of the 20<sup>th</sup> century, the simulation period (58 years) was set from 1961, the beginning of crop yield data recording, to 2018, when a field campaign was carried out to gain observation data. Modelling was carried out following two implementations: (i) TOT considering soil and SOC redistribution due to the combined effect of water and tillage; (ii) WAT only considering water processes.

Topographic information is based on a LiDAR digital elevation model (DEM) with a spatial resolution of 5 m (DEM 4G<sup>®</sup>; Czech Office for Surveying, Mapping and Cadaster, 2017).

For modelling SOC dynamics, two different periods of crop compositions were assumed to account for the extensive changes in the Czech agricultural system that took place in 1989. For the period 1961 - 1989, a standard crop rotation from the study region was used, including lucerne (*Medicago sativa*), winter wheat (*Triticum aestivum*), potatoes (*Solanum tuberosum*), spring barley (*Hordeum vulgare*), corn (*Zea mays*), and spring barley (*Hordeum vulgare*). For the second period 1990 - 2018, the actual crop rotation for the study area was set according to information from local farmers as follows: winter wheat (*Triticum aestivum*), corn (*Zea mays*), winter wheat (*Triticum aestivum*), and oilseed rape

(*Brassica napus subsp. napus*). According to the farmers, the crops were sown into stubbles and post-harvest residues have been left on the field in the second period.

The grasslands and pathways between parcels are also considered for the assessment of the overall erosion-induced C balance of the study area (Figure A.1). Seasonal crop cover distribution for those areas is assumed for the whole simulated period.

**SOIL REDISTRIBUTION.** The following input parameters were used for modelling water and tillage soil redistribution with SPEROS-C. Calculating  $k_{til}$  with Eq. A.4 resulted in a value of  $505 \text{ kg m}^{-1}$ . Corresponding data (tillage depth = 0.3 m, tillage speed =  $10.0 \text{ km h}^{-1}$ ) was taken from a previous study (Hrabalíková et al., 2016). An  $R$  factor of  $0.049 \text{ MJ mm m}^{-2} \text{ h}^{-1} \text{ yr}^{-1}$  was derived from the measured precipitation of the period 1985-2018 (RISWC, 2018). A  $K$  factor of  $41 \text{ kg m}^2 \text{ h m}^{-2} \text{ MJ}^{-1} \text{ mm}^{-1}$  was calculated from texture and SOC measurements following the approach of Auerswald et al. (2016). We used annual  $C$  factor values that differ between the first and second period. Overall, the crop rotations resulted in a  $C$  factor ranging from 0.048 (lucerne) to 0.74 (corn) and mean combined  $CP$  factors of 0.257 and 0.304 resulted for the first and second period, respectively. The  $P$  factor is set to 1 (no protection) and 0.86 for the first and second period, respectively. This resulted from the percentage difference between  $CP$  factor (0.352 vs. 0.304) because the crops were sown into stubbles and post-harvest residues in the second period. As the majority of erosive rainfalls occur in summer, the annual  $CP$  factor was corrected according to the percentage distribution of the  $R$  factor (RISWC, 2018). For the transport coefficient ( $k_{tc}$ ) a value of 55 m is used that was already calibrated earlier for small catchments in the Czech Republic (Krása et al., 2019). On grasslands, only water-induced soil redistribution is considered ( $CP$  factors of 0.005). We assume that 50 % of the transported sediment is trapped at the field border ( $P_{con} = 50$ ).

**SOC DYNAMICS.** The C turnover model was parametrised based on annual crop yields grown in the region of the study site from 1961 to 2018 (Czech Statistical Office, 2022). Crop-specific HI values were taken from the literature (Table A.1). The mean annual air temperature of  $10.5 \text{ }^\circ\text{C}$  was measured at a meteorological station located approximately in the centre of the study area for the period December/2016 - December/2017 (mean data from hourly records). As there is no livestock in the study area, C input from manure was excluded. The mean clay content of 22 % (ranging from 14 % to 48 %) and bulk density of  $1260 \text{ kg m}^{-3}$  (ranging from  $1070$  to  $1490 \text{ kg m}^{-3}$ ) were calculated based on data from the field campaign in 2018. Annual turnover rates

were set to  $k_Y = 0.8$  and  $k_O = 0.006$  (Andrén and Kätterer, 1997). The humification coefficients for crop and manure were set to  $h_c = 0.125$  and  $h_m = 0.31$  (Kätterer and Andrén, 1999).

Table A.1: The annual mean yield (range in brackets) for the two periods 1961 - 1989 and 1990 - 2018 and the crop-specified harvest index (HI) that is used to calculate dry aboveground biomass (AGBM).

Crop	Mean yield <sup>†</sup> (range) [kg m <sup>-2</sup> ]		Harvest index (HI)
	1961 - 1989	1990 - 2018	
Winter wheat	0.41 (0.27 - 0.57)	0.51 (0.39 - 0.66)	0.39 <sup>1)</sup>
Spring barley	0.39 (0.27 - 0.52)	-	0.39 <sup>1)</sup>
Corn	0.25 (0.17 - 0.38)	0.68 (0.34 - 1.11)	0.50 <sup>1)</sup>
Potatoes	1.63 (1.21 - 1.91)	-	0.53 <sup>2)</sup>
Oilseed rape	-	0.97 (0.72 - 1.31)	0.95 <sup>3)</sup>
Lucerne	7.81 <sup>6)</sup>	-	0.30 <sup>4)</sup>
Grassland	1.95 <sup>5)</sup>	1.95 <sup>5)</sup>	-

<sup>†</sup> the annual yields are taken from the Czech Statistical Office (2022)

<sup>1)</sup> Bolinder et al. (1999)    <sup>2)</sup> Prince et al. (2001)    <sup>3)</sup> Gobin (2010)

<sup>4)</sup> Diepenbrock (2000)    <sup>5)</sup> Kuzyakov and Domanski (2000)

<sup>6)</sup> AGBM = annual yield

The total C input from crops depends on the amount of C from crop residues left on the surface after harvest and C input by roots (Andrén and Kätterer, 1997). It is generally difficult to obtain all the SOC turnover model input parameters, and this is even more true if a period of nearly 60 years with different land management is supposed to be modelled. The most important and sensitive parameters for the SOC models are the C input allocation parameters (root to shoot ratio and residue to AGBM ratio) and the parameters allocating C in different soil depths ( $u$  and  $z$  in Eq. A.11). For a calibration of those parameters, a mean SOC depth profile was derived from 26 soil profiles of a nearby area (approx. 50 km distance) with a similar land management history, comparable soil conditions and unaffected by soil redistribution. This mean SOC depth profile is then modelled by varying the above-mentioned parameters based on an inverse modelling approach. Thereby, each parameter was sampled from a reasonable vast parameter space (see the supplementary material A.6) in a Monte Carlo framework ( $n = 1000$ ). The goodness-of-fit between modelled and observed (undisturbed) SOC depth profile is evaluated by the Nash Sutcliffe model efficiency (MEF) (Nash and Sutcliffe, 1970) and the root mean square error (RMSE). The optimised modelling of the mean profile (Figure A.2) is achieved with a root-to-shoot ratio of

0.47, a residue to AGBM ratio of 0.26, a decomposition with depth  $u$  of 2.6, and a root growth constant  $zz$  of 2.9, respectively.

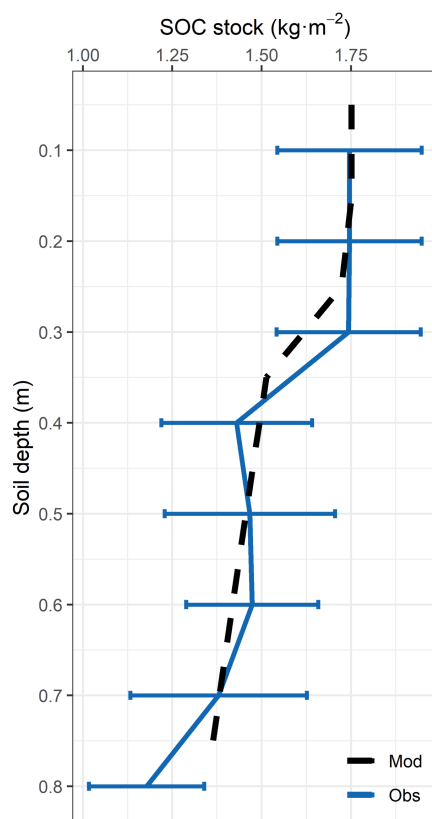


Figure A.2: Comparison between the mean observed (*Obs*, blue line) soil profiles ( $n = 26$ ) of a non-eroded area with  $\pm 95\%$  confidence intervals as the error bars and carbon (C) turnover model output obtained by the parameter set that yielded the highest Nash Sutcliffe model efficiency (MEF) of 0.85 (root mean square error (RMSE) = 0.07; *Mod*, black dashed line) in 1000 Monte Carlo simulations.

#### A.2.5 Model validation and statistical analysis

The quality of the model simulation is assessed by comparing it with the observed topsoil SOC stocks. The observed data was gained by predictive modelling using aerial hyperspectral data and ground truth data in a previous study by Žížala et al. (2017) with a prediction accuracy ( $R^2 = 0.91$ ). As the remotely sensed data showed artificially high SOC stocks along field borders (approx. 20 m to the inside of each field) due to border effects, those pixels are not included in the validation (ca. 5% of the area). The pixels are grouped into classes of 0.1 m of soil redistribution to reduce the noise resulting from the high spatial resolution of the hyperspectral data. The SOC stocks depth distribution is further validated against observed SOC stocks at 65 locations and three depth intervals (0-0.2 m, 0.2-0.4 m, 0.4-0.6 m if applicable) for erosion and deposition sites separately. Goodness-

of-fit between observed and modelled SOC stocks are quantified by Spearman's rank correlation coefficient ( $\rho$ ), MEF, and RMSE.

The results are statistically described by a mean or a median with the 1<sup>st</sup> (25 %) and 3<sup>rd</sup> (75 %) quartiles. As modelled soil redistribution in some cases shows artificially high rates especially along field borders (i. e. missing DEM update), redistribution rates ranging between -0.5 and 0.5 m after 58 years of simulation are removed (ca. 0.9 % of the data). Statistical significance is determined at level of  $p < 0.05$  (\*) and  $p < 0.01$  (\*\*). Data processing and statistical analyses are performed in R studio (R Core Team, 2022). All maps are produced in QGIS (QGIS Development Team, 2022).

### A.3 RESULTS

#### A.3.1 Soil redistribution after 58 years

The modelled 58 years of cumulative soil redistribution by water and tillage is dominated by water erosion. Water erosion is most prominent along the steepest slopes and along thalwegs, while tillage erosion prevails on hilltops and slope shoulders (Figure A.3). Both redistribution agents result in deposition along the footslopes but tillage-induced deposition can also be found along downslope field borders and thalwegs. On grasslands, the redistribution pattern mainly follows the topographic conditions.

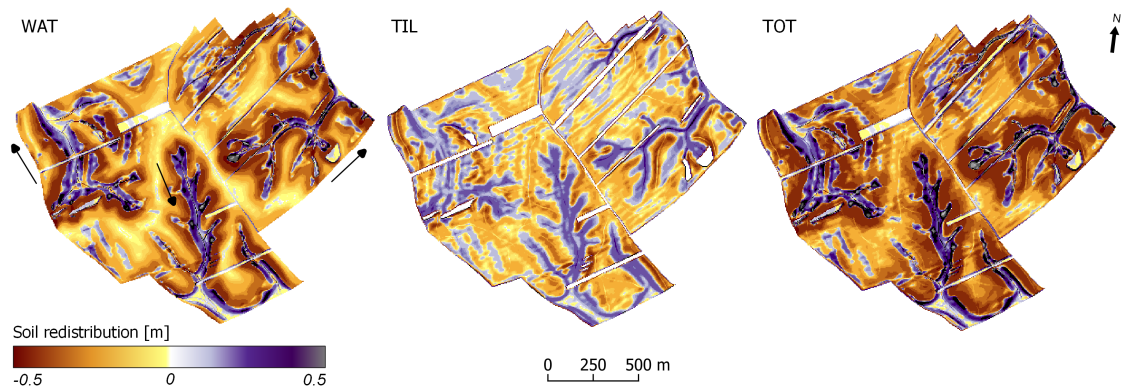


Figure A.3: Patterns of modelled soil redistribution by water (WAT), tillage (TIL), and total erosion (TOT). It is assumed that the grasslands between the fields (see Figure A.1) are only affected by water erosion and deposition. Grey lines represent 10 m contours, while black arrows in WAT indicate flow directions in thalwegs.

For erosion sites (70 % of the area), the modelled median soil loss was 0.12 m in 58 years, while for deposition sites (30 % of the area) the simulation results in a median deposition of 0.19 m. Overall, the modelled median contribution of TIL erosion to TOT is 33 %.

## A.3.2 SOC patterns

**MODEL VALIDATION.** After grouping the modelled and remote sensing-based topsoil SOC stocks into erosion classes (of 0.1 m loss or gain in 58 years) we found a strong and significant correlation between both (Figure A.4;  $R^2 = 0.85^{**}$ ). Using a pixel-by-pixel comparison, including a lot of small-scale SOC variability, especially in the remote sensing data, the modelled SOC patterns based on TOT and WAT could significantly explain data variability (TOT:  $R^2 = 0.38^{**}$ , and WAT:  $R^2 = 0.29^{**}$ , respectively). Regardless of the implementation, the highest topsoil SOC is found at sites with the lowest erosion (class of -0.1 - 0.0 m) and deposition rates (class of 0.0 - 0.1 m), while the lowest topsoil SOC is observed at highly eroded areas.

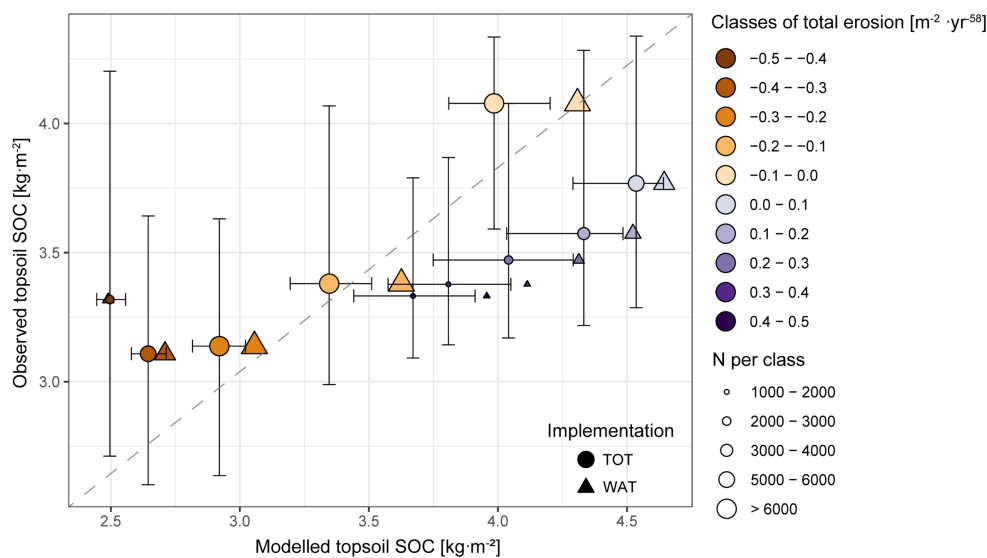


Figure A.4: Mean modelled topsoil soil organic carbon (SOC) (first 0.2 m) versus mean observed topsoil SOC derived from hyperspectral images (Žižala et al., 2017) per erosion group (TOT indicated by circles and WAT by triangles). The horizontal and vertical error bars show the 1<sup>st</sup> and 3<sup>rd</sup> quartiles of observed topsoil SOC and modelled SOC modified by TOT. The grey dashed line represents the 1:1 line.

Modelled SOC stocks for erosional and depositional sites for TOT and WAT were compared to the measured SOC stocks at 65 locations from the sampling campaign (Figure A.5; Table A.2). The overall observed median SOC stock up to 0.6 m soil depth is  $8.7 \text{ kg m}^{-2}$ , whereas the modelled SOC stock for TOT and WAT is  $8 \text{ kg m}^{-2}$  and  $8.3 \text{ kg m}^{-2}$ , respectively. Generally, the best fit is reached for the first soil layer for both implementations, and it decreases with depth (Table A.2). The observed median SOC stock in the plough layer ( $3.4 \text{ kg m}^{-2}$ ) is better predicted by TOT ( $3.7 \text{ kg m}^{-2}$ ) than by WAT ( $4 \text{ kg m}^{-2}$ ). Both implementations show an overestimation of the SOC stocks in deeper soil layers

(i.e. 0.2 - 0.4 m, 0.4 - 0.6 m). SOC stocks are also overestimated in the plough layer when erosional and depositional sites are considered separately. The overestimation is higher for WAT at erosional sites whereby SOC stocks at depositional sites are in good agreement with both.

Table A.2: Goodness-of-fit between observed and modelled SOC stocks ( $\text{kg m}^{-2}$ ) for TOT and WAT and three soil layers (0 - 0.2 m,  $n = 65$ ; 0.2 - 0.4 m,  $n = 10$ ; 0.4 - 0.6 m,  $n = 5$ ) quantified by Spearman's rank correlation coefficient ( $\rho$ ), Nash Sutcliffe model efficiency (MEF), and root mean square error (RMSE). Level of significance of the correlation coefficient is shown accordingly:  $p < 0.05$  (\*),  $p < 0.01$  (\*\*).

	Implementation	$\rho$	RMSE	MEF
0 - 20 cm	TOT	0.50**	0.97	0.12
	WAT	0.44**	1.09	-0.12
20 - 40 cm	TOT	0.78*	1	-0.38
	WAT	0.36	1.07	-0.58
40 - 60 cm	TOT	-0.3	1.18	-5.93
	WAT	-1*	1.17	-5.77
0 - 60 cm	TOT	0.53**	0.98	0.14
	WAT	0.5**	1.09	-0.06

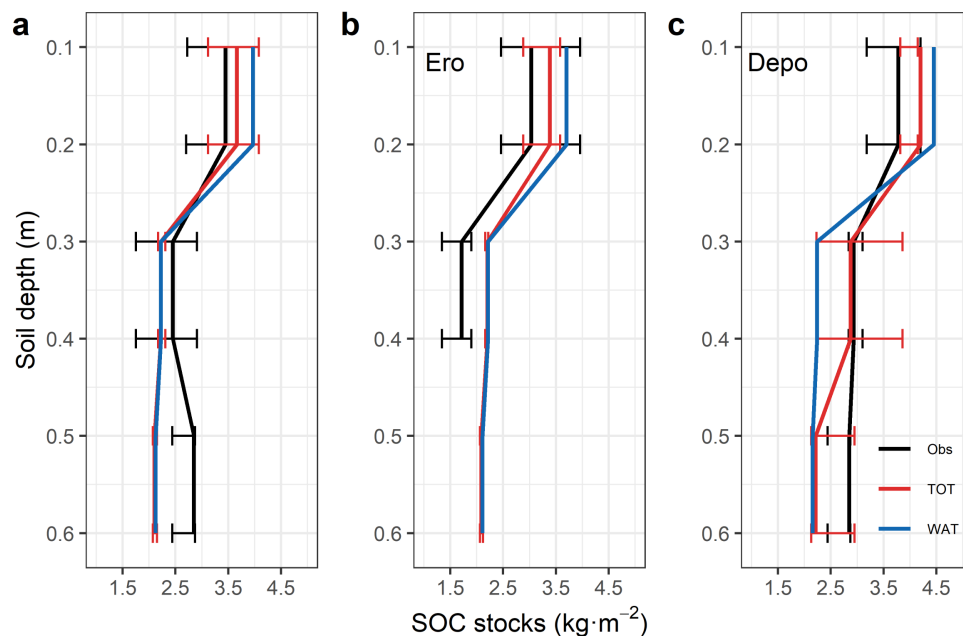


Figure A.5: Comparison of modelled TOT and WAT and observed (*Obs*) median SOC stocks ( $\text{kg m}^{-2}$ ). (a) Median values all sample sites, (b) eroded areas and (c) depositional areas. Error bars show 1<sup>st</sup> and 3<sup>rd</sup> quartiles at each depth interval (0 - 0.2, 0.2 - 0.4, 0.4 - 0.6 m).

**SOC STOCKS AFFECTED BY TOT AND WAT.** Modelled SOC stocks reveal a high spatial heterogeneity corresponding to the pattern of soil redistribution processes (Figure A.6). For the plough layer (0–0.2 m), TOT and WAT show in general a similar spatial pattern of soil redistribution and hence, SOC stocks distribution, i.e., highest SOC stocks can be found at the areas with the lowest erosion rates and at depositional sites including grasslands, where sediment is mostly trapped. On the contrary, lowest SOC stocks are found along the steepest parts of the study area, which are prone to relatively high erosion rates. However, some differences in the amount of SOC stocks can be seen if the effect of tillage is considered. Overall, the modelled median SOC stocks for the plough layer are lower for the TOT ( $3.66 \text{ kg m}^{-2}$ ) than for the WAT ( $4 \text{ kg m}^{-2}$ ).

Even though the area is dominated by water-induced soil redistribution, the influence of tillage is clearly visible at hilltops and slope shoulders. Those slope positions reveal generally lower SOC stocks for TOT than for WAT. Moreover, higher SOC stocks appear at footslopes where tillage deposition outweighs water erosion.

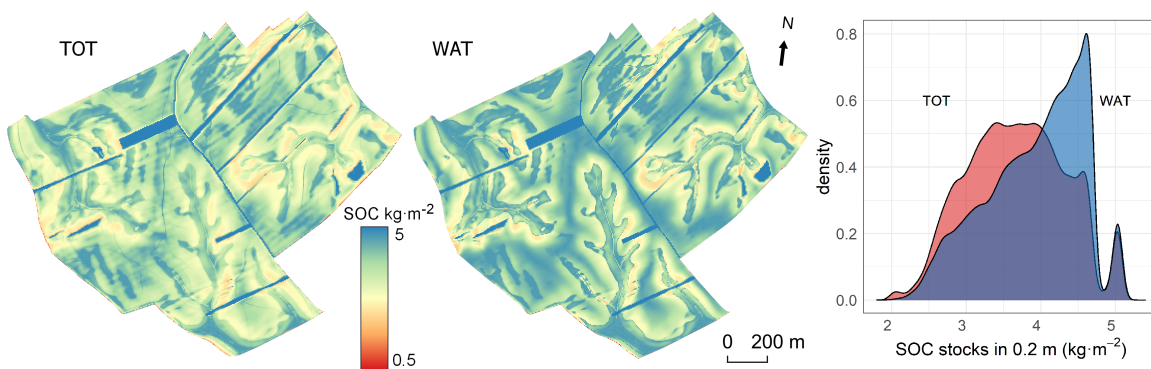


Figure A.6: Maps and density distributions of SOC stocks ( $\text{kg m}^{-2}$ ) after 58 years of modelling TOT (plot: red) and WAT (plot: blue) up to 0.2 m of modelling depth (plough layer). The highest SOC stocks appear on grasslands due to higher sequestration.

### A.3.3 Erosion-induced C balance

The overall erosion-induced C balance of the undulating agricultural landscape was calculated based on C sequestration and mineralisation at erosional and depositional sites and C export from the test area due to water erosion. C burial below 1 m was calculated separately. Per definition the erosion-induced C balance is negative, if soil redistribution leads to an overall C release to the atmosphere, while it is positive if it leads to a larger soil C sink.

The difference of the cumulative vertical soil redistribution-induced C fluxes between TOT and WAT shows that the fluxes into the soil or the atmosphere are significantly influenced by tillage redistribu-

tion (Figure A.7). At erosional sites, dynamic replacement initiated a positive C flux into the C depleted soils. In contrast, at depositional sites, the fluxes are negative, due to slow but steady mineralisation of additionally deposited SOC. Thereby, the soil's function as a C sink is more pronounced at erosional sites for TOT (including TIL) compared to WAT. The modelled cumulative C sequestration at erosional sites results in a soil influx of  $348 \text{ g m}^{-2}$  and  $475 \text{ g m}^{-2}$  for WAT and TOT, respectively. This represents an increase of 37% in C sequestration if the contribution of tillage is considered. At depositional sites, the modelled cumulative C efflux into the atmosphere is  $-285 \text{ g m}^{-2}$  and  $-296 \text{ g m}^{-2}$  (difference of 4%) for the WAT and TOT, respectively. Note that the grasslands contribute a loss of  $-0.7 \text{ g m}^{-2}$  to the annual mean C flux as they were assumed to act as depositional sites (data not shown).

The annual mean C export from the study site due to water redistribution reaches  $-2.53 \text{ g m}^{-2}$  for WAT and  $-2.44 \text{ g m}^{-2}$  for TOT. The lower C export for TOT is mainly caused by SOC rich sediment, which is transported from hilltops and slope shoulders and then accumulated at depositional sites due to tillage and therefore not accessible for water erosion. Moreover, the minor peaks in the curves indicate changes of the annual *CP* factor over the simulation period.

The erosion-induced C balance of the study site considers the area-weighted fluxes at erosional and depositional sites between soil and the atmosphere and the exported C out of the study area. The overall erosion-induced C balance is negative for the first half of the modelling period (C lost to the atmosphere) and positive for the second half of the modelling period (C stored in the soils). This results from the larger lateral loss of C with surface runoff resulting from having potatoes in the crop rotation which caused a short-term increase in water erosion rates.

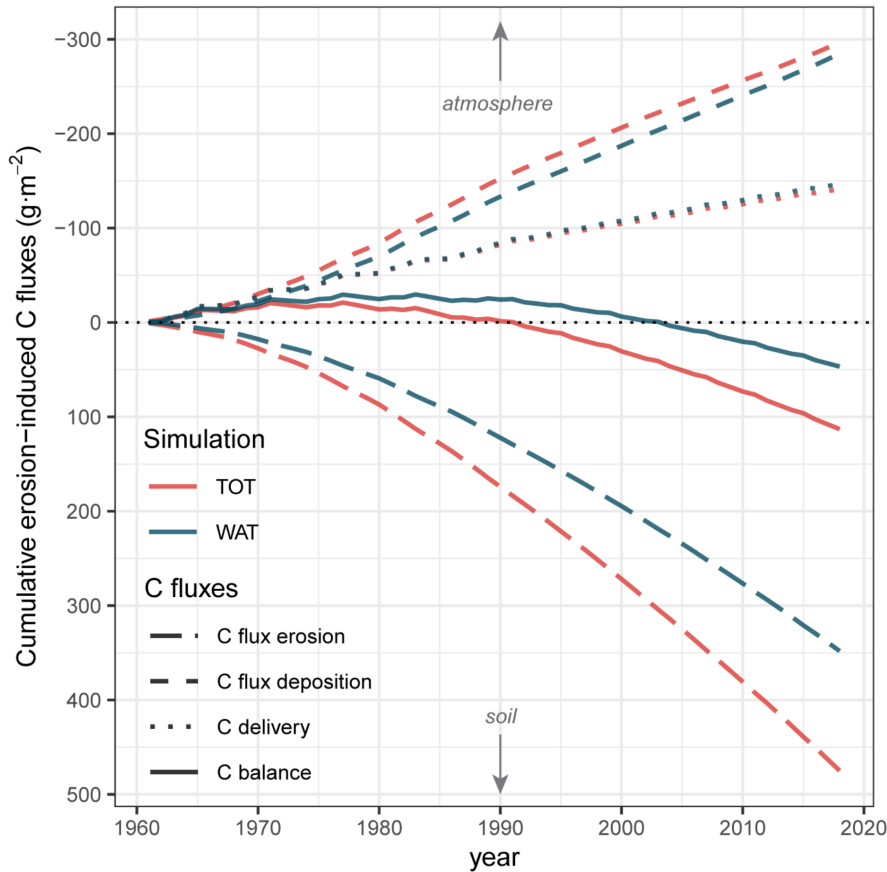


Figure A.7: Cumulative erosion-induced C fluxes ( $\text{g m}^{-2}$ ) after 58 years (1961 - 2018) for erosion (long dashed line) and deposition sites (dashed line), lateral C delivery (dotted line) and overall C balance (solid line) of the study site for TOT (red) and WAT (blue) simulation, respectively.

## A.4 DISCUSSION

### A.4.1 Erosion-induced spatial SOC patterns

The SPEROS-C model simulation results in a soil redistribution pattern that is typical for hilly agricultural regions like the chernozem region of the Czech Republic. The spatial variability of the SOC stocks is highly affected by soil redistribution due to the combined effect of water and tillage redistribution for the model period over the past 58 years. Modelled TOT rates and SOC stocks patterns are also in good agreement with a regional field study showing a soil loss of 0.23 m and the lowest SOC stocks at hilltops and slope shoulders for the period 1960-2018 (Juřicová et al., 2022). The results show net soil loss and thus lower SOC stocks at those slope positions, which can only be explained by considering tillage redistribution. The accumulation of SOC rich sediment is found at lower slope parts and thalwegs, which is also shown in this study.

It could be shown that neglecting tillage redistribution substantially underestimates the amount of transported sediment, resulting in lower accumulation rates at footslopes. This also reveals how the processes of water and tillage redistribution are interlinked in terms of different amounts of mobilised sediment from hilltops by tillage that is later available for being transported in concentrated flow by water. These findings have further consequences for the estimation of SOC stocks in Colluvisols. Especially for the chernozem region where the presence of deep colluvial soils (up to several meters) resulting from an ongoing accumulation of soil sediment is typical (Zádorová and Peňížek, 2018; Zádorová et al., 2015, 2011). The Colluvisols represent the largest soil C pool due to long-term burial of SOC rich soil sediments (Berhe and Kleber, 2013; Chabbi et al., 2009). This is an important process preserving C from decomposition as C is buried in an oxygen limited environment that reduces microbial access and mineralisation (Berhe et al., 2012, 2007; Berhe and Kleber, 2013).

Even though our findings are in line with the previous modelled studies (e.g. Nadeu et al., 2015; Van Oost et al., 2003; Wilken et al., 2017b), there are still recently published studies or reviews that are neglecting the role of tillage in the terms of soil redistribution (Borrelli et al., 2017; Lugato et al., 2018; Panagos et al., 2015) or its impact on C dynamics (Lal, 2018, 2019). This might result in misunderstanding of the role of soil redistribution of tillage and water in C dynamics. Thereby, our results point at the need to include sediment transport via tillage in regional and global scale C turnover modelling studies.

#### A.4.2 *Erosion-induced C balance*

The results of this study support the general finding that soil and corresponding SOC redistribution due to water and tillage is an essential modulator of the C source or sink function of soil systems (Doetterl et al., 2016). It can also be seen that this effect increases with time. Therefore, tillage-induced soil redistribution strengthens the soil's C sink function, due to enhanced dynamic replacement in erosional zones, deep C burial in depositional zones and restricted C export from the study area. Similar results can be found only in a few studies that assessed the roles of water- and tillage-induced soil redistribution on C dynamics separately (Van Oost et al., 2005a; Wilken et al., 2017b). Van Oost et al. (2005a) found a higher positive erosion-induced C balance for combined water and tillage redistribution ( $3.08/3.84 \text{ g m}^{-2} \text{ yr}^{-1}$ ) than the erosion-induced C balance for water redistribution alone ( $0.61/0.59 \text{ g m}^{-2} \text{ yr}^{-1}$ ) at two study sites (3.9 and 4.1 ha) located in Denmark and the UK. Wilken et al. (2017b) further showed that neglecting the contribution of tillage leads to a net erosion-induced C loss of  $-4.8 \text{ g m}^{-2}$  from a small 7.8 ha arable catchment in a loess area of Southern Germany. On the other hand, relatively low contribution

of tillage ( $k_{til} \approx 85 \text{ kg m}^{-1} \text{ yr}^{-1}$ ) leads to a  $-0.4 \text{ g m}^{-2}$  lower C loss for a small catchment after modelling for 50 years. Only a simulation with a high contribution of tillage ( $k_{til} \approx 254 \text{ kg m}^{-1} \text{ yr}^{-1}$ ) causes  $10.3 \text{ g m}^{-2}$  of C gain. This difference between TOT and WAT can be traced back to the fact that tillage redistribution is the dominant erosion agent in their study areas (Wilken et al., 2017b), which is not the case for this study. Even though our study area is dominated by water erosion, the results reveal that even when tillage has a subordinate role its contribution is important for assessing erosion-induced C balance.

The SPEROS-C model results show a good agreement with observed overall SOC stock distribution with depth and are consistent with regional and local studies (Juřicová et al., 2022; Žižala et al., 2017) as well as with studies modelling rates of SOC redistribution and turnover (e.g. Długoś et al., 2012; Nadeu et al., 2015; Van Oost et al., 2005b; Wilken et al., 2017b). Nevertheless, our study has some limitations, mainly concerning model assumptions and input parameters that should be considered while interpreting the results. One shortcoming is that C inputs from primary productivity are assumed to be spatially homogeneous. However, several studies found spatially variable C input associated with spatially distributed crop yields that are related to erosion patterns (Heckrath et al., 2006; Quinton et al., 2022; Öttl et al., 2021). McCarty and Ritchie (2002) showed that high erosion rates result in a net loss of crop productivity, thus less C input to soils. This could partly explain the overestimation of modelled SOC stocks for some of the observation sites. However, a sufficient amount of used fertilizer could balance the crop production on eroded sites with decreased soil fertility. Although loess sediment mixed with the rest of the humic horizon in the plough layer has less favourable plant growth conditions than less eroded Chernozem, it is usually still sufficient (e.g. water holding capacity) for crop growth.

## A.5 CONCLUSIONS

Tillage redistribution can no longer be considered as a new area of research. However, its role is still underrepresented in a way in which it affects the erosion-induced C balance and sequestration of agroecosystems. Even though our study region is dominated by water erosion, we identified the substantial contribution of tillage affecting SOC stocks and erosion-induced C fluxes. Our findings show that neglecting the contribution of tillage leads to a considerable overestimation of SOC stocks on eroded parts of hilly arable fields. Furthermore, tillage redistribution reinforces the C sink function of soils, which leads to a positive net C flux of the study site after modelling 58 years. Moreover, tillage redistribution also results in less C export from the study site as SOC rich sediment is moved from hilltops and slope shoulders and is not further accessible for surface runoff by water. Although tillage

redistribution is a major contributor to soil degradation and hence, a risk for food security, it is a highly relevant process for C storage in cropland soils. Our results suggest that climate mitigation strategies, which are often based on conservative agricultural management (i. e. no-till) to increase SOC sequestration, might be less effective as the erosion-induced C sink function declines.

#### A.6 SUPPLEMENTARY MATERIAL

Table A.3: Model input parameters with abbreviations used in the text in brackets, parameter ranges used in the Monte Carlo simulation and final, calibrated values, parameters taken from literature, and goodness-of-fit parameters for the comparison of observed and modelled soil organic carbon (SOC) depth profiles.

Calibrated parameters				
	value		unit	reference
	range	final value		
Root:Shoot ratio ( <i>RS</i> )	0.1 - 0.5	0.47	-	
Residue to AGBM ratio ( <i>Res:AGBM</i> )	0.1 - 0.5	0.26	-	Monte Carlo simulations n = 1000
Decomposition depth attenuation ( <i>u</i> )	2 - 3	2.6	-	
Root growth constant ( <i>zz</i> )	2 - 6	2.9	-	
Parameters from literature				
C turnover rate - young pool ( <i>k<sub>Y</sub></i> )		0.8	yr <sup>-1</sup>	Andrén and Kätterer (1997)
C turnover rate - old pool ( <i>k<sub>O</sub></i> )		0.006	yr <sup>-1</sup>	Andrén and Kätterer (1997)
C content		45	%	Van Oost et al. (2005b)
Humification coefficient - crops ( <i>h<sub>c</sub></i> )		0.125	-	Kätterer and Andrén (1999)
Humification coefficient - manure ( <i>h<sub>m</sub></i> )		0.31	-	Kätterer and Andrén (1999)
Reference soil depth ( <i>z<sub>r</sub></i> )		0.25	m	Van Oost et al. (2005b)
Aboveground biomass ( <i>AGBM</i> = crop yield / harvest index; range for different crops)		0.7 - 1.6	kg m <sup>-2</sup>	annual data (1961-2018; Czech Statistical Office)
Cover crop aboveground biomass ( <i>AGBM<sub>cc</sub></i> )		7.81	kg m <sup>-2</sup>	∅ annual yield (1961-1989; Czech Statistical Office)
Cover crop root to shoot ratio ( <i>RS<sub>cc</sub></i> )		0.73	kg m <sup>-2</sup>	Bolinder et al. (2002)
Goodness-of-fit coefficients				
Mean error ( <i>ME</i> )		-0.03	kg m <sup>-2</sup>	
Absolute error ( <i>AE</i> )		0.01	kg m <sup>-2</sup>	
Root mean square error ( <i>RMSE</i> )		0.07	kg m <sup>-2</sup>	
Model efficiency ( <i>MEF</i> )		0.85	-	Nash and Sutcliffe (1970)

## LIST OF FIGURES

---

Figure 2.1	Summary of the thesis . . . . .	10
Figure 2.2	Drawing of historical ploughs . . . . .	14
Figure 2.3	Comparison of tillage implements . . . . .	16
Figure 3.1	Experimental design of the tillage experiments	27
Figure 3.2	Implements used within tillage experiments .	28
Figure 3.3	Schematic drawing of the detection system . .	29
Figure 3.4	Spatial pattern of the position of the RFIDs . .	31
Figure 3.5	Direction and distance of the RFID translocation	32
Figure 3.6	Boxplots of the RFID translocation distance . .	33
Figure 3.7	Boxplots of the $k_{til}$ . . . . .	34
Figure 4.1	Impact of desurfacing on crop yields . . . . .	42
Figure 4.2	The study area . . . . .	46
Figure 4.3	Erosion-affected soil pattern in the study area	47
Figure 4.4	Spatial patterns of modeled erosion . . . . .	52
Figure 4.5	EVI vs. modeled erosion for one field . . . . .	53
Figure 4.6	EVI <sub>z</sub> versus erosion for the study area . . . . .	55
Figure 4.7	Net effect of soil redistribution on the EVI . . .	56
Figure 5.1	Changes in soil properties and crop yields . .	63
Figure 5.2	The effects of soil redistribution on soil properties	64
Figure 5.3	Effects of topsoil removal on yields . . . . .	65
Figure 5.4	Modelled biomass production and EVI . . . . .	74
Figure 5.5	Modelled cumulative biomass production . . .	75
Figure 5.6	Comparison of AQUACROP with statistics . .	82
Figure 5.7	Modelled soil loss and gain . . . . .	83
Figure 5.8	Topography and arable fields in the test area .	85
Figure 5.9	Monthly precipitation at the station Dedelow .	85
Figure 6.1	Study area . . . . .	91
Figure 6.2	Input parameters for modelling . . . . .	96
Figure 6.3	Depth profile of SOC stocks . . . . .	100
Figure 6.4	Exemplary aerial photos . . . . .	101
Figure 6.5	Modelled spatial patterns . . . . .	103
Figure 6.6	Modelled versus observed topsoil SOC . . . .	104
Figure 6.7	Temporal variation of the model output . . . .	106
Figure A.1	Study site . . . . .	164
Figure A.2	Observed and modelled soil profiles . . . . .	171
Figure A.3	Patterns of modelled soil redistribution . . . .	172
Figure A.4	Mean modelled vs. observed topsoil SOC . . .	173
Figure A.5	Modelled and observed SOC stocks . . . . .	174
Figure A.6	Maps and density distributions of SOC stocks	175
Figure A.7	Cumulative erosion-induced C fluxes . . . . .	177

## LIST OF TABLES

---

Table 3.1	Soil moisture and bulk density . . . . .	34
Table 3.2	Comparison of tillage erosion coefficients . . .	36
Table 5.1	Cumulative $k_{til}$ estimated from literature . . . .	81
Table 5.2	Soil properties of references Calcic Luvisols . .	84
Table 5.3	Hydraulic properties of undisturbed soil . . .	84
Table 6.1	Model input parameters for SOC modelling . .	99
Table 6.2	Modelled vs. classified erosion . . . . .	102
Table 6.3	Literature review of the $k_{til}$ values . . . . .	113
Table A.1	Annual mean yield . . . . .	170
Table A.2	Goodness-of-fit of modelled SOC stocks . . . .	174
Table A.3	Model input parameters . . . . .	180

## LIST OF ABBREVIATIONS

---

<b>AGBM</b>	aboveground biomass
<b>C</b>	carbon
<b>CaCO<sub>3</sub></b>	carbonate
<b>CO<sub>2</sub></b>	carbon dioxide
<b>COP21</b>	21 <sup>st</sup> Conference of the Parties to the United Nations Framework Convention on Climate Change (UNFCCC)
<b>DEM</b>	digital elevation model
<b>DFG</b>	German Research Foundation
<b><i>E<sub>til</sub></i></b>	tillage-induced soil redistribution
<b><i>E<sub>tot</sub></i></b>	total soil redistribution due to tillage and water
<b><i>E<sub>wat</sub></i></b>	water-induced soil redistribution
<b>EVI</b>	Enhanced Vegetation Index
<b>HI</b>	harvest index
<b>ICBM</b>	Introductory Carbon Balance Model
<b>IPCC</b>	Intergovernmental Panel on Climate Change
<b><i>k<sub>til</sub></i></b>	tillage transport coefficient
<b>MEF</b>	Nash Sutcliffe model efficiency
<b>N</b>	nitrogen
<b>P</b>	phosphorous
<b>RMSE</b>	root mean square error
<b>RPAS</b>	remotely piloted aircraft system
<b>RUSLE</b>	Revised Universal Soil Loss Equation
<b>SLCH</b>	soil loss due to crop harvesting
<b>SOC</b>	soil organic carbon
<b>SOM</b>	soil organic matter
<b>UNFCCC</b>	United Nations Framework Convention on Climate Change
<b>USLE</b>	Universal Soil Loss Equation



## PUBLICATIONS OF THE AUTHOR

---

### *Articles published in ISI peer-reviewed journals*

- Quinton, J. N., L. K. Öttl and P. Fiener (2022). 'Tillage exacerbates the vulnerability of cereal crops to drought'. In: *Nature Food* 3.6, pp. 472–479.
- Öttl, L. K., F. Wilken, K. Auerswald, M. Sommer, M. Wehrhan and P. Fiener (2021). 'Tillage erosion as an important driver of in-field biomass patterns in an intensively used hummocky landscape'. In: *Land Degradation & Development* 32.10, pp. 3077–3091.
- Öttl, L. K., F. Wilken, A. Hupfer, M. Sommer and P. Fiener (2022). 'Non-inversion conservation tillage as an underestimated driver of tillage erosion'. In: *Scientific Reports* 12.20704.

### *Articles submitted to peer-reviewed journals*

- Juřicová, A., L. K. Öttl, F. Wilken, T. Chuman, D. Žiřala, R. Minařík and P. Fiener (submitted to *Soil & Tillage Research*). *Tillage erosion as an underestimated driver of carbon dynamics*.
- Öttl, L. K., F. Wilken, A. Juřicová, P. V. G. Batista and P. Fiener (submitted to *Soil*). *A millennium of arable land use - the long-term impact of water and tillage erosion on landscape-scale carbon dynamics*.



## EIDESSTATTLICHE ERKLÄRUNG

---

Hiermit versichere ich, Lena Katharina Öttl, dass ich die vorliegende Dissertation mit dem Titel *“Tillage erosion – An important driver of yield variability and carbon dynamics in a hummocky arable landscape in Northeast Germany”* selbständig verfasst und keine anderen als die angegebenen Quellen und Hilfsmittel verwendet habe. Alle Ausführungen, die anderen Schriften wörtlich oder inhaltlich entnommenen wurden, sind als solche kenntlich gemacht.

Ich habe diese kumulative Dissertation am Institut für Geographie der Fakultät für Angewandte Informatik an der Universität Augsburg erarbeitet und in englischer Sprache angefertigt.

Diese Dissertation wird erstmalig und ausschließlich an der Universität Augsburg eingereicht. Die dem Promotionsverfahren zugrundeliegende Promotionsordnung vom 21. Mai 2014, geändert durch die Satzung vom 27. Mai 2015, ist mir bekannt.

Augsburg, Juli 2023

---

Lena Katharina Öttl